Chemical Studies on Tyrosinase Inhibitory and Antioxidant Activity of Bromophenols from Rhodomelaceae Algae

A Dissertation

Submitted to the Graduate School of Fisheries Sciences, Hokkaido University, in Partial Fulfillment of the Requirements for the Degree of Doctor of Philosophy in Fisheries Sciences

By

Md. Reazul Islam

Division of Marine Life Science

Hokkaido University

Japan

January 2018

Table of Contents

ACKNOWLEDGEMENTS

First of all, I want to acknowledge my supervisor Dr. Hideyuki KURIHARA sensei for his guidance, encouragement, and continuous monitoring of research progress throughout the study. He was always open his door for all questions and discussions concerning all aspects of the work. I am also grateful for his scrutinizing and improving this manuscript.

I want to express my gratitude to Dr. Hideshi SEKI and Dr. Masashi HOSOKAWA sensei for constructive criticism to improve this manuscript. I am also indebted to them for reviewing and improving this thesis.

I would like to thanks my former lab Professor Dr. Koretaro TAKAHASHI sensei for his inspiration, amicable behavior and friendly attitude that make my Japanese life easier and enjoyable.

I also express my gratitude to Dr. Eri Fukushi and Mr. Yusake Takata for MS and NMR analysis.

I also would like to thank all of my lab members, friends for their help during my research work and making our laboratory environment enjoyable.

I would like to express gratefulness to my parents, all family members including my wife, for their mental support and continuous inspiration.

Finally, I want to thanks the Ministry of Education, Culture, Sports, Science and Technology of Japan to offer my scholarship.

ABBREVIATIONS

Acronym	Full Name
mRNA	Messenger ribonucleic acid
DHI	Dihydroxyindole
DHICA	Dihydroxyindole-2-carboxylic acid
ROS	Reactive oxygen species
RNS	Reactive nitrogen species
PTB1B	Protein tyrosine phosphatase 1 B
T2DM	Diabetes mellitus type 2
HMG-CoA	3-Hydroxy-3-methylglutaryl-CoA
MeOH	Methanol
$CHCl_3$	Chloroform
EtOAc	Ethyl acetate
BuOH	*n*-Butanol
AA	Acetic acid
FA	Formic acid
Abs	Absorbance
Fr	Fraction
TLC	Thin layer chromatography
PLC	Preparative thin layer chromatography
R_f	Rate of flow
IC_{50}	50% Inhibitory concentration
EC_{50}	50% Effective concentration
RP	Reversed phase
NP	Normal phasse
HPLC	High performance liquid chromatography
NMR	Nuclear magnetic resonance
COSY	Correlation spectroscopy
HSQC	Heteronuclear single quantum coherence spectroscopy
HMBC	Heteronuclear multiple bond correlation
ROESY	Rotating frame nuclear Overhauser effect spectroscopy
NOE	Nuclear Overhauser effect
MHz	Megahertz
$(CD_3)_2CO$	Deuterated acetone
CD_3OD	Deuterated methanol
MS	Mass spectrometry
FD-MS	Field desorption mass spectrometry
UV	Ultraviolet
DPPH	2,2-Diphenyl-1-picrylhydrazyl
ABTS	2,2´-Azino-bis(3-ethylbenzothiazoline-6-sulfonic acid) diammonium salt
CUPRAC	Cupric reducing antioxidant capacity
FRAP	Ferric reducing antioxidant power
TPTZ	2,4,6-Tris(2-pyridyl)-*s*-triazine
EDTA	Ethylenediamine-*N,N,N',N'*-tetraacetic acid
BHA	2(3)-*tert*-Butyl-4-hydroxyanisole

General Introduction

Melanin, a dark macromolecular pigment, is commonly found in animals. This pigment determines color of skin, eyes and hair, and gives protection by absorbing ultraviolet (UV) sunlight [1]. Human phenotypic appearance is also determined by melanin. It protects damage from stress caused by UV radiation of sun and reactive oxygen species in microorganisms. Melanin also provides protection from high temperature, chemical stress, and biochemical threat (such as host defenses against invading microbes) [2]. The melanin formation begins with oxidation of tyrosine to dopaquinone catalyzed with tyrosinase which undergoes polymerization to produce it [3]. Enzymatic browning mediated with tyrosinase may decrease market price, consumer acceptance and shelf life of fruits, vegetables, and beverages [4].

Polyphenol oxidases are copper-containing enzymes that include tyrosinase and catechol oxidase [5]. Tyrosinase (EC 1.14.18.1) catalyzes hydroxylation of the monophenol L-tyrosine to the *o*-diphenol, L-3,4-dihydroxyphenyl alanine (L-dopa) and oxidation of L-dopa to the L-dopaquinone whereas catechol oxidase (EC 1.10.3.2) catalyzes only L-dopa to L-dopaquinone [6]. Thus, tyrosinase catalyzes both monophenolase and diphenolase redox reaction followed by series of chemical reactions which result the formation of melanin (Figure GI-1) and/or brown color in foods [4]. In melanogenesis process, oxidation of L-tyrosine to L-dopaquinone mediated with tyrosinase is a rate-limiting step as subsequent reactions proceed spontaneously. Eumelanin is formed through a series of cyclization and oxidation reactions of dopaquinone to dopachrome that later convert to dihydroxyindole (DHI) and dihydroxyindole-2-carboxylic acid (DHICA). Finally DHI and DHICA are further polymerized to produce eumelanin [1, 3, 7, 8]. In the presence of cysteine or glutathione, dopaquinone is converted to cysteinyldopa or glutathionyldopa. Subsequently, pheomelanins are formed from cyclization and polymerization of cysteinyldopa or glutathionyldopa. Mixed-type melanins are formed from the interaction between the eumelanin and pheomelanin [9].

Hyperpigmentation can create serious esthetic problem due to excessive production of melanin [10]. Melanin is produced by melanocyte cell in under-layer of epidermis. Hyperpigmentation is developed by excessive concentration of melanocyte cell under UV light stimuli. Enzymatic browning is another problem resulted from the enzymatic activity of tyrosinase in fruits, vegetables, beverages, and crustaceans [11]. This problem occurs when

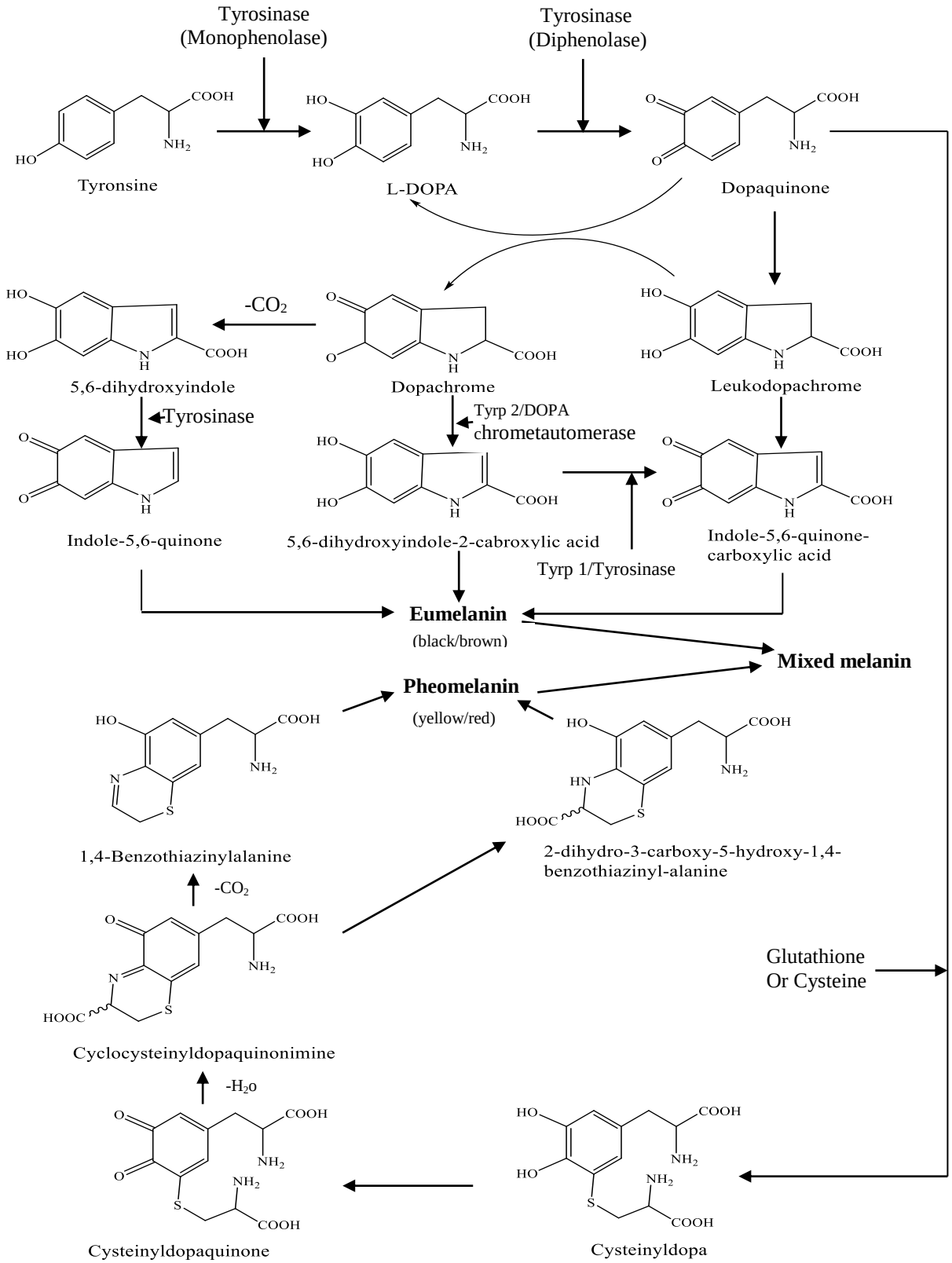

Figure GI-1. Schematic diagram of melanin formation in mammals [4, 8, 9].

tyrosinase and its polyphenolic substrate are mixed after brushing, peeling, and crushing operations, which lead to the rupture of cell structure [12]. It brings undesirable changes such as nutrient composition, shelf-life, and consumer acceptance are negatively affected from enzymatic browning [4]. So enzymatic browning is one of the major concerns in food industry.

Figure GI-2. Woman suffering from hyperpigmenation.

Figure GI-3. Enzymatic browning on banana.

Pictures source: www.googleimage.com

Last several decades, tyrosinase inhibitors have been drawn attention to prevent hyperpigmentation and enzymatic browning. There are few approaches to prevent excessive melanin production: inhibition of tyrosinase catalytic activity, inhibition of tyrosinase mRNA transcription, aberration of tyrosinase glycosylation, acceleration of tyrosinase degradation, inhibition of inflammation-induced melanogenic response [3, 4, 13]. Inhibition of tyrosinase activity is one of the popular strategies to prevent hyperpigmentation and enzymatic browning [4].

Kojic acid, a fungal metabolite used as a cosmetic skin-whitening agent and food additive to prevent enzymatic browning [14]. Kojic acid shows competitive and mixed type inhibition potency against mushroom tyrosinase. It also acts as copper chelator at the active site of tyrosinase [3]. Hydroquinone and arbutin are other two phenolic compounds that are used in cosmetic industry as a skin-whitening agent. These compounds are criticized for cytotoxicity [15] including carcinogenic effect [16]. In addition, different plant extracts such as licorice root, mulberry, aloes, green tea, etc. have also been used as whitening agents in cosmetics [4]. Inhibitors having high efficacy and safety are the two important properties that must be fulfilled before using in cosmetic industry. In case of food industries, inhibitor

should not deteriorate sensory properties. So, there is an urgency to find new potent tyrosinase inhibitor.

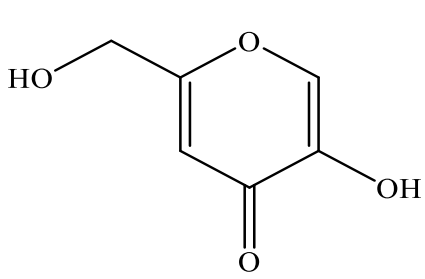

1

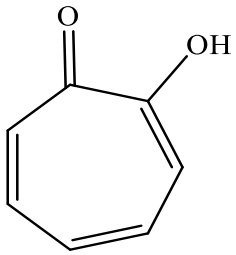

2

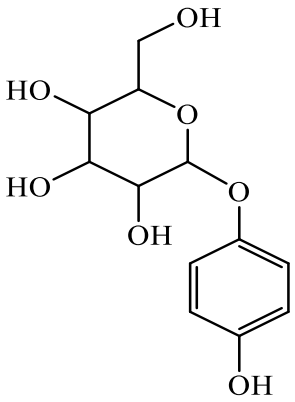

3

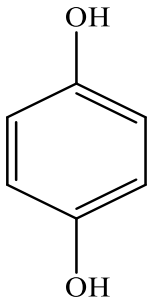

4

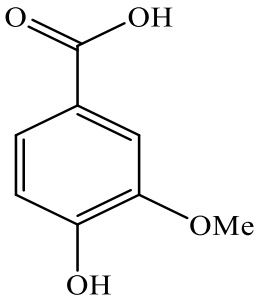

5

Figure GI-4. Structure of kojic acid (**1**), tropolone (**2**), arbutin (**3**), hydroquinone (**4**), vanillic acid (**5**) (commonly used tyrosinase inhibitors).

Free radicals are continuously generated as byproducts of oxygen metabolism in the life process [17]. Free radicals are also referred as reactive oxygen species (ROS) and reactive nitrogen species (RNS) and act as oxidizing agents [18]. There is a balance between generation of ROS and RNS to minimize molecular, cellular and tissue damage. Imbalance between the generation of free radicals and antioxidant defenses causes oxidative stress, associated with aging, atherosclerosis, cancer, diabetes, inflammation, Alzheimer's and Parkinson's diseases [17, 19]. Antioxidants have the ability to protect body damage caused by free radicals [20]. In addition, many food ingredients contain unsaturated fatty acids that are susceptible to quality deterioration, especially under oxidative stress [21]. Thus, addition of antioxidants is the best strategy to get rid of this problem.

Synthetic compounds butylated hydroxyanisole (BHA), butylated hydroxytoluene (BHT), propyl gallate (PG), and *tert*-butylhydroquinone (TBHQ) are widely used as antioxidants [22]. However, synthetic antioxidants are criticized for pathological lipid alternation [23] and carcinogenic effect [24]. There is an increasing interest of finding effective natural antioxidants to replace synthetic antioxidants. Naturally occurring phenolic compounds received significant attention to many researchers as antioxidants with diverse pharmacological activity [17, 25, 26, 27]. The *in vitro* antioxidant test is the most extensively method for searching natural antioxidants based on mechanisms such as the ability to quench free radicals by hydrogen donation and the ability to transfer one electron [28].

Several mechanisms of antioxidant compounds are recognized as: i) scavenging species that initiate peroxidation; ii) chelating metal ions that catalyze generation of reactive species; iii) quenching superoxide anion ($^{\bullet}O_2^-$) to prevent formation of peroxides; iv) breaking the autooxidative chain reaction; v) reducing localized O_2 concentration [29]. Plant phenolics can be divided into four general groups: phenolic acids (gallic, caffeic, rosmarinic acids), flavonoids (quercetin, catechin), phenolic diterpenes (carnosol, carnosic acid), and volatile oils (eugenol, thymol) [21, 30]. Phenolic acids generally act as antioxidants by trapping free radicals. Flavonoids can scavenge free radicals and chelate metals. Flavonoids can decrease transition metal enhancement of oxidation by donating hydrogen radical. Number and position of –OH group in phenolic compound is very sensitive as it can donate hydrogen, scavenge free radicals, quenching $^{\bullet}O_2$, chelate metal ions and act as reducing agent [21].

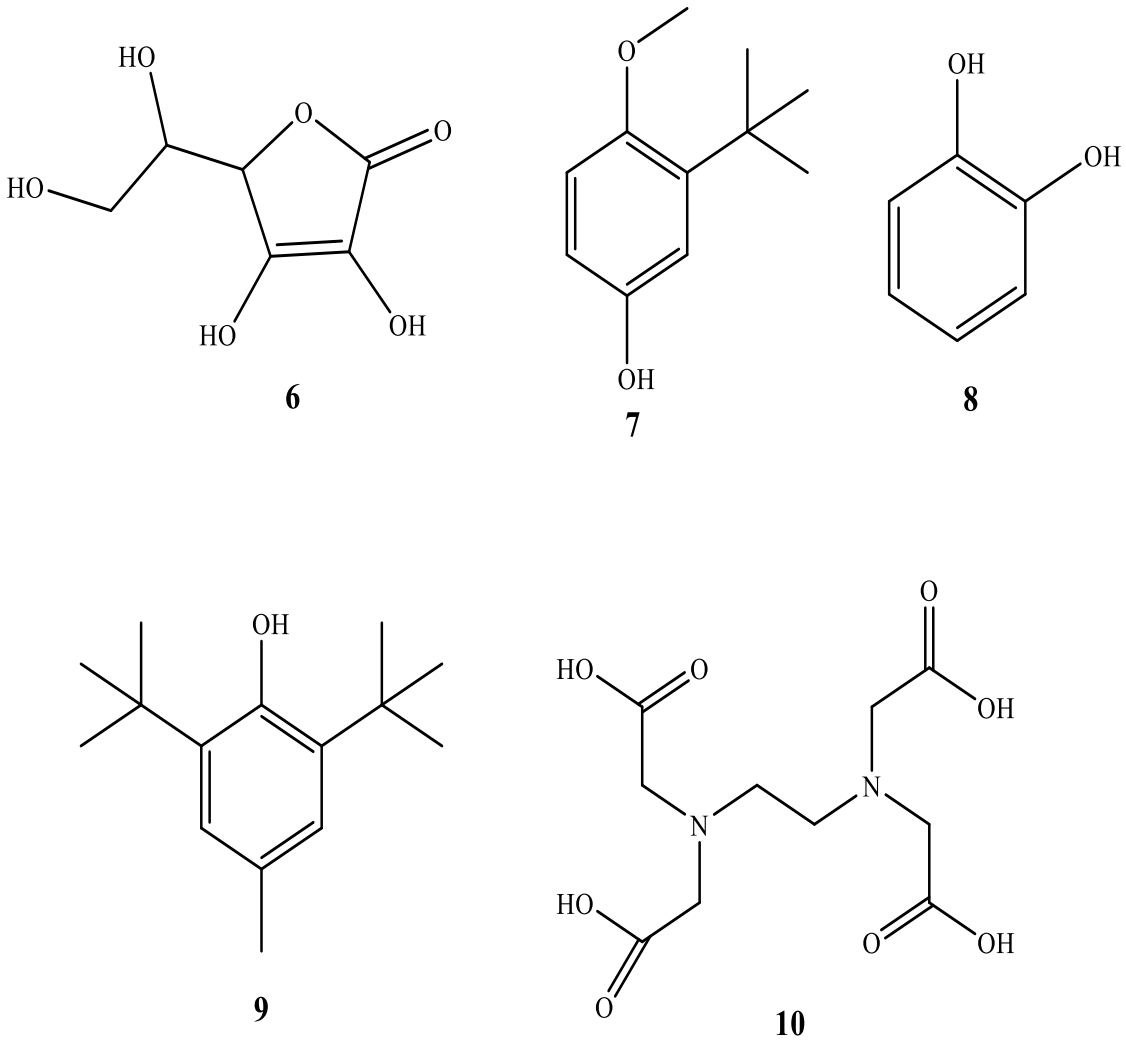

Figure GI-5. Structure of ascorbic acid (**6**), BHA (**7**), catechol (**8**), BHT (**9**) and EDTA (**10**) (commonly used natural and synthetic antioxidants).

Researchers are using many *in vitro* tests to measure the antioxidant potency of naturally occurring compounds. Metal-reducing assay (FRAP, CUPRAC, Folin-Ciocalteau test) can suggest the potency to donate electron and reduce oxidizing substances. Radical scavenging assay is another commonly used for *in vitro* test. Different radicals (DPPH and ABTS radical cation) and reactive oxygen species (superoxide anion, hydrogen peroxide, peroxyl radical, hydroxyl radical, singlet oxygen and peroxynitrite) were used for compounds radical scavenging measurement. The presence of transition metals (Cu^{2+}, Fe^{2+}, Fe^{3+}) in a system can induce and accelerate oxidation. Thus, chelating transition metals are also used to determine antioxidant ability of compounds [18].

Marine algae have been used as foodstuffs in East Asian countries and sources of food additives such as agar, alginates, and carrageenans in western countries [24]. It is also a source of structurally diverse bioactive compounds showing many bioactivities. Bromophenols are the most commonly found compound particularly from red algae of the family Rhodomelaceae. Seawater contains bromide (about 0.65 mg/kg) and bromophenols are biosynthesized as secondary metabolites in the presence of bromoperoxidases, hydrogen peroxide and bromide [31-33]. Its ecological importance not fully understood but may act as defense and deterrence agents [34]. Bromophenols consists of one or several benzene rings with varying number of bromine and hydroxyl-substituents. Monomer (bromophenols with single benzene ring) and dimer (bromophenols with double benzene rings) are predominantly found in red algae. Certain red algae contain relatively higher amount of bromophenols including those collected from low tide [35]. However, bromophenols were also reported from brown algae, green algae, ascidians and sponges [36-40].

A series of bromophenols were purified from red algae possessing antioxidant properties. Antioxidant properties rely on the number of hydroxy groups in the bromophenols [17, 24]. Mainly bromophenols antioxidant activity measured on *in vitro* biochemical basis but there was single report of cellular antioxidant activity of bromophenols from the red alga *Vertebrata lanosa* [41] (Figure GI-6). Bromophenols also inhibit proliferation of cancer cell line. Bromophenols showing anticancer activity were isolated from the brown alga *Leathesia nana*, the red algae *Rhodomela confervoides* and *Osmundaria colensoi* and the green alga *Avrainvillea nigricians*. Cytotoxicity has been found a variety of human cancer cell lines including A549, BGC823, MCF-7, BEL-7402, HCT-8, A2780. Activities largely rely on number and position of bromine substitution including phenolic groups and side chains [31] (Figure GI-7).

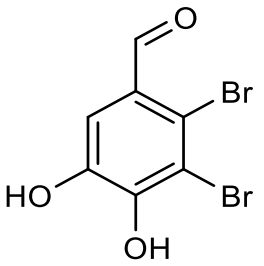

11

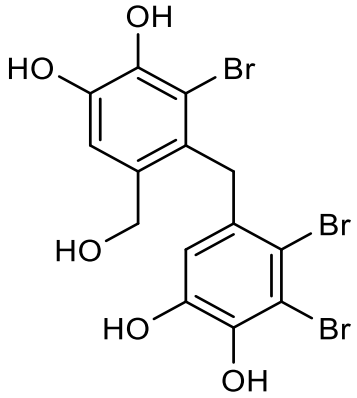

12

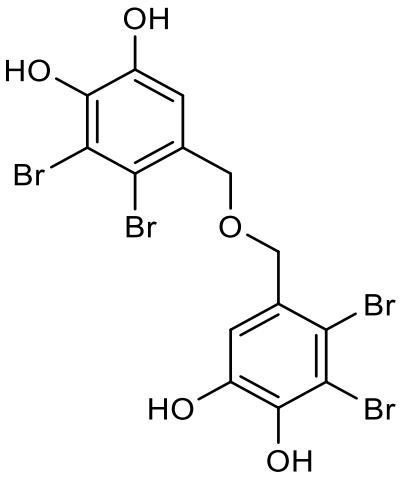

13

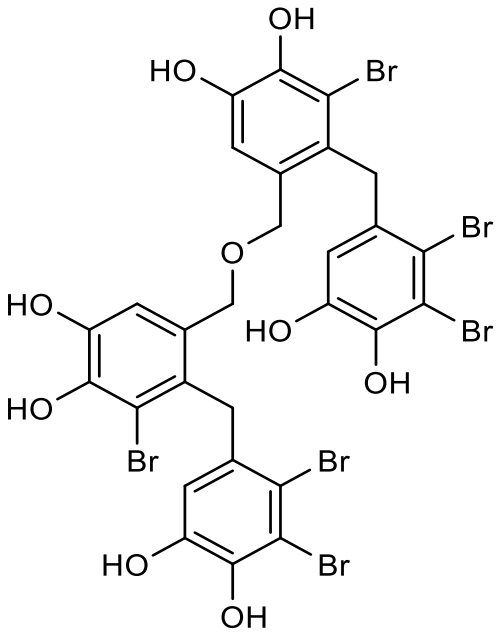

14

Figure GI-6. Bromophenols with cellular antioxidant activity from the red alga *Vertebrata lanosa* [41].

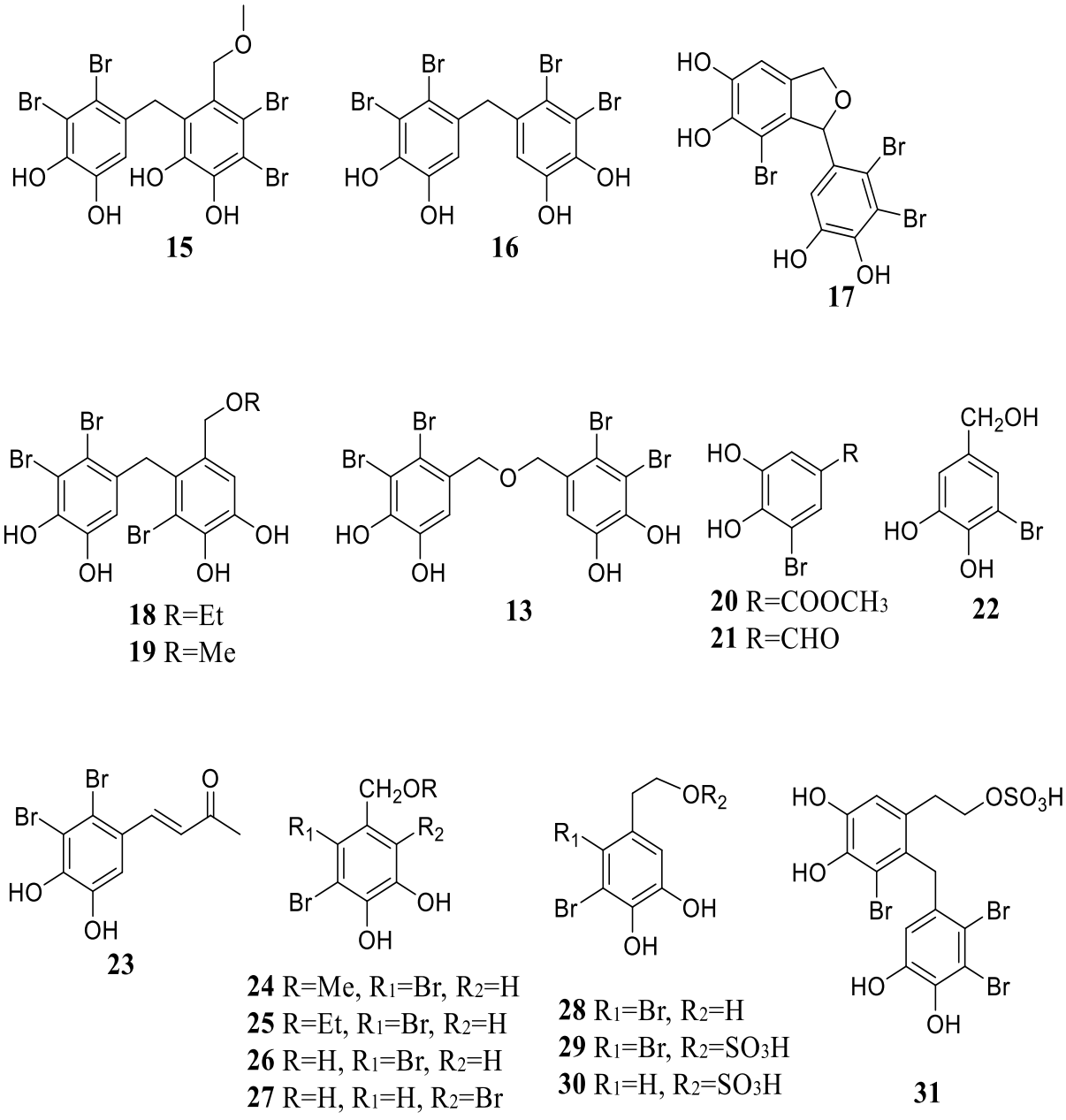

Figure GI-7. Bromophenols with anticancer activity [31].

Marine alga derived bromophenol showed promising antimicrobial activity. Bromophennols from the red alga *Rhodomela confervoides* displayed growth inhibitory effect against Gram positive and Gram negative bacteria [42]. New Zealand red alga *Osmundaria colensoi* derived bromophenols exhibit antibacterial activity against MC155 strain of *Mycobacterium smegmatis* [43]. Bromophenols from *Polysiphonia morrowii* also exhibit activity against fish pathogenic virus, infectious hematopoietic necrosis virus, and infectious pancreatic necrosis virus [44]. Mechanism behind antimicrobial activity not fully investigated but researchers found bromination can play an important role [31] (Figure GI-8).

Traditionally marine algae have been used as folk medicine for treatment of diabetes. Bromophenols derivatives from the red alga *Rhodomela confervoides* inhibit PTB1B activity and decrease the blood glucose levels in diabetic rats [45]. The red algae *Grateloupia elliptica*, *Polyopes lancifolia* and *Odonthalia corymbifera* were reported to produce alpha-glucosidase inhibitory bromophenols [46-49]. This enzyme plays a significant role in carbohydrate digestion and is a key target for anti-diabetic drugs. Alpha-glucosidase inhibitory activity increased with number of bromine substitution in the molecules [31] (Figure GI-9).

Bromophenols from marine algae also exhibit inhibition against various enzymes such as bromophenols from the red alga *Symphyocladia latiuscula* displayed aldose reductase inhibitory activity. This type of inhibitor can be used for the treatment of diabetes, eye and nerve damage in T2DM patients [31, 50]. Thrombin inhibitory bromopheonls were isolated from the brown alga *Leathesia nana* and possess the potentiality for cardiovascular disease treatment [51, 52] (Figure GI-10). The green alga *Avrainvillea rawsoni* was reported to generate HMG-CoA reductase inhibitory bromophenols and can be used as cholesterol-lowering drugs [53] (Figure GI-10).

The red alga *Vidalia obtusaloba* was known to produce anti-inflammatory bromophenols and could reduce swelling of mouse ear via inhibition of phospholipase A_2 metabolic pathway [54]. Bromophenols also showed properties as flame retardants and fungicides [31] (Figures GI-11 to GI-13). However, feeding deterrent bromophenols were isolated from *Odonthalia corymbifera* [55], and anti-human rhinoviral bromophenols from *Neorhodomela aculeata* [56]. Mostly bromophenols bioactivities were measured on *in vitro* basis but it possess the ability to be potential drug candidates. Limited information available on toxicity of bromophenols but few studies reveals low toxicity of bromophenols.

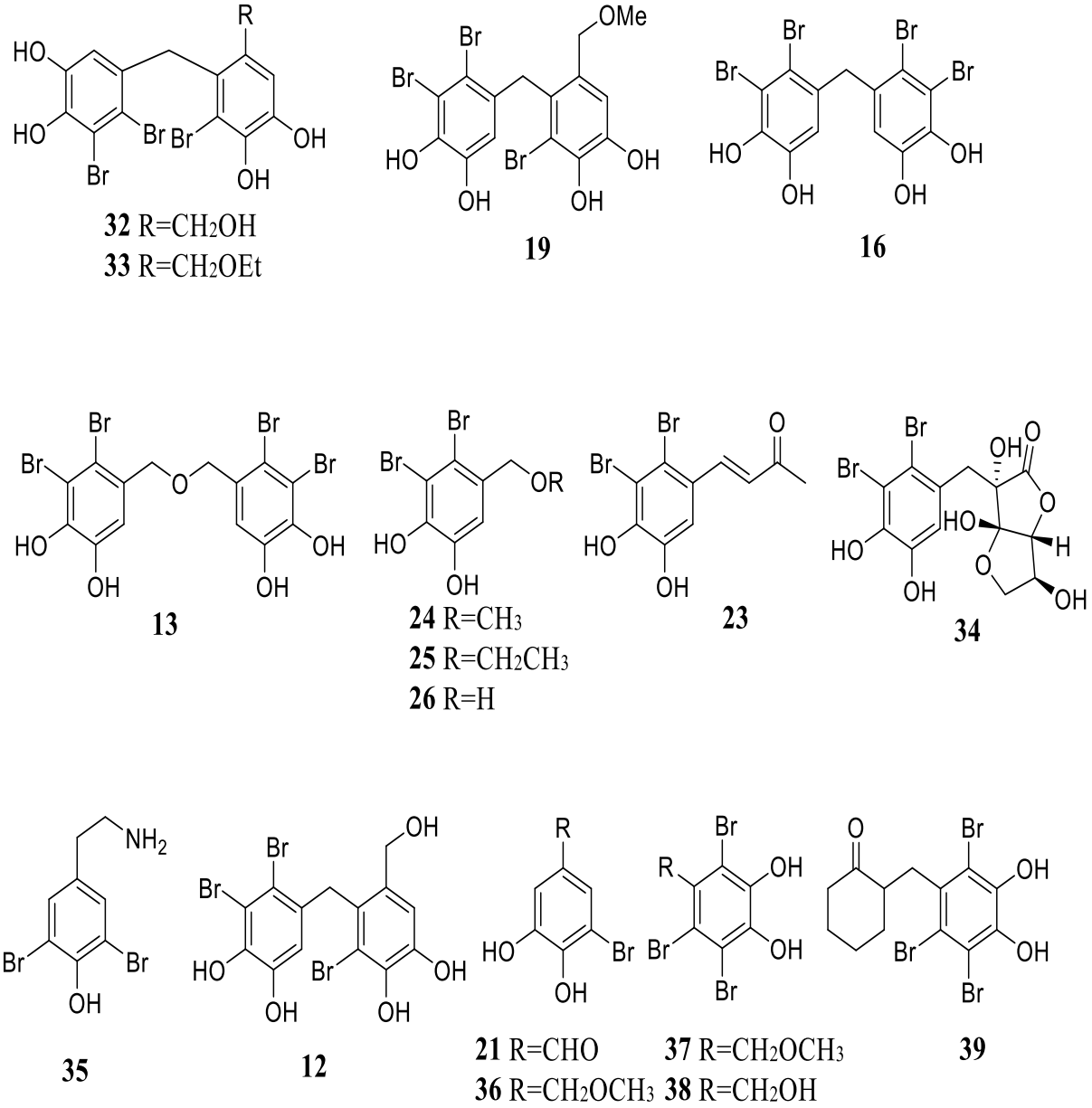

Figure GI-8. Bromophenols with antimicrobial activity [31].

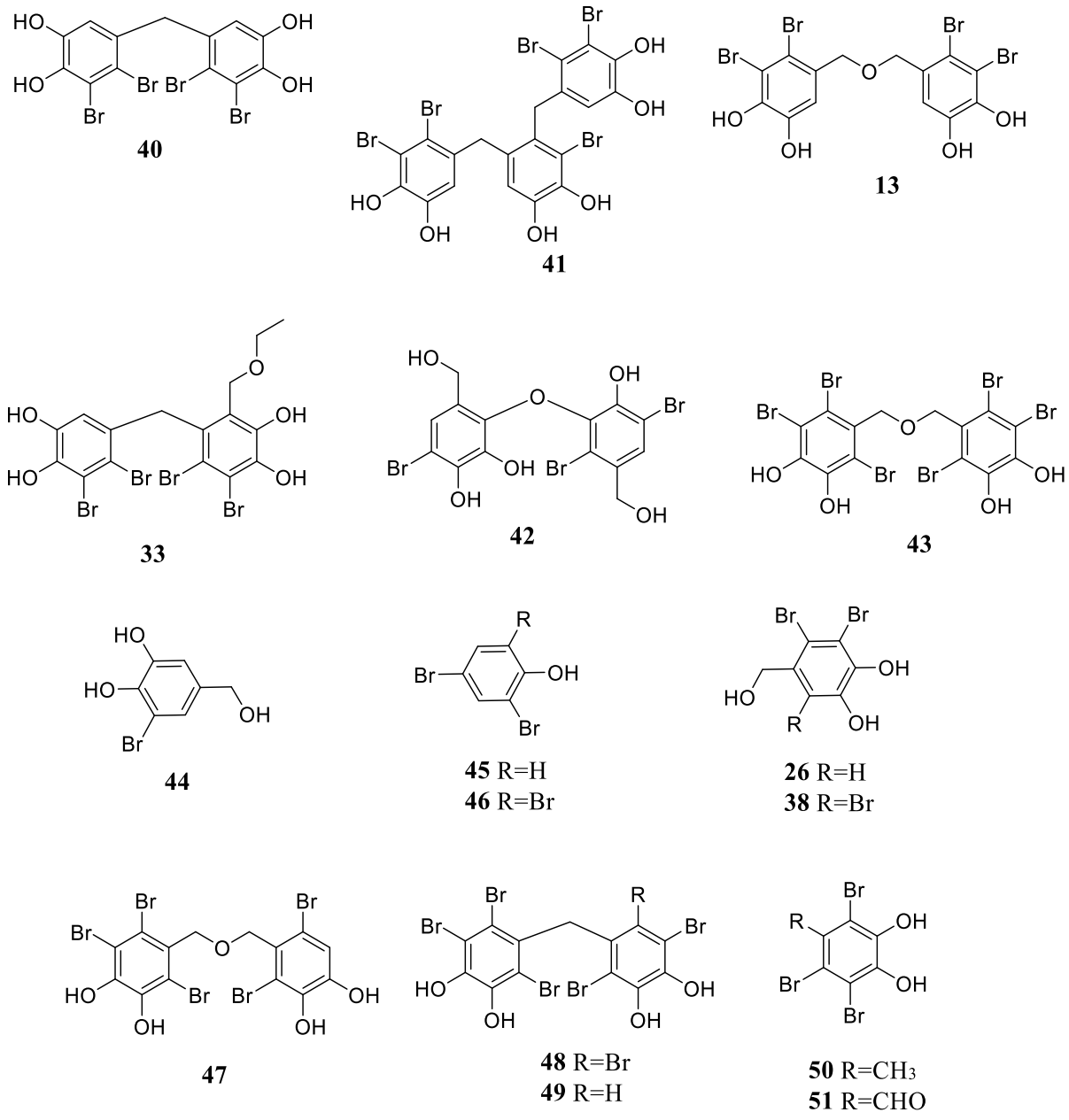

Figure GI-9. Bromophenols with anti-diabetic activity [31].

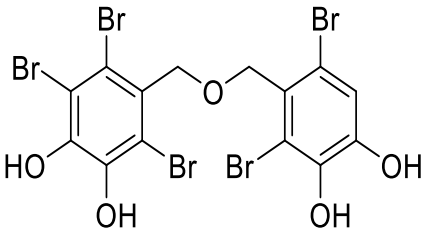

47

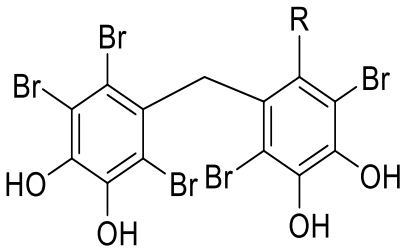

48 R=Br
49 R=H

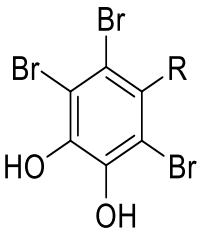

50 R=CH_3
51 R=CHO

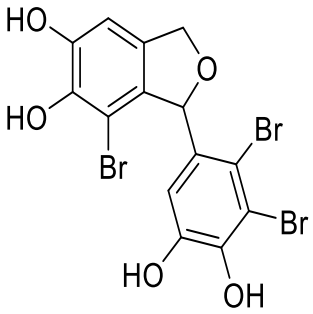

17

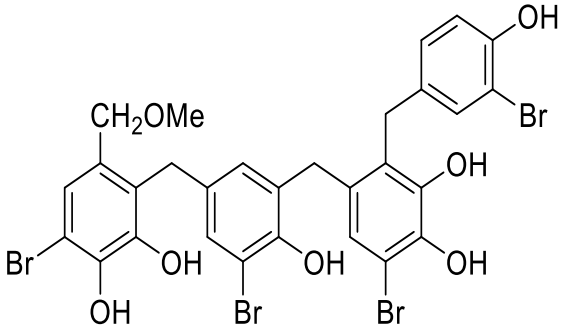

52

Figure GI-10. Bromophenols with various enzyme inhibitory activities [31, 50].

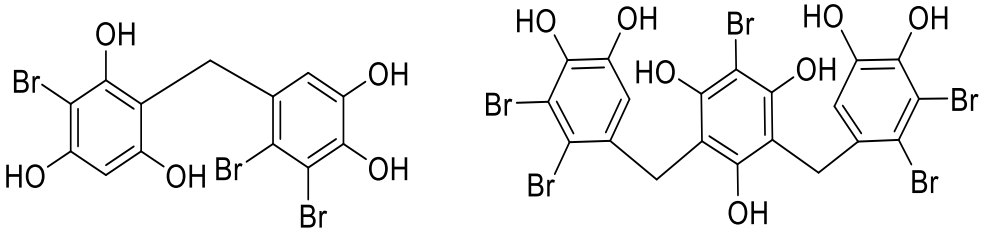

53 **54**

Figure GI-11. Bromophenols with anti-inflammatory activity [31].

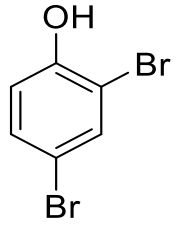

45

Figure GI-12. Bromophenol with flame retardants activity [31].

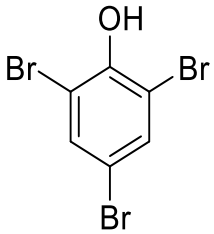

46

Figure GI-13. Bromophenol with fungicides activity [31].

In the course of search for tyrosinase inhibitor and antioxidant, naturally occurring bromophenols were isolated from the two red algae, *Neorhodomela aculeata* and *Odonthalia corymbifera* of the Rhodomelaceae family. Thus, the main objectives of this research are as followed:

1. Screening of marine algae and identify the potential marine algae for isolation of tyrosinase inhibitors and antioxidant compounds.

2. Isolation and purification of bioactive compounds, structural elucidation by MS and NMR analysis, and studying their structure-activity relationship.

3. Investigating kinetic study of some isolated compounds against tyrosinase activity.

4. Comparison of isolated compounds with related synthetic compounds to elucidate plausible inhibition mechanisms against tyrosinase.

Chapter 1
Screening of Antioxidant Algal Extract and Isolation of Novel Bromophenols

1.1. Introduction

Marine algae are the prolific sources of structurally diverse bioactive compounds [31]. More than 1058 naturally occurring compounds were isolated and purified from red algae of family Rhodomelaceae since 1960s to till now. Bromophenol is found as a metabolite in marine alga, specifically in marine red alga. The genera *Polysiphonia*, *Rhodomela*, and *Symphyocladia* are the most prolific sources of bromophenols [57]. However, there are few reports on presence of bromophenol in brown algae [36, 37], green alga [38], ascidians [39] and sponges [40]. Bromophenols were divided into monomers to tetramers on the basis of number of benzene rings. Algal bromophenols consist of brominated hydroxylated benzyl (BHB) unit. Rhodomelaceae algae contain large number of monomers and dimers of mono to tribrominated 3,4-dihydroxybenzyl alcohols and alkyl ethers as typical BHB units [47]. Many kinds of the dimers have been isolated and constructed with two BHB units via ether and methylene bridges [57]. However, hybrid-type bromophenols from *Rhodomela confervoides* [58] and *Symphyocladia latiuscula* [59] were reported to contain unique sulfoxide and methyl sulfone moieties coupled with BHB unit. BHB unit coupled with an amino acid or nucleoside unit through a C-N bound were found from *R. confervoides* [60]. There are few reports on isolation of bromophenol trimers [54, 61-63], tetramers [53, 64] and hybrid bromophenols [17, 43, 59, 60, 65, 66]. In the present research, two new algal bromophenols, a hybrid compound of a BHB unit and cyclopentenedione moiety named odonthadione (**R1**) and a trimer of BHB units named odonthalol (**R2**) were isolated from the red alga *Odonthalia corymbifera* (S. G. Gmelin) Greville (Rhodomelaceae). Eight known bromophenols (two monomers and six dimers) were also isolated from the family Rhodomelaceae as well.

1.2. Materials and Methods

1.2.1. General Experimental Procedures

NMR spectra were recorded on a Bruker AMX-500 (Karlsruhe, Germany) NMR spectrometer at 500 MHz for proton and 125 MHz for carbon in $(CD_3)_2CO$ or CD_3OD. Field desorption-MS (FD-MS) spectra were recorded on a JEOL JMS-T100GCV mass spectrometer (Tokyo, Japan). High performance liquid chromatography (HPLC) was performed using SHIMADZU LC-10AT$_{vp}$ apparatus (Kyoto, Japan) equipped with a diode array detector SHIMADZU SPD-M10A$_{vp}$ and RP HPLC column (Mightysil® RP-18, Kanto Chemical Co. Inc., Tokyo, Japan). Silica gel (Chromatorex®, Fuji Silysia, Japan), reversed-

phase (RP-18) silica gel (Nacalai Tesque Inc. Kyoto, Japan) and Sephadex® LH-20 (GE Healthcare, Uppsala, Sweden) were used for column chromatography (CC). Thin layer chromatography (TLC) was performed on glass plate with precoated silica gel (60 F_{254}, RP-18 F_{254} Merck, Darmstadt, Germany). TLC spots were visualized under UV lamp or by spraying with 5% H_2SO_4.

1.2.2. Collection of Algae

Marine algae were collected from three different sites in Hokkaido prefecture (Hakodate, Otaru, and Nemuro city), Japan in 2015, 2016 and 2017, respectively. The species identification was done by Associate Professor Hideyuki Kurihara and supervised by Professor Hiroyuki Mizuta (Faculty of Fisheries Sciences, Hokkaido University). Voucher specimens were deposited in our laboratory.

1.2.3. Screening of Marine Algae

Collected algae were washed with tap water and cut into small pieces. The algal extracts were prepared with 95% methanol (MeOH) and concentrated for 3 days (twice). Prepared extracts were screened against DPPH radical scavenging assay for the selection of alga for further purification of bioactive compounds (Tables 1-1 to 1-11). The marine red algae *Neorhodomela aculeata* and *Odonthalia corymbifera* (Rhodomelaceae) were selected for purification on the basis of assay results. These algae were collected at the coast of Hakodate city, Japan in 2015 and 2016, respectively.

1.2.4. DPPH Radical Scavenging Assay [67]

Tested sample solution (50 µl) in MeOH was added to 40 µg/ml DPPH radical solution (950 µl) in MeOH in a test tube and mixed vigorously. In the dark, the mixture was left for 30 min and measured absorbance at 517 nm. Catechol and BHA were used as positive control. The EC_{50} value was expressed as sample concentration which can quench fifty percent of DPPH free radicals. The radical scavenging activity was calculated using the following equation:

$$\text{Scavenging activity (\%)} = \{A_0 – A_S/A_0\} \times 100$$

Where A_0 is the absorbance of control, A_S is the absorbance of sample. The IC_{50} values were determined graphically from the regression curve by plotting sample concentration against percent scavenging activity.

Table 1-1. Screening of algae collected at Usujiri area, Hakodate in April, 2015.

Specimen Name	Scientific Name	Air Dried Wt. (g)	1st Extract Wt. (g)	2nd Extract Wt. (g)	DPPH Radical Scavenging (%)[a,b]
[Phaeophyceae]					
Matsumo	*Analipus japonicus*	147	3.569	0.863	8.6±1.4
Watamo	*Colpomenia bullosa*	166	1.739	1.520	20.7±5.3
Kayamonori	*Scytosiphon lomentaria*	13	0.538	0.083	6.2±1.4
Fushisujimoku	*Sargassum confusum*	390	14.459	4.452	13.2±2.2
Umitoranoo	*Sargassum thunbergii*	285	9.821	2.428	34.5±1.8
Akamoku	*Sargassum horneri*	34	2.766	0.100	31.4±2.7
[Rhodophyceae]					
Akaba	*Neodilsea yendoana*	7	0.428	0.246	9.1±0.8
Hirakotoji	*Chondrus pinnulatus*	11	0.806	0.197	5.5±1.5
Fukurofunori	*Gloiopeltis furcata*	451	14.296	2.166	3.3±0.8
Akabaginnanso	*Mazzaella japonica*	4	0.028	0.026	5.3±1.8
Kurohaginnanso	*Chondrus yendoi*	1391	42.822	8.401	5.5±0.9
Kushibenihiba	*Ptilota filicina*	45	2.791	0.330	19.9±2.3
Moroitoesa	*Polysiphonia morrowii*	7	0.411	0.072	88.1±2.2
Fujimatsumo	*Neorhodomela aculeata*	113	4.969	0.851	86.6±0.3
Hakesakinokogirihiba	*Odonthalia corymbifera*	93	6.400	0.800	91.2±0.4
Hosobafujimatsumo	*Rhodomela teres*	70	3.490	0.502	77.6±1.6

[a]Final sample concentration 100 μg/ml.

[b]Mean±standard error (n=3).

Table 1-2. Screening of algae collected at Usujiri area, Hakodate in June, 2015.

Specimen Name	Scientific Name	Air Dried Wt. (g)	1st Extract Wt. (g)	2nd Extract Wt. (g)	DPPH Radical Scavenging (%)[a,b]
[Chlorophyceae]					
Anaaosa	*Ulva pertusa*	103	3.105	0.596	32.1±1.6
[Phaeophyceae]					
Matsumo	*Analipus japonicus*	1700	43.800	17.100	9.5±2.1
Nebarimo	*Leathesia difformis*	52	1.321	0.156	12.6±4.2
Kayamonori	*Scytosiphon lomentaria*	48	1.453	0.032	7.8±0.3
Chigaiso	*Alaria crassifolia*	164	12.529	1.814	41.2±3.8
Makonbu	*Saccharina japonica*	107	7.618	0.524	21.3±0.9
Fushisujimoku	*Sargassum confusum*	4800	143.400	28.600	15.2±2.7
Umitoranoo	*Sargassum thunbergii*	3500	111.500	35.600	30.8±1.6
[Rhodophyceae]					
Makusa	*Gelidium elegans*	94	4.746	0.743	44.7±0.4
Hirakotoji	*Chondrus pinnulatus*	1340	35.718	17.316	8.3±1.1
Akabaginnanso	*Mazzaella japonica*	610	13.476	2.749	11.2±0.8
Kushibenihiba	*Ptilota filicina*	25	0.983	0.225	13.9±0.9
Fujimatsumo	*Neorhodomela aculeata*	3000	71.800	16.500	88.6±1.8
Hakesakinokogirihiba	*Odonthalia corymbifera*	664	28.247	4.932	95.3±1.7

[a]Final sample concentration 100 μg/ml.

[b]Mean±standard error (n=3).

Table 1-3. Screening of algae collected at Nemuro, in July, 2015.

Specimen Name	Scientific Name	Air Dried Wt. (g)	1st Extract Wt. (g)	2nd Extract Wt. (g)	DPPH Radical Scavenging (%)[a,b]
[Chlorophyceae]					
Anaaosa	*Ulva pertusa*	48	1.822	0.552	15.5±1.4
Ezomiru	*Codium yezoense*	900	14.505	7.194	9.5±0.8
[Phaeophyceae]					
Matsumo	*Analipus japonicus*	360	8.989	2.842	7.8±1.1
Nagamatsumo	*Chordaria flagelliformis*	1800	32.261	17.683	26.1±2.1
Ezofukuro	*Coilodesme japonica*	250	5.785	1.220	29.4±0.9
Aname	*Agarum clathratum*	1380	26.700	14.000	65.4±0.9
Tororokonbu	*Saccharina gyrata*	530	15.547	2.463	9.9 ±0.5
Hibamata	*Fucus distichus* subsp. *evanescens*	970	36.500	17.600	70.3±1.4
Nebutomoku	*Stephanocystis crassipes*	2300	74.300	31.800	33.3±1.3
[Rhodophyceae]					
Darusu	*Palmaria palmata*	20	1.858	0.538	20.4±4.2
Hirakotoji	*Chondrus pinnulatus*	64	2.412	0.734	6.8±2.6
Kurohaginnanso	*Chondrus yndoi*	530	13.792	2.961	2.1±0.7
Akabaginnanso	*Mazzaella japonica*	35	1.208	0.085	9.9±1.3
Egonori	*Campylaephora hyponaeoides*	950	2.246	2.858	15.2±1.8
Igisu	*Ceramium kondoi*	89	0.529	0.183	12.1±3.4
Fujimatsumo	*Neorhodomela aculeata*	160	33.293	4.880	85.7±1.8
Hakesakinokogirihiba	*Odonthalia corymbifera*	330	4.423	0.338	90.7±1.1

[a]Final sample concentration 100 μg/ml.

[b]Mean±standard error (n=3).

Table 1-4. Screening of algae collected at Oshoro area, Otaru in July, 2015.

Specimen Name	Scientific Name	Air Dried Wt. (g)	1st Extract Wt. (g)	2nd Extract Wt. (g)	DPPH Radical Scavenging (%)[a,b]
[Chlorophyceae]					
Anaaosa	*Ulva pertusa*	26	0.689	0.241	8.6±0.6
[Phaeophyceae]					
Ezoyahazu	*Dictyopteris divaricata*	65	4.976	1.132	12.9±1.3
Umitoranoo	*Sargassum thunbergii*	1300	40.617	15.001	22.6±0.8
Azumanejimoku	*Sargussum yamadae*	240	38.359	6.505	24.4±1.9
[Rhodophyceae]					
Makusa	*Gelidium elegans*	163	9.225	1.921	23.1±1.2
Marubatsunomata	*Chondrus nipponicus*	232	7.000	1.540	18.3±1.8
Hirakotoji	*Chondrus pinnulatus*	22	1.182	0.249	13.9±2.4
Haneigisu	*Ceramium japonicum*	183	6.826	0.657	6.4±2.3
Fujimatsumo	*Neorhodomela aculeata*	790	37.799	11.351	81.5±0.8

[a]Final sample concentration 100 μg/ml.

[b]Mean±standard error (n=3).

Table 1-5. Screening of algae collected at Usujiri area, Hakodate (early) in May, 2016.

Specimen Name	Scientific Name	Air Dried Wt. (g)	1st Extract Wt. (g)	2nd Extract Wt. (g)	DPPH Radical Scavenging (%)[a,b]
[Phaeophyceae]					
Matsumo	*Analipus japonicus*	119	4.010	0.410	19.8±0.9
Kayamonori	*Scytosiphon lomentaria*	582	10.040	1.820	18.6±0.2
Chigaiso	*Alaria crassifolia*	575	14.219	4.638	27.8±2.2
Fushisujimoku	*Sargassum confusum*	2050	73.529	18.129	35.3±2.1
Umitoranoo	*Sargassum thunbergii*	1090	40.139	10.519	32.9±1.6
[Rhodophyceae]					
Sangomo	*Corallina officinalis*	7	0.080	0.015	23.2±0.6
Makusa	*Gelidium elegans*	1350	45.799	12.633	37.8±0.8
Akaba	*Neodilsea yendoana*	264	12.520	2.770	21.1±3.6
Hirakotoji	*Chondrus pinnulatus*	182	12.330	2.520	19.0±0.9
Kurohaginnanso	*Chondrus yendoi*	161	4.600	0.880	25.9±1.7
Akabaginnanso	*Mazzaella japonica*	148	3.923	0.627	19.6±1.7
Matsunori	*Polyopes affinis*	5	0.125	0.024	15.2±0.9
Kushibenihiba	*Ptilota filicina*	141	4.029	0.602	23.2±1.2
Fujimatsumo	*Neorhodomela aculeata*	2430	51.039	15.109	78.4±2.3
Hakesakinokogirihiba	*Odonthalia corymbifera*	1140	69.629	16.220	84.6±1.1
Hosobafujimatsumo	*Rhodomela teres*	419	19.489	4.749	89.6±0.9

[a]Final sample concentration 100 μg/ml.

[b]Mean±standard error (n=3).

Table 1-6. Screening of algae collected at Usujiri area, Hakodate (late) in May, 2016.

Specimen Name	Scientific Name	Air Dried Wt. (g)	1st Extract Wt. (g)	2nd Extract Wt. (g)	DPPH Radical Scavenging (%)[a,b]
[Phaeophyceae]					
Matsumo	*Analipus japonicus*	239	7.462	1.579	15.6±1.8
Ezoyahazu	*Dictyopteris divaricata*	232	7.340	1.540	9.5±1.5
Kayamonori	*Scytosiphon lomentaria*	63	1.260	0.480	19.2±1.1
Chigaiso	*Alaria crassifolia*	274	7.450	2.810	21.7±0.6
Umitoranoo	*Sargassum thunbergii*	188	8.147	1.364	22.6±2.1
Nebarimo	*Leathesia difformis*	6	0.233	0.025	17.4±3.6
Makonbu	*Saccharina japonica*	68	4.281	0.737	13.6±1.1
Tororokonbu	*Saccharina gyrata*	37	1.336	0.356	9.4±0.6
[Rhodophyceae]					
Makusa	*Gelidium elegans*	315	11.057	2.651	35.6±2.7
Akaba	*Neodilsea yendoana*	1470	49.080	14.351	15.9±1.2
Fukurofunori	*Gloiopeltis furcata*	383	9.338	1.350	8.2±0.6
Tsunomata	*Chondrus ocellatus*	7	0.439	0.113	3.9±1.6
Hirakotoji	*Chondrus pinnulatus*	213	12.360	2.420	11.4±0.4
Kurohaginnanso	*Chondrus yndoi*	8	0.185	0.028	7.6±2.6
Akabaginnanso	*Mazzaella japonica*	40	1.178	0.192	12.8±2.2
Karekigusa	*Tichocarpus crinitus*	625	32.700	7.540	14.4±3.6
Kushibenihiba	*Ptilota filicina*	6	0.517	0.040	16.7±1.5
Fujimatsumo	*Neorhodomela aculeata*	1400	36.598	13.420	88.2±1.1
Hakesakinokogirihiba	*Odonthalia corymbifera*	692	30.960	10.430	91.1±1.5

[a]Final sample concentration 100 μg/ml.

[b]Mean±standard error (n=3).

Table 1-7. Screening of algae collected at Oshoro area, Otaru in June, 2016.

Specimen Name	Scientific Name	Air Dried Weight (g)	1st Extract Wt. (g)	2nd Extract Wt. (g)	DPPH Radical Scavenging (%)[a,b]
[Chlorophyceae]					
Anaaosa	*Ulva pertusa*	9	0.328	0.075	9.1±1.7
Sujiaonori	*Ulva prolifera*	503	5.280	2.276	6.2±0.4
Tamajuzumo	*Chaetomorpha moniligera*	6	0.502	0.102	25.7±1.8
[Phaeophyceae]					
Ezoyahazu	*Dictyopteris divaricata*	730	31.546	7.119	5.8±2.1
Tsurumo	*Chorda asiatica*	599	18.220	3.480	20.5±1.9
Uganomoku	*Stephanocystis hakodatensis*	180	7.019	2.175	7.7±0.1
Hondawara	*Sargassum fulvellum*	1250	39.920	11.790	18.3±2.0
Fushisujimoku	*Sargassum confusum*	1040	38.470	7.680	27.1±1.6
[Rhodophyceae]					
Makusa	*Gelidium elegans*	293	8.430	1.505	23.4±1.6
Akaba	*Neodilsea yendoana*	1060	35.680	6.975	6.9±0.3
Marubatsunomata	*Chondrus nipponicus*	560	16.630	3.418	5.0±0.7
Hirakotoji	*Chondrus pinnulatus*	16	0.569	0.080	12.7±2.4
Haneigisu	*Ceramium japonicum*	66	9.391	2.640	19.5±0.9
Yuna	*Chondria crassicaulis*	49	6.128	1.112	9.6±2.3
Urasozo	*Laurencia nipponica*	840	18.910	3.190	36.2±0.6
Mitsudesozo	*Laurencia okamurae*	385	0.988	0.072	28.8±2.2
Fujimatsumo	*Neorhodomela aculeata*	122	1.114	0.253	89.7±1.1
Isomurasaki	*Symphyocladia latiuscula*	28	9.980	1.567	79.4±2.1

[a]Final sample concentration 100 μg/ml.

[b]Mean±standard error (n=3).

Table 1-8. Screening of algae collected at Nemuro, in July, 2016.

Specimen Name	Scientific Name	Air Dried Wt. (g)	1st Extract Wt. (g)	2nd Extract Wt. (g)	DPPH Radical Scavenging (%)[a,b]
[Chlorophyceae]					
Anaaosa	*Ulva pertusa*	39	2.400	0.520	15.9±0.3
Tsuyanashishiogusa	*Cladophora opaca*	72	7.930	3.340	17.0±0.1
[Phaeophyceae]					
Nagamatsumo	*Chordaria flagelliformis*	207	3.500	0.401	5.4±1.9
Ezofukuro	*Coilodesme japonica*	66	8.280	2.830	10.5±0.5
Aname	*Agarum clathratum*	1150	35.834	5.244	30.5±1.8
Hibamata	*Fucus distichus* subsp. *evanescens*	2170	109.958	29.404	28.1±0.4
Nebutomoku	*Stephanocystis crassipes*	4	1.000	0.252	20.5±1.7
[Rhodophyceae]					
Darusu	*Palmaria palmata*	240	6.671	1.275	8.6±2.1
Umizoumen	*Nemalion vermiculare*	124	2.367	0.716	3.3±1.4
Akabaginnanso	*Mazzaella japonica*	85	1.724	0.204	13.2±2.5
Karekigusa	*Tichocarpus crinitus*	1830	55.420	28.153	18.7±0.8
Katababenihiba	*Neoptilota asplenioides*	5	0.220	0.036	21.2±1.1
Kushibenihiba	*Ptilota filicina*	790	13.044	4.789	17.5±0.6
Isomurasaki	*Symphyocladia latiuscula*	23	1.171	0.240	73.4±1.3

[a]Final sample concentration 100 μg/ml.

[b]Mean±standard error (n=3).

Table 1-9. Screening of algae collected at Usujiri area, Hakodate in April, 2017.

Specimen Name	Scientific Name	Air Dried Wt. (g)	1st Extract Wt. (g)	2nd Extract Wt. (g)	DPPH Radical Scavenging (%)[a,b]
[Chlorophyceae]					
Anaaosa	*Ulva pertusa*	22	0.674	0.096	5.1±1.1
[Phaeophyceae]					
Matsumo	*Analipus japonicus*	92	1.914	1.868	3.2±0.5
Watamo	*Colpomenia bullosa*	1512	27.907	7.817	14.7±1.6
Kayamonori	*Scytosiphon lomentaria*	1526	41.588	11.778	6.2±0.2
Chigaiso	*Alaria crassifolia*	667	13.705	6.190	21.1±1.7
Fushisujimoku	*Sargassum confusum*	1490	3.298	0.6369	32.1±2.5
Umitoranoo	*Sargassum thunbergii*	989	36.570	9.290	33.3±0.6
[Rhodophyceae]					
Akaba	*Neodilsea yendoanna*	229	4.314	3.308	4.6±0.7
Matsunori	*Polyopes affinis*	25	2.338	0.634	3.2±1.1
Egonori	*Campylaephora hypnaeoides*	127	3.386	0.613	20.7±2.6
Kushibenihiba	*Ptilota filicina*	5	0.206	0.042	16.2±1.4
Fujimatsumo	*Neorhodomela aculeata*	1948	39.340	32.170	69.7±3.1
Hakesakinokogirihiba	*Odonthalia corymbifera*	108	5.140	0.500	88.4±0.9
Hosobafujimatsumo	*Rhodomela teres*	272	14.930	3.440	72.5±3.6

[a]Final sample concentration 100 μg/ml.

[b]Mean±standard error (n=3).

Table 1-10. Screening of algae collected at Nemuro, in May, 2017.

Specimen Name	Scientific Name	Air Dried Wt. (g)	1st Extract Wt. (g)	2nd Extract Wt. (g)	DPPH Radical Scavenging (%)[a,b]
[Chlorophyceae]					
Ezomiru	*Codium yezoense*	211	0.253	0.134	8.2±0.8
[Phaeophyceae]					
Keurushigusa	*Desmarestia viridis*	397	0.193	0.034	7.9±4.1
Aname	*Agarum clathratum*	1054	16.970	3.772	50.1±4.3
Sujime	*Costaria costata*	112	0.324	0.102	25.1±0.9
Hibamata	*Fucus distichus* subsp. *evanescens*	4708	0.995	0.288	31.3±1.6
Nebutomoku	*Stephanocystis crassipes*	1700	0.396	0.194	27.6±5.1
[Rhodophyceae]					
Benifukuronori	*Halosaccion yendoi*	489	8.286	1.361	17.3±1.4
Darusu	*Palmaria palmata*	302	5.805	0.963	9.5±2.5
Akabaginnansou	*Mazzaella japonica*	487	4.778	0.909	6.5±1.4
Kushibenihiba	*Ptilota filicina*	106	1.580	0.271	16.1±5.3
Fujimatsumo	*Neorhodomela aculeata*	334	6.449	1.246	78.9±1.6
Hakesakinokogirihiba	*Odonthalia corymbifera*	100	2.727	0.388	93.5±2.7

[a]Final sample concentration 100 μg/ml.

[b]Mean±standard error (n=3).

Table 1-11. Screening of algae collected at Usujiri area, Hakodate in June, 2017.

Specimen Name	Scientific Name	Air Dried Wt. (g)	1st Extract Wt. (g)	2nd Extract Wt. (g)	DPPH Radical Scavenging (%)[a,b]
[Phaeophyceae]					
Kayamonori	*Scytosiphon lomentaria*	152	0.778	0.080	18.6±1.2
Fushisujimoku	*Sargassum confusum*	38	1.086	0.262	35.8±1.4
Umitoranoo	*Sargassum thunbergii*	42	1.866	0.326	28.4±3.1
[Rhodophyceae]					
Makusa	*Gelidium elegans*	6.2	0.543	0.213	21.1±0.6
Akaba	*Neodilsea yendoana*	128	7.075	1.824	4.8±2.3
Igisu	*Ceramium kondoi*	6	0.751	0.104	5.1±0.8
Urasozo	*Laurencia nipponica*	56	16.740	1.690	20.7±0.4
Fujimatsumo	*Neorhodomela aculeata*	156	31.132	11.036	75.8±2.5
Hakesakinokogirihiba	*Odonthalia corymbifera*	91	5.602	1.522	95.1±1.8
Isomurasaki	*Symphyocladia latiuscula*	6	0.510	0.189	75.5±1.9

[a]Final sample concentration 100 μg/ml.

[b]Mean±standard error (n=3).

1.2.5. Isolation and Purification of Novel Compounds R1 and R2.

The red alga *Odonthalia corymbifera* (1832 g, air dried weight) was collected twice (early and late) in May, 2016 at Usujiri area, Hakodate. Both MeOH extracts were combined and partitioned into *n*-hexane, ethyl acetate (EtOAc), *n*-butanol and water-soluble fractions (Table 1-2-5-1, Figure 1-2-5-1). The EtOAc-soluble fraction (19.5 g) was chromatographed over silica gel, eluted with gradient of increasing methanol (0-100%) in chloroform to get eleven fractions (Fr 1-11) (Table 1-2-5-2, Figures 1-2-5-2a & 1-2-5-2b). Factions were examined for DPPH radical scavenging activity for assay-guided purification. Fraction 6 was subjected to RP column chromatography using 70% aqueous methanol as eluent to obtain eleven fractions 6.1-6.11 (Table 1-2-5-3, Figure 1-2-5-3). Fractions 6.4-6.6 were combined and further fractionated by Sephadex LH-20 (eluent, 70% MeOH) (Table 1-2-5-4, Figure 1-2-5-4) and purified on preparative TLC developed with toluene:ethyl acetate:acetic acid (10:10:1, v/v/v) (Table 1-2-5-5). The final purification was performed by RP HPLC using 70% aqueous methanol as mobile phase to yield compound **R1** (6.5 mg) (Figures 1-2-5-5 & 1-2-5-6).

Fraction 6.8 was purified again by Sephadex LH-20 (eluent, 70% MeOH) (Table 1-2-5-6, Figure 1-2-5-7) and preparative TLC (toluene:ethyl acetate:acetic acid; 10:10:1, v/v/v) (Table 1-2-5-7). The finally purified compound **R2** (2.8 mg) was obtained after RP HPLC using 70% aqueous methanol as eluent (Figures 1-2-5-8 & 1-2-5-9).

Table 1-2-5-1. Yields and radical scavenging activity after organic solvent partitioning of *Odonthalia corymbifera*.

Solvent Partitioning Fraction	Yield (g)	DPPH Radical Scavenging (%)[a,b]
n-Hexane	1.5	76.6±0.7
Ethylacetate	19.5	91.4±0.1
n-Butanol	12.4	34.8 ±1.1
Water	60.9	NA[c]

[a]Sample concentration 50 μg/ml.

[b]Mean±standard error (n=3).

[c]No Activity.

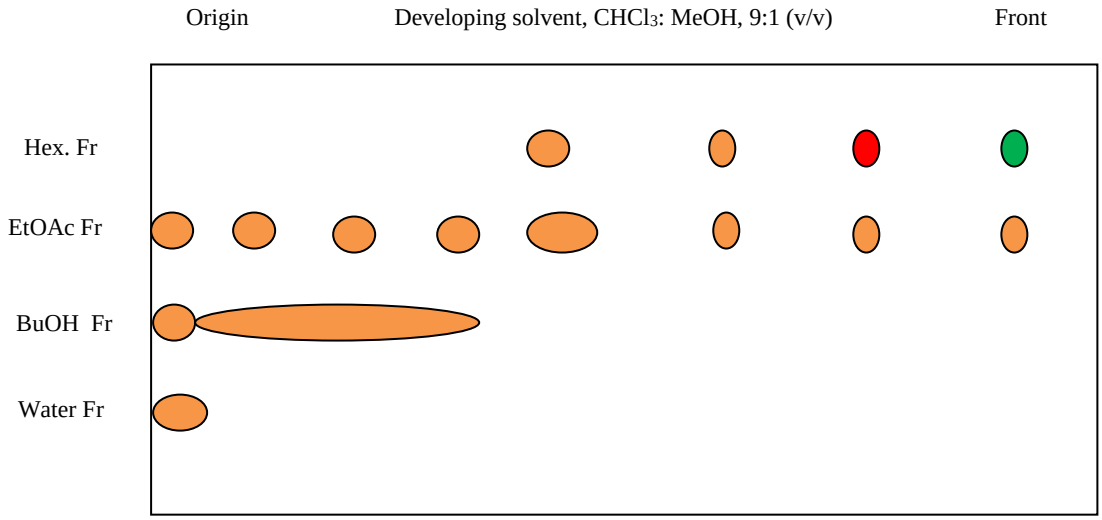

Figure 1-2-5-1. TLC chromatogram after solvent partitioning of *O. corymbifera*. Spots were visualized after spraying with 5% H_2SO_4.

Table 1-2-5-2. DPPH radical scavenging activity of individual fractions obtained after silica gel column chromatography[a] of the EtOAc-soluble fraction of *O. corymbifera*.

Fraction	Eluent (v/v)	Yield (mg)	DPPH Radical Scavenging (%)[b,c]
1	$CHCl_3$(100)	0.0	NE[d]
2	$CHCl_3$(100)	0.0	NE
3	$CHCl_3$: MeOH (90:10)	280	30.2±0.7
4	$CHCl_3$: MeOH (90:10)	5300	89.7±0.5
5	$CHCl_3$: MeOH (80:20)	6440	91.8±0.6
6	$CHCl_3$: MeOH (80:20)	1900	93.2±0.4
7	$CHCl_3$: MeOH (70:30)	1080	94.1±0.6
8	$CHCl_3$: MeOH (70:30)	730	92.8±0.3
9	$CHCl_3$: MeOH (50:50)	610	90.6±0.7
10	$CHCl_3$: MeOH (50:50)	680	89.6±0.6
11	$CHCl_3$: MeOH (0:100)	520	87.6±0.7

[a]Column size ϕ 4.2 × 37 cm. Each fraction contains 500 ml eluent.

[b]Final sample concentration 50 μg/ml.

[c]Mean±standard error (n=3).

[d]Not Examined.

Table 1-2-5-3. DPPH radical scavenging activity of individual fractions obtained from reverse phase column chromatography[a] of fraction 6.

Fraction	Eluent (v/v)	Yield (mg)	DPPH Radical Scavenging (%)[b,c]
6.1	Acetone:water (30:70)	0.0	NE[d]
6.2	Acetone:water (30:70)	430	20.8±6.3
6.3	Acetone:water (40:60)	254	62.7±3.7
6.4	Acetone:water (40:60)	150	86.7±0.6
6.5	Acetone:water (50:50)	95	88.5±0.4
6.6	Acetone:water (50:50)	99	93.9±0.3
6.7	Acetone:water (60:40)	1000	89.4±0.8
6.8	Acetone:water (60:40)	200	85.4±0.7
6.9	Acetone:water (70:30)	130	65.7±0.9
6.10	Acetone:water (70:30)	125	59.4±1.6
6.11	Acetone:water (100:0)	109	53.2±1.2

[a]Column size ϕ 3.0 × 21 cm. Each fraction contains 150 ml eluent.

[b]Final sample concentration 25 μg/ml.

[c]Mean±standard error (n=3).

[d]Not Examined.

Table 1-2-5-4. DPPH radical scavenging activity of fractions obtained from Sephadex LH-20 chromatography of combined fractions 6.4-6.6.[a]

Fraction	Tube No.	Yield (mg)	DPPH Radical Scavenging (%)[b,c]
6.4.1	1-7	18	62.7±7.9
6.4.2	8-10	25	89.9±0.4
6.4.3	11-25	52	87.5±1.1
6.4.4	26-37	55	93.6±0.3
6.4.5	38-45	26	93.9±2.3
6.4.6	46-50	10	88.2±0.9

[a]Column size ϕ 1.0 × 23 cm. 70% MeOH as eluent. Each tube contains 8 ml eluent.

[b]Final sample concentration 25 μg/ml.; [c]Mean±standard error (n=3).

Table 1-2-5-5. DPPH radical scavenging activity of fractions obtained after PLC of fraction 6.4.2.[a]

Fraction	R_f Value	Yield (mg)	DPPH Radical Scavenging (%)[b,c]
6.4.2.1 (**R1**)	0.3	9	49.9±0.0
6.4.2.2	0.2	5	26.4±5.1

[a]Developing solvent, toluene:EtOAc:acetic acid, 10:10:1 (v/v/v).

[b]Final sample concentration 10 μg/ml.

[c]Mean±standard error (n=3).

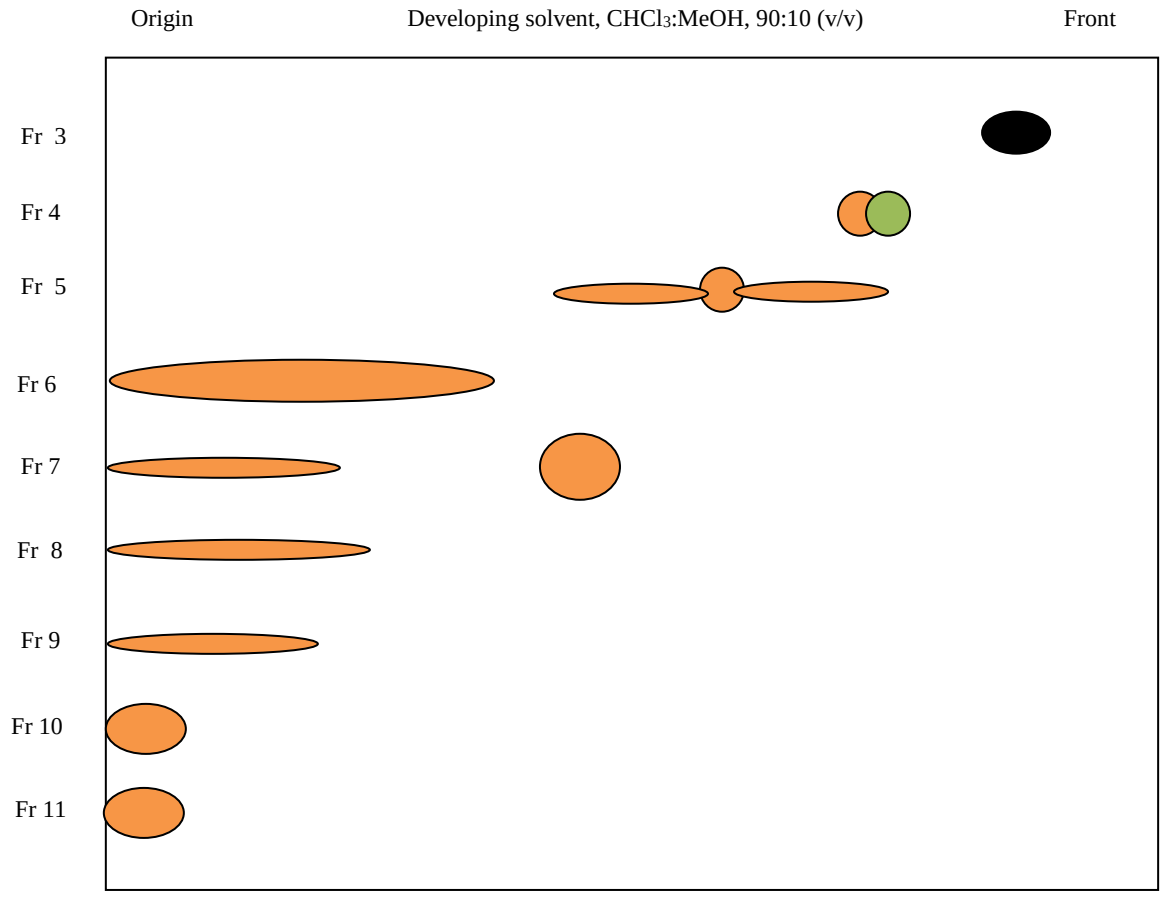

Figure 1-2-5-2a. TLC chromatogram of individual fractions obtained after silica gel column chromatography of EtOAc-soluble fraction. Spots were visualized after spraying with 5% H_2SO_4.

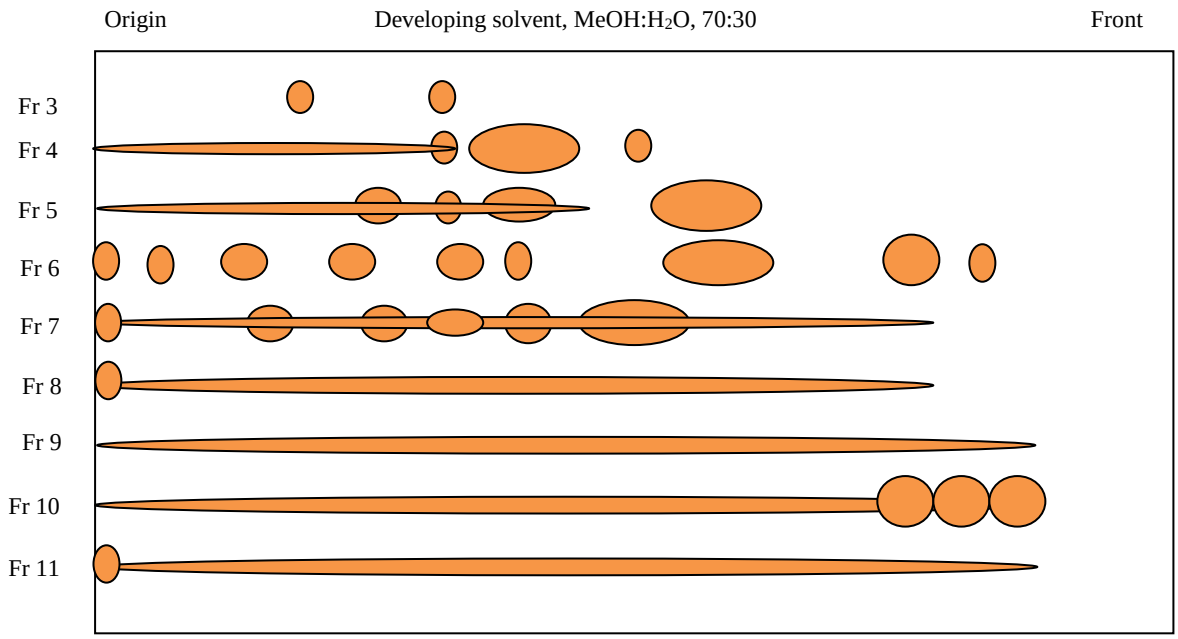

Figure 1-2-5-2b. RP-TLC chromatogram of individual fractions obtained after silica gel column chromatography of EtOAc soluble fraction. Spots were visualized after spraying with 5% H_2SO_4.

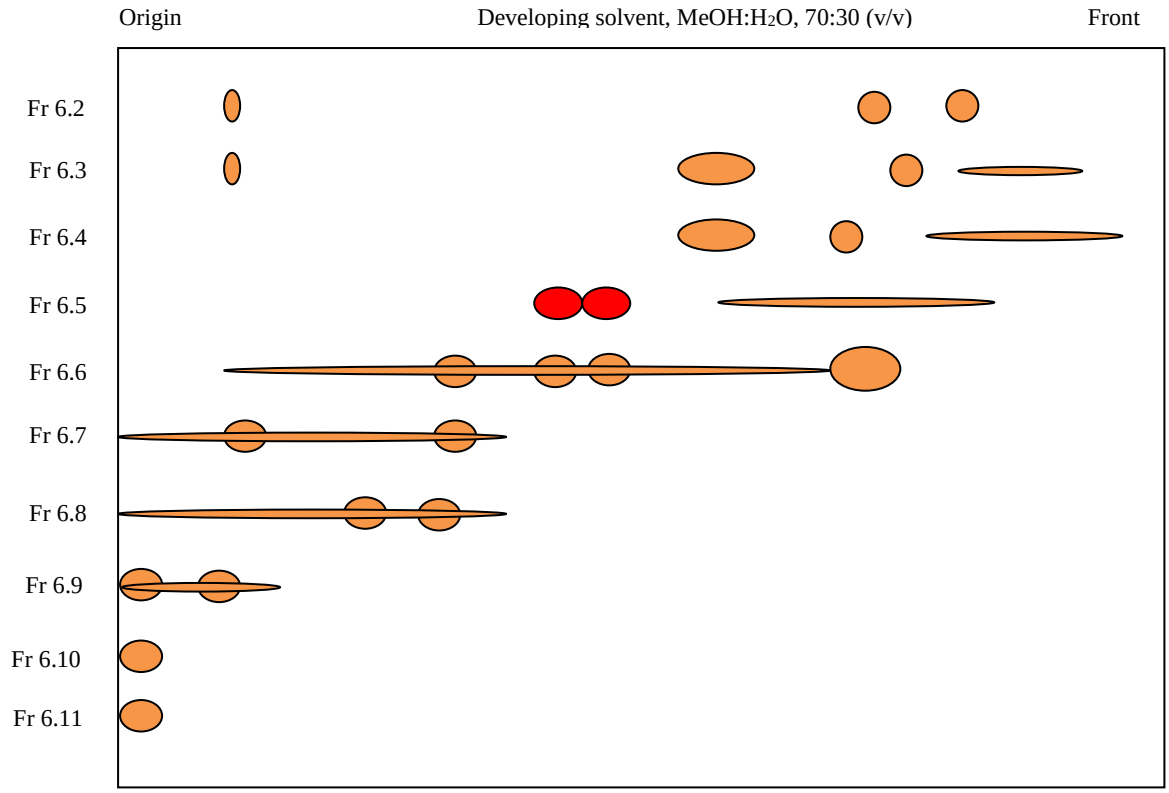

Figure 1-2-5-3. RP-TLC chromatogram of individual fractions obtained after reverse phase column chromatography of Fr 6. Spots were visualized after spraying with 5% H_2SO_4.

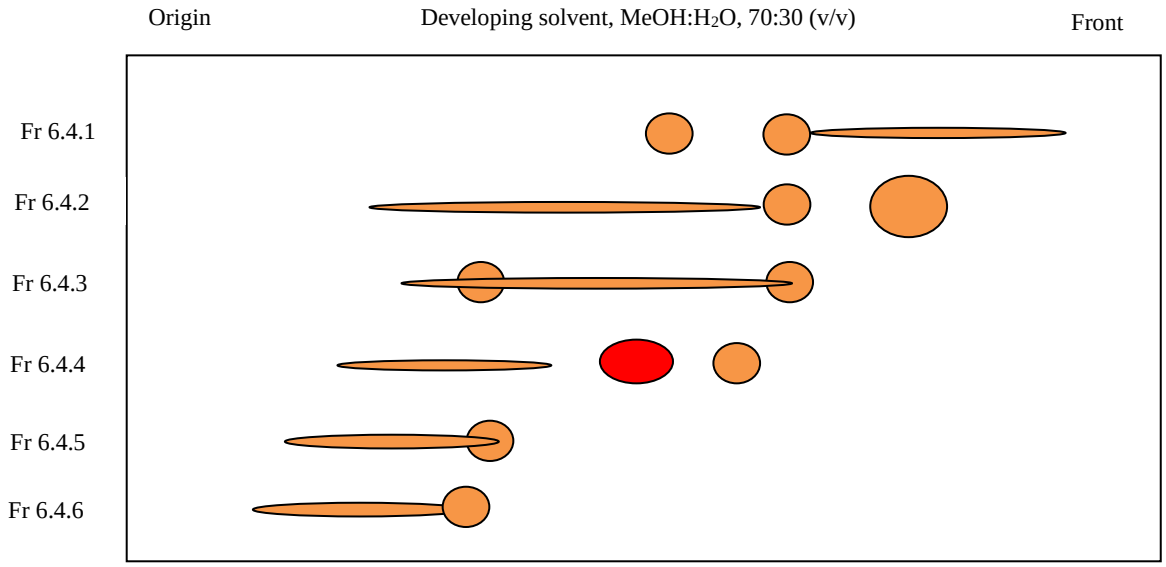

Figure 1-2-5-4. RP-TLC chromatogram of fractions obtained after Sephadex LH-20 chromatography of combined fractions 6.4-6.6. Spots were visualized after spraying with 5% H_2SO_4.

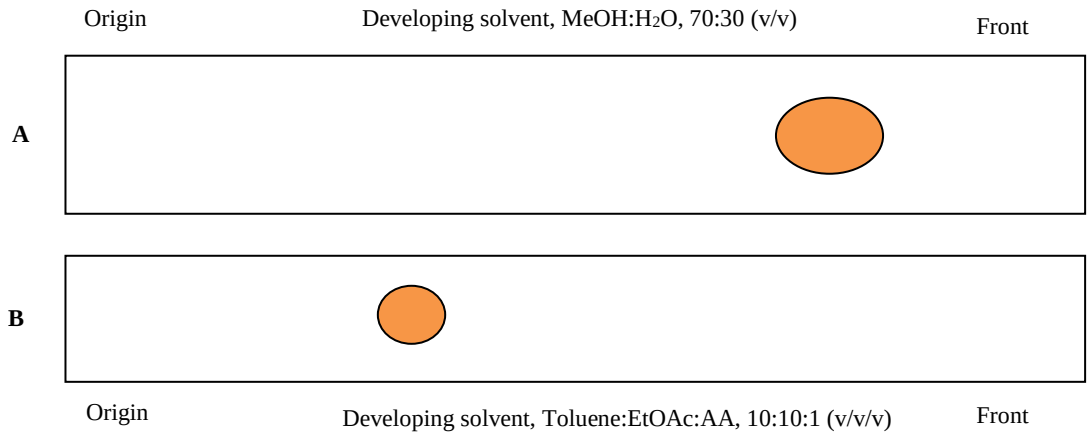

Figure 1-2-5-5. **A**. RP-TLC and **B**. NP-TLC chromatogram of compound **R1**. Spots were visualized after spraying with 5% H_2SO_4.

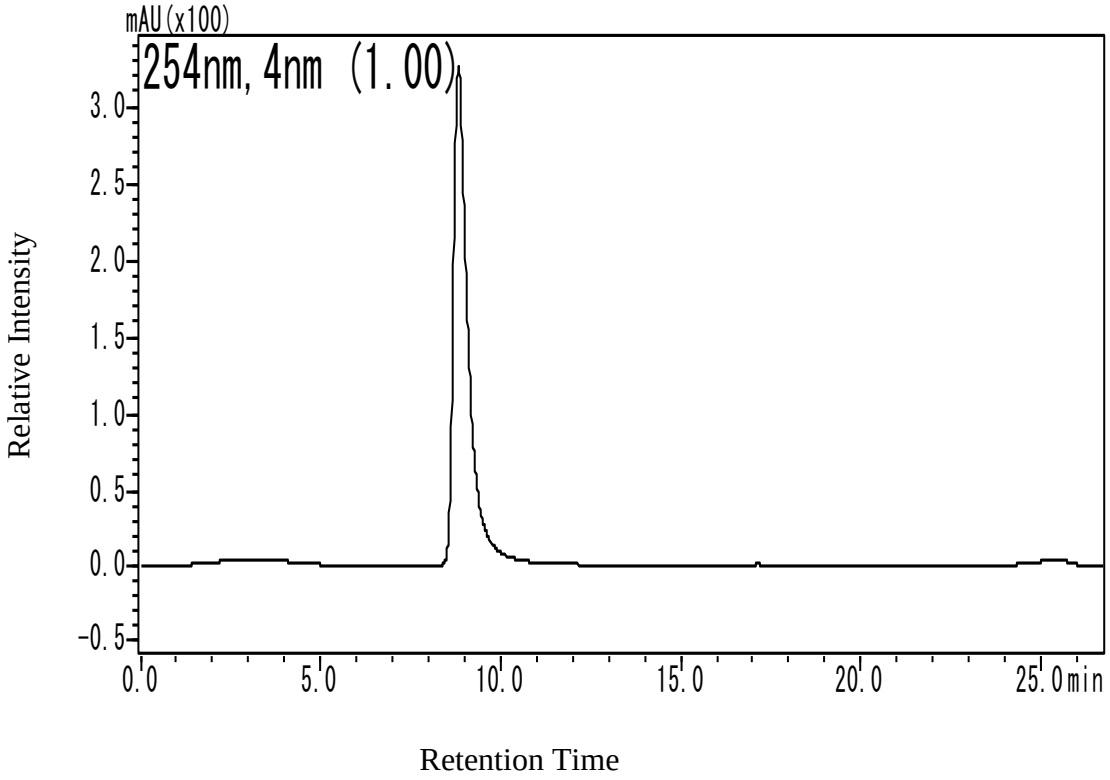

Figure 1-2-5-6. HPLC chromatogram of compound **R1**. Column: Mightysil RP-18 250-4.6 (5 μm); eluent: 70% aqueous MeOH; flow rate: 0.5 ml/min; detection: UV 254 nm.

Table 1-2-5-6. DPPH radical scavenging activity of fractions obtained from Sephadex LH-20 of fraction 6.8.[a]

Fraction	Tube No.	Yield (mg)	DPPH Radical Scavenging (%)[b,c]
6.8.1	1-10	7.5	66.1±1.0
6.8.2	11-15	6.8	86.7±0.4
6.8.3	16-25	3.4	91.3±0.8
6.8.4	26-32	5.1	71.1±2.9

[a]Column size ϕ 1.0 × 24 cm. 70% MeOH as eluent. Each tube contains 8 ml eluent.

[b]Final sample concentration 25 μg/ml.

[c]Mean±standard error (n=3).

Table 1-2-5-7. DPPH radical scavenging activity of a fraction obtained after PLC of fraction 6.8.1.[a]

Fraction	R_f Value	Yield (mg)	DPPH Radical Scavenging (%)[b,c]
6.8.1.1 (**R2**)	0.4	5.5	53.6±0.0

[a]Developing solvent, toluene:EtOAc:acetic acid, 10:10:1 (v/v/v).

[b]Final sample concentration 10 µg/ml.

[c]Mean±standard error (n=3).

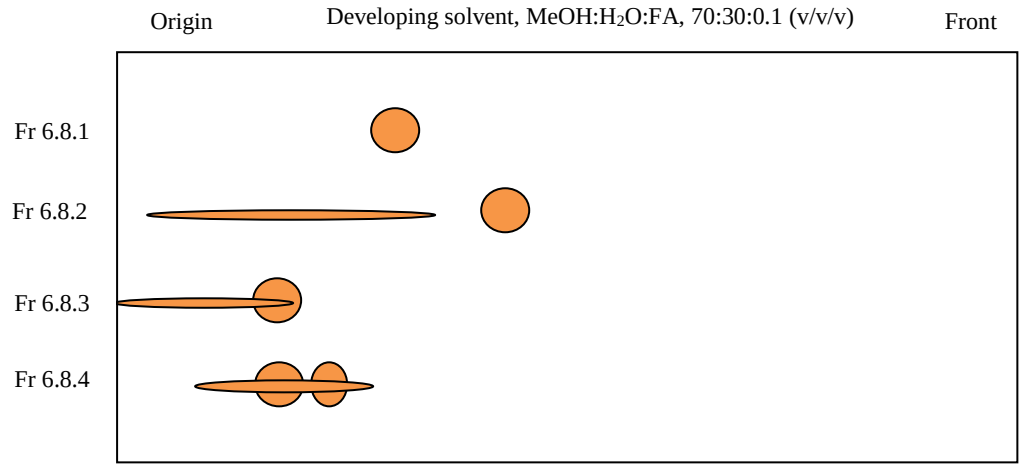

Figure 1-2-5-7. RP-TLC chromatogram of fractions obtained after Sephadex LH-20 chromatography of fraction 6.8. Spots were visualized after spraying with 5% H_2SO_4.

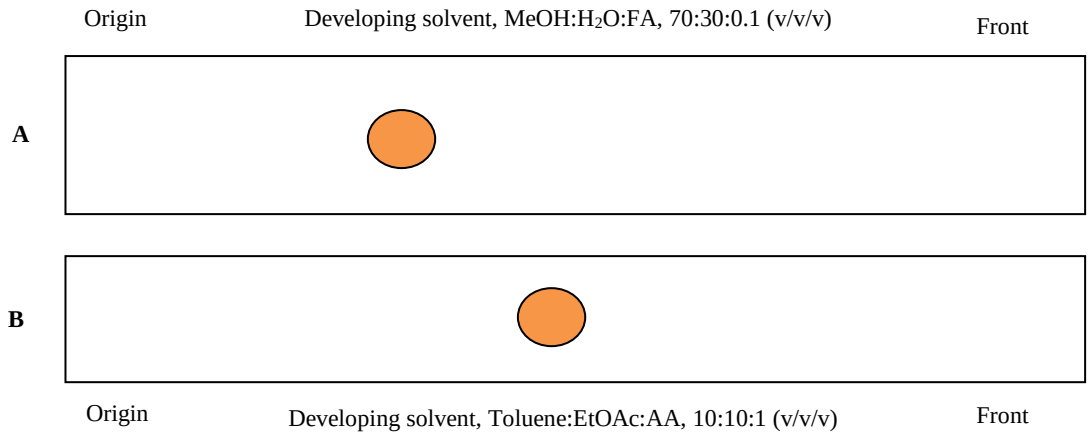

Figure 1-2-5-8. **A**. RP-TLC and **B**. NP-TLC chromatogram of compound **R2**. Spots were visualized after spraying with 5% H_2SO_4.

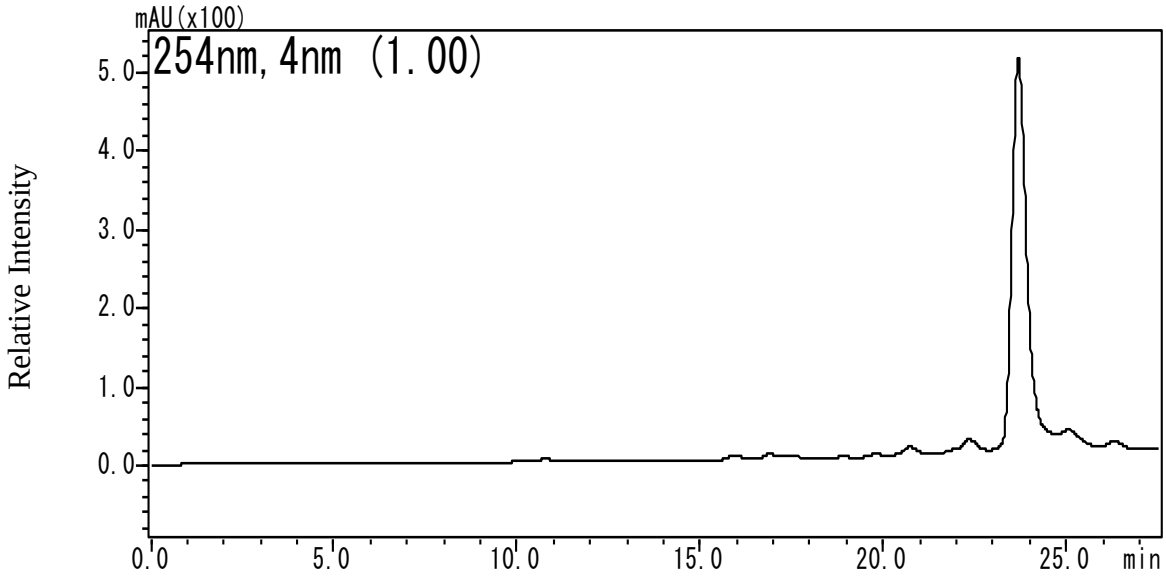

Figure 1-2-5-9. HPLC chromatogram of compound **R2**. Column: Mightysil RP-18 250-4.6 (5 μm); eluent: 70% aqueous MeOH; flow rate: 0.5 ml/min; detection: UV 254 nm.

1.3. Results and Discussion

1.3.1. Structural Elucidation of Novel Compound **R1**.

Appearance of compound **R1** was light brown amorphous solid. UV (MeOH) spectrum gave absorption maxima at λ_{max} (log ε) 212 (4.28), 230 sh (3.94), 290 (3.32) nm and it suggest the presence of catechol moiety from absorption at 290 nm absorbance (Figure 1-3-1-1). IR ($CHCl_3$) spectrum gave a C=O vibration peak at 1704 cm^{-1} (Figure 1-3-1-2). This peak suggested presence of ketonic group. Compound **R1** was determined as a dibrominated compound from molecular and isotopic ion peaks at *m/z* 404/406/408. Molecular formula was $C_{13}H_{10}Br_2O_5$ based on HRMS data. The ^{1}H NMR spectrum showed a conjugated olefinic proton at δ 7.10, an aromatic proton at δ 6.89, an equivalent methylene at δ 4.51, a non-equivalent methylene at δ 3.09/3.05, and a methine at δ 3.22 in acetone-d_6 (Table 1-3-1-1, Figures 1-3-1-3 to 1-3-1-7). The last methine proton signal was disappeared in methanol-d_4 (Figures 1-3-1-8 to 1-3-1-11). This phenomenon strongly suggested the methine proton was exchangeable. The ^{13}C NMR and HSQC spectrum revealed six aromatic, two ketonic, two olefinic, two methylenes, and one methine carbons. Among them, six aromatic and one methylene carbon are typical signals for the BHB unit (positions 1a to 7a). The methylene protons in BHB unit and a methine proton were correlated not only one another but also with both ketonic carbons in HMBC experiment (Figure 1-3-1-13). However, the olefinic and methylene protons were correlated with respective different ketonic carbons. Therefore, remaining structure other than the BHB unit was determined as 4-hydroxymethyl-4-cyclopenten-1,3-dion-2-yl moiety. Thus structure of compound **R1** named odonthadione was determined as shown in Figure 1-3-1-12. This compound does not optically active under specific rotation measurement $[\alpha]_D^{27}$ =0 (*c* 2.6, acetone). This reason is seemed that compound **R1** is racemic mixture because the hydrogen at 2-position in 1,3-diketone moiety was easily exchangeable in protic solvent like the case of ^{1}H NMR spectrum in methanol-d_4. The compound **R1** is a novel hybrid algal bromophenol (Figure 1-3-1-12), especially this is the first report on a naturally occurring cyclopentendione moiety.

There were few reports on isolation of hybrid bromophenols from the marine red algae *Rhodomela confervoides*, *Symphyocladia latiuscula* and *Osmundaria colensoi* [17, 43, 59, 60, 65, 66]. This research has successfully isolated a novel hybrid bromophenol (**R1**) from the red alga *Odonthalia corymbifera*. All the hybrid bromophenols consist of couplings between the BHB unit and electron-rich atoms (in nucleophiles) (Figure 1-3-1-14). These

couplings would be derived by bimolecular nucleophilic substitution (S_N2) reaction. Leaving group would be substituted at 7-position in the BHB unit. The other parts, α-carbons of carbonyl groups (in the case of **1**, **34**, **39** and **57**) and nitrogen atoms (in the case of **55**, **56**, **58** and **59**), are attacked to the 7-position of the BHB unit as nucleophiles. A part of bromophenol dimers have been speculated to be derived by nucleophilic substitution. The BHB unit possessing leaving group could play an important role in bromophenol dimer formation like hybrid formation.

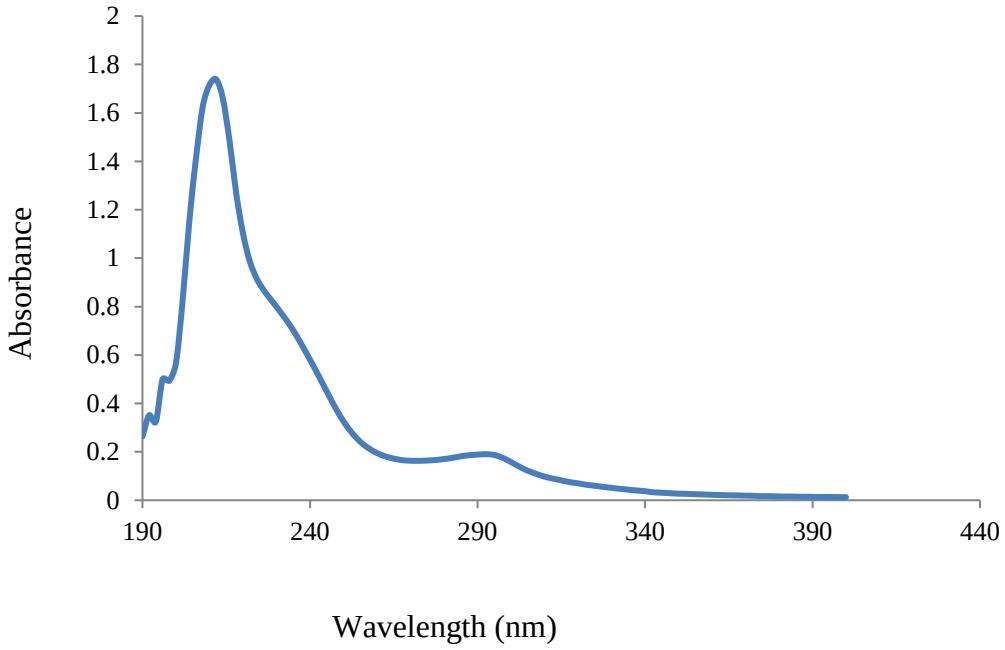

Figure 1-3-1-1. UV spectrum of compound **R1**.

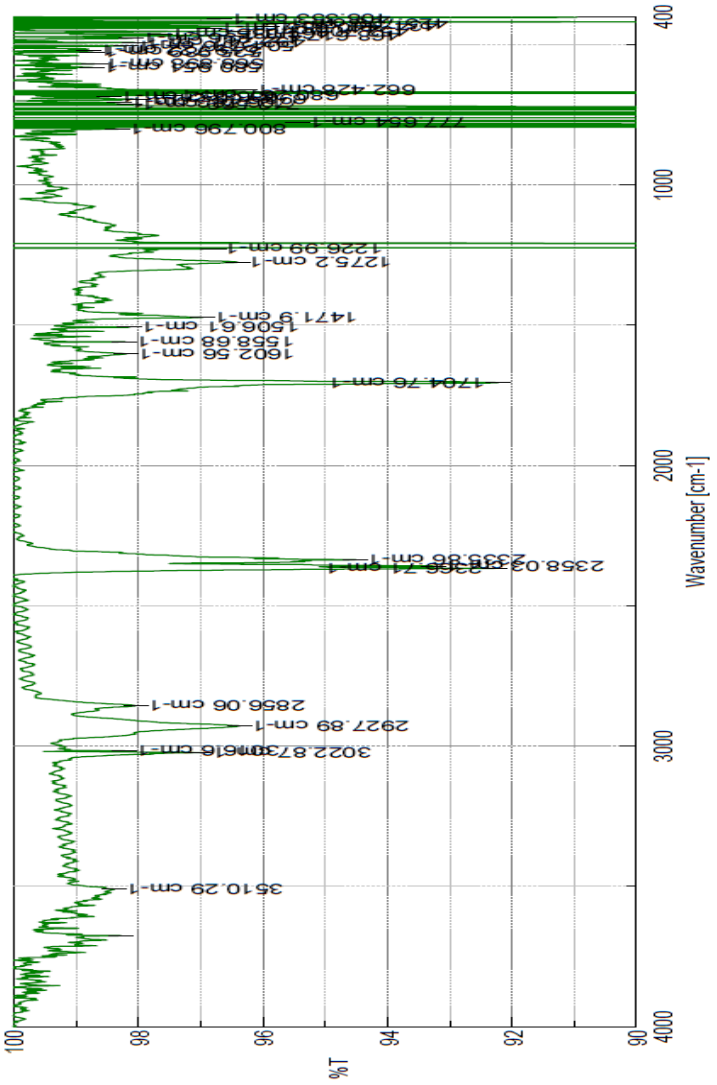

Figure 1-3-1-2. IR spectrum of compound **R1**.

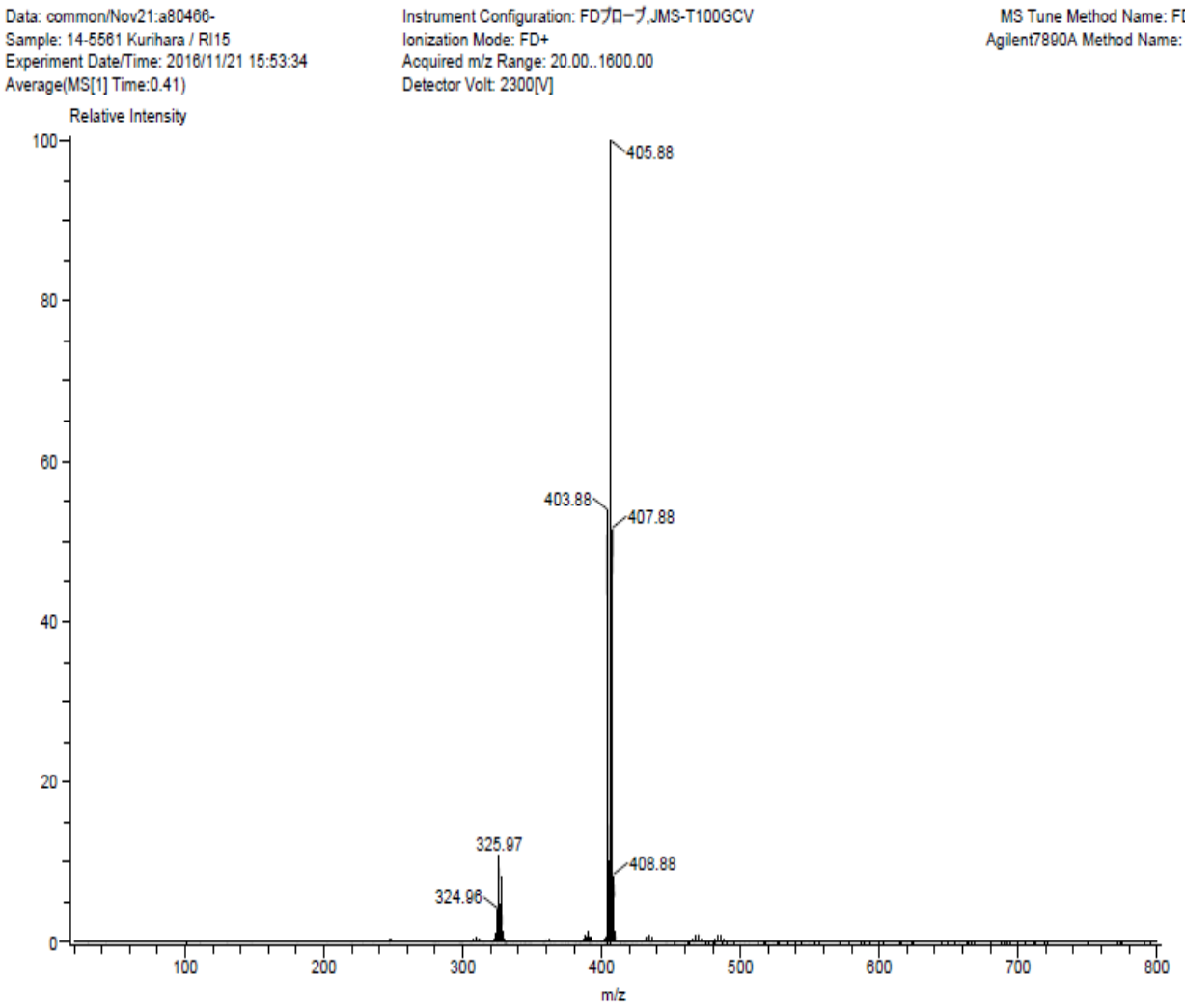

Figure 1-3-1-3. FD-MS spectrum of compound **R1**.

DU=/u, USER=agr, NAME=17an007, EXPNO=1, PROCNO=1
F1=18.295ppm, F2=-2.361ppm, MI=0.50cm, MAXI=10000.00cm, PC=3.000

#	ADDRESS [Hz]	FREQUENCY [PPM]	INTENSITY
1	17760.9	3547.572	7.0933	1.02
2	18304.8	3378.928	6.7561	1.51
3	21322.6	2427.531	4.8538	17.72
4	21913.5	2241.233	4.4813	1.99
5	23779.3	1653.030	3.3052	2.43
6	23784.1	1651.529	3.3022	4.02
7	23789.0	1649.979	3.2991	4.66
8	23793.9	1648.429	3.2960	3.20
9	24153.8	1534.949	3.0691	1.44
10	24164.2	1531.698	3.0626	1.38
11	25620.9	1072.429	2.1443	12.50

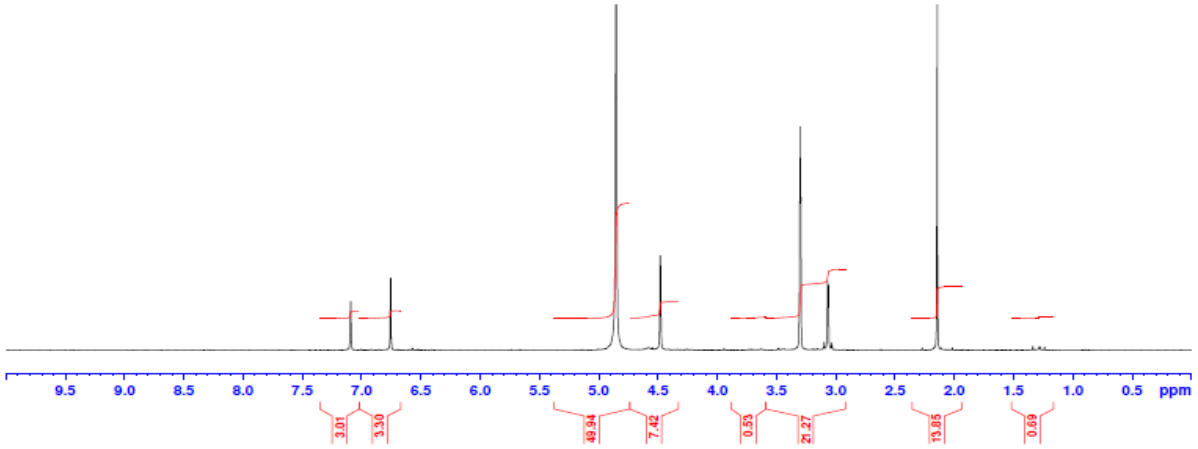

Figure 1-3-1-4. ^{1}H-NMR spectrum of compound **R1** (acetone-d_6, 500 MHz).

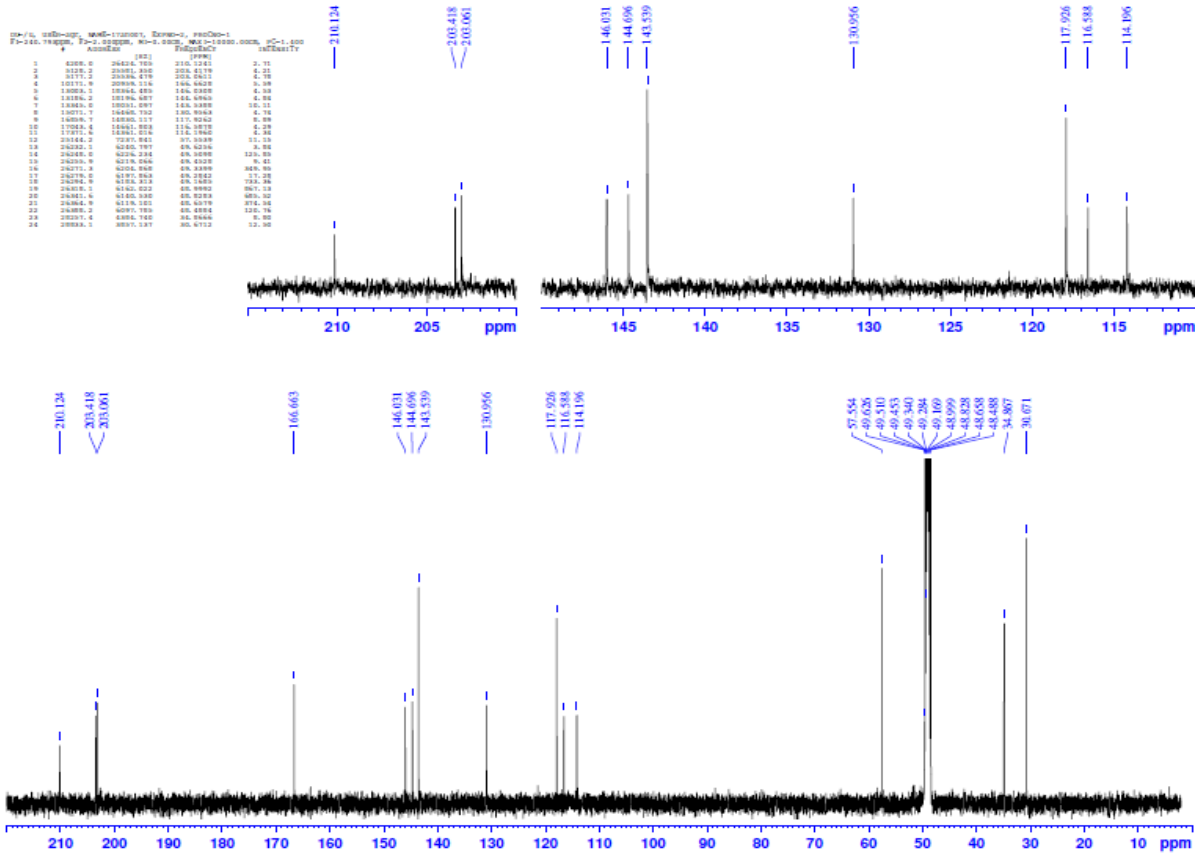

Figure 1-3-1-5. ^{13}C-NMR spectrum of compound **R1** (acetone-d_6, 125 MHz).

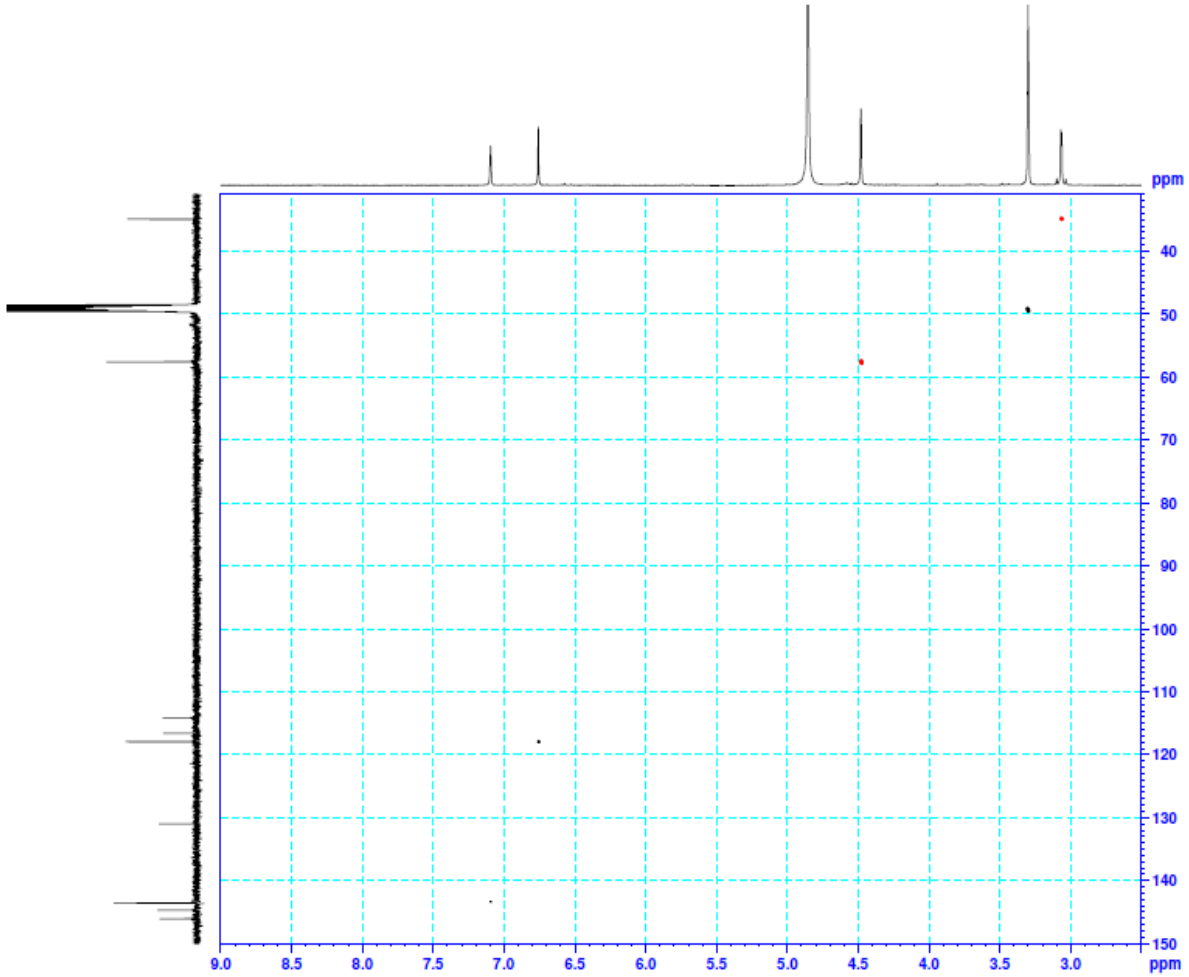

Figure 1-3-1-6. Editing HSQC spectrum of compound **R1** (acetone-d_6).

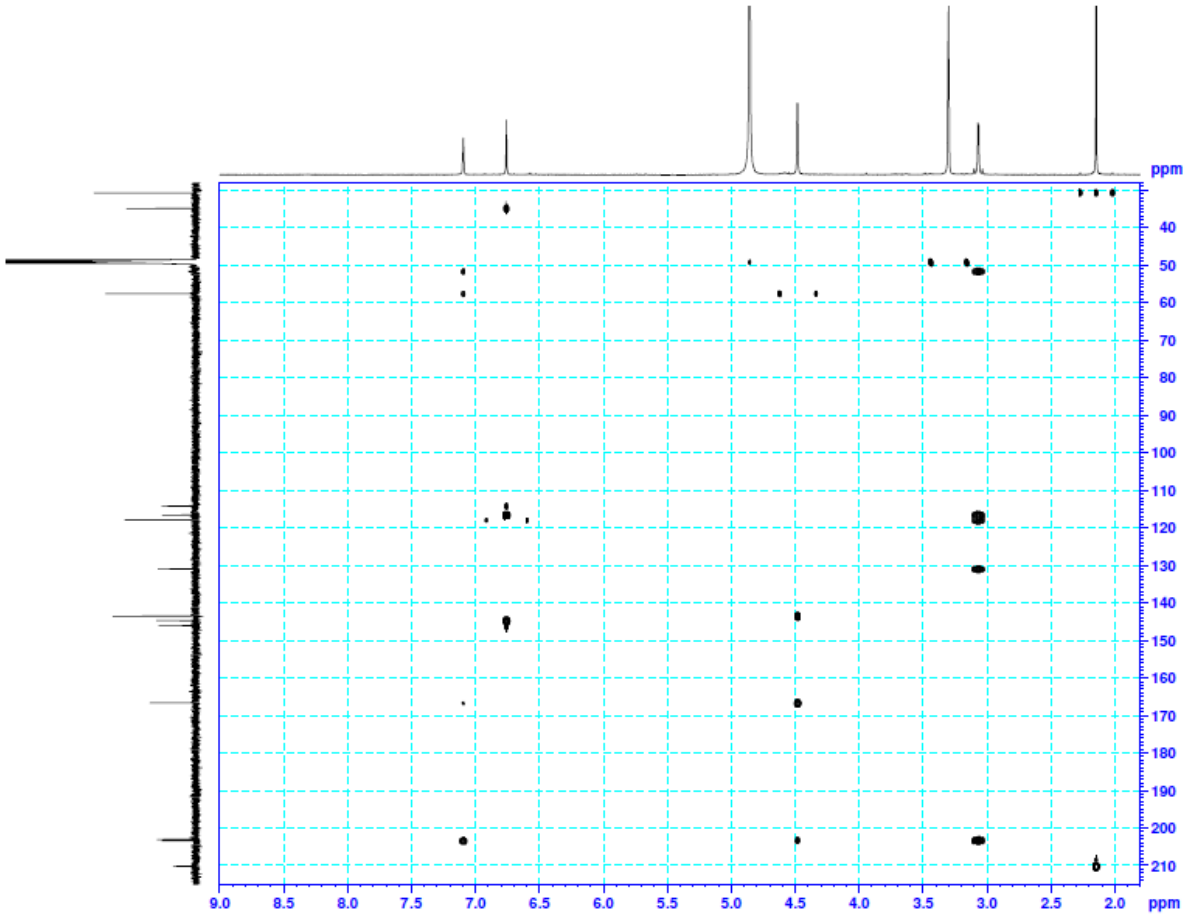

Figure 1-3-1-7. HMBC spectrum of compound **R1**.

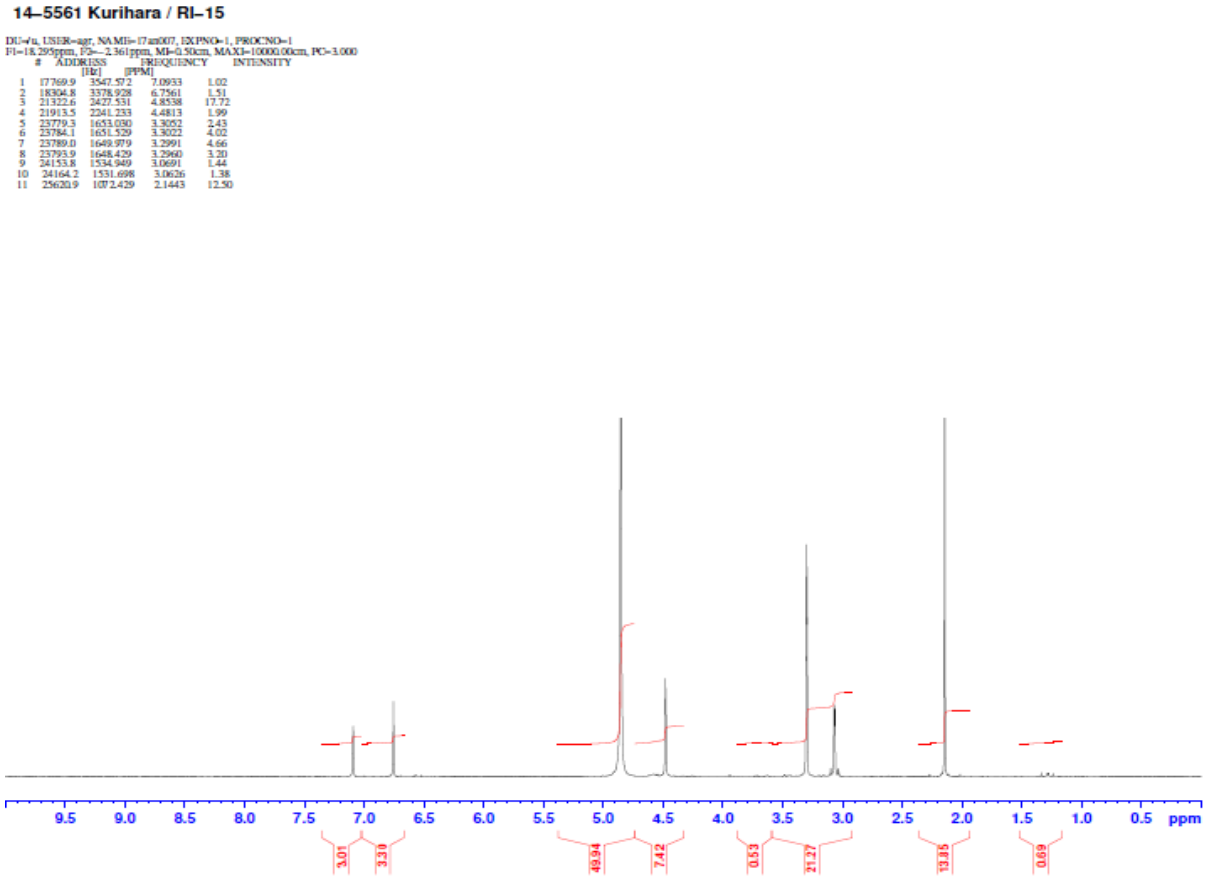

Figure 1-3-1-8. ^{1}H-NMR spectrum of compound **R1** (methanol-d_4 500 MHz).

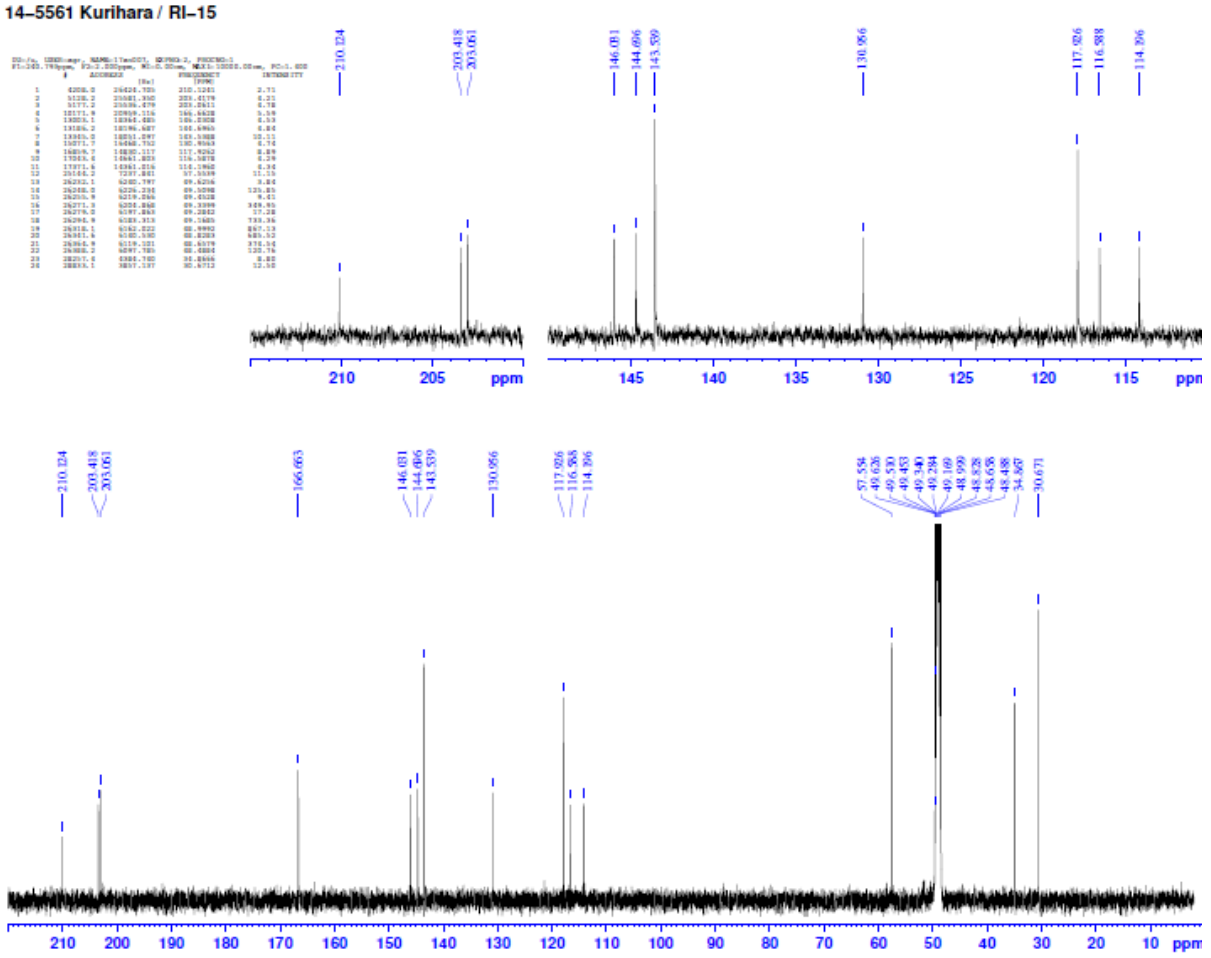

Figure 1-3-1-9. ^{13}C-NMR spectrum of compound **R1** (methanol-d_4 125 MHz).

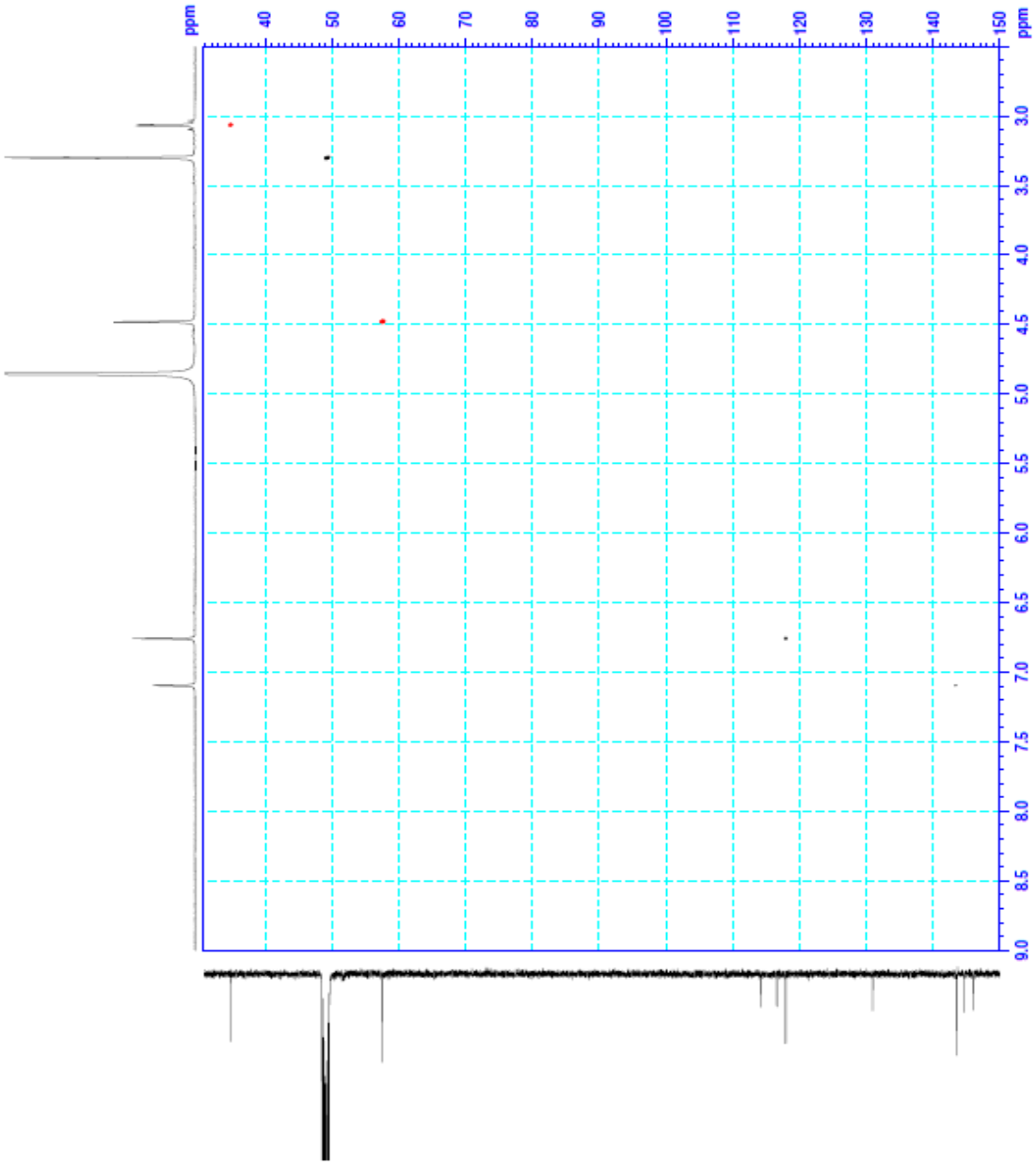

Figure 1-3-1-10. Editing HSQC spectrum of compound **R1**.

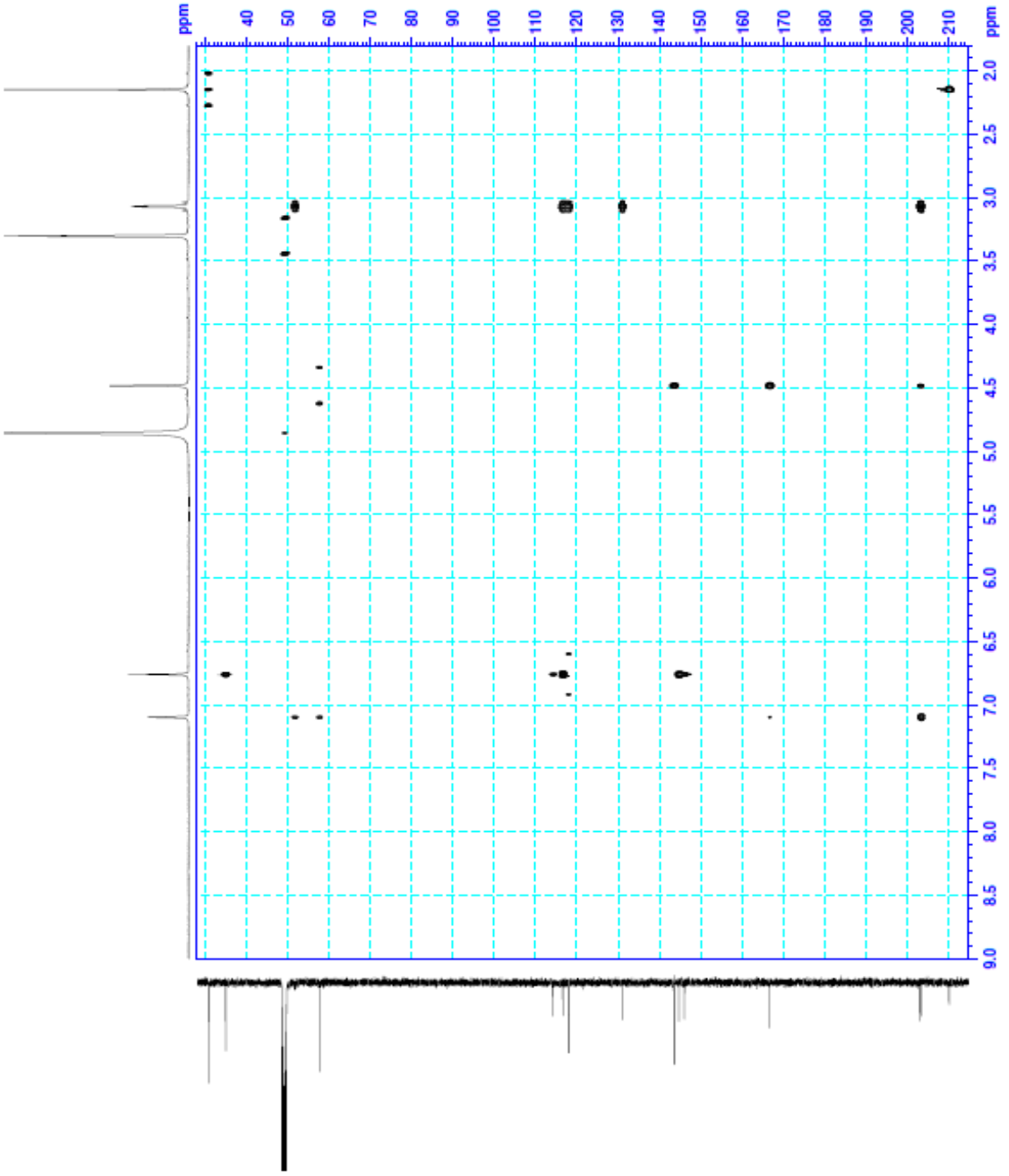

Figure 1-3-1-11. HMBC spectrum of compound **R1** (methanol-d_4).

Table 1-3-1-1. ^{1}H (500 MHz) and ^{13}C NMR (125 MHz) data of odonthadione (compound **R1**) in acetone-d_6 and methanol-d_4.

Position	δ_C in acetone-d_6	δ_H (J in Hz)	HMBC	δ_C in methanol-d_4	δ_H (J in Hz)
1a	131.1			131.0	
2a	116.4			116.6	
3a	113.6			114.2	
4a	144.1			144.7	
5a	145.2			146.0	
6a	118.0	6.89, s	2a, , 4a, 5a, 7a	117.9	6.76, s
7a	34.3	3.09, dd (14.6, 7.0)	1a, 2a, 6a, 1b, 2b,	34.9	3.07, dd (14.6, 7.0)
		3.05, dd (14.6, 7.0)	3b		3.06, dd (14.6, 7.0)
1b	201.6			203.4[a]	
2b	51.3	3.22, t (7.0)	1a, 7a, 1b, 3b	51.8	NO[b]
3b	202.6			203.6[a]	
4b	166.2			166.7	
5b	143.0	7.10, s	1b	143.5	7.09, s
6b	57.3	4.51, s	3b, 4b, 5b	57.6	4.48, s

[a]Exchangeable.

[b]Not observed.

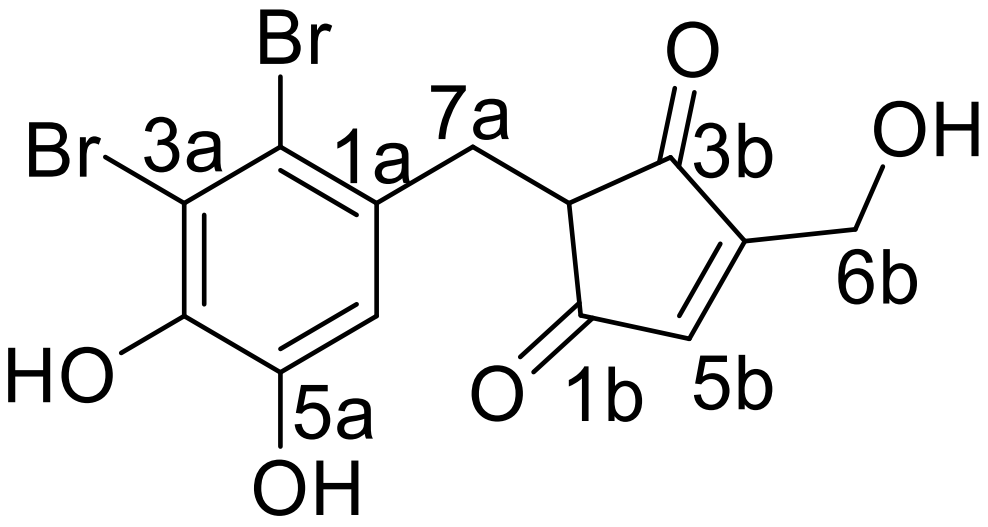

Figure 1-3-1-12. Structure of novel compound **R1**.

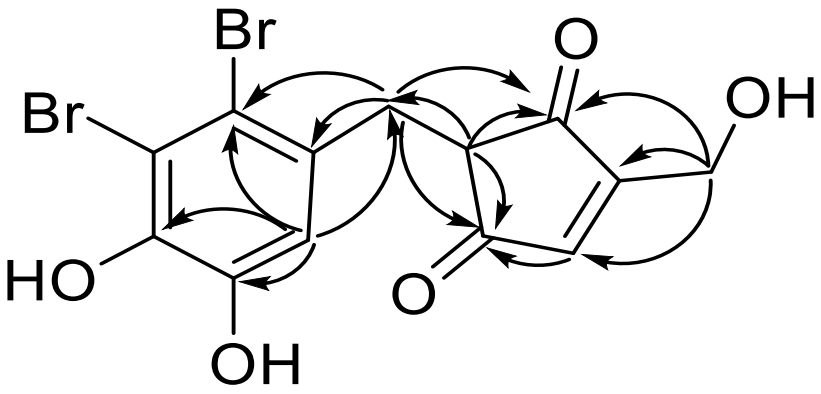

Figure 1-3-1-13. HMBC correlations of novel compound **R1**.

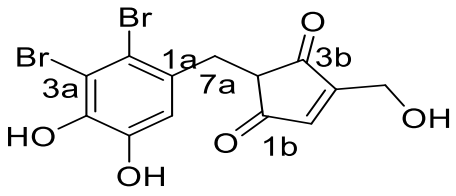

Odonthadione

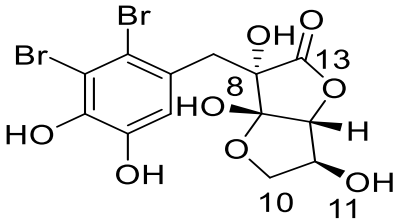

34

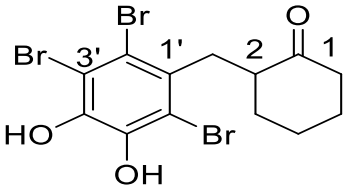

39

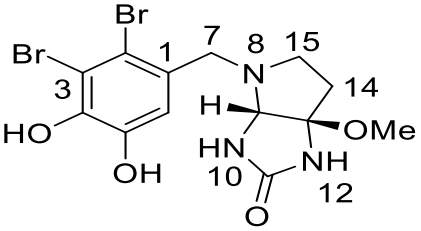

55

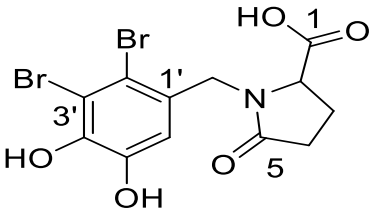

56

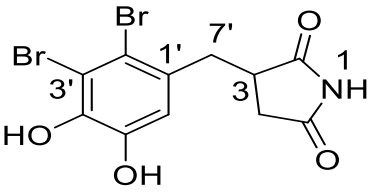

57

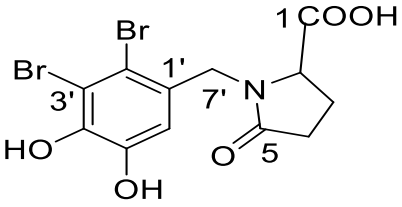

58

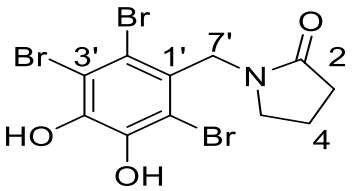

59

Figure 1-3-1-14. Structure of naturally occurring hybrid bromophenols.

1.3.2. Structural Elucidation of Novel Compound **R2**.

Appearance of compound **R2** was brown amorphous solid. UV (CH_3OH) spectrum gave absorption maxima at λ_{max} (log ε) 210 (4.57), 232 sh (4.00), 290 (3.57) nm and showed absorbance of catechol moiety like compound **R1** (Figure 1-3-2-1). IR ($CHCl_3$) spectrum gave a characteristic phenolic compounds peak (Figure 1-3-2-2). HRMS data of compound **R2** suggests to be a tetrabrominated compound from peak cluster of *m/z* at 740/742/744/746/748 and its molecular formula of $C_{23}H_{20}Br_4O_8$ (Figure 1-3-2-3). This molecular formula is evaluated as BHB unit trimer. The ^{1}H NMR spectrum (Table 1-3-2-1, Figure 1-3-2-4) showed three aromatic, two methylene, and two methoxy proton signals, along with a broad proton signal (δ_H 3.94). The ^{13}C NMR spectrum revealed eighteen aromatic, two methylene and two methoxy carbon signals (Table 1-3-2-1, Figure 1-3-2-5). These signals were characterized to be an oligomer of BHB units. One remaining carbon signal was not determined because no correlation was observed with the broad proton signal of low signal height in HSQC experiment. Unfortunately HMBC correlations of compound **R2** were limited within individual BHB units (Figures 1-3-2-6 & 1-3-2-7). Thus little information was observed for determination of connection among different units.

For increasing information of NMR signals, compound **R2** in methanol was quantitatively converted with trimethylsilyldiazomethane in hexane to pentamethyl ether (**R2-M**) at room temperature. Compound **R2-M** was appeared as pale yellow amorphous solid. Molecular ion peak of derivative **R2-M** increased 70 mass units compared to that of compound **R2** in HRFDMS (Figure 1-3-2-8). New five methoxy signals were appeared result enhancement of 70 mass in NMR spectra of **R2-M** (Table 1-3-2-1, Figures 1-3-2-9 to 1-3-2-13). These data suggested presence of five free phenolic hydroxy groups in compound **R2**. Therefore, one remaining oxygen atom would be used to form an ether linkage. The five methoxy groups were completely assigned to individual positions with consideration of HMBC and ROESY correlations (Figure 1-3-2-15). All other proton and carbon signals of derivative **R2-M** except for carbon signals C-3a, C-3b and C-3c were also assigned from the 2D NMR data. The three aromatic carbons signals at δ_C 122.7, 122.6, and 106.5, showing no correlation with the three aromatic proton signals in the HMBC experiment, are assigned to be the brominated aromatic carbons at *para*-positions (3a, 3b and 3c) of aromatic protons from their ^{13}C NMR chemical shifts. Thus the remaining four aromatic carbons at the positions 2a, 2b, 7b, and 4c are suggested to connect among the three BHB units. Their carbon chemical shifts lead to determine combinations of connectivity, that is to say,

alkylated aromatic C-2a (δ_C 129.1) is directly connected with alkylated aromatic C-1b (δ_C 130.5) via a methylene bridge at C-7b (δ_C 32.9). On the other hand, oxygenated aromatic C-2b (δ_C 142.6) is connected with oxygenated aromatic C-4c (δ_C 151.1) via an ether bridge. Thus structures of compound **R2** named odonthalol and its pentamethylated derivative **R2-M** are determined as trimers of bromophenols (Figure 1-3-2-14). Partial structure of units A and B of odonthalol (**R2**) had already isolated from the same alga [68]. Connectivity between units B and C of **R2** may due to debrominated phenol coupling reaction like the previously isolated bromophenols possessing a diaryl ether bridge [49]. To the best of our knowledge, odonthalol is a novel algal bromophenol trimer whose BHB units are uniquely connected via ether and methylene bridges.

Bromophenol trimers consist of three BHB units which were already isolated from the marine red algae *Halopytis pinastroides*, *Vidalia obtusaloba*, and *Rhodomela convervoides* (Figures 1-3-2-16) [54, 61-63]. To the best of our knowledge only four trimers were reported so far [57]. This research successfully isolated a novel bromophenol trimer named odonthalol (**R2**) from the red alga *Odonthalia corymbifera*. Structurally trimers were unique from each other considering BHB units were connected via diaryl methylene and ether bridges which were not observed in other reported trimers.

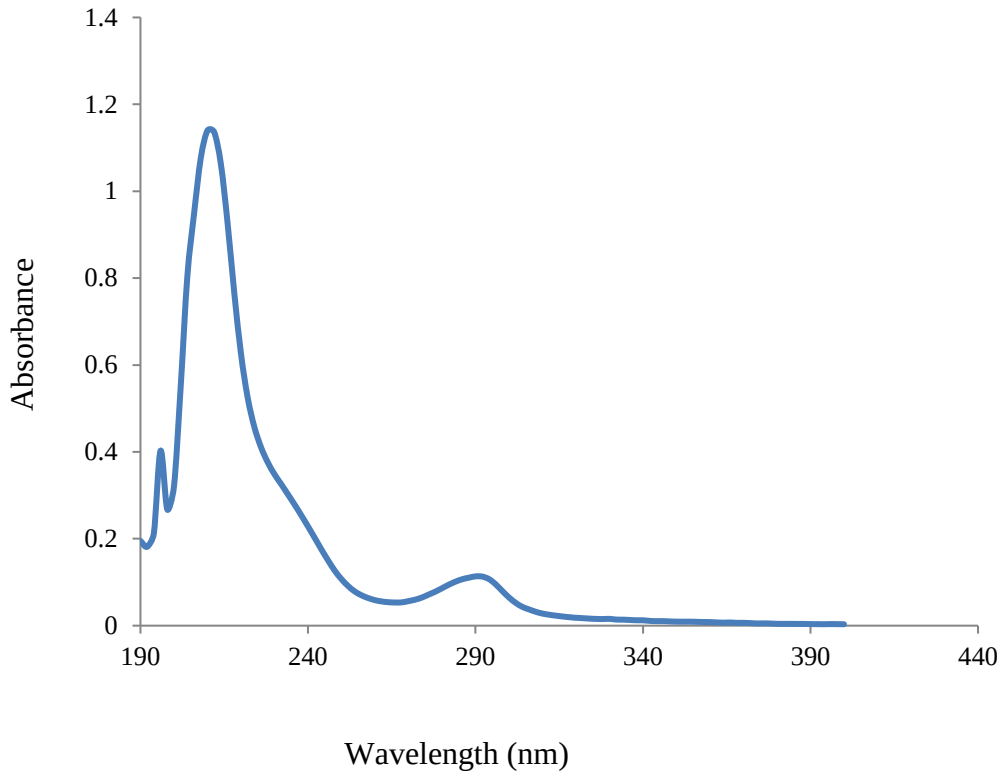

Figure 1-3-2-1. UV spectrum of compound **R2**.

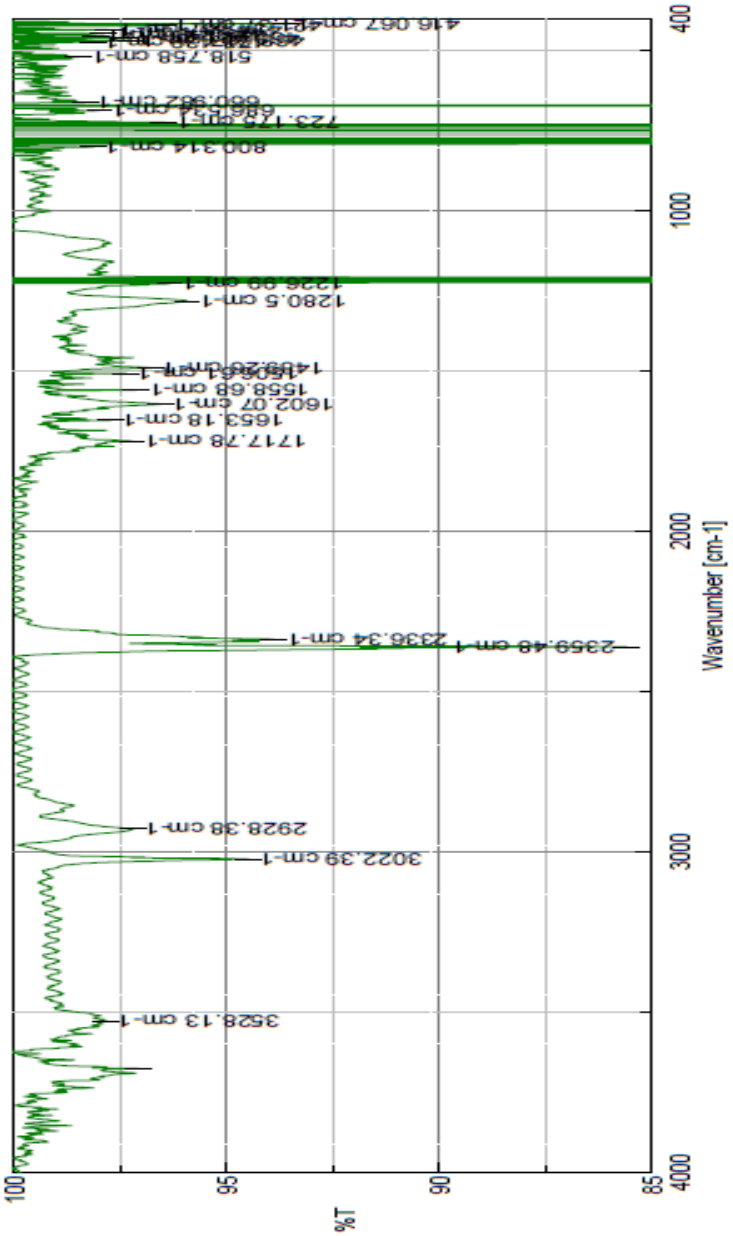

Figure 1-3-2-2. IR spectrum of compound **R2**.

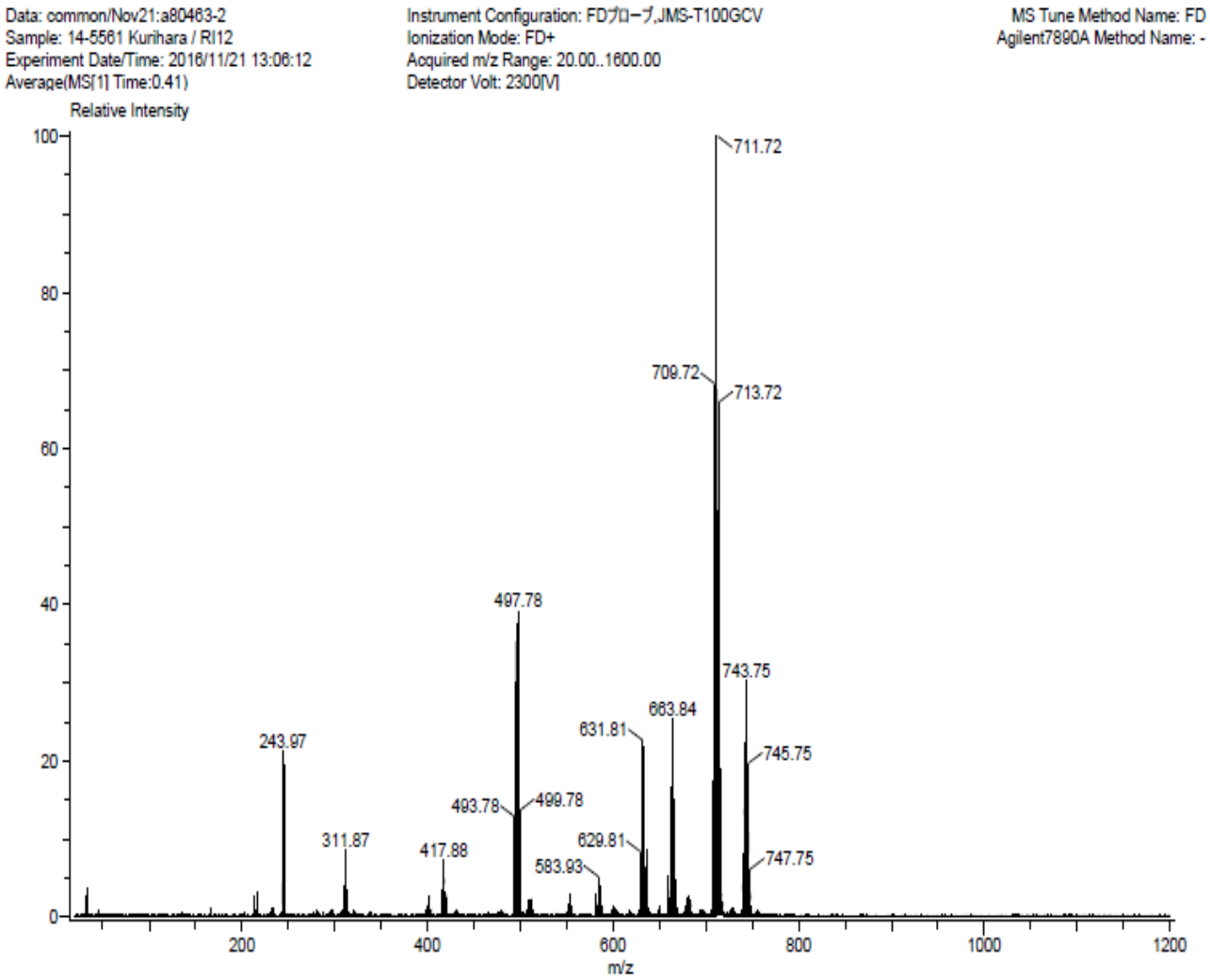

Figure 1-3-2-3. FD-MS spectrum of compound **R2**.

		[Hz]	[PPM]	
1	15541.6	4251.716	8.5012	0.05
2	18016.6	3471.432	6.9411	0.85
3	18271.0	3391.228	6.7807	1.16
4	19381.1	3041.247	6.0809	1.00
5	21806.4	2276.695	4.5521	0.05
6	22090.3	2187.126	4.3731	2.41
7	22420.1	2083.167	4.1653	0.79
8	22774.2	1971.542	3.9421	0.09
9	23376.2	1781.737	3.5625	0.06
10	23398.4	1774.736	3.5485	0.07
11	23683.8	1684.753	3.3686	0.05
12	23795.8	1649.464	3.2981	4.24
13	24034.9	1574.074	3.1473	3.96
14	24535.0	1416.420	2.8321	0.15
15	24915.1	1296.571	2.5925	0.05
16	25507.0	1109.976	2.2194	0.05
17	25535.4	1101.030	2.2015	0.08
18	25645.2	1066.419	2.1323	0.09
19	25733.5	1038.568	2.0766	12.50
20	25756.5	1031.302	2.0621	1.54
21	25761.7	1029.685	2.0588	1.61
22	25768.0	1027.689	2.0548	1.59
23	25777.3	1024.764	2.0490	1.92
24	25784.2	1022.583	2.0446	2.07
25	25791.0	1020.430	2.0403	4.03
26	25797.9	1018.275	2.0360	3.00
27	25804.6	1016.145	2.0318	1.69
28	25937.6	974.220	1.9479	0.07
29	27000.4	639.173	1.2780	0.04
30	27144.7	593.660	1.1870	0.14
31	27248.7	560.873	1.1215	0.06
32	27270.9	553.884	1.1075	0.12
33	27293.1	546.876	1.0935	0.07
34	27625.1	442.211	0.8842	0.05
35	27750.0	402.823	0.8054	0.04

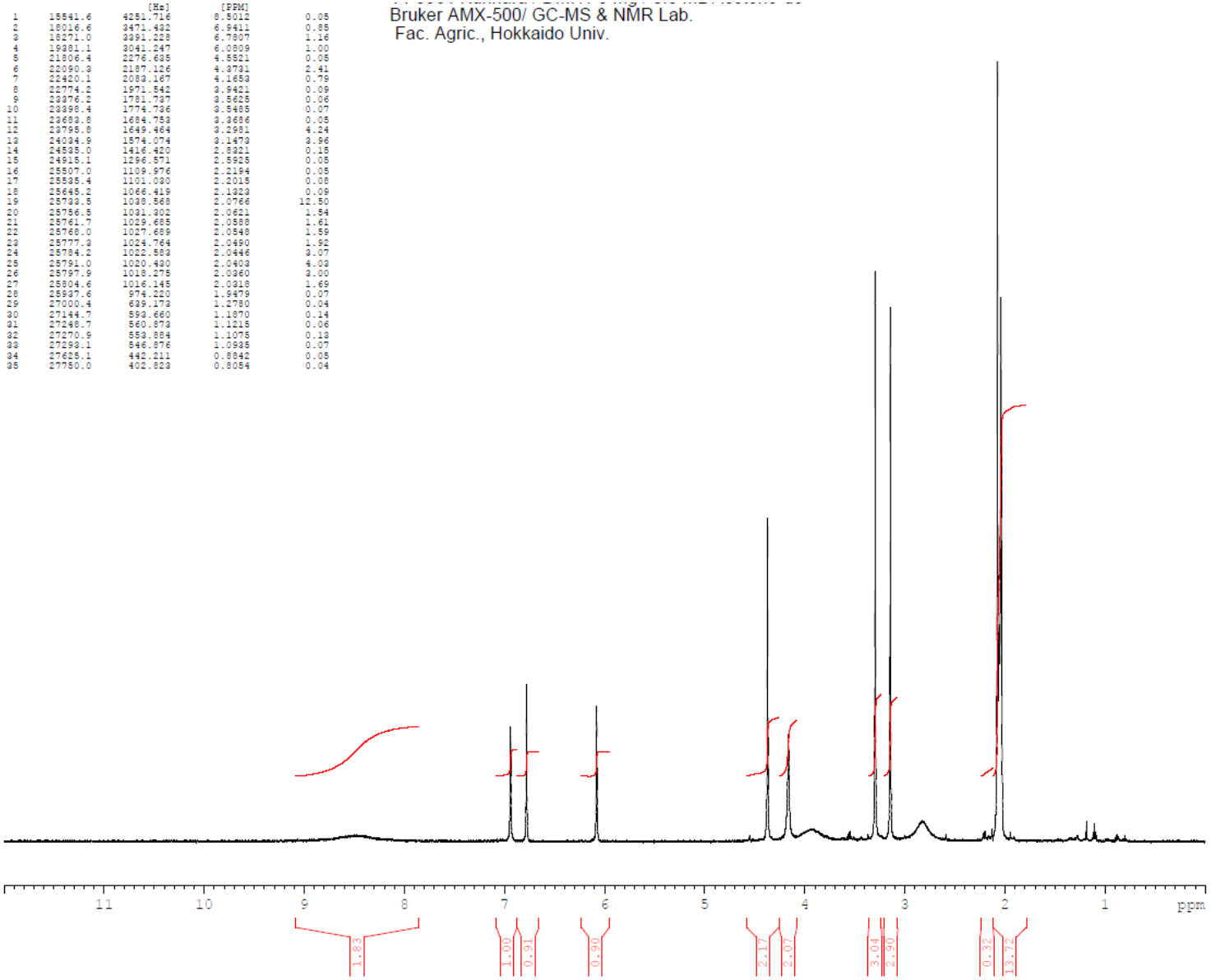

Figure 1-3-2-4. ^{1}H-NMR spectrum of compound **R2** (acetone-d_6, 500 MHz).

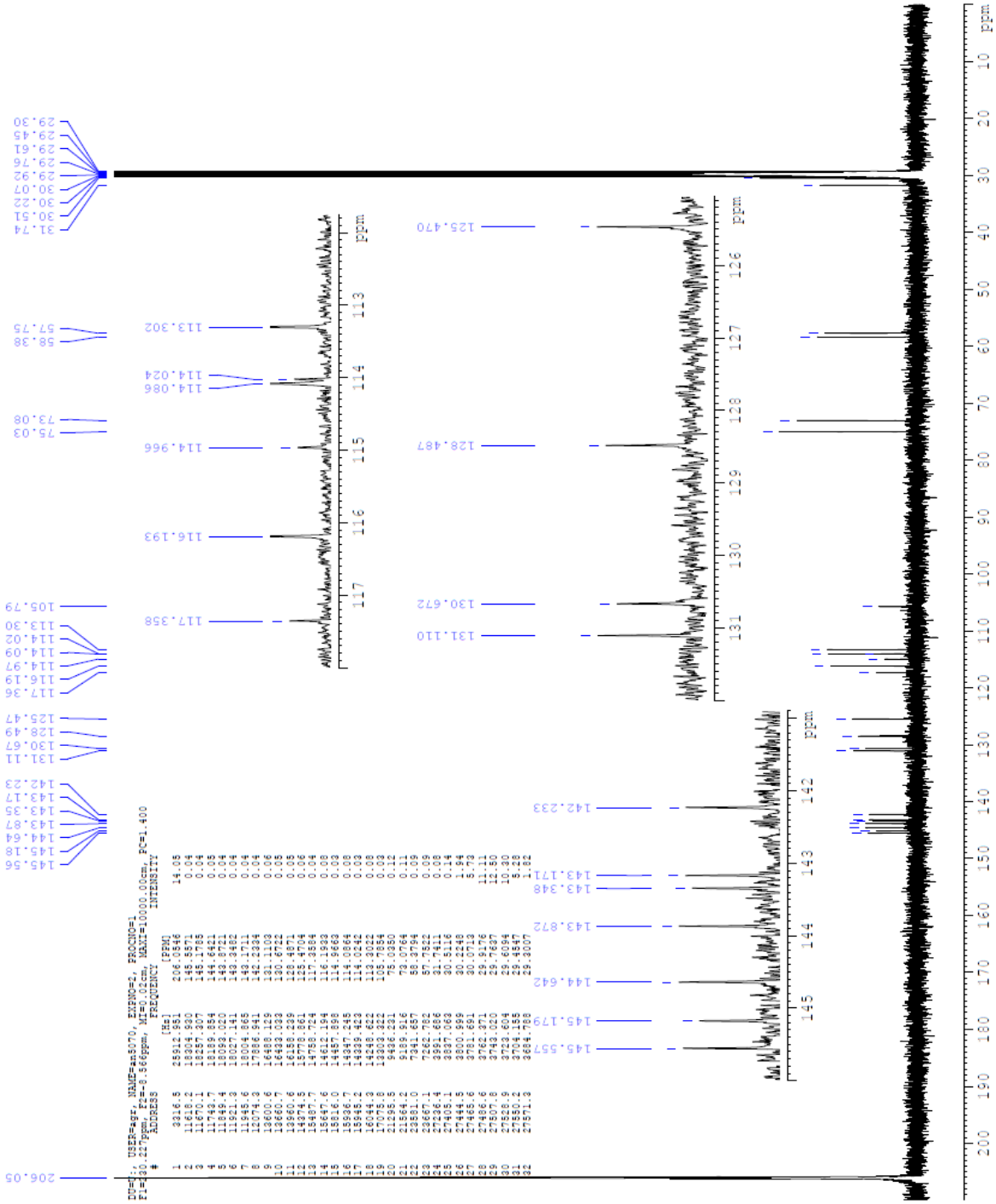

Figure 1-3-2-5. ^{13}C-NMR spectrum of compound **R2** (acetone-d_6, 125 MHz).

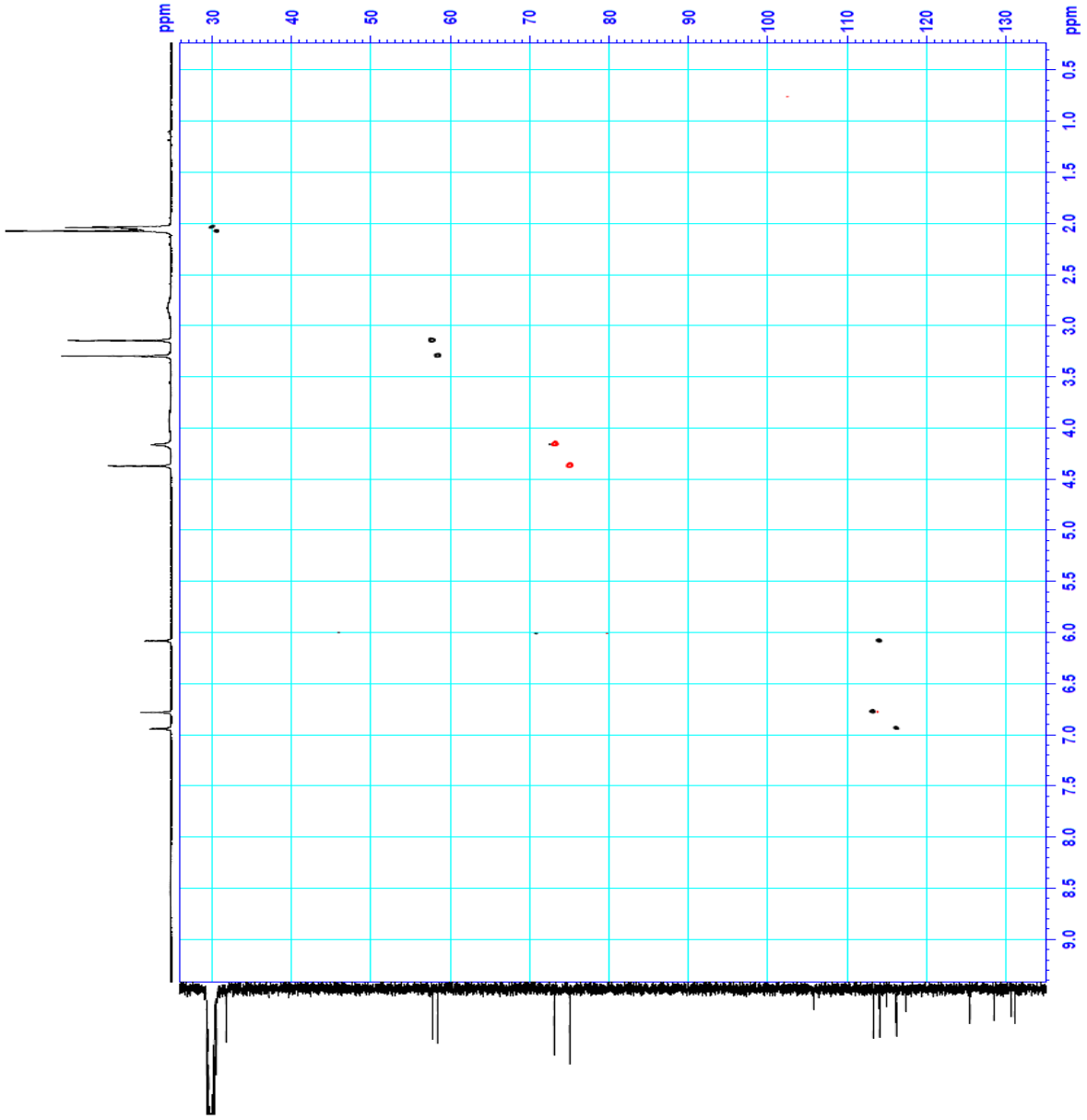

Figure 1-3-2-6. Editing HSQC spectrum of compound **R2** (acetone-d_6).

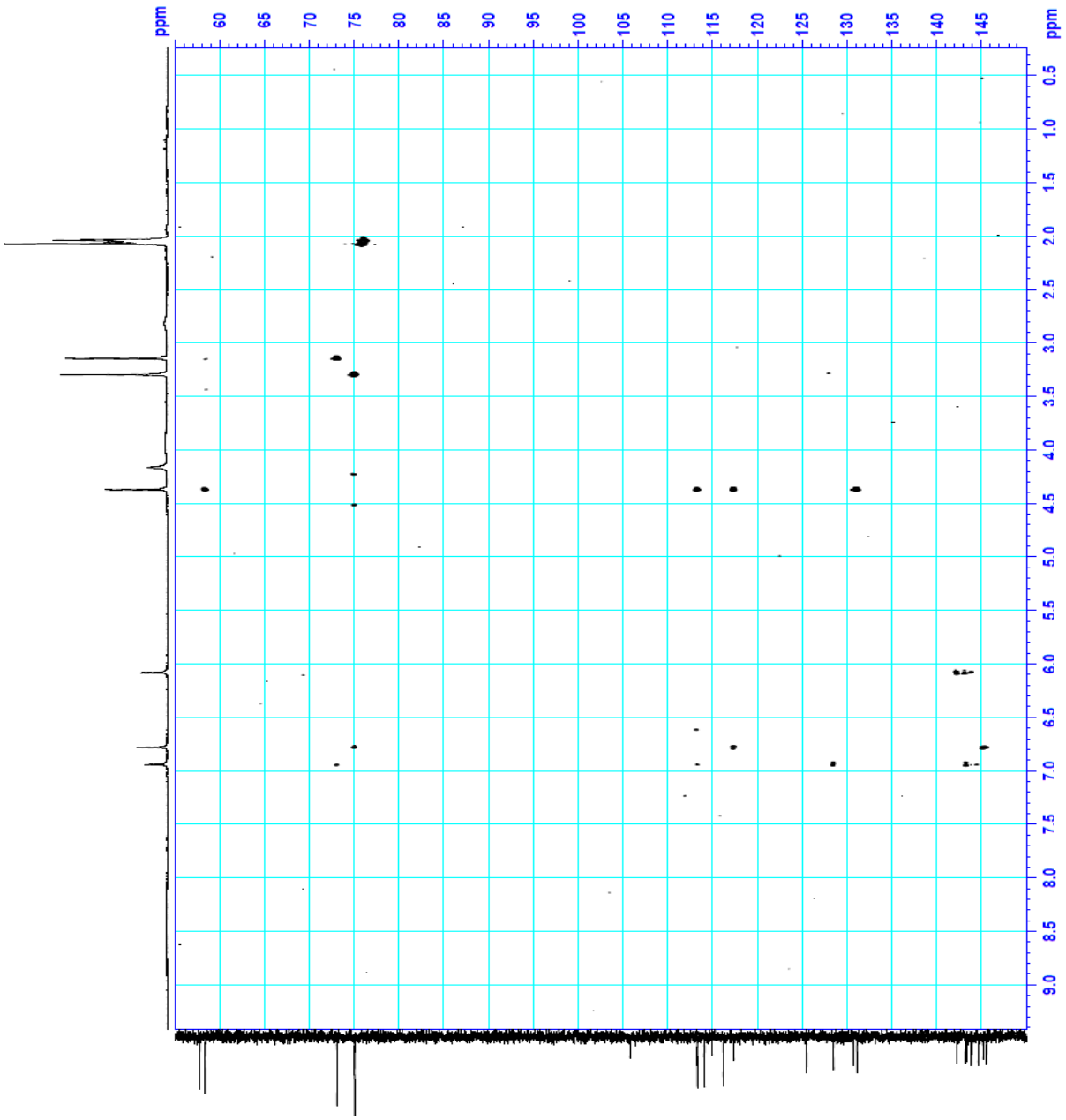

Figure 1-3-2-7. HMBC spectrum of compound **R2**.

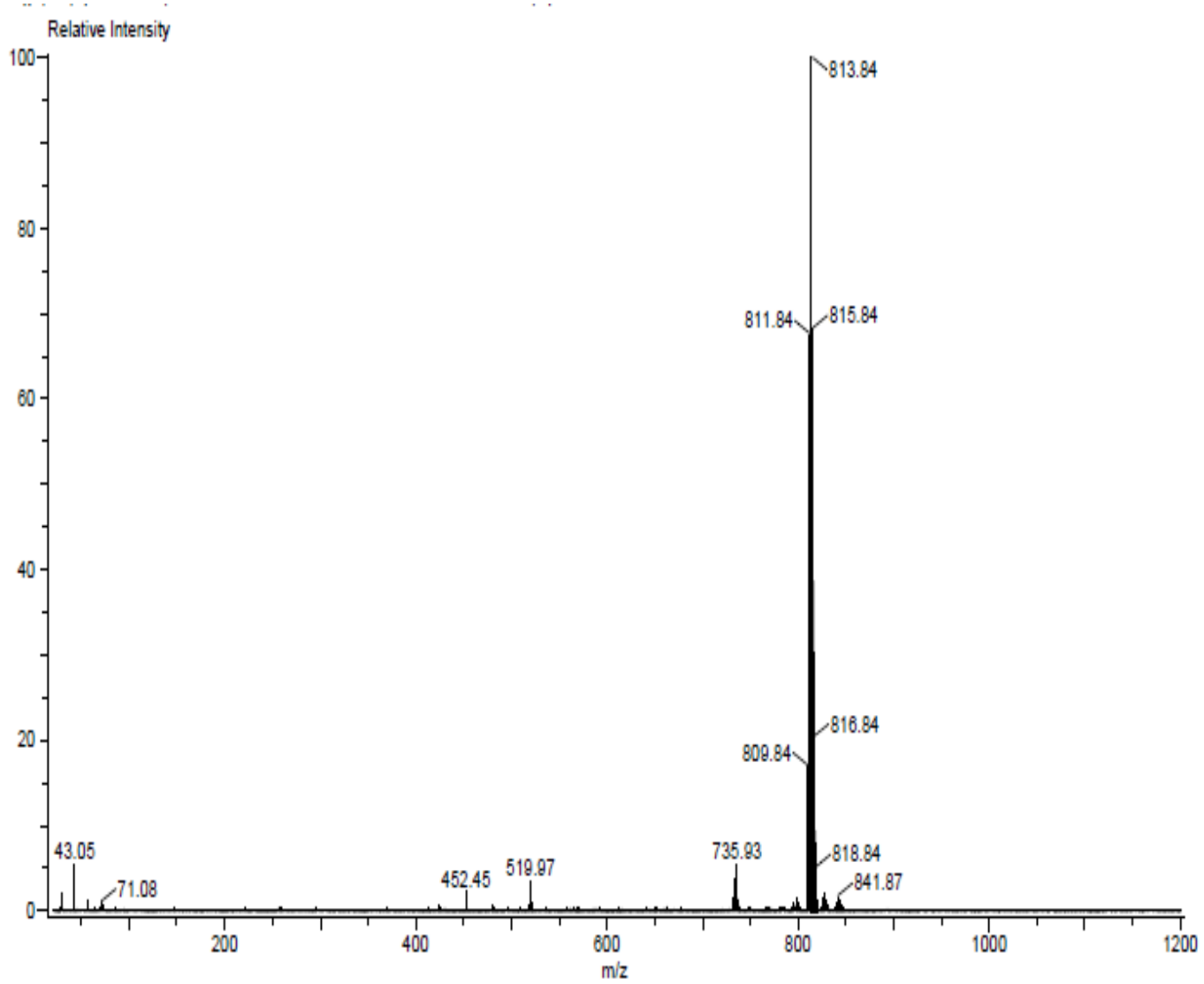

Figure 1-3-2-8. FD-MS spectrum of compound **R2-M**.

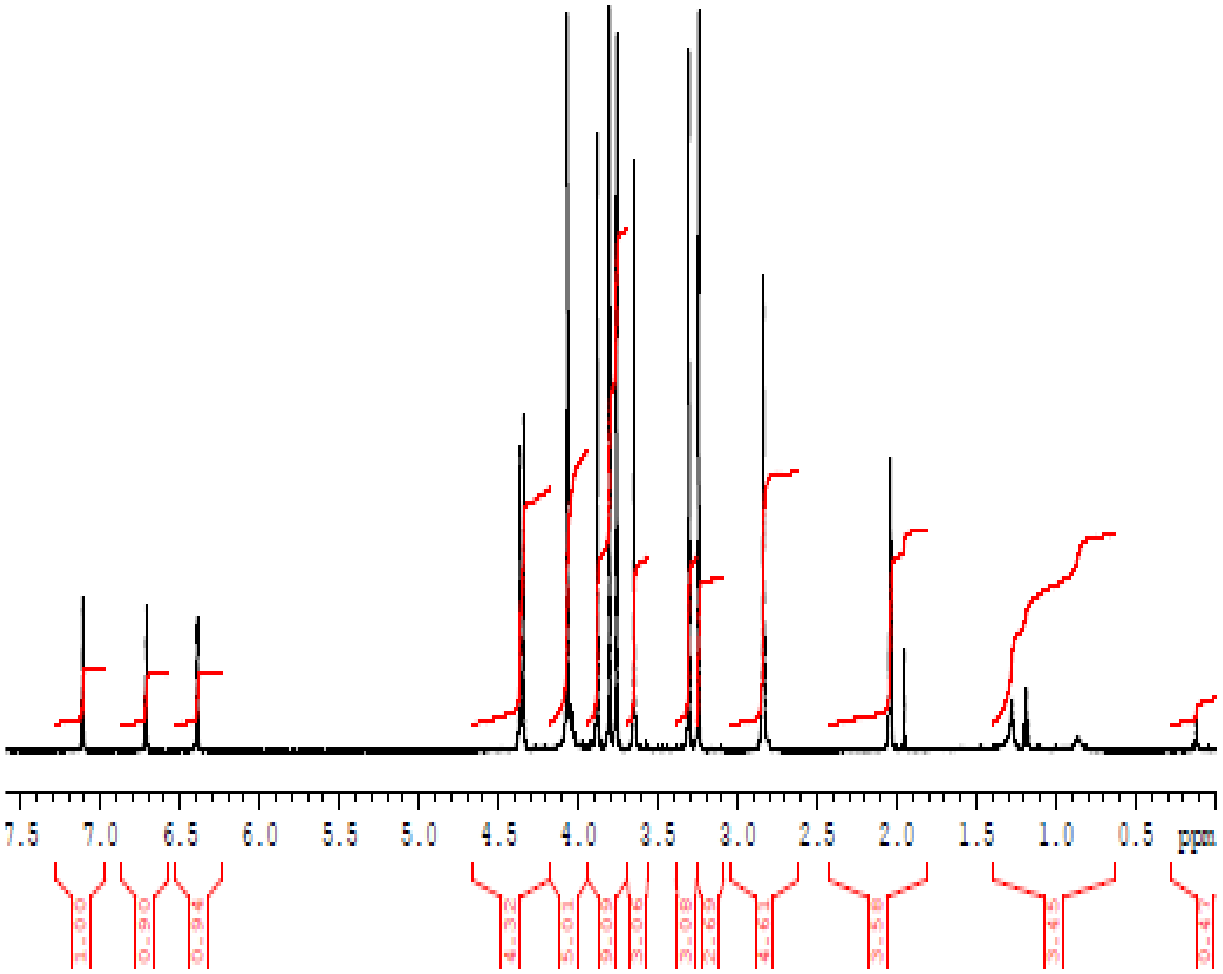

Figure 1-3-2-9. ^{1}H-NMR spectrum of compound **R2-M** (acetone-d_6, 500 MHz).

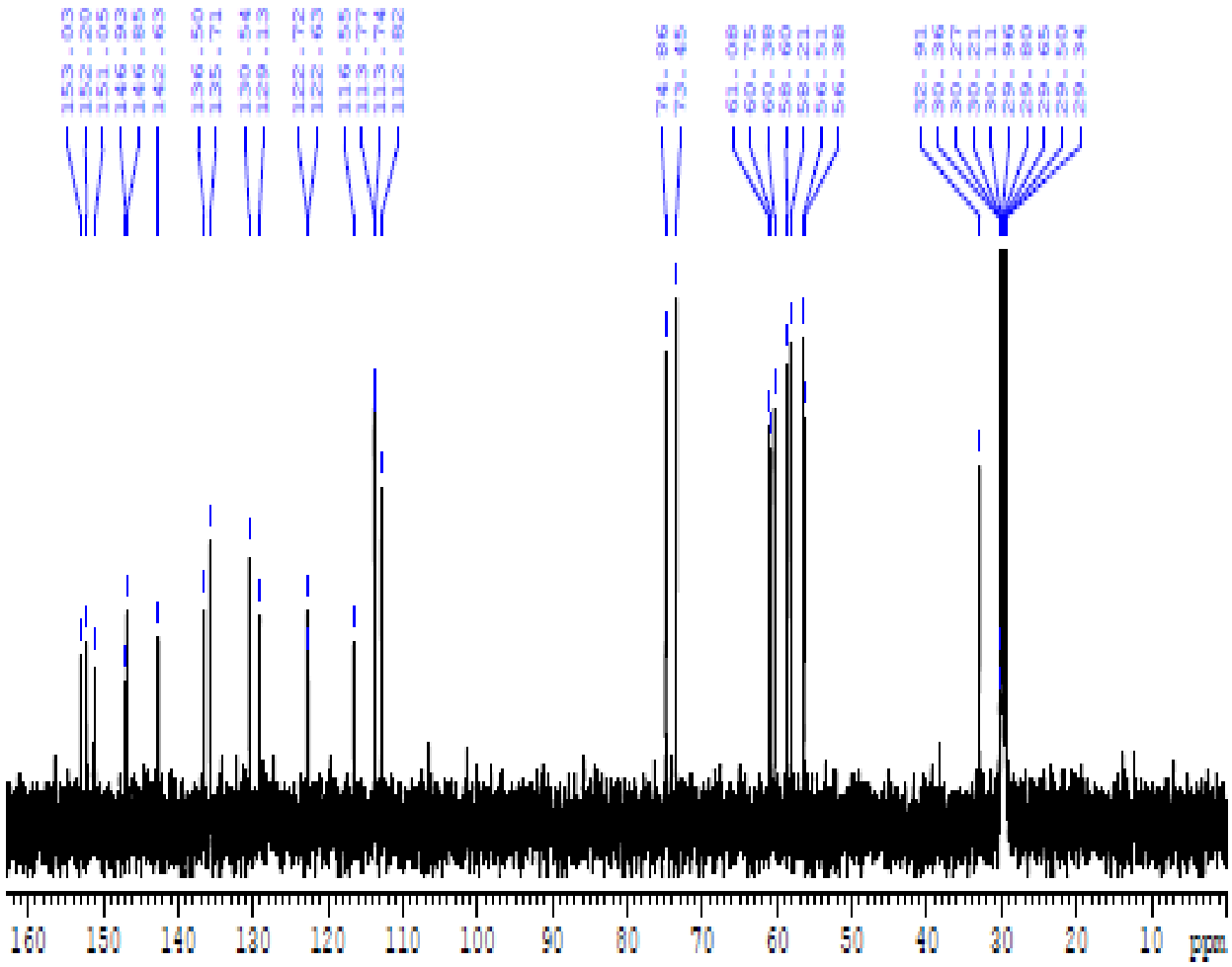

Figure 1-3-2-10. ^{13}C-NMR spectrum of compound **R2-M** (acetone-d_6, 125 MHz).

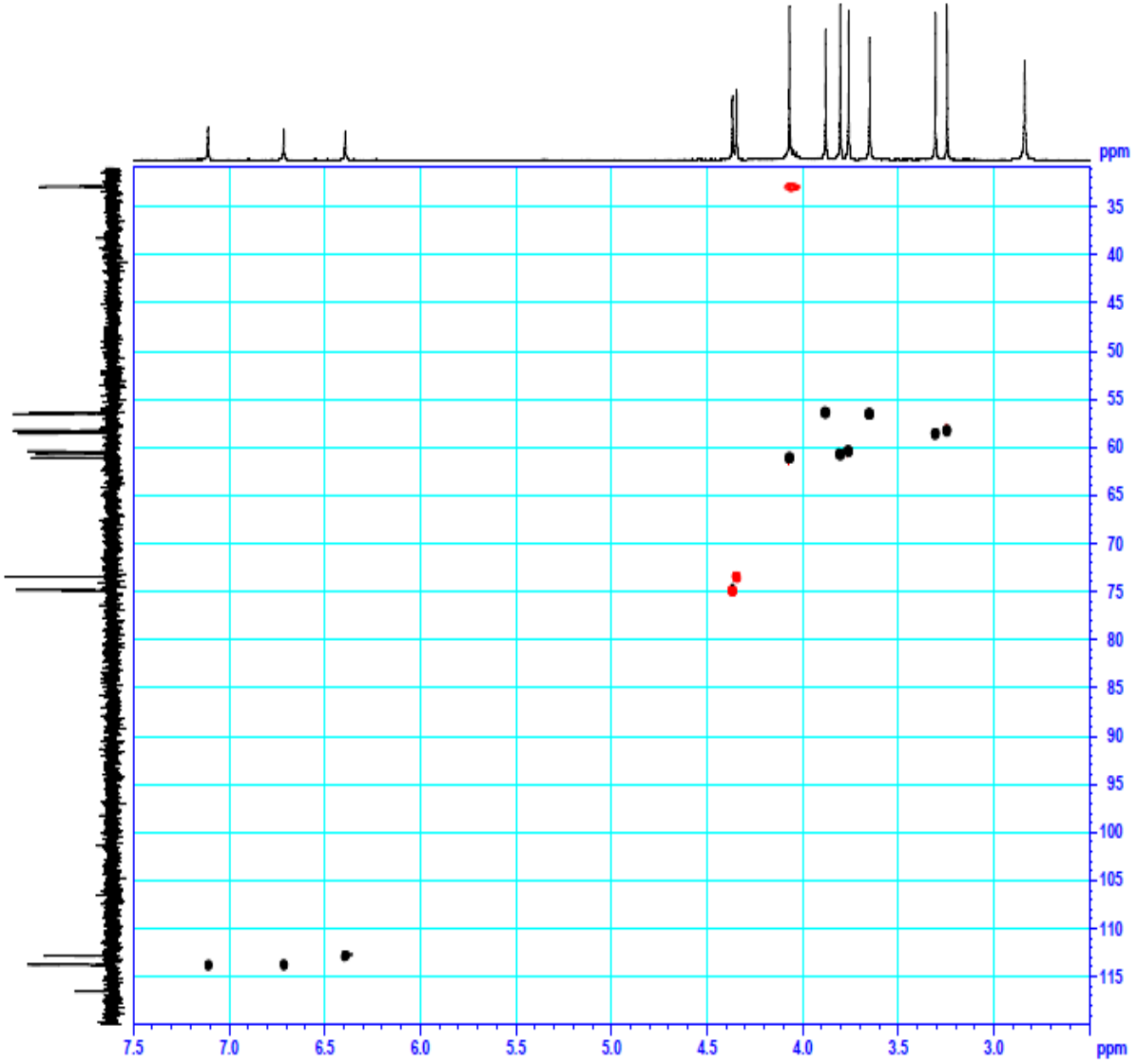

Figure 1-3-2-11. Editing HSQC spectrum of compound **R2-M** (acetone-d_6).

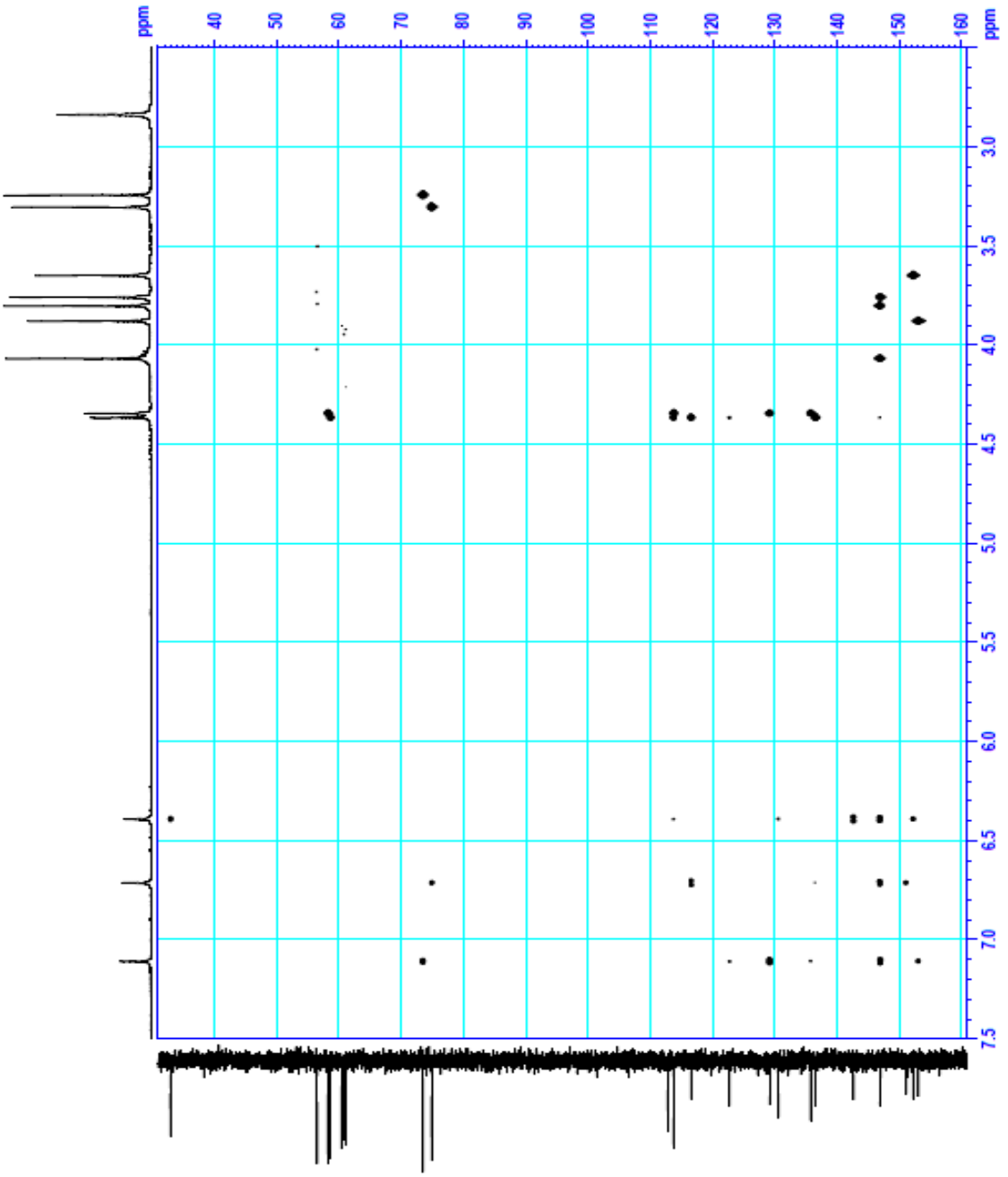

Figure 1-3-2-12. HMBC spectrum of compound **R2-M** (acetone-d_6).

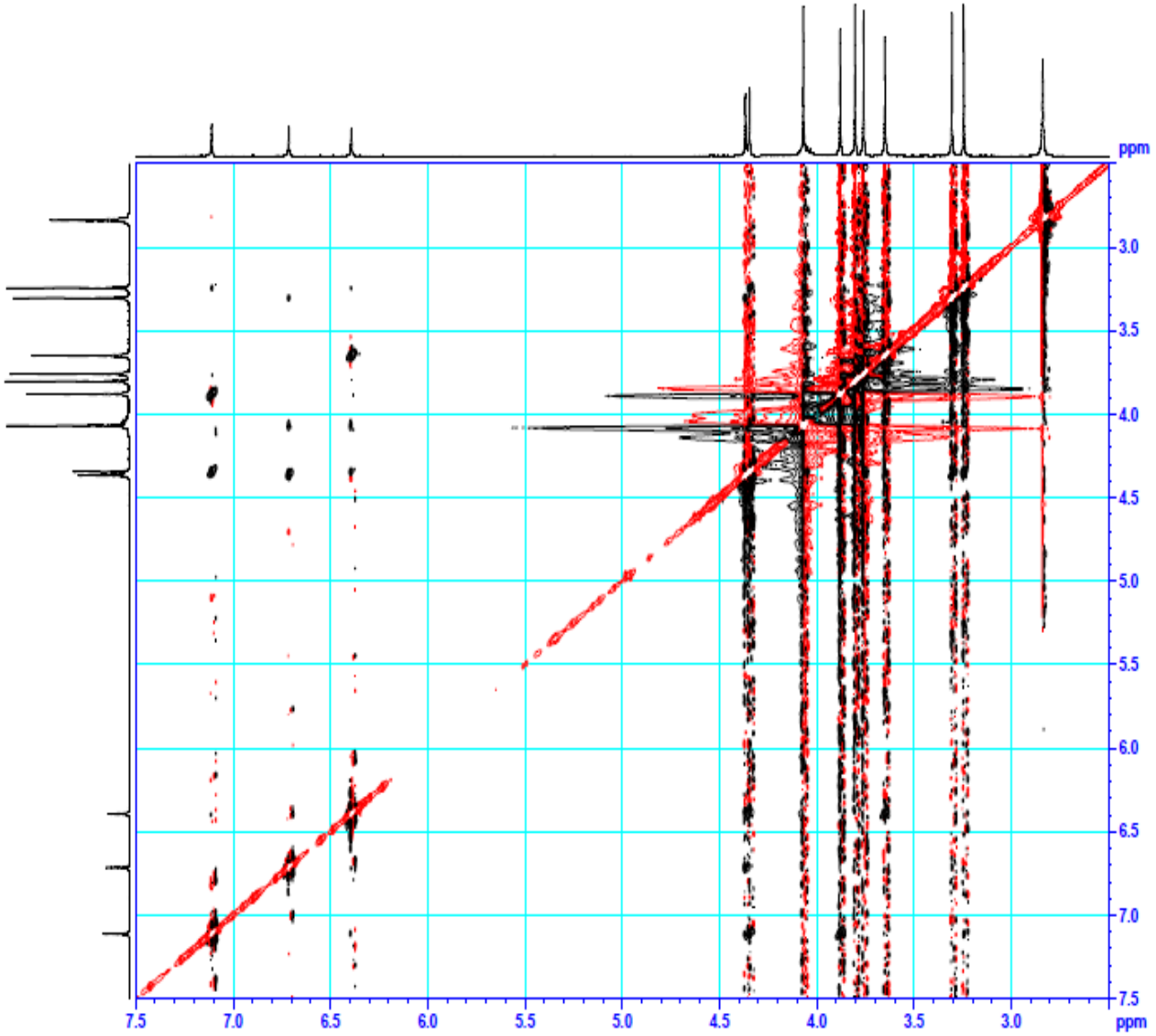

Figure 1-3-2-13. ROESY spectrum of compound **R2-M** (acetone-d_6).

Table 1-3-2-1. ^{1}H (500 MHz) and ^{13}C NMR (125 MHz) data of odonthalol (**R2**) and its permethylated derivative (**R2-M**) in acetone-d_6.

	Compound **R2**			Compound **R2-M**			
Position	δ_C, type	δ_H	HMBC	δ_C, type	δ_H	HMBC	ROESY
1a	130.7[a], C			135.7, C			
2a	128.5, C			129.1, C			
3a	115.0[b], C			122.7[f], C			
4a	144.6[c], C			146.9, C			
5a	143.4[c], C			153.0, C			
6a	116.2, CH	6.94, s	2a, 4a, 5a, 7a	113.8, CH	7.11, s	1a, 2a, 4a, 5a, 7a	7a, 8a, 5a-OMe
7a	73.1, CH_2	4.16, brs	ND[g]	73.5, CH_2	4.35, s	1a, 2a, 6a, 8a	6a, 6b
8a	57.8, CH_3	3.14, s	7a	58.2, CH_3	3.22, s	7a	6a, 6b
4a-OMe				60.4, CH_3	3.75, s	4a	
5a-OMe				56.4, CH_3	3.88, s	5a	6a
1b	125.5[a], C			130.5, C			
2b	143.2[d], C			142.6, C			
3b	105.8, C			106.5, C			
4b	142.2[d], C			146.9, C			
5b	143.9, C			152.2, C			
6b	114.1, CH	6.08, s	2b, 4b, 5b	112.8, CH	6.39, s	1b, 2b, 4b, 5b, 7b	7a, 8a, 5b-OMe, 5c-OMe
7b	31.7, CH_2	3.94, brs	ND[g]	32.9, CH_2	4.07, brs	ND[g]	
4b-OMe				60.8, CH_3	3.80, s	4b	
5b-OMe				56.5, CH_3	3.64, s	5b	6b
1c	131.1, C			136.5, C			
2c	117.4, C			116.6, C			
3c	114.0[b], C			122.6[f], C			
4c	145.6[e], C			151.1, C			
5c	145.2[e], C			146.9, C			
6c	113.3, CH	6.78, s	2c, 4c, 5c, 7c	113.7, CH	6.71, s	1c, 2c, 4c, 5c, 7c	6b, 7c, 8c, 5c-OMe
7c	75.1, CH_2	4.37, s	1c, 2c, 6c, 8c	74.9, CH_2	4.36, s	1c, 2c, 6c, 8c	6c
8c	58.8, CH_3	3.29, s	7c	58.6, CH_3	3.30, s	7c	6c
5c-OMe				61.1, CH_3	4.06, s	5c	6c

[a-f] Data are interchangeable within same character.

[g] Not detected because of a broad proton signal.

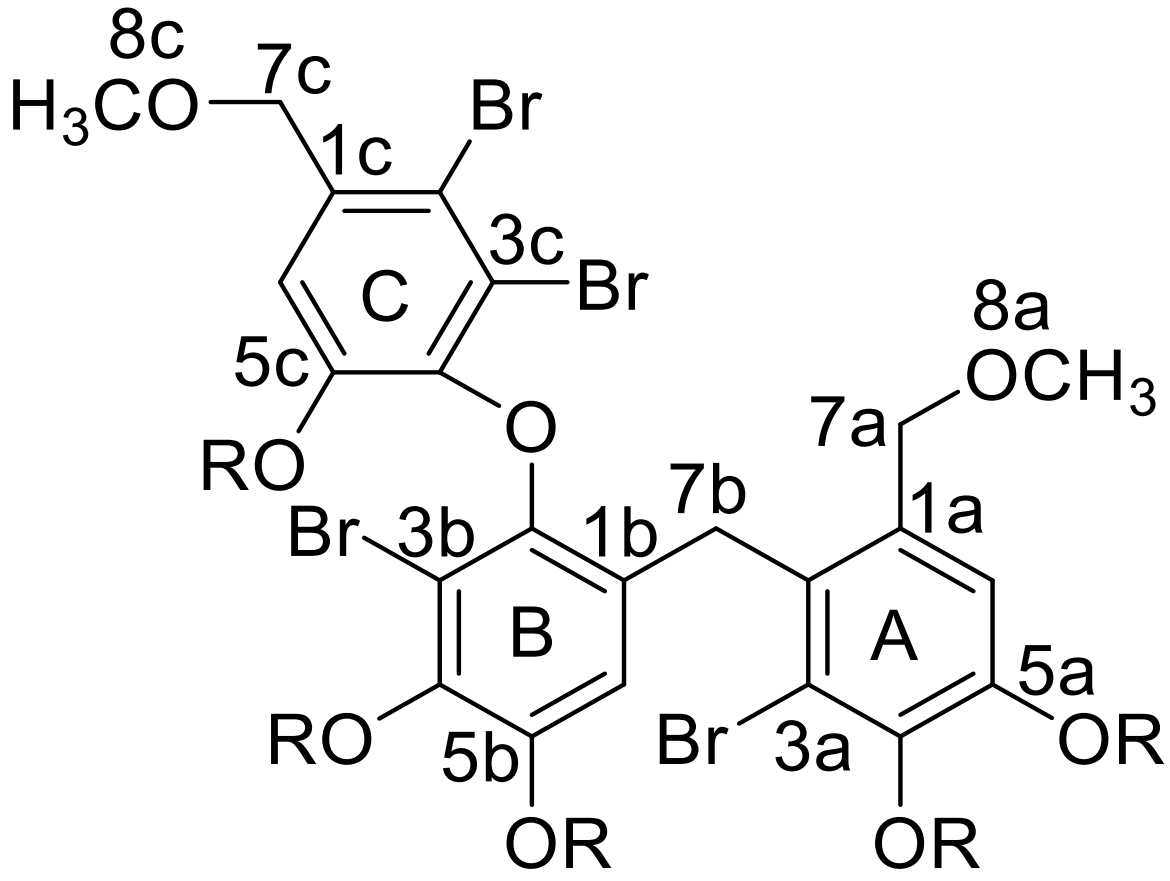

Figure 1-3-2-14. Structure of novel compound **R2** (R=H, odothalol) and its premethylated derivative **R2-M** (R=Me).

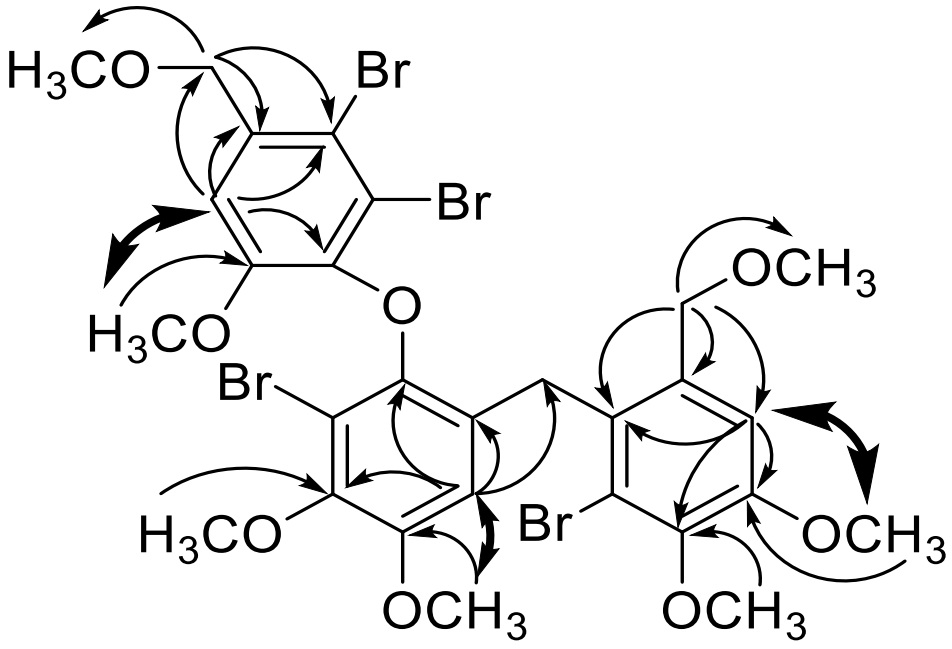

Figure 1-3-2-15. Key HMBC (single arrows) and ROESY (double arrows) correlations of compound **R2-M**.

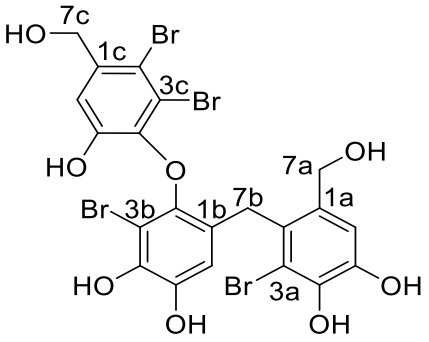

Odonthalol

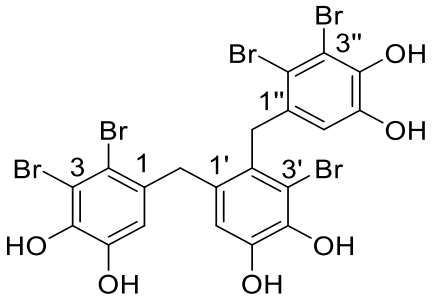

41

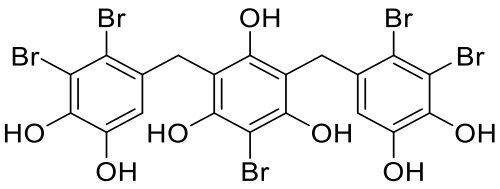

54

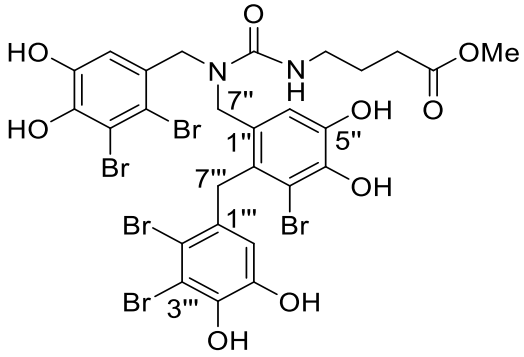

60

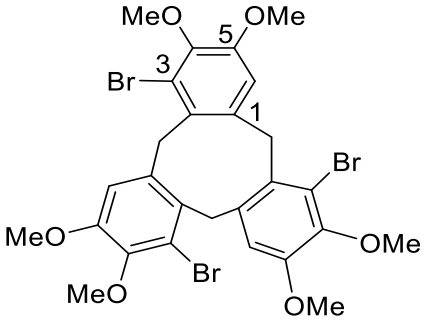

61

Figure 1-3-2-16. Structure of naturally occurring bromophenols trimers.

1.4. Conclusion

The marine red algae of family Rhodomelaceae is the prolific sources of secondary metabolite bromophenols. Bromophenols were also found from different marine organisms. Last few years researchers have been isolated many bromophenols and most of them were structurally very unique. Two marine red algae *Neorhodomela aculeata* and *Odonthalia corymbifera* are the members of family Rhodomelaceae. These marine algae were collected at Hakodate, Japan in the course of searching bromophenols. Researchers have already isolated bromophenols from these marine algae. But this study successfully isolated two novel compounds (**R1** & **R2**). Compound **R1** was a hybrid type bromophenols consist of coupling between BHB unit and cyclopentene moiety with two ketone groups. Hybrid type bromophenols not usually purified from these marine algae and this compound was structurally unique having two ketone groups. While compound **R2** was found as trimer of three BHB units. So far only four trimers have been purified and this compound will include as a new member of this group. Previously reported trimers BHB units were connected via methylene bridges but in compound **R2** BHB units were connected via methylene and ether bridges which were structurally very unique.

Chapter 2
Isolation of Known Bromophenols from Two Rhodomelaceae Algae

2.1. Introduction

Bromophenol, a halogenated phenolic compound is usually isolated from marine algae. The family of Rhodomelaceae algae is the prolific sources of halogenated compounds. These halogenated compounds represent unique secondary metabolite in terms of structural and biological diversity [57]. Most halogenated compounds of Rhodomelaceae origin are brominated and few chlorinated. On the basis of structural characteristics halogenated terpenoids, nonterpenoids C_{15}-acetogenins, indoles were mainly isolated from genus *Laurencia*, while halogenated phenols (bromophenols) were isolated from *Polysiphonia*, *Rhodomela*, *Symphyocladia* and *Odonthalia* genera. Bromophenols were found to be reported as monomer to tetramer and BHB unit was common feature of these compounds. But still researchers are keen to search novel type compounds and disclose new functionality of bioactive compounds. Two red algae of this family *Neorhodomela aculeata* and *Odonthalia corymbifera* are commonly found at the coast of Hakodate, Japan. These algae were collected in the year of 2015 and 2016, respectively. Ten bromophenols were isolated from these algae including two novel compounds.

2.2. Materials and Methods

2.2.1. General Experimental Procedure

This content was described in Chapter 1.

2.2.2. Isolation and purification of bromophenols from *Neorhodomela aculeata*.

The ethyl acetate solvent partitioning fraction (12.1 g) of *N. aculeata* (air dried algal weight, 3000 g; Usujiri, Hakodate 2015) (Table 2-2-2-1, Figure 2-2-2-1) was subjected to silica gel column chromatography, eluted with gradient of increasing acetone (0-100%) in hexane and ethyl acetate (20-100%) in methanol to obtain seventeen fractions (I-XVII) (Table 2-2-2-2, Figure 2-2-2-2). Fractions IX and X were combined and loaded onto octadecylsilyl (ODS) gel, eluted with a gradient of methanol (30%→100%) in water to afford nine fractions IX.I-IX.IX (Table 2-2-2-3, Figure 2-2-2-3). Fraction IX.III was further purified by RP HPLC using 60% aqueous methanol as a mobile phase to obtain compound **R3** (12 mg) (Table 2-2-2-4, Figures 2-2-2-4 & 2-2-2-5). Compound **R4** (10 mg) was purified from fraction IX.II by preparative TLC developed with chloroform:methanol:acetic acid (90:10:1, v/v/v) (Table 2-2-2-5, Figure 2-2-2-5).

Table 2-2-2-1. Yields and scavenging activity after organic solvent partitioning of *N. aculeata.*

Solvent Partitioning Fraction	Yield (g)	DPPH Radical Scavenging (%)[a,b]
n-Hexane	3.8	60.8±1.5
Ethyl acetate	12.1	89.1±2.7
n-Butanol	18.1	12.9±0.6
Water	45.7	NA[c]

[a]Final sample concentration 100 μg/ml.

[b]Mean±standard error (n=3).

[c]No Activity.

Table 2-2-2-2. DPPH radical scavenging activity of individual fractions obtained after silica gel column chromatography[a] of EtOAc-soluble fraction.

Fraction	Eluent (v/v)	Yield (mg)	DPPH Radical Scavenging (%)[b,c]
I	Hexane	0.0	NE[d]
II	Hexane	0.0	NE
III	Hexane:acetone (90:10)	0.0	NE
IV	Hexane:acetone (90:10)	0.0	NE
V	Hexane:acetone (80:20)	10	NE
VI	Hexane:acetone (80:20)	30	5.2±2.2
VII	Hexane:acetone (70:30)	40	19.2±1.8
VIII	Hexane:acetone (70:30)	398	94.6±0.1
IX	Hexane:acetone (50:50)	584	95.9±0.5
X	Hexane:acetone (30:70)	885	93.1±0.1
XI	Hexane:acetone (30:70)	1813	92.3±0.3
XII	Hexane:acetone (0:100)	777	88.3±0.2
XIII	Hexane:acetone (0:100)	936	89.5±0.6
XIV	EtOAC:MeOH (80:20)	1031	89.4±0.3
XV	EtOAC:MeOH (80:20)	418	89.5±0.3
XVI	EtOAC:MeOH (50:50)	1404	89.4±0.2
XVII	EtOAC:MeOH (0:100)	1214	89.8±0.1

[a]Column size ϕ 4.0 × 42 cm. Each fraction contains 500 ml eluent.

[b]Final sample concentration 50 μg/ml.

[c]Mean±standard error (n=3).

[d]Not Exmined.

Table 2-2-2-3. DPPH radical scavenging activity of individual fractions obtained from reverse phase column chromatography[a] of combined fraction IX-X.

Fraction	Eluent (v/v)	Yield (mg)	DPPH Radical Scavenging (%)[b,c]
IX.I	Methanol:water (30:70)	203	30.8±4.6
IX.II	Methanol:water (30:70)	462	88.8±2.4
IX.III	Methanol:water (50:50)	247	87.1±0.5
IX.IV	Methanol:water (50:50)	177	78.4±0.1
IX.V	Methanol:water (70:30)	984	80.1±2.1
IX.VI	Methanol:water (70:30)	108	49.4±0.8
IX.VII	Methanol:water (90:10)	245	53.9±2.6
IX.VIII	Methanol:water (90:10)	89	27.1±3.2
IX.IX	Methanol:water (100:0)	117	15.5±0.6

[a]Column size ϕ 2.3 × 21 cm. Each fraction contains 90 ml eluent.

[b]Final sample concentration 10 μg/ml.

[c]Mean±standard error (n=3).

Table 2-2-2-4. DPPH radical scavenging activity of compound **R3** after RP HPLC of fraction IX.III[a]

Fraction	Yield (mg)	DPPH Radical Scavenging (%)[b,c]
Compound **R3**	12	51.2±0.1

[a] Eluent 60% MeOH

[b]Final sample concentration 5 μg/ml.

[c]Mean±standard error (n=3).

Table 2-2-2-5. DPPH radical scavenging activity of fraction obtained after PLC of fraction IX.II.[a]

Fraction	R_f Value	Yield (mg)	DPPH Radical Scavenging (%)[b,c]
IX.II.I (**R4**)	0.5	10	54.2±0.5

[a]Developing solvent, $CHCl_3$:MeOH:AA, 90:10:1 (v/v/v).

[b]Final sample concentration 3.3 µg/ml.

[c]Mean±standard error (n=3).

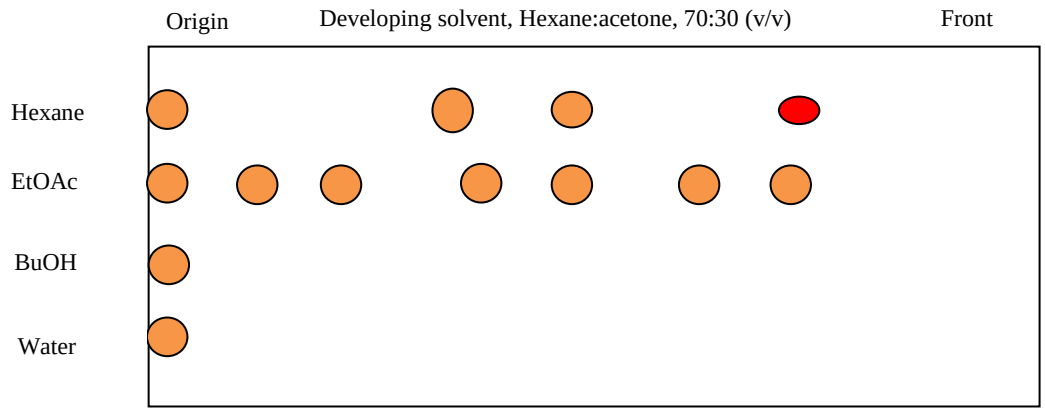

Figure 2-2-2-1. TLC chromatogram after solvent partitioning of *N. aculeata*. Spots were visualized after spraying with 5% H_2SO_4.

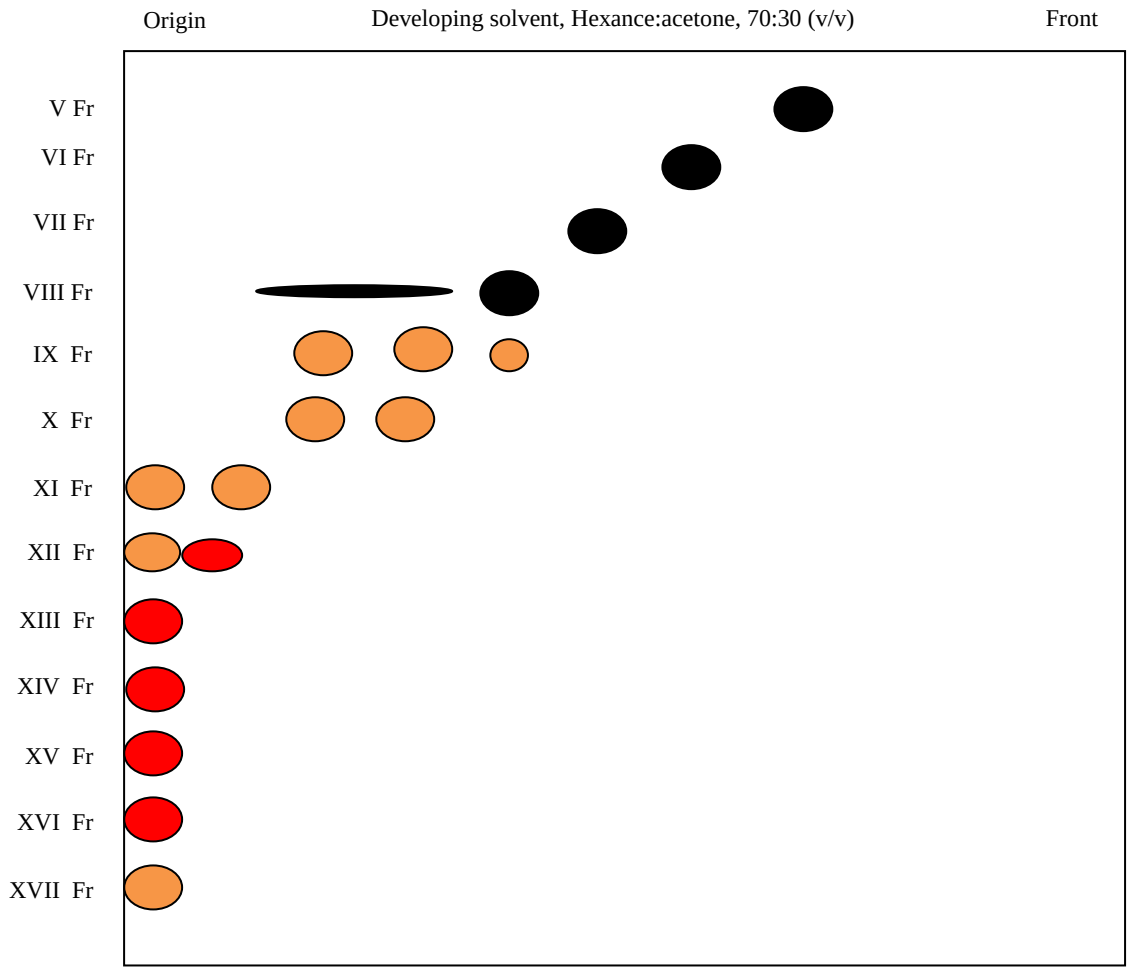

Figure 2-2-2-2. TLC chromatogram of individual fractions obtained after silica gel column chromatography of EtOAc-soluble fraction. Spots were visualized after spraying with 5% H_2SO_4.

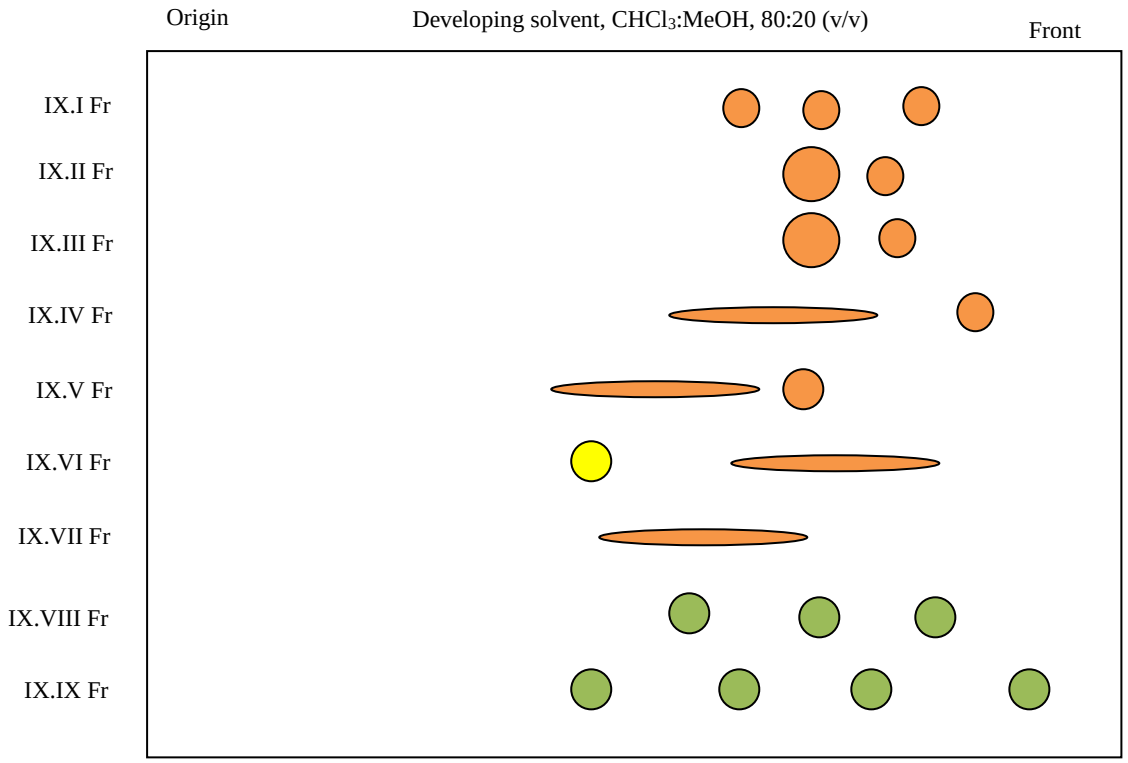

Figure 2-2-2-3. TLC chromatogram of individual fractions obtained after reverse phase column chromatography of combined fractions IX-X. Spots were visualized after spraying with 5% H_2SO_4.

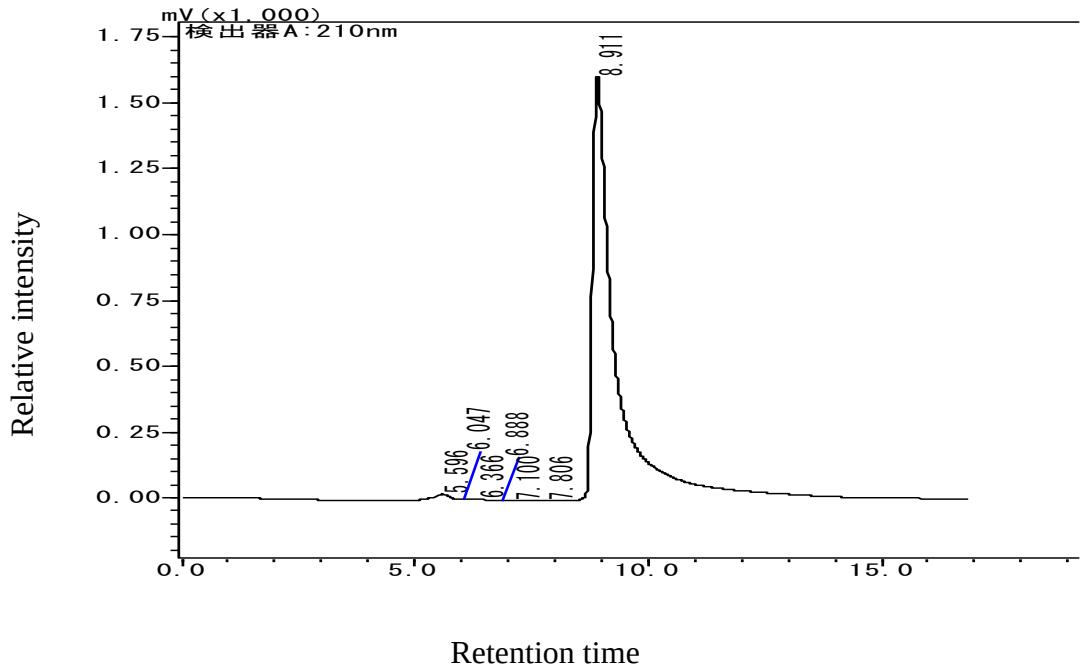

Figure 2-2-2-4. HPLC chromatogram of compound **R3**. Column: Mightysil RP-18 250-4.6 (5 μm); eluent: 60% aqueous MeOH; flow rate: 0.5 ml/min; detection: UV 210 nm.

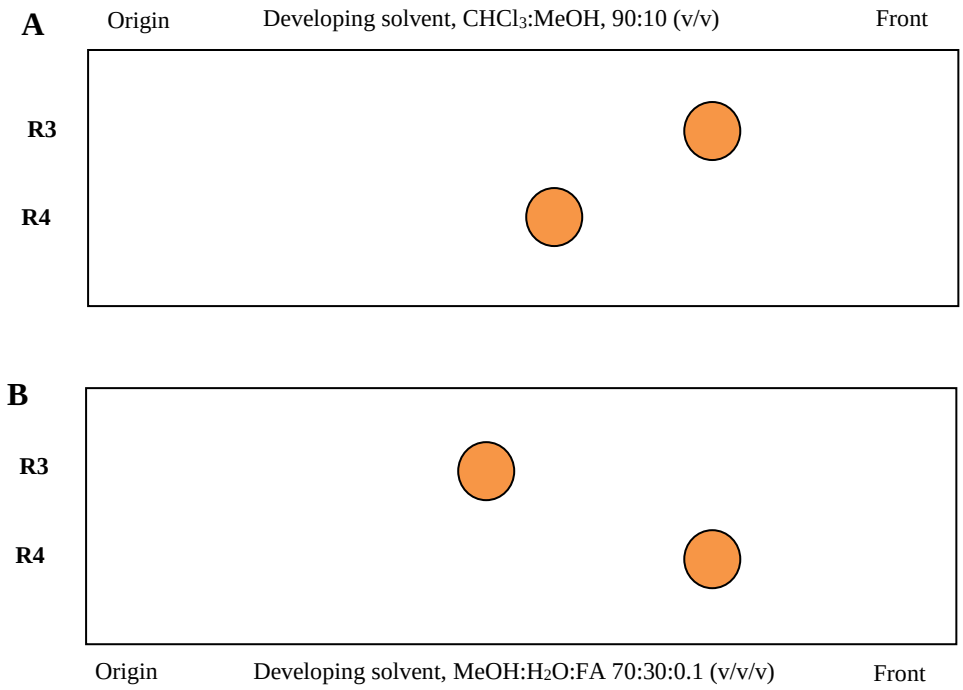

Figure 2-2-2-5. **A**. NP-TLC and **B**. RP-TLC chromatogram of compounds **R3** and **R4**. Spots were visualized after spraying with 5% H_2SO_4.

2.2.3. Isolation and Purification of Bromophenols from *Odonthalia corymbifera*.

Extract preparation, solvent partitioning and 1st column chromatography of *O. corymbifera* were described in section 1.2.5.

Fraction 5 was subject to RP column chromatography using 70% aqueous methanol as eluent to obtain six fractions (Table 2-2-3-1, Figure 2-2-3-1). Fraction 5.2 was further fractionated by Sephadex LH-20 (eluent, 70% MeOH) (Table 2-2-3-2, Figure 2-2-3-2). Final purification was performed on preparative TLC (toluene:ethyl acetate:acetic acid,10:10:1, v/v/v) to obtain compound **R5** (4.2 mg) (Table 2-2-3-3, Figure 2-2-3-7). Fraction 5.3 offered two compounds **R6** (3 mg) and **R7** (1.5 mg) (Figure 2-2-3-7) after purification by Sephadex LH-20 (eluent, 70% MeOH) (Table 2-2-3-4, Figure 2-2-3-3) and RP HPLC (mobile phase, 70% MeOH) (Figures 2-2-3-4 to 2-2-3-6). Compound **R8** (10.8 mg) was obtained after PLC of fraction 5.4 (Table 2-2-3-5, Figure 2-2-3-7) developed with toluene:ethyl acetate:acetic acid, 10:10:1, (v/v/v).

Fraction 7 was subjected to reverse phase column chromatography which offered nine fractions (70% MeOH used as eluent) (Table 2-2-3-6, Figure 2-2-3-8). After PLC (toluene:ethyl acetate:acetic acid, 10:10:1, v/v/v) (Table 2-2-3-7, Figure 2-2-3-9) and RP HPLC (70% MeOH as eluent) (Figure 2-2-3-10), compound **R9** (6.3 mg) was purified from fraction 7.3 (Figure 2-2-3-11). While, fraction 7.5 was purified on PLC plate developed with toluene:ethyl acetate:acetic acid,10:10:1, (v/v/v) (Table 2-2-3-8) which had yield compound **R10** (10.5 mg) (Figure 2-2-3-11).

The isolation scheme of bromophenols from *O. corymbifera* and *N. aculeata* were illustrated in Figures 2-2-3-12 & 2-2-3-13, respectively.

Table 2-2-3-1. DPPH radical scavenging activity of fractions obtained from reverse phase column chromatography of fraction 5.[a]

Fraction	Tube No.	Yield (mg)	DPPH Radical Scavenging (%)[b,c]
5.1	1-27	772	82.6±0.7
5.2	28-41	2890	89.2±0.6
5.3	42-49	215	89.1±0.4
5.4	50-55	500	69.1±3.2
5.5	56-62	400	53.1±1.5
5.6	63-70	150	46.5±0.9

[a]Column size ϕ 2 × 20 cm. 70% MeOH as eluent. Each tube contains 4 ml eluent.

[b]Final sample concentration 25 μg/ml.

[c]Mean±standard error (n=3).

Table 2-2-3-2. DPPH radical scavenging activity of fractions obtained after Sephadex LH-20 of fraction 5.2.[a]

Fraction	Tube No.	Yield (mg)	DPPH Radical Scavenging (%)[b,c]
5.2.1	1-10	510	82.6±0.3
5.2.2	11-19	689	91.3±0.4
5.2.3	20-24	264	91.7±0.3
5.2.4	25-30	190	81.4±0.3
5.2.5	31-35	150	76.2±1.1

[a]Column size ϕ 1 × 22 cm. 70% MeOH as eluent. Each tube contains 4 ml eluent.

[b]Final sample concentration 20 μg/ml.

[c]Mean±standard error (n=3).

Table 2-2-3-3. DPPH radical scavenging activity of compound **R5** obtained after PLC of fraction 5.2.4.[a]

Fraction	R_f Value	Yield (mg)	DPPH Radical Scavenging (%)[b,c]
5.2.4.1 (compound **R5**)	0.55	4.2	51.5±0.1

[a]Developing solvent, Toluene:EtOAc:AA, 10:10:1 (v/v/v).

[b]Final sample concentration 4 μg/ml.

[c]Mean±standard error (n=3).

Table 2-2-3-4. DPPH radical scavenging activity of fractions obtained after Sephadex LH-20 of fraction 5.3.[a]

Fraction	Tube No.	Yield (mg)	DPPH Radical Scavenging (%)[b,c]
5.3.1	1-30	30	81.4±0.3
5.3.2	31-40	51	89.3±0.4
5.3.3	41-44	45	90.1±0.3
5.3.4	45-47	67	85.9±0.4
5.3.5	48-55	36	83.9±1.1

[a]Column size ϕ 1 × 22 cm. 70% MeOH as eluent. Each tube contains 4 ml eluent.

[b]Final sample concentration 20 μg/ml.

[c]Mean±standard error (n=3).

Table 2-2-3-5. DPPH radical scavenging activity of compound **R8** obtained after PLC of fraction 5.4.[a]

Fraction	R_f Value	Yield (mg)	DPPH Radical Scavenging (%)[b,c]
5.4.1 (Compound **R8**)	0.45	10.8	50.5±0.1

[a]Developing solvent, Toluene:EtOAc:AA, 10:10:1 (v/v/v).

[b]Final sample concentration 5 μg/ml.

[c]Mean±standard error (n=3).

Table 2-2-3-6. DPPH radical scavenging activity of fractions obtained from reverse phase column chromatography of fraction 7.[a]

Fraction	Tube No.	Yield (mg)	DPPH Radical Scavenging (%)[b,c]
7.1	1-17	108	82.3±0.6
7.2	18-20	90	92.1±0.2
7.3	21-24	142	95.5±0.6
7.4	25-29	70	91.4±0.6
7.5	30-34	27	86.6±0.5
7.6	35-45	155	77.4±0.9
7.7	46-50	31	66.7±1.4
7.8	51-57	61	47.7±1.2
7.9	58-68	24	44.3±3.1

[a]Column size ϕ 2 × 20 cm. 70% MeOH as eluent. Each tube contains 5 ml eluent.

[b]Final sample concentration 25 μg/ml.

[c]Mean±standard error (n=3).

Table 2-2-3-7. DPPH radical scavenging activity of fraction obtained after PLC of fraction 7.3.[a]

Fraction	R_f Value	Yield (mg)	DPPH Radical Scavenging (%)[b,c]
7.3.1 (Not pure)	0.25	7.6	62.3±0.2

[a]Developing solvent, Toluene:EtOAc:AA, 10:10:1 (v/v/v).

[b]Final sample concentration 4 μg/ml.

[c]Mean±standard error (n=3).

Table 2-2-3-8. DPPH radical scavenging activity of compound **10** obtained after PLC of fraction 7.5.[a]

Fraction	R_f Value	Yield (mg)	DPPH Radical Scavenging (%)[b,c]
7.5.1 (Compound **R10**)	0.5	10.5	51.2±0.1

[a]Developing solvent, Toluene:EtOAc:AA, 10:10:1 (v/v/v).

[b]Final sample concentration 5 μg/ml.

[c]Mean±standard error (n=3).

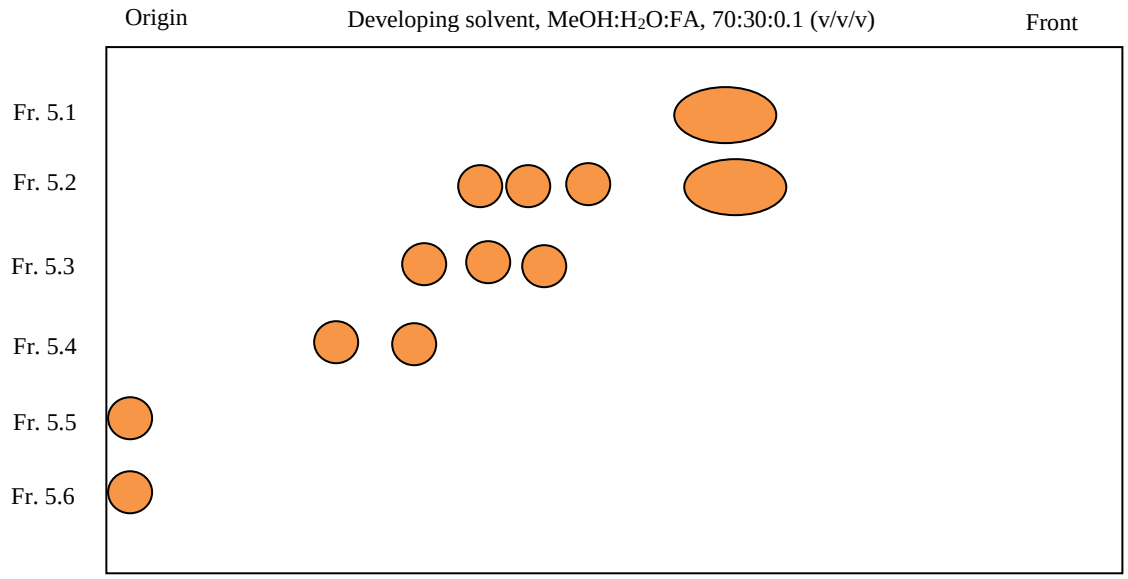

Figure 2-2-3-1. RP-TLC chromatogram of individual fractions obtained after reverse phase column chromatography of fraction 5. Spots were visualized after spraying with 5% H_2SO_4.

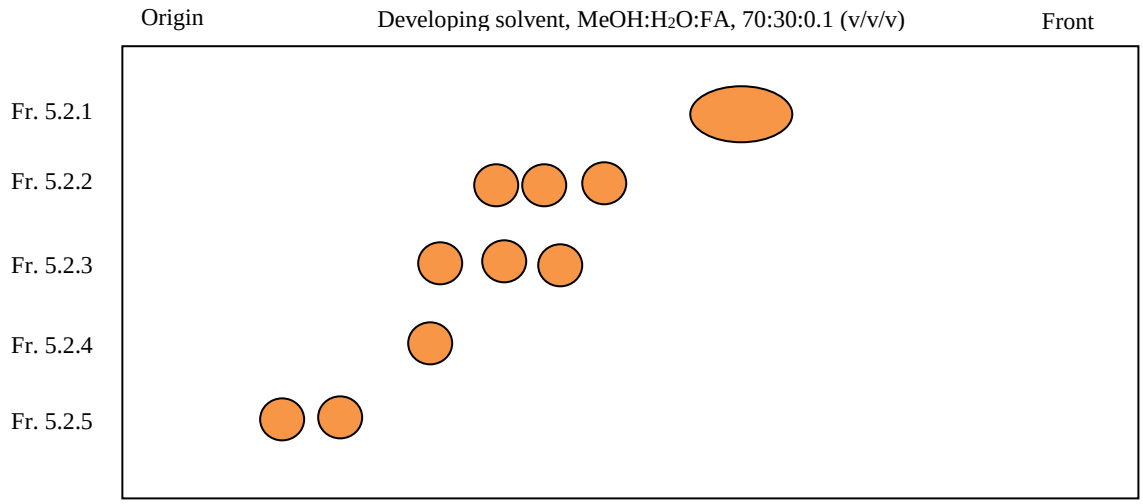

Figure 2-2-3-2. RP-TLC chromatogram of individual fractions obtained after Sephadex LH-20 of fraction 5.2. Spots were visualized after spraying with 5% H_2SO_4.

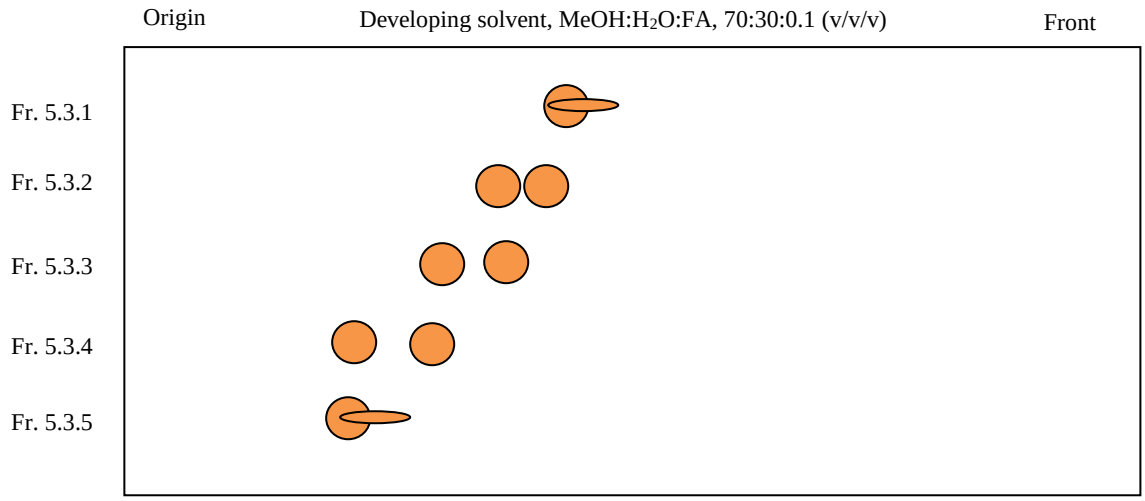

Figure 2-2-3-3. RP-TLC chromatogram of individual fractions obtained after Sephadex LH-20 of fraction 5.3. Spots were visualized after spraying with 5% H_2SO_4.

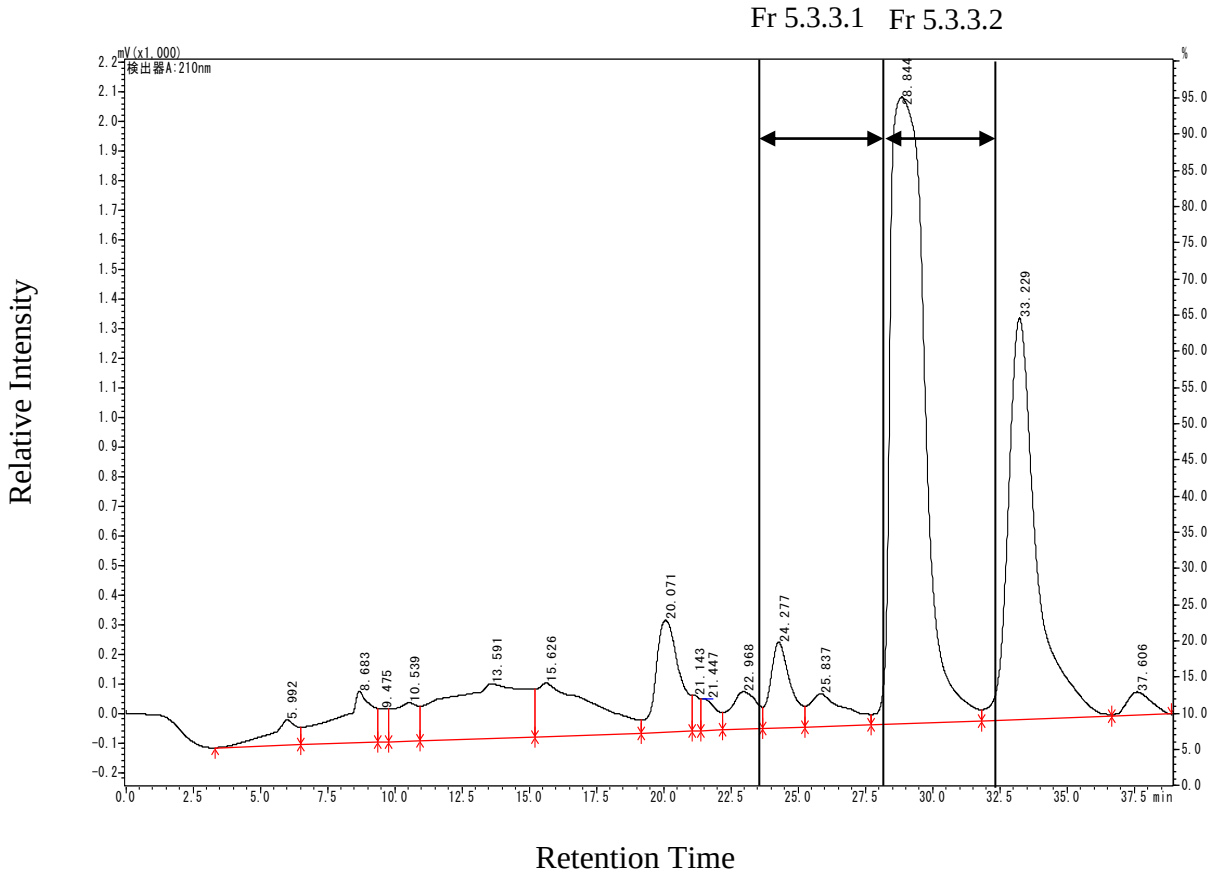

Figure 2-2-3-4. HPLC chromatogram of fraction 5.3.3. Column: Mightysil RP-18 250-4.6 (5 μm); eluent: 70% aqueous MeOH; flow rate: 0.5 ml/min; detection: UV 210 nm.

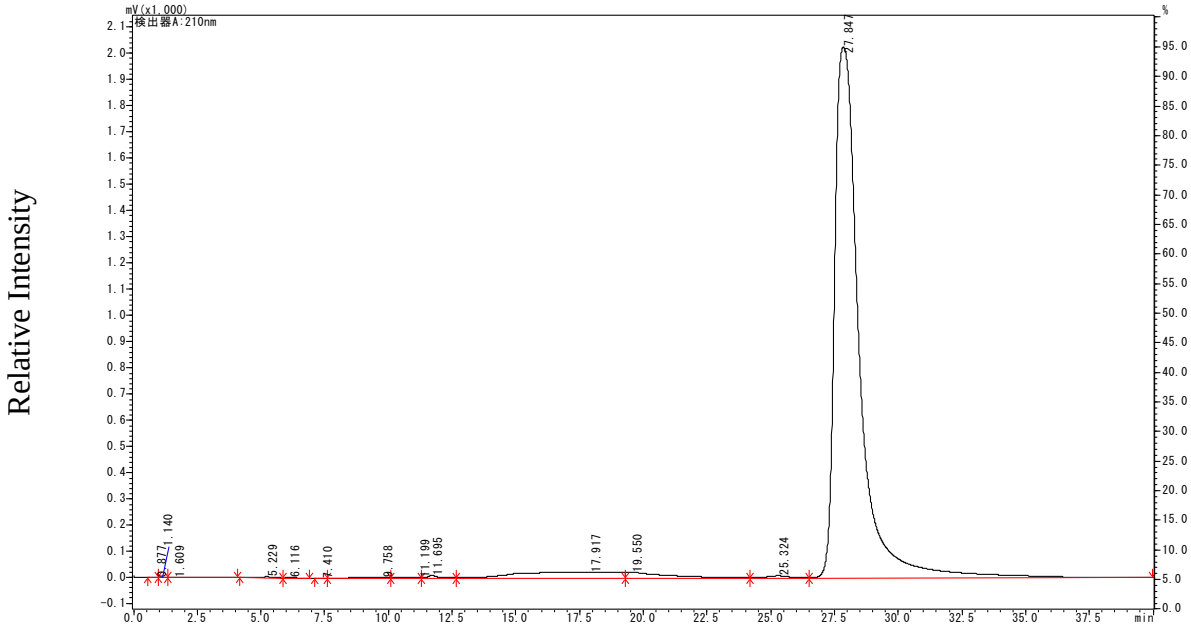

Figure 2-2-3-5. HPLC chromatogram of fraction 5.3.3.1 (compound **R6**). Column: Mightysil RP-18 250-4.6 (5 μm); eluent: 70% aqueous MeOH; flow rate: 0.5 ml/min; detection: UV 210 nm.

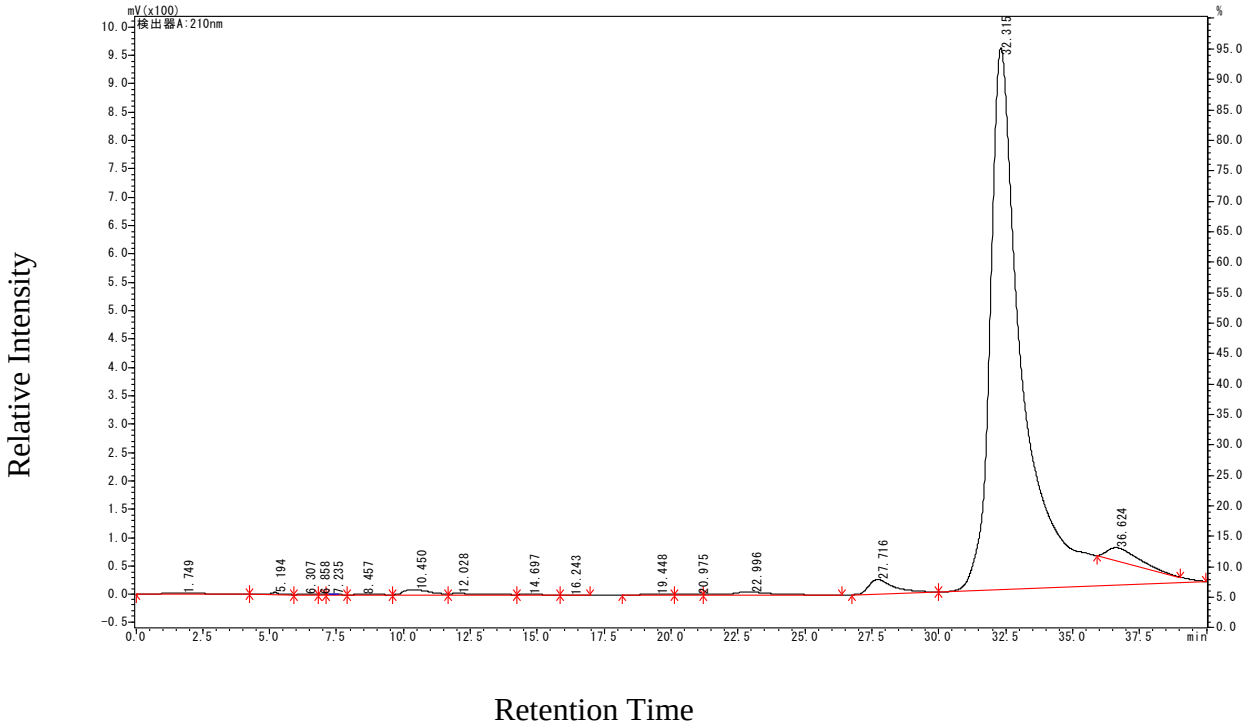

Figure 2-2-3-6. HPLC chromatogram of fraction 5.3.3.2 (compound **R7**). Column: Mightysil RP-18 250-4.6 (5 μm); eluent: 70% aqueous MeOH; flow rate: 0.5 ml/min; detection: UV 210 nm.

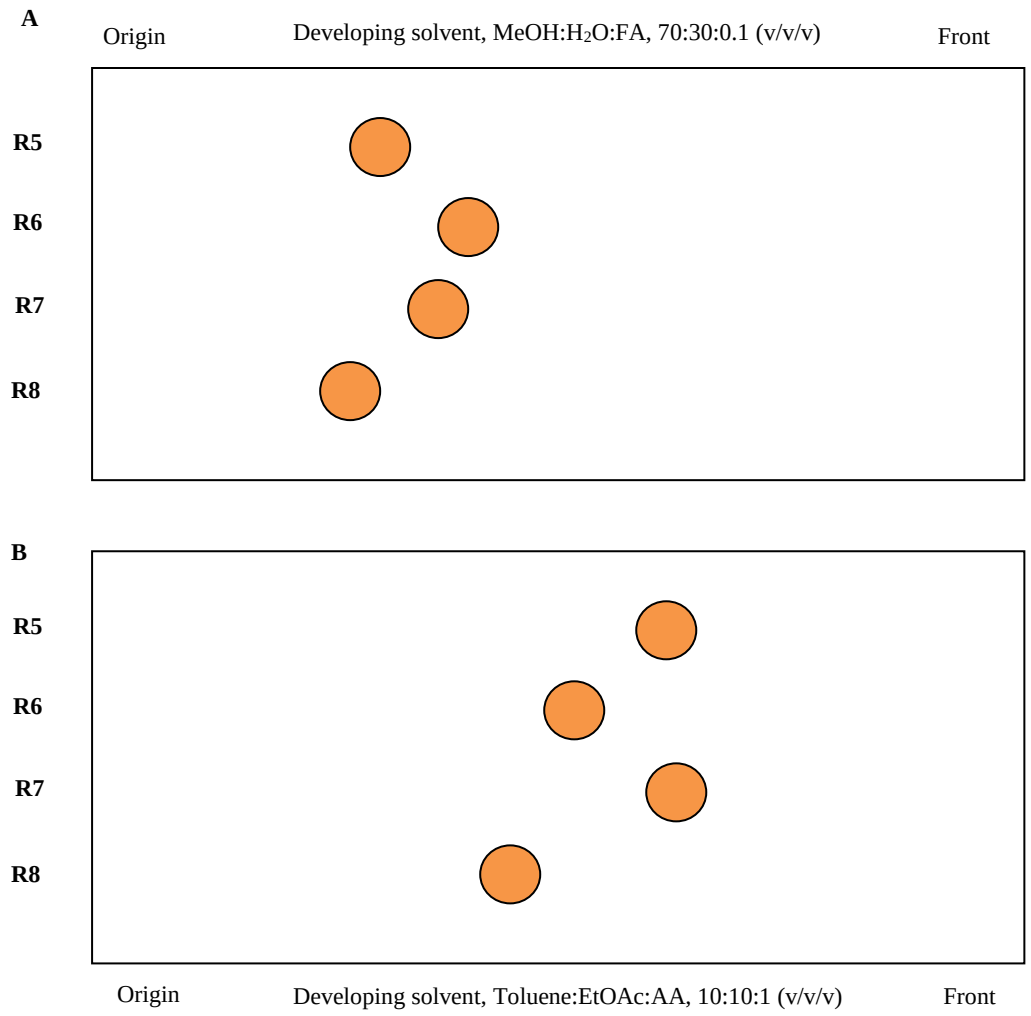

Figure 2-2-3-7. **A**. RP-TLC and **B**. NP-TLC chromatogram of compounds **R5-R8**. Spots were visualized after spraying with 5% H_2SO_4.

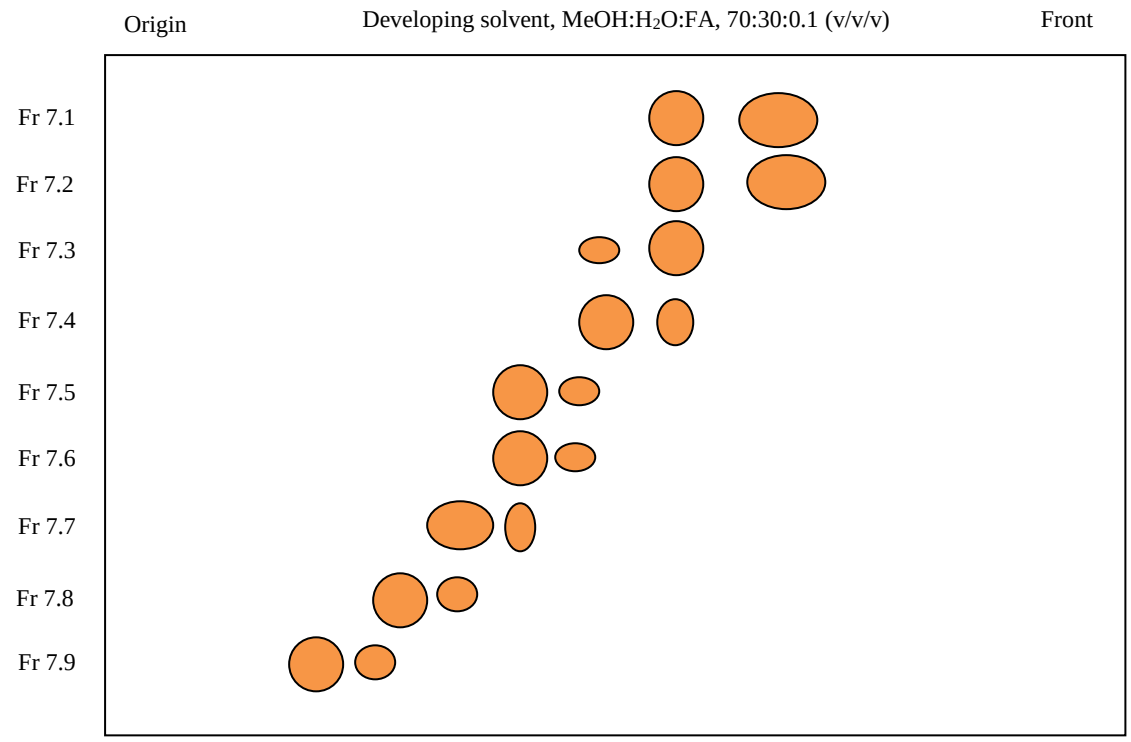

Figure 2-2-3-8. RP-TLC chromatogram of individual fractions obtained after reverse phase column chromatography of fraction 7. Spots were visualized after spraying with 5% H_2SO_4.

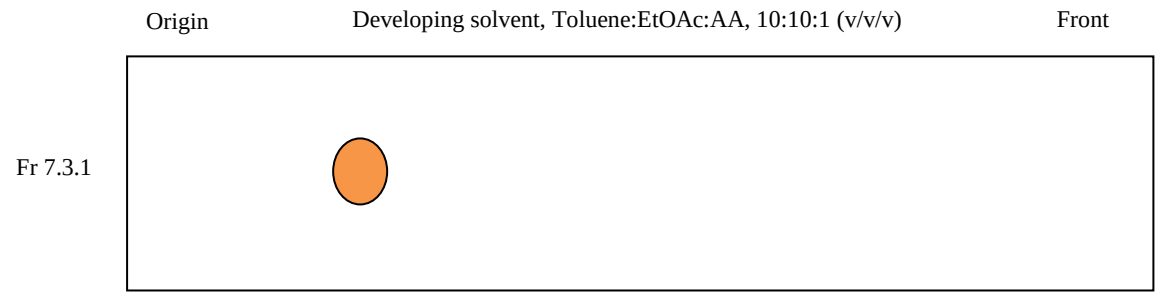

Figure 2-2-3-9. RP-TLC chromatogram of fraction obtained after PLC of fraction 7.3. Spots were visualized after spraying with 5% H_2SO_4.

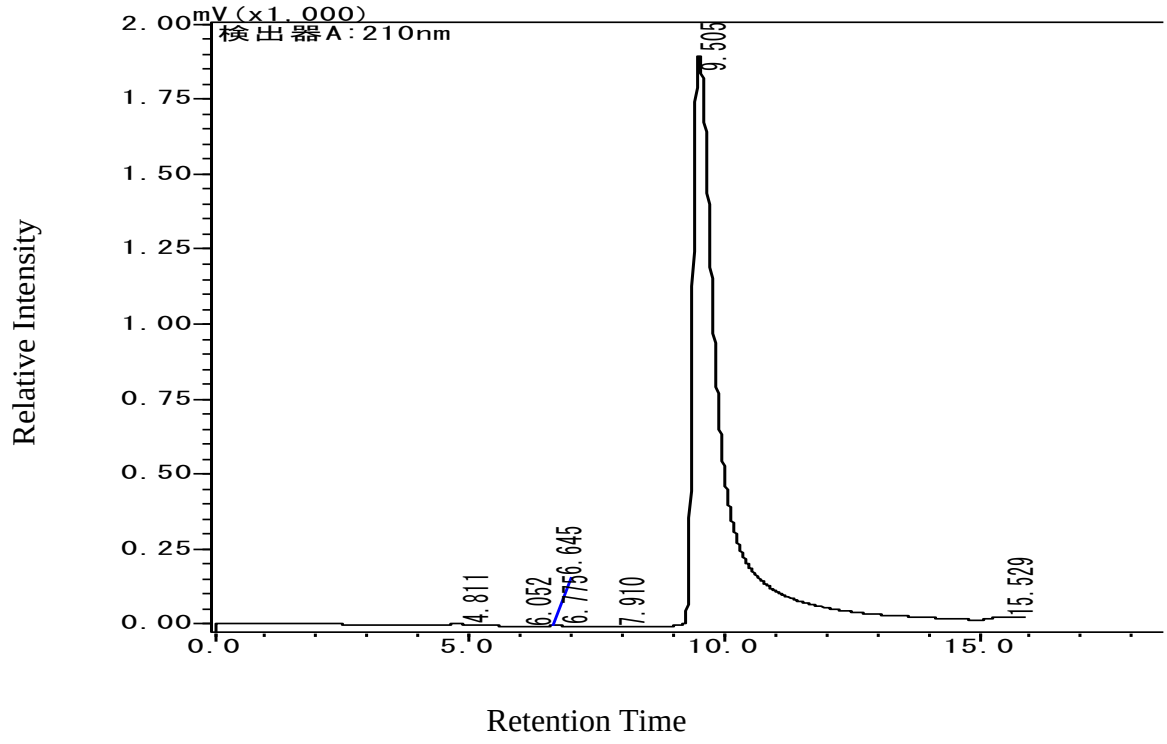

Figure 2-2-3-10. HPLC chromatogram of fraction 7.3.1 (compound **R9**). Column: Mightysil RP-18 250-4.6 (5 μm); eluent: 70% aqueous MeOH; flow rate: 0.5 ml/min; detection: UV 210 nm.

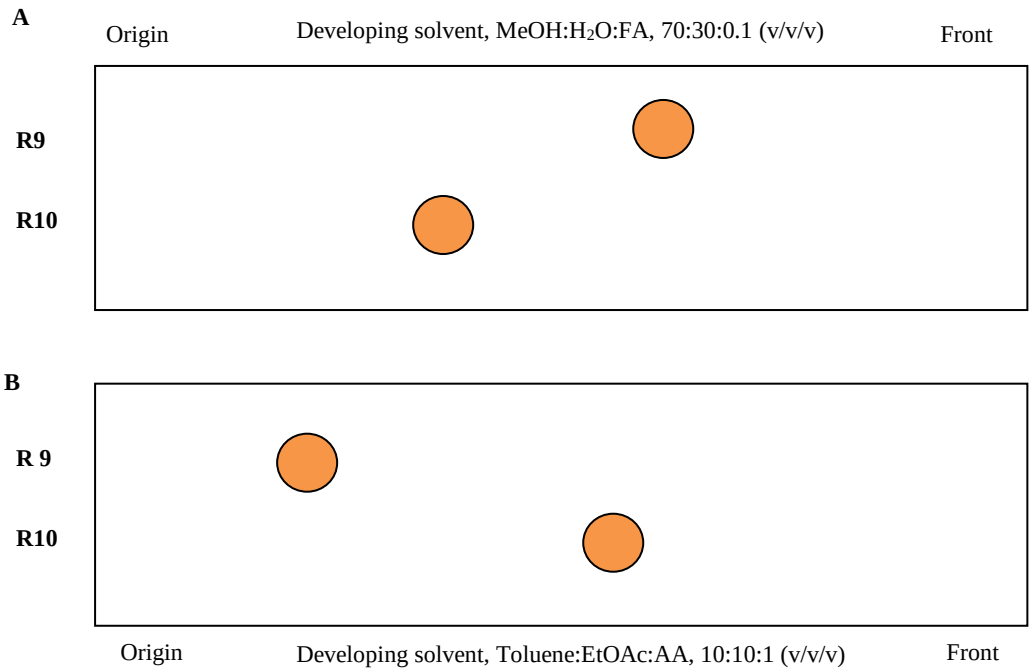

Figure 2-2-3-11. **A**. RP-TLC and **B**. NP-TLC chromatogram of compounds **R9** and **R10**. Spots were visualized after spraying with 5% H_2SO_4.

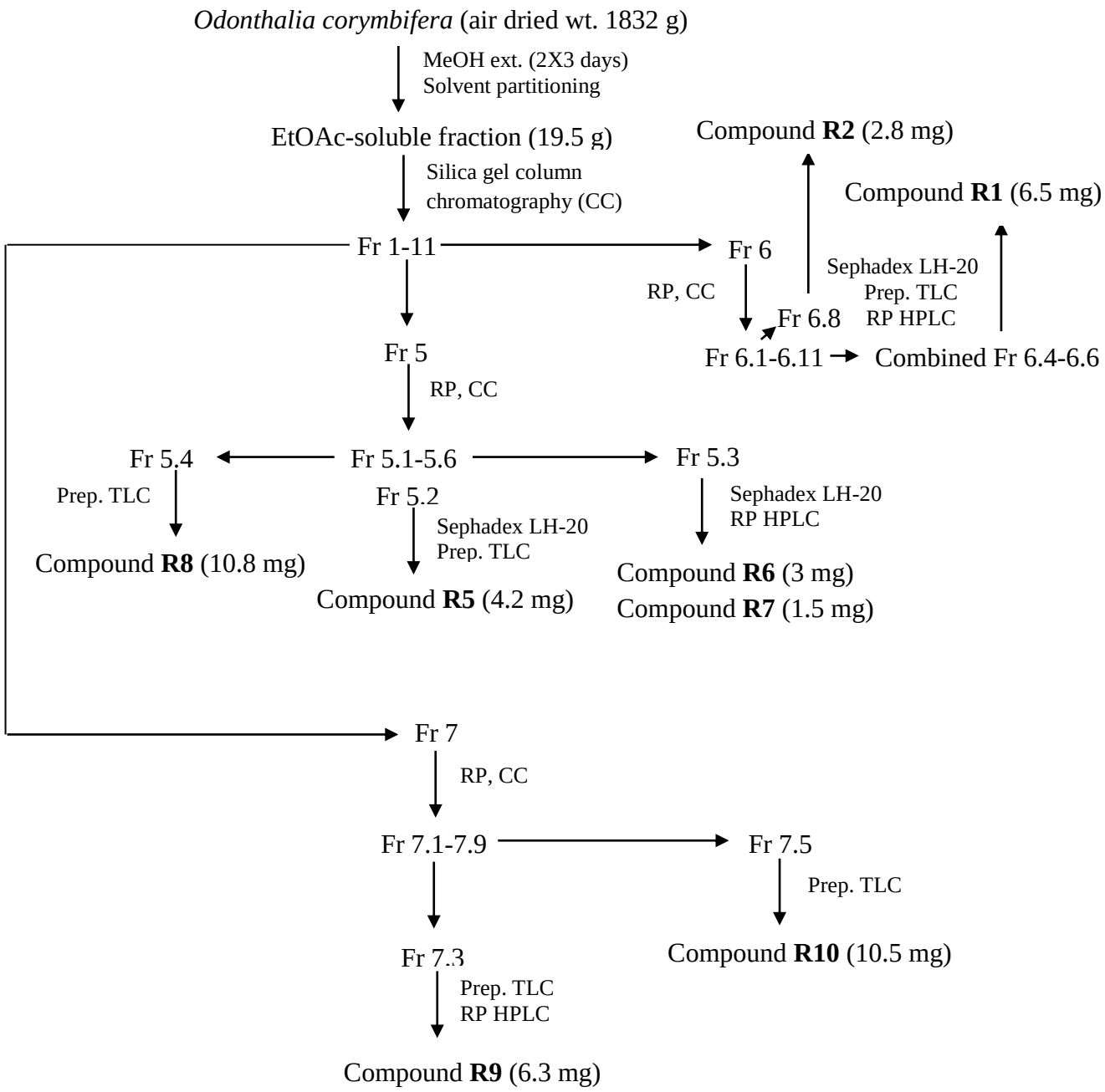

Figure 2-2-3-12. Bromophenols isolation scheme of *O. corymbifera*.

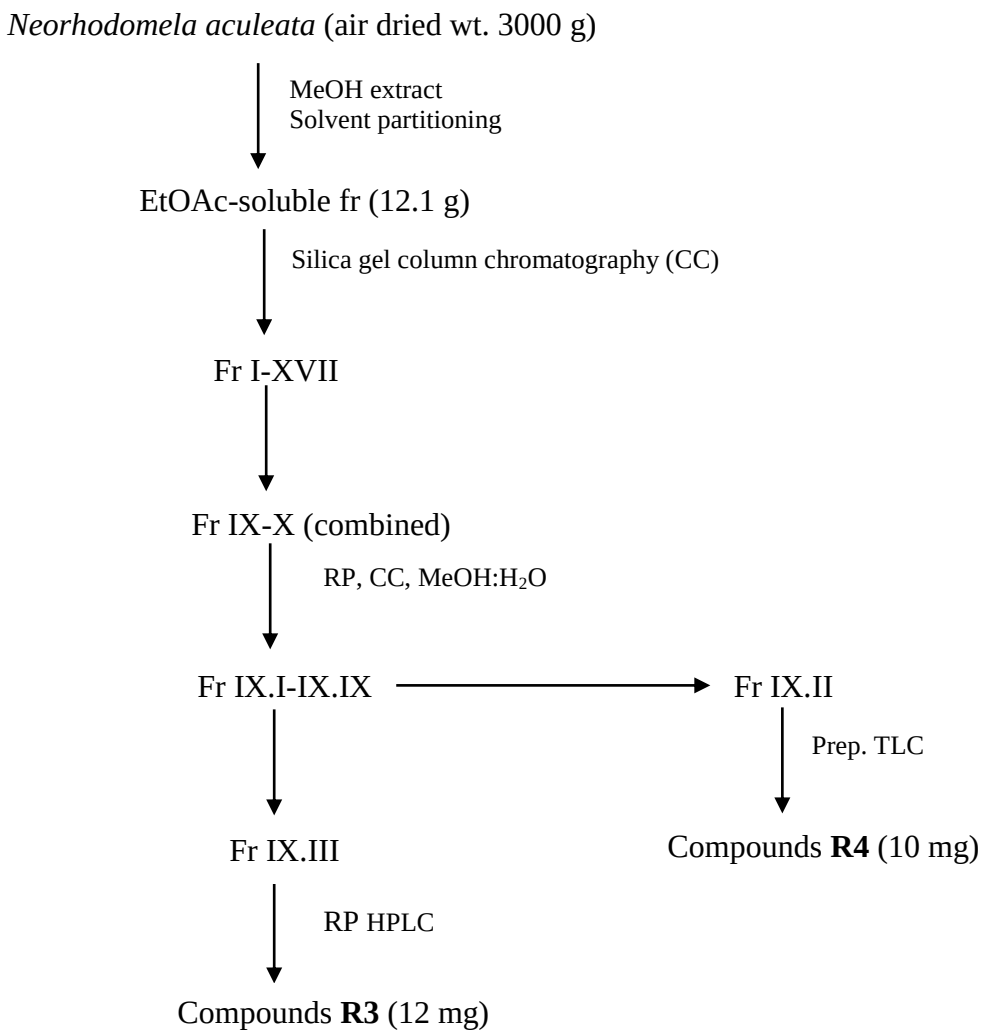

Figure 2-2-3-13. Bromophenols isolation scheme of *N. aculeata*.

2.3. Results and Discussion

2.3.1. Structural Elucidation of Compounds **R3** and **R4**

Compound **R3** was purified as light brown sticky substance. Presence of two bromine atom was confirmed from the molecular ion cluster at *m/z* 296/298/300 with a ratio of 1:2:1 (Figure 2-3-1-2). From its FD-MS analysis, the molecular formula was determined as $C_7H_6{}^{79}Br_2O_3$ at *m/z* 295.8694 (calcd for 295.8684). The ^{1}H NMR spectrum of compound **R3** in acetone-d_6 showed the presence of a single aromatic compound at δ_H 7.18 ppm and a methylene group at δ_H 4.56 ppm on a catechol (Table 2-3-1-1). The methylene ^{13}C signals assigned at 65.04 ppm while six aromatic carbon signals found at 113.4-145.6 ppm (Figures 2-3-1-3 to 2-3-1-6). The structure of compound **R3** was determined as 2,3-dibromo-4,5-dihydroxybenzyl alcohol (lanosol) (Figure 2-3-1-1) [56].

Compound **R4** was purified as brown sticky substance. The molecular ion cluster at *m/z* 310/312/314 with a ratio of 1:2:1 (Figure 2-3-1-8) revealed presence of two bromine atom. From its FD-MS analysis, the molecular formula was determined as $C_8H_8{}^{79}Br_2O_3$ at *m/z* 309.88406 (calcd for 309.88402). The ^{1}H NMR spectrum of compound **R4** in acetone-d_6 showed the presence of a single aromatic compound at δ_H 7.06 ppm and a methylene group at δ_H 4.40 ppm on a catechol (Table 2-3-1-2). A methoxy proton signal found at δ_H 3.38 ppm. The methylene ^{13}C signals assigned at 75.08 ppm; one methoxy carbon signal at 58.36 ppm while six aromatic carbon signals found at 113.4-145.6 ppm (Figures 2-3-1-9 to 2-3-1-12). The structure of compound **R4** was determined as 2,3-dibromo-4,5-dihydroxybenzyl methyl ether (Figure 2-3-1-7) [56].

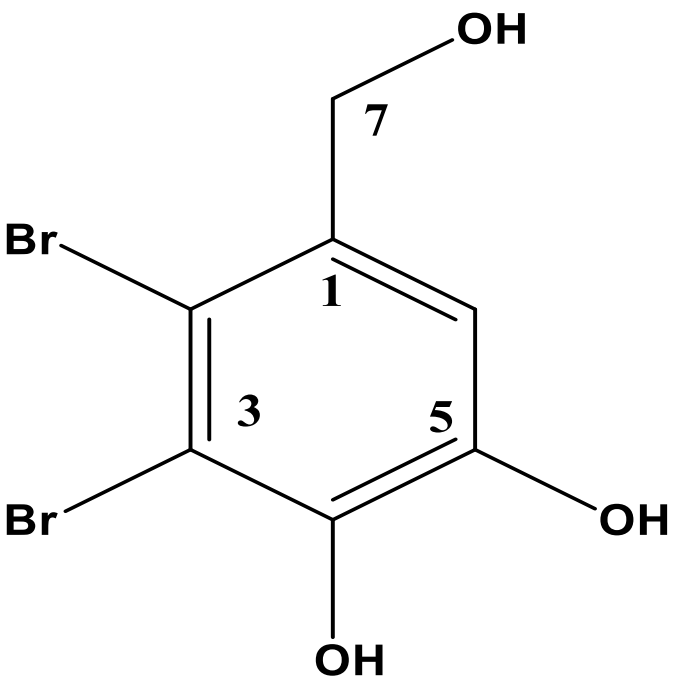

Figure 2-3-1-1. Structure of 2,3-dibromo-4,5-dihydroxybenzyl alcohol (lanosol) (compound **R3**).

Table 2-3-1-1. Comparison of compound **R3** observed and literature NMR data [56].

No.	^{1}H NMR (δ_H, ppm)		^{13}C NMR (δ_C, ppm)	
	Observed data	Literature data	Observed data	Literature data
1			135.1	134.1
2			113.5[a]	112.6
3			113.4[a]	112.4
4			145.6[b]	143.1
5			143.9[b]	144.8
6	7.18 (s, 1H)	7.20 (s, 1H)	114.6	113.7
7	4.56 (s, 2H)	4.62 (s, 2H)	65.0	64.2

[a,b]Data are interchangeable.

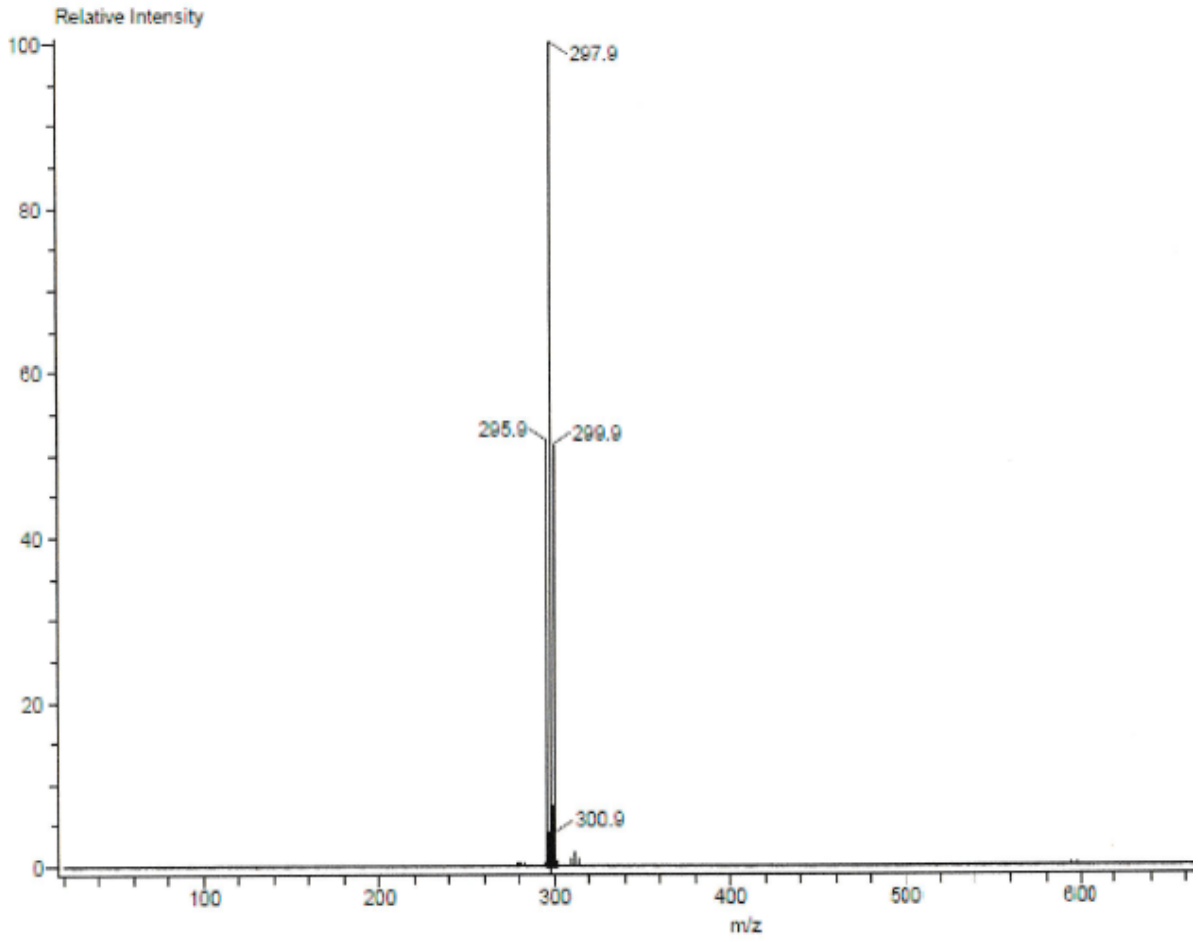

Figure 2-3-1-2. FD-MS spectrum of compound **R3**.

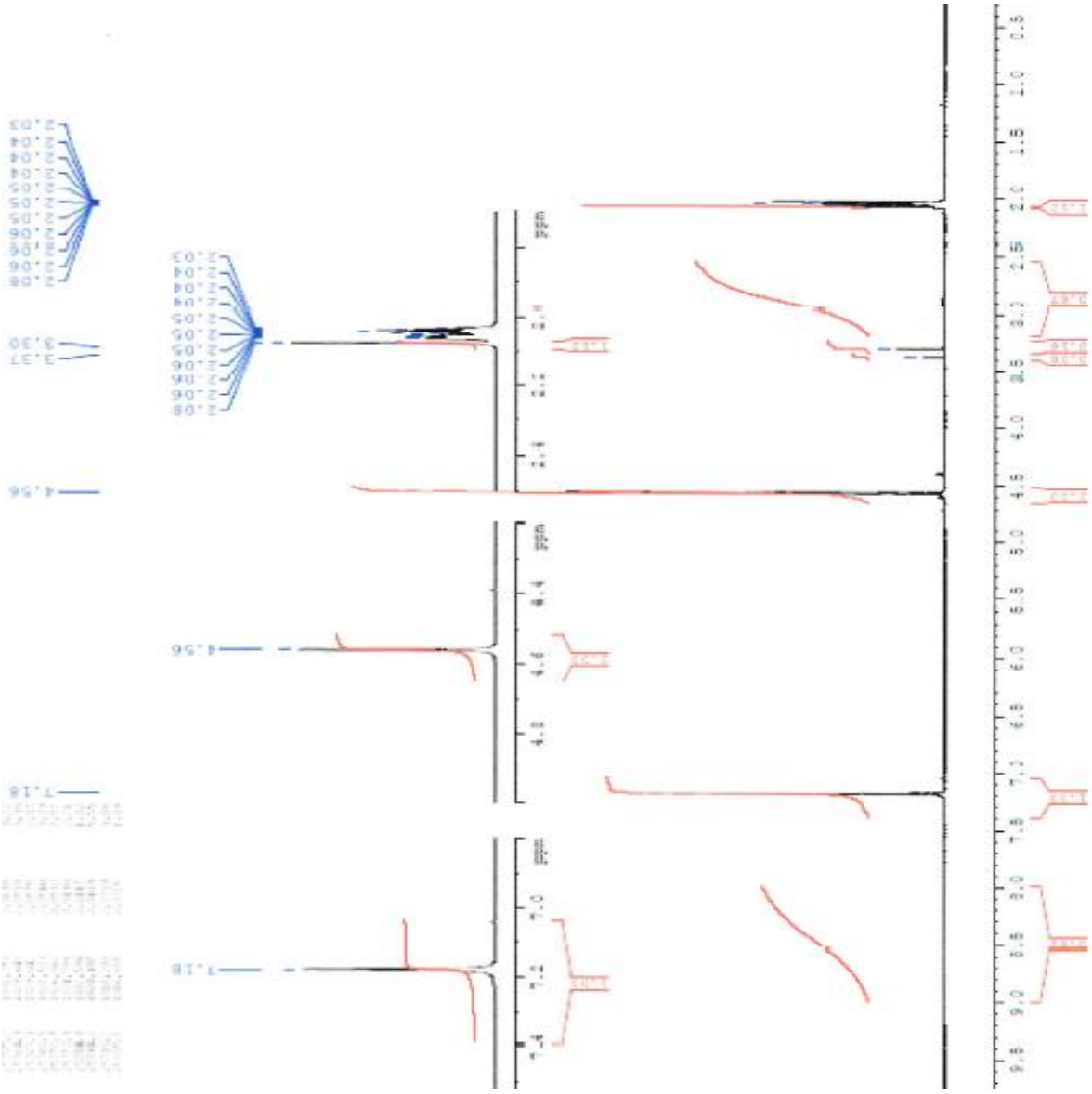

Figure 2-3-1-3. ^{1}H-NMR spectrum of compound **R3** (acetone-d_6, 500 MHz).

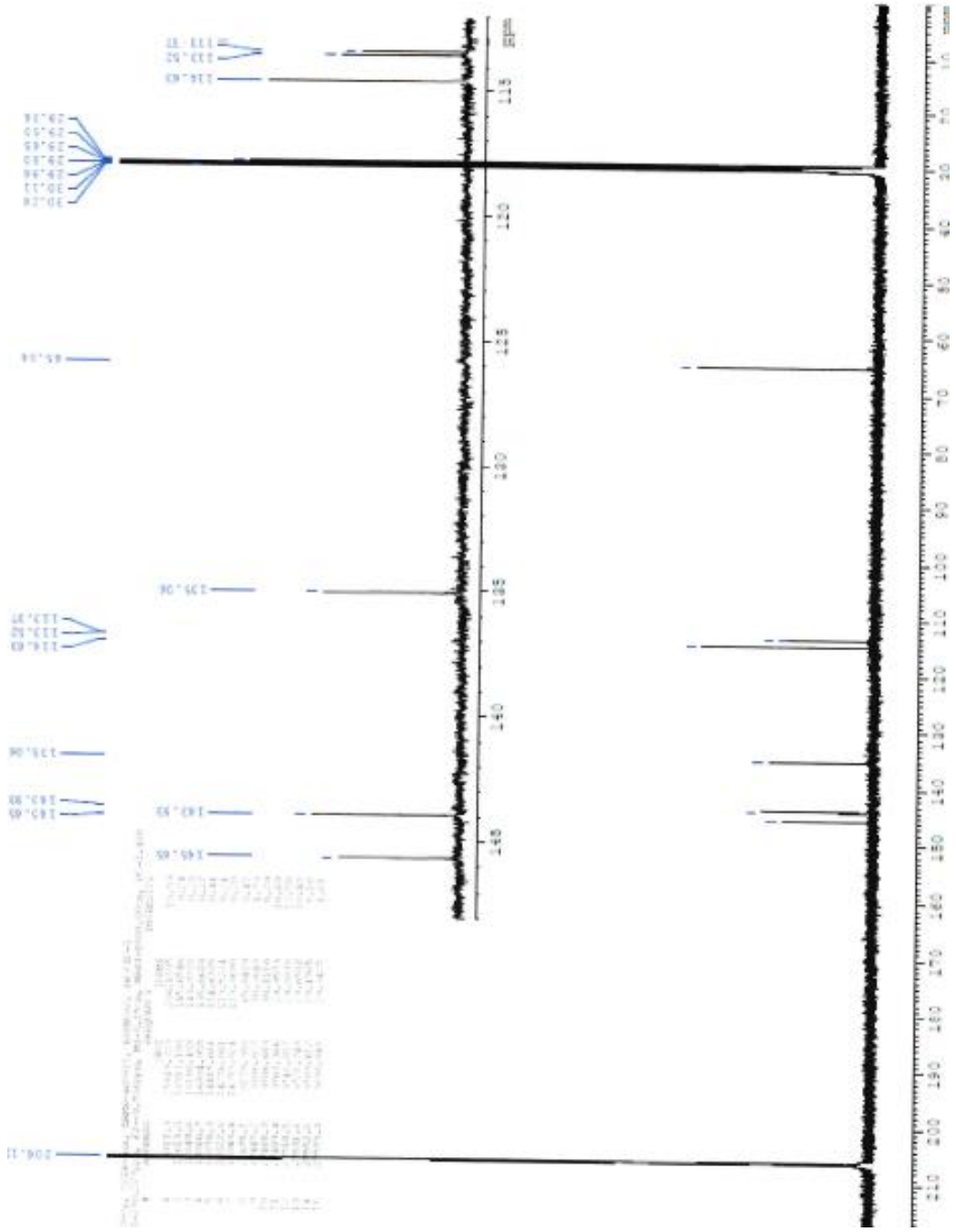

Figure 2-3-1-4. ^{13}C-NMR spectrum of compound **R3** (acetone-d_6, 125 MHz).

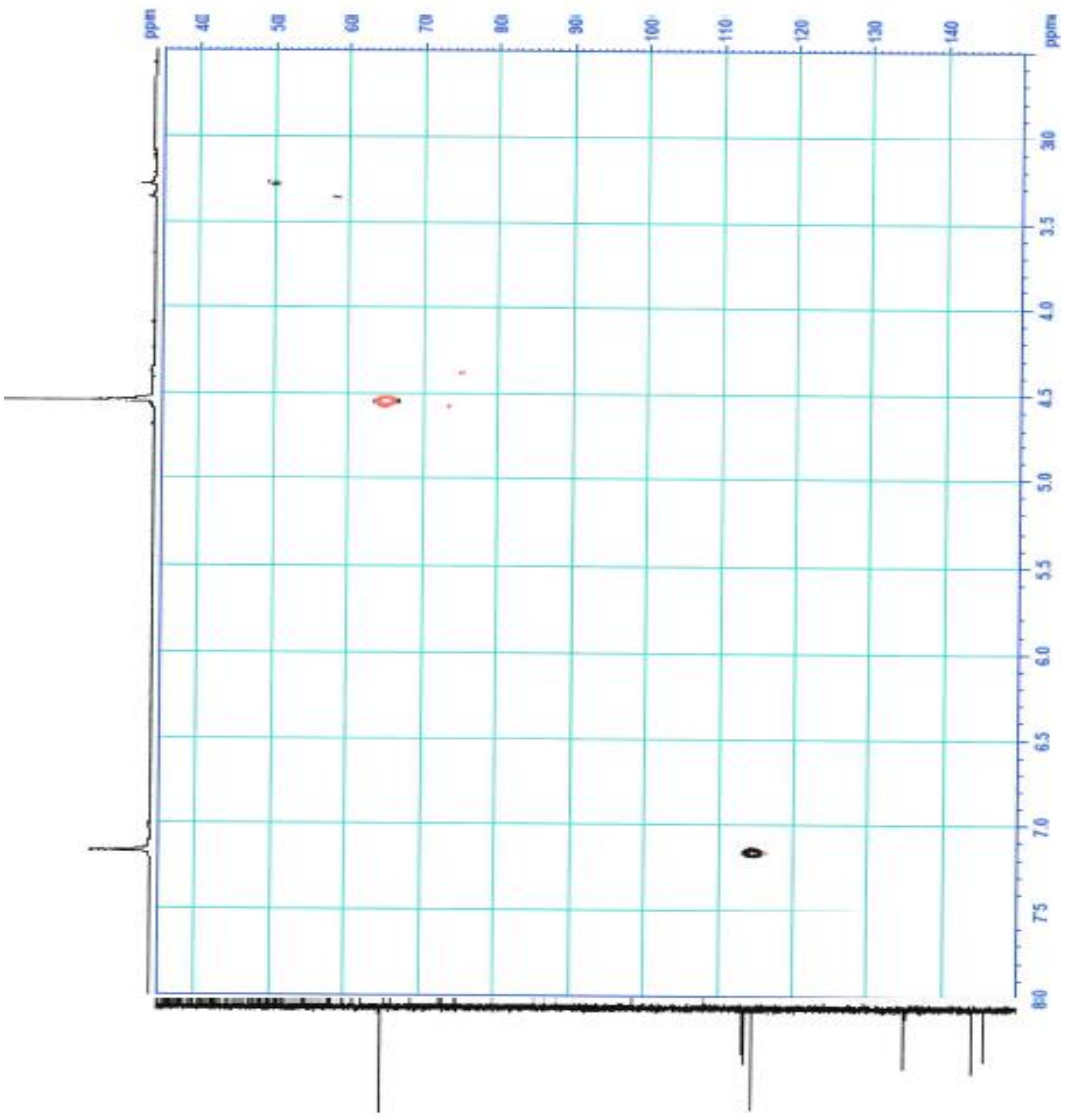

Figure 2-3-1-5. Editing HSQC spectrum of compound **R3**.

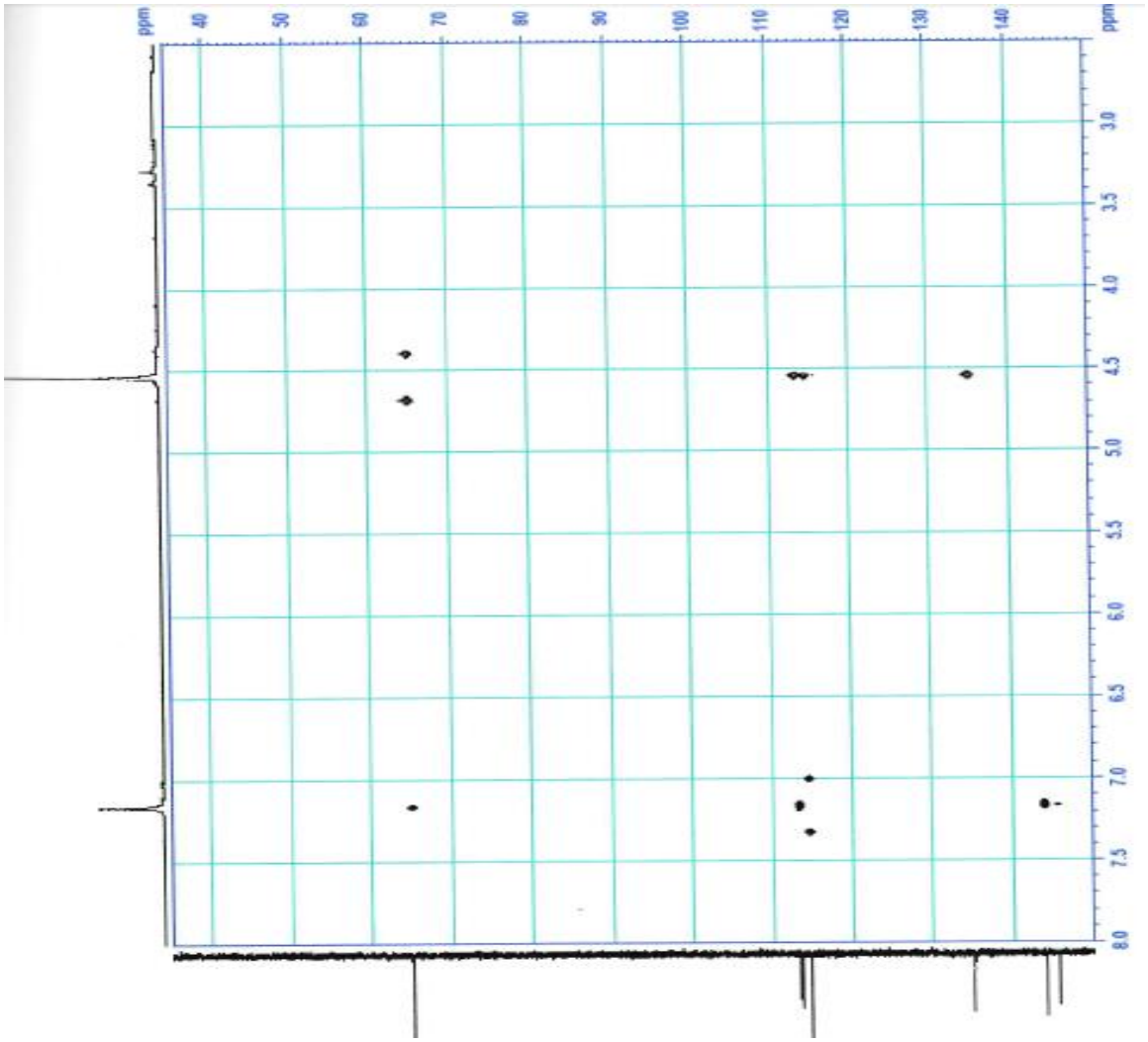

Figure 2-3-1-6. HMBC spectrum of compound **R3**.

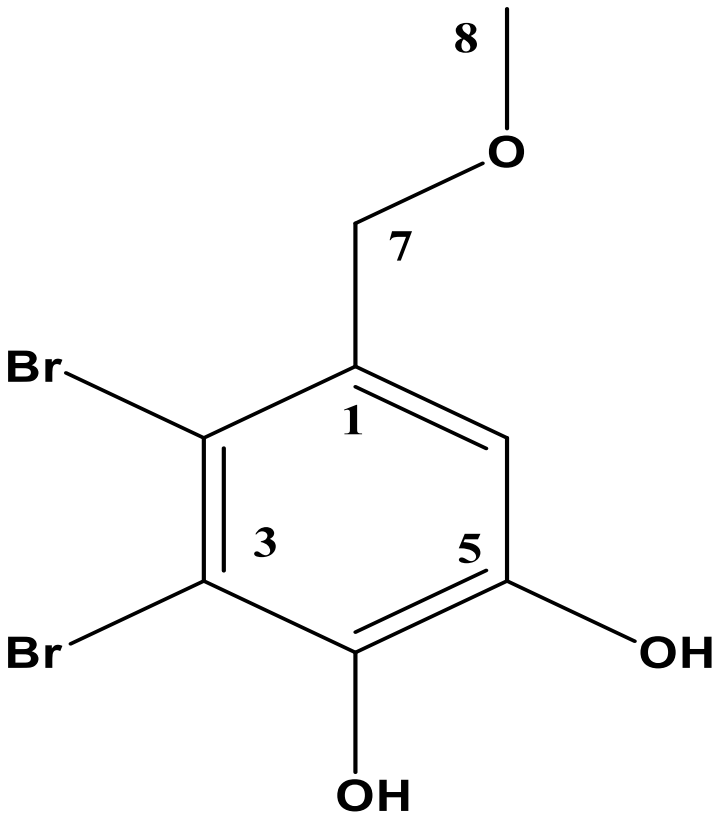

Figure 2-3-1-7. Structure of 2,3-dibromo-4,5-dihydroxybenzyl methyl ether (compound **R4**).

Table 2-3-1-2. Comparison of compound **R4** observed and literature NMR data [56].

No.	^{1}H NMR (δ_H, ppm)		^{13}C NMR (δ_C, ppm)	
	Observed data	Literature data	Observed data	Literature data
1			131.5	131.6
2			114.4	114.8
3			113.6	114.4
4			144.5	143.7
5			145.6	144.9
6	7.06 (s, 1H)	7.07 (s, 1H)	115.3	114.8
7	4.40 (s, 2H)	4.41 (s, 2H)	75.1	75.0
8	3.38 (s, 3H)	3.39 (s, 3H)	58.3	58.4

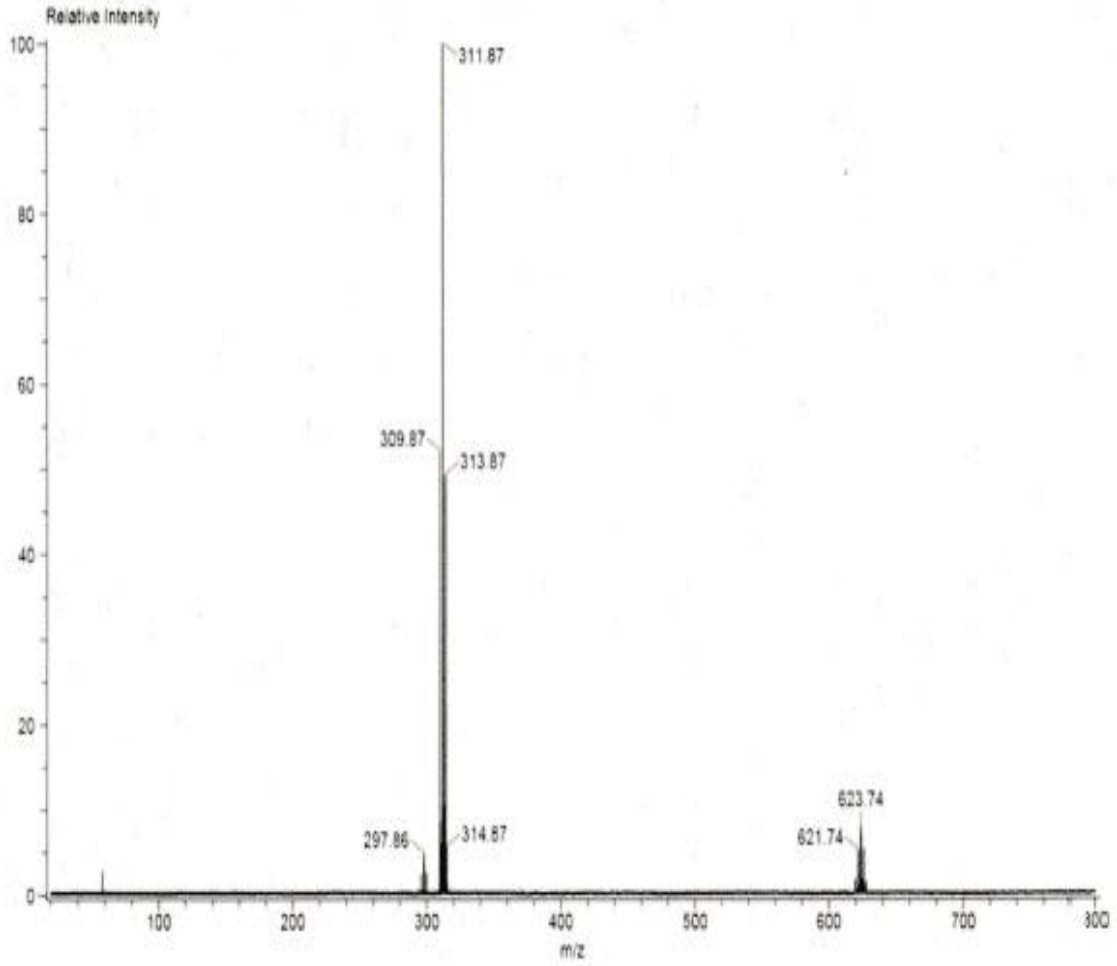

Figure 2-3-1-8. FD-MS spectrum of compound **R4**.

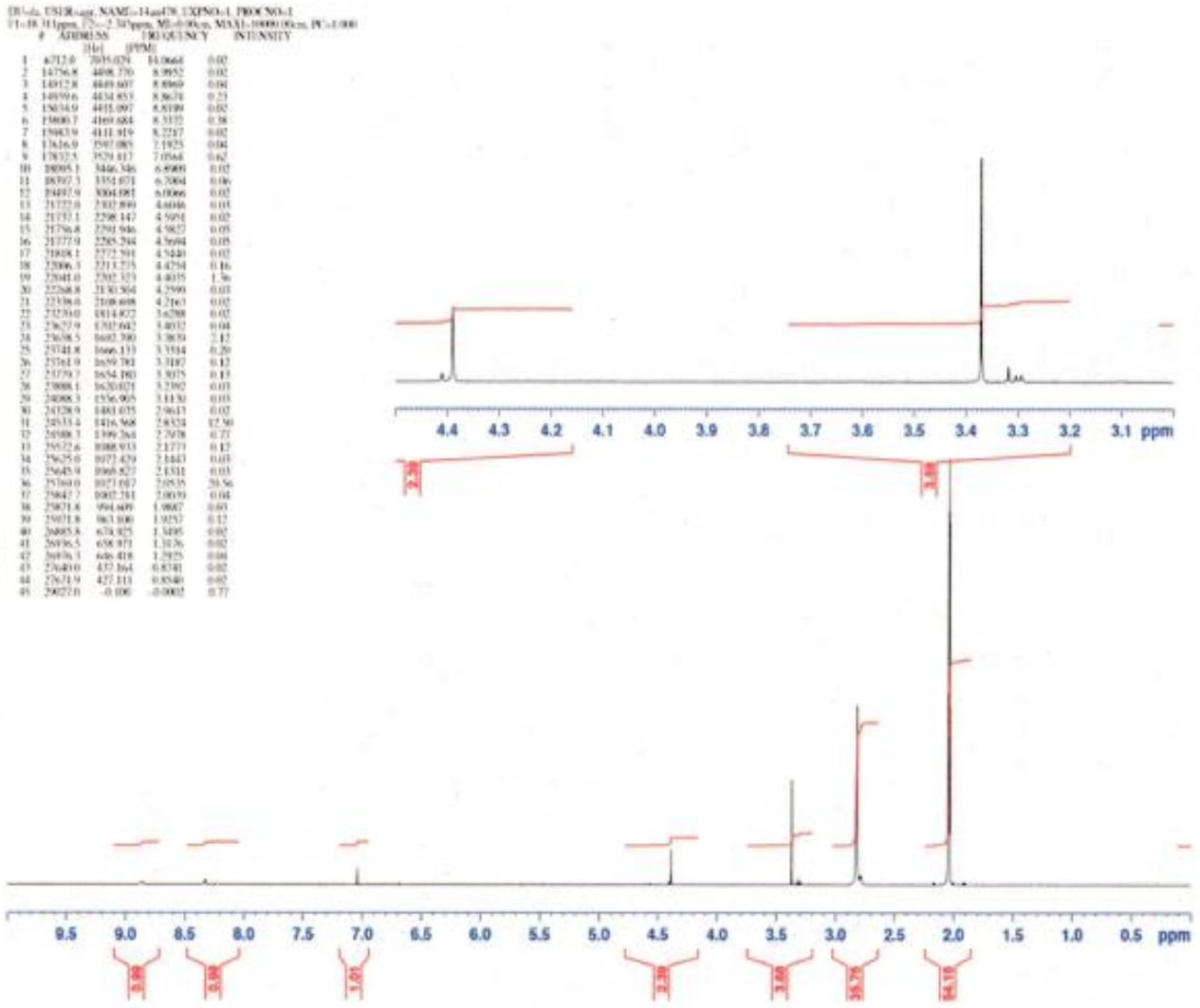

Figure 2-3-1-9. ^{1}H-NMR spectrum of compound **R4** (acetone-d_6, 500 MHz).

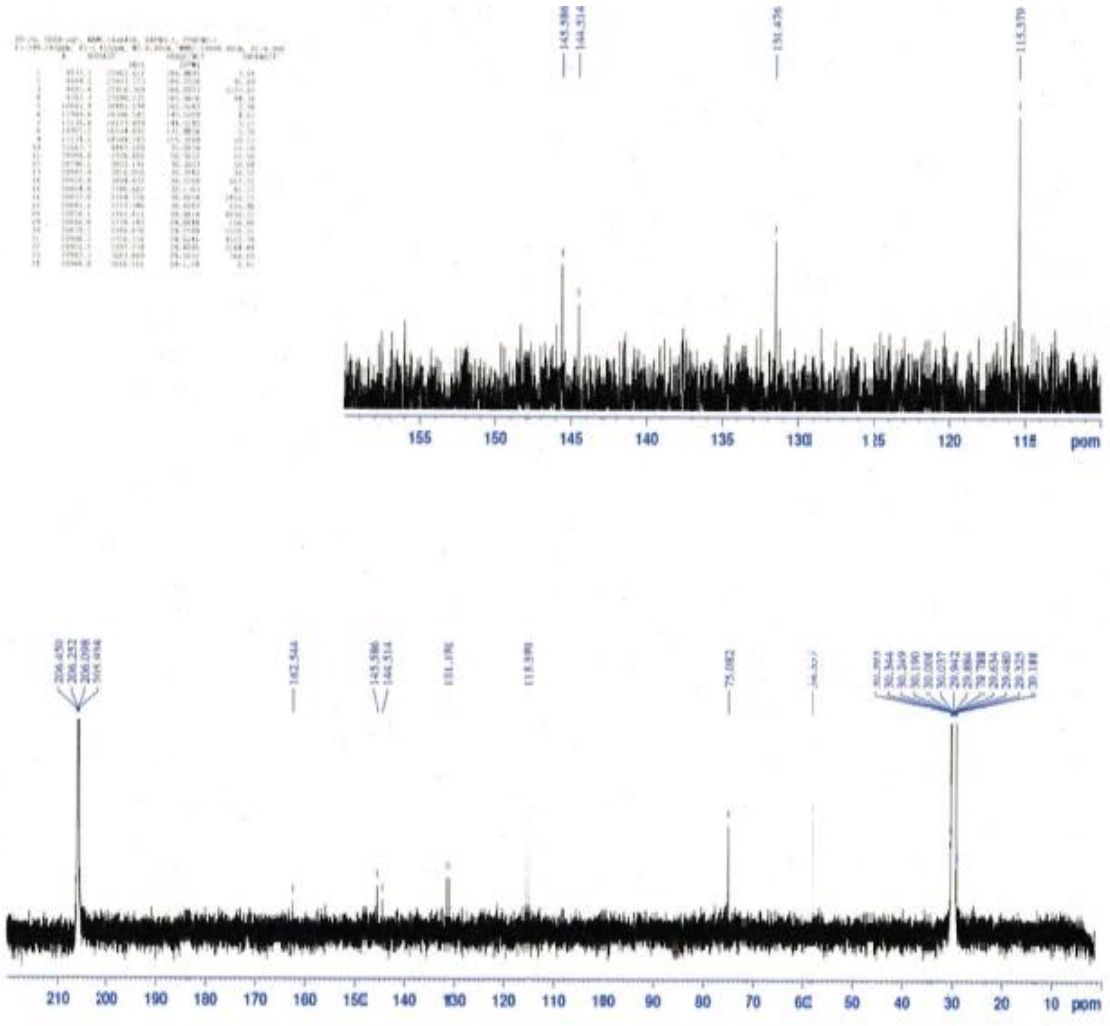

Figure 2-3-1-10. ^{13}C-NMR spectrum of compound **R4** (acetone-d_6, 125 MHz).

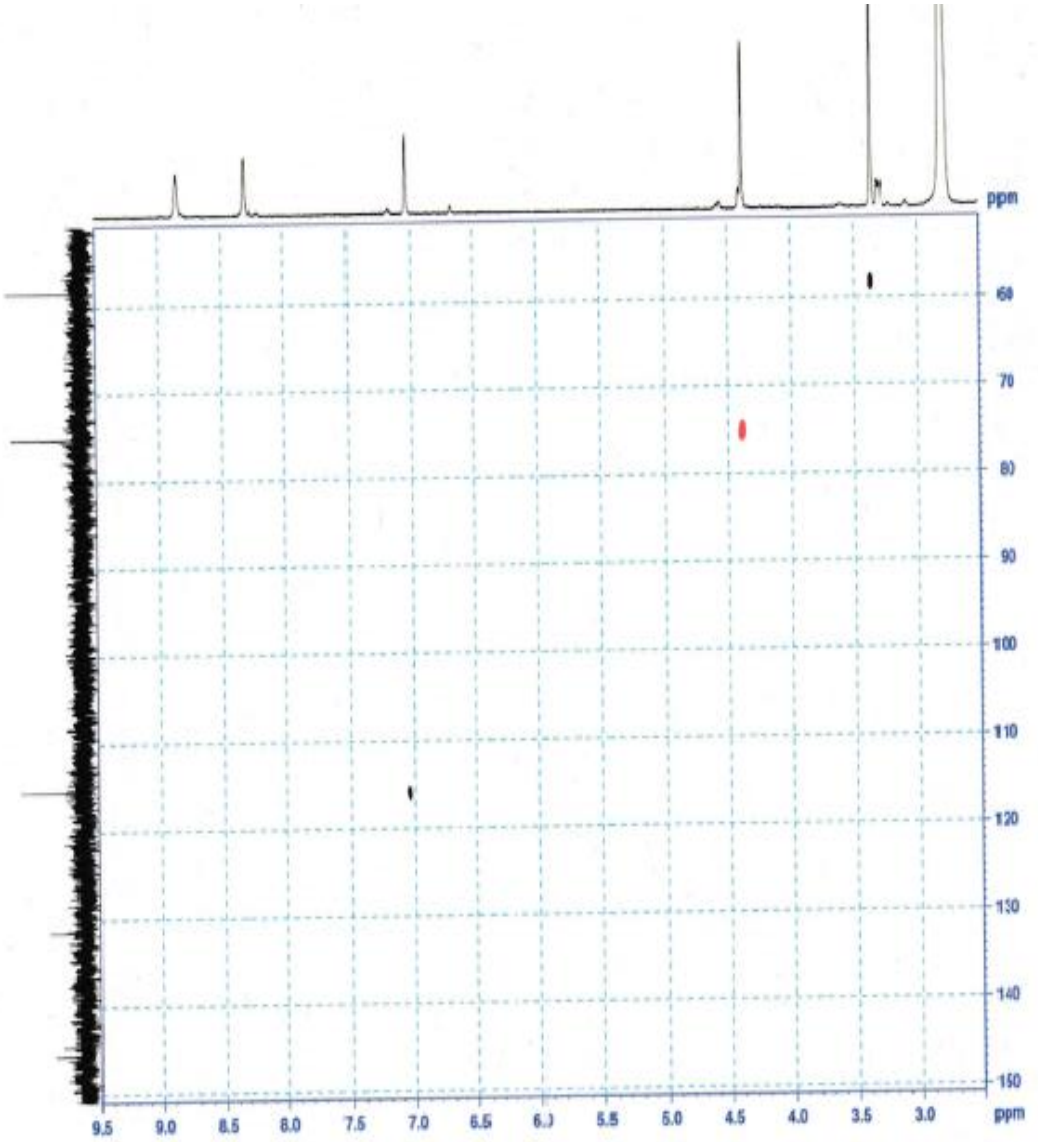

Figure 2-3-1-11. Editing HSQC spectrum of compound **R4**.

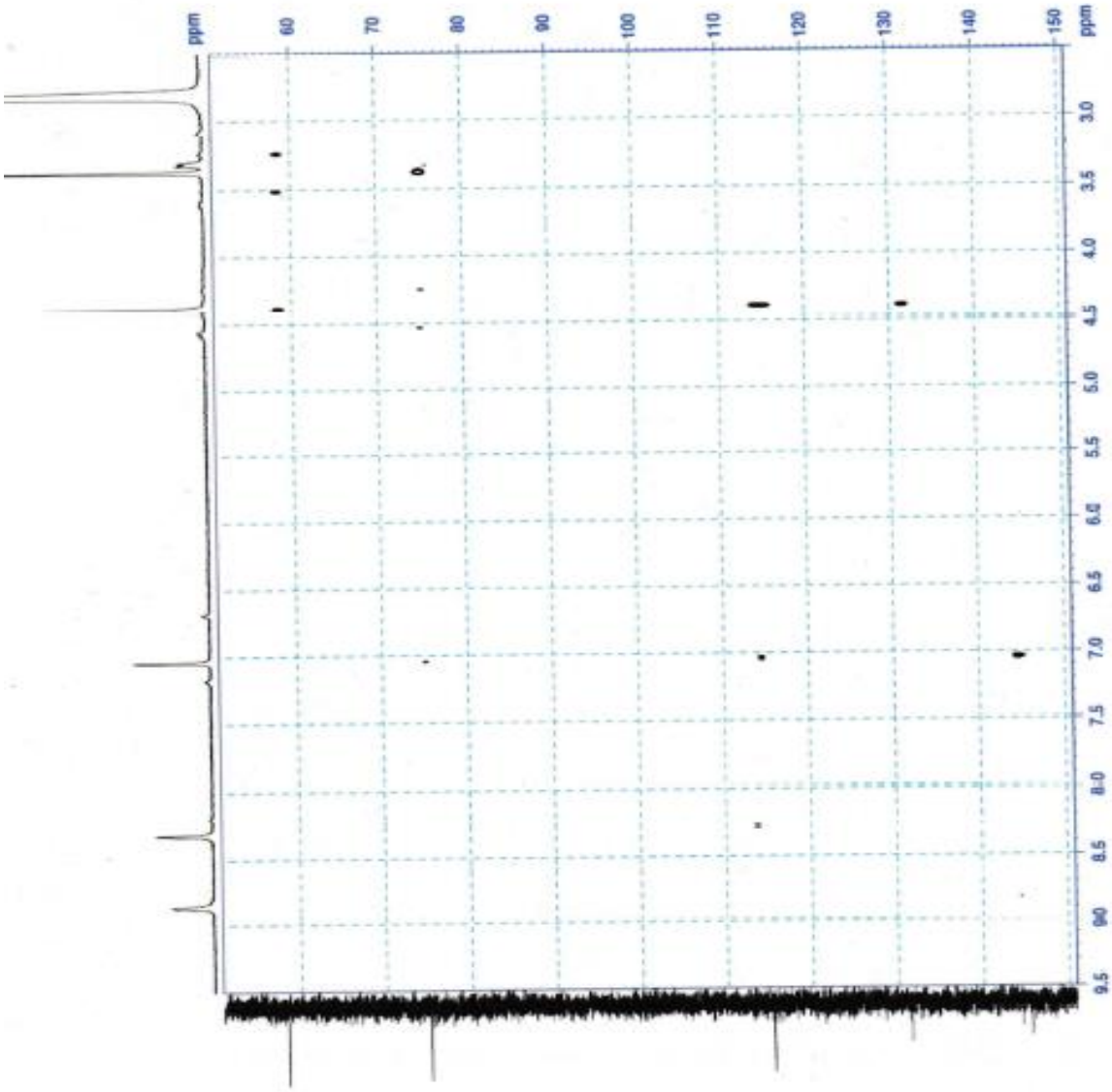

Figure 2-3-1-12. HMBC spectrum of compound **R4**.

2.3.2. Structural Elucidation of Compounds **R5**, **R6**, **R7** and **R8**

Compound **R5** was purified as brown sticky substance. Presence of bromine atom was confirmed from the molecular ion cluster at *m/z* 544/546/548/550/552 with a ratio of 1:4:6:4:1 (Figure 2-3-2-2). From its FD-HRMS analysis, the molecular formula was determined as $C_{13}H_8{}^{79}Br_4O_4$ at *m/z* 543.71720 (calcd for 543.71561). The ^{1}H NMR spectrum of compound **R5** in acetone-*d*$_6$ showed the presence of a single aromatic compound at δ_H 6.56 ppm (s, 2H, H-6, 6') and a methylene group at δ_H 4.04 ppm (s, 2H, H-7). The methylene ^{13}C signals assigned at 44.8 ppm while six aromatic carbon signals found at 113.9-145.6 ppm (Figures 2-3-2-3 to 2-3-2-6, Table 2-3-2-1). The structure of compound **R5** was determined as *bis* (2,3-dibromo-4,5-dihydroxyphenyl) methane (Figure 2-3-2-1) [56].

Compound **R6** was purified as light brown sticky substance. Charactristics molecular ion cluster indicate presence of bromine atom at *m/z* 510/512/514/516 with a ratio of 1:3:3:1 (Figure 2-3-2-8). From its FD-HRMS analysis, the molecular formula was determined as $C_{15}H_{13}{}^{79}Br_3O_4$ at *m/z* 509.8306 (calcd for 509.8313). The ^{1}H NMR spectrum of compound **R6** in methanol-*d*$_4$ showed the presence of two aromatic proton at δ_H 6.14 and 6.91 ppm. Two methylene proton at δ_H 4.41 and 4.14 ppm and one methoxy proton at 3.29 ppm. The methylene ^{13}C signals assigned at 75.6 and 38.2 ppm and methoxy carbon at 58.5 ppm, respectively while twelve aromatic carbon signals found at 114.0-146.1 ppm (Figures 2-3-2-9 to 2-3-2-12, Table 2-3-2-2). From the characteristics chemical shift suggested presence of typical 2,3-dibromo-4,5-dihydroxybenzyl moiety. HMBC correlations were observed from H-7' to C-8' and H-8' to C-7'. It established the position of methoxymethyl moiety. Connectivity of two units were determined from H-7 to C-1, C-2, C-6, C-2', C-3' and C-4'; H-7' to C-1', C-2' and C-6' of HMBC spectrum. Finally the structure of compound **R6** was determined as 2'-bromo-5',6'-dihydroxy-1'-(2,3-dibromo-4,5-dihydroxybenzyl)benzyl methyl ether (Figure 2-3-2-7) [55, 56, 69].

The FDMS of compound **R7** gave a characteristic tetrabrominated fragment ion peak at 588/590/592/594/596 (1:3:4:2:1) (Figure 2-3-2-14). The molecular formula was established as $C_{15}H_{12}{}^{79}Br_4O_5$ at 587.7404 (calcd 587.7418) by FD-HRMS analysis. The ^{1}H NMR spectrum showed four singlets at δ 6.12, 4.41, 4.11 and 3.30 ppm attributed to an aromatic proton, two methylenes and one methoxy moiety, respectively. The protonated carbon were assigned by HSQC experiment and the oxygenated quaternary carbons were recognized by the chemical shifts (δ>143 ppm) (Figures 2-3-2-15 to 2-3-2-18). All of the data revealed that

compound **R7** consists of one tetrasubstituted and one pentasubstituted benzyl moiety. The characteristics chemical shift of protons and carbons indicated the presence of the 2,3-dibromo-4,5-dihydroxybenzyl moiety. The HMBC correlations from H-7' to C-8' and H-8' to C-7' revealed presence of methoxymethyl moiety. In addition, the HMBC correlations from H-7 to C-1, C-2, C-6, C-1' and C-6'; H-7' to C-1', C-2' and C-6' established the connectivity between two units. The substitution patterns of the two benzyl moieties were confirmed by carefully comparing the NMR data of compound **R7** with those of the related compounds in the literature (Table 2-3-2-3) [36]. The structure of compound **R7** was determined as 2',3'-dibromo-4',5'-dihydroxy-6'-(2,3-dibromo-4,5-dihydroxybenzyl)benzyl methyl ether (Figure 2-3-2-13).

Compound **R8** was found to have four bromine atoms from the molecular ion peak cluster at *m/z* 574/576/578/580/582 in the FD-HRMS (Figure 2-3-2-20). The ^{13}C NMR spectrum showed six aromatic and one benzylic carbon signals. The HMBC experiment showed that the benzylic carbon (C-7) and proton (H-7) were coupled with the aromatic proton (H-6) and carbon (C-6), respectively (Figures 2-3-2-21 to 2-3-2-24, Table 2-3-2-4). These couplings revealed that the benzylic methylene group is located in an ortho-position to the aromatic proton. The brominated aromatic carbon at C-2 was coupled with the protons at H-6 and H-7, suggesting the presence of a Br atom at the other ortho-position of the benzylic methylene group. The aromatic proton at H-6 was coupled with two oxygenated aromatic carbons at C-4 and C-5. Thus, it was suggested that compound contains a 2,3-dibromo-4,5-dihydroxybenzyl moiety. A symmetrical structure was also confirmed by the HMBC correlations of compound **R8** since both long range couplings were observed between both the benzylic C-7 and H-7. Thus, the structure of compound **R8** was determined to be *bis*(2,3-dibromo-4,5-dihydroxybenzyl) ether (Figure 2-3-2-19) [49].

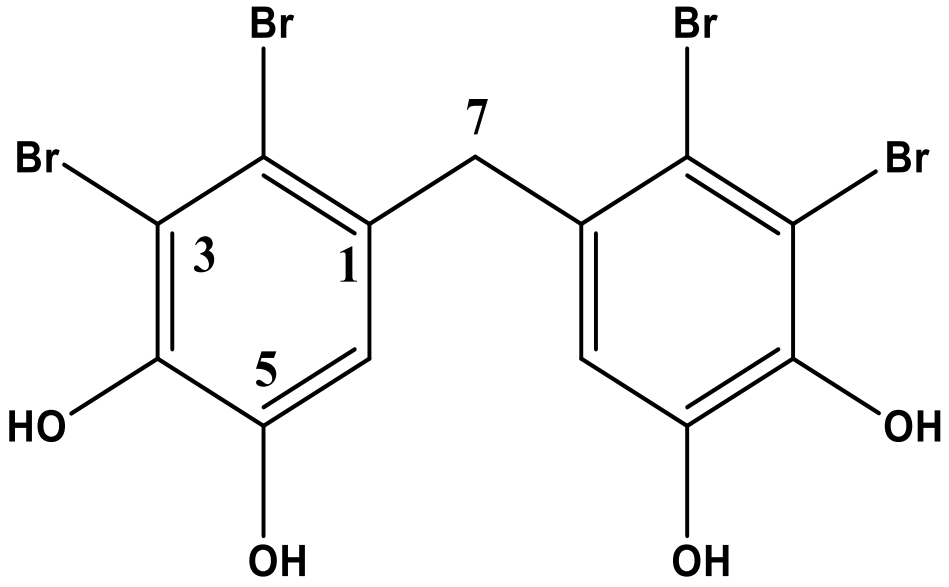

Figure 2-3-2-1. Structure of *bis* (2,3-dibromo-4,5-dihydroxyphenyl) methane (compound **R5**).

Table 2-3-2-1. Comparison of compound **R5** observed and literature NMR data [56].

No.	^{1}H NMR (δ_H, ppm)		^{13}C NMR (δ_C, ppm)	
	Observed data	Literature data	Observed data	Literature data
1			132.4	132.0
2			116.7	116.4
3			113.9	113.6
4			144.0	143.8
5			145.6	145.4
6	6.56 (s, 1H)	6.58 (s, 1H)	116.8	116.5
7	4.04 (s, 2H)	4.04 (s, 2H)	44.8	44.5

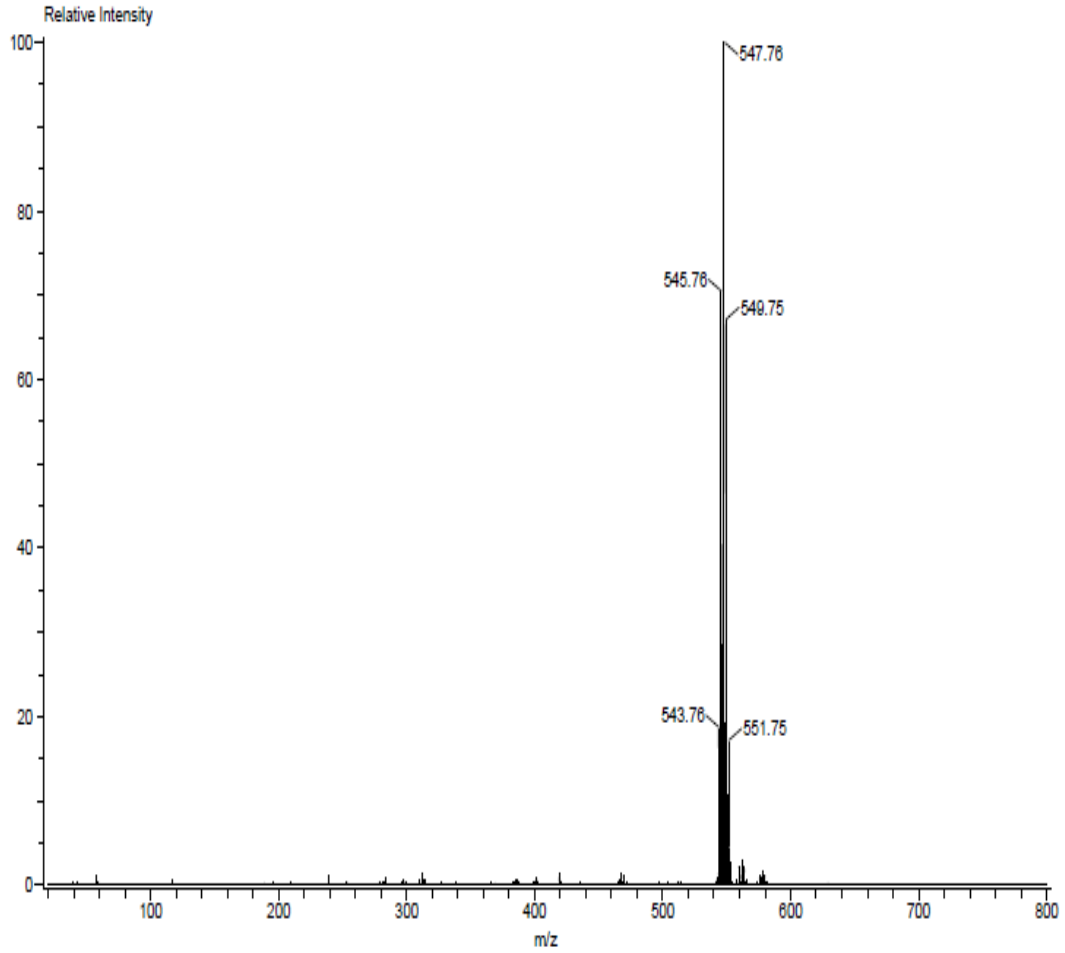

Figure 2-3-2-2. FD-MS spectrum of compound **R5**.

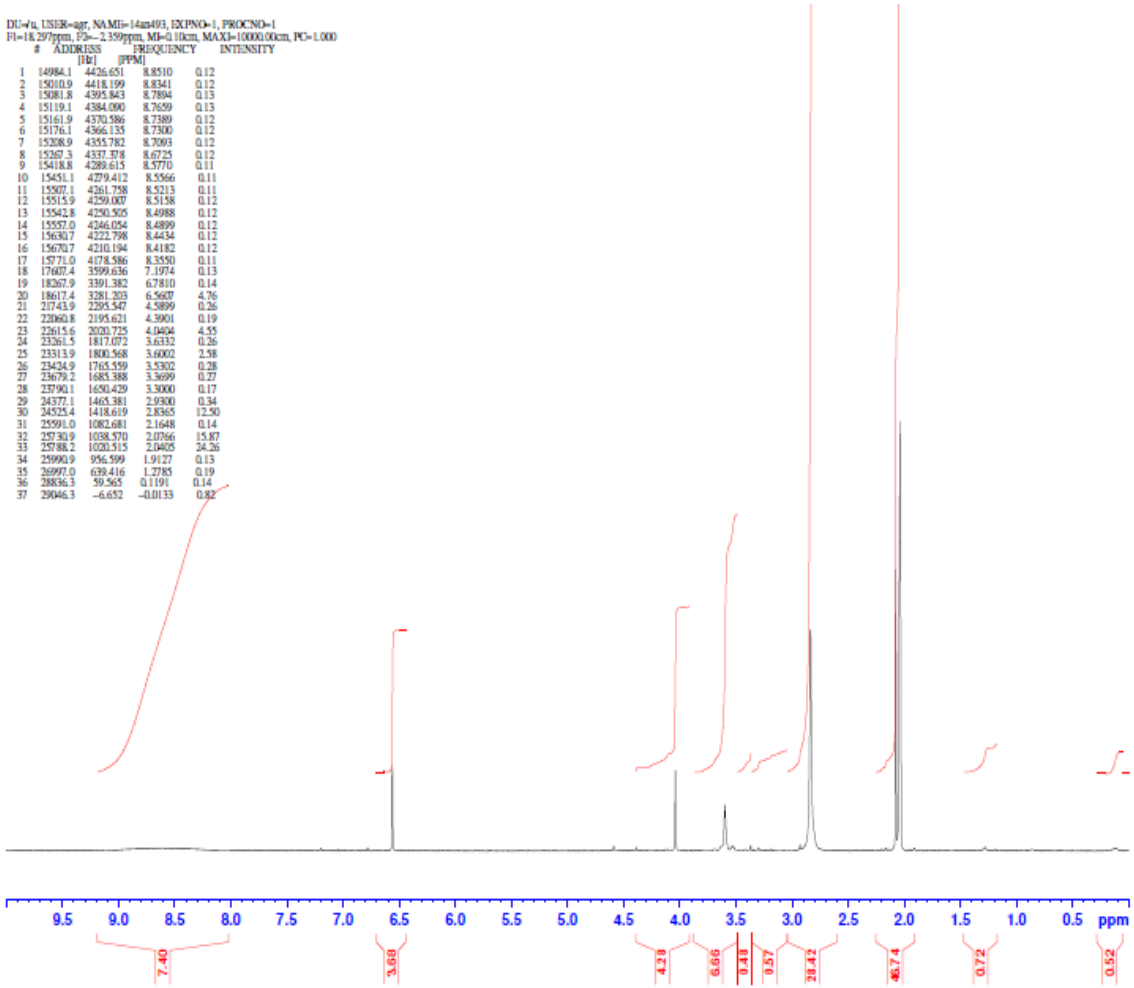

Figure 2-3-2-3. ^{1}H-NMR spectrum of compound **R5** (acetone-d_6, 500 MHz).

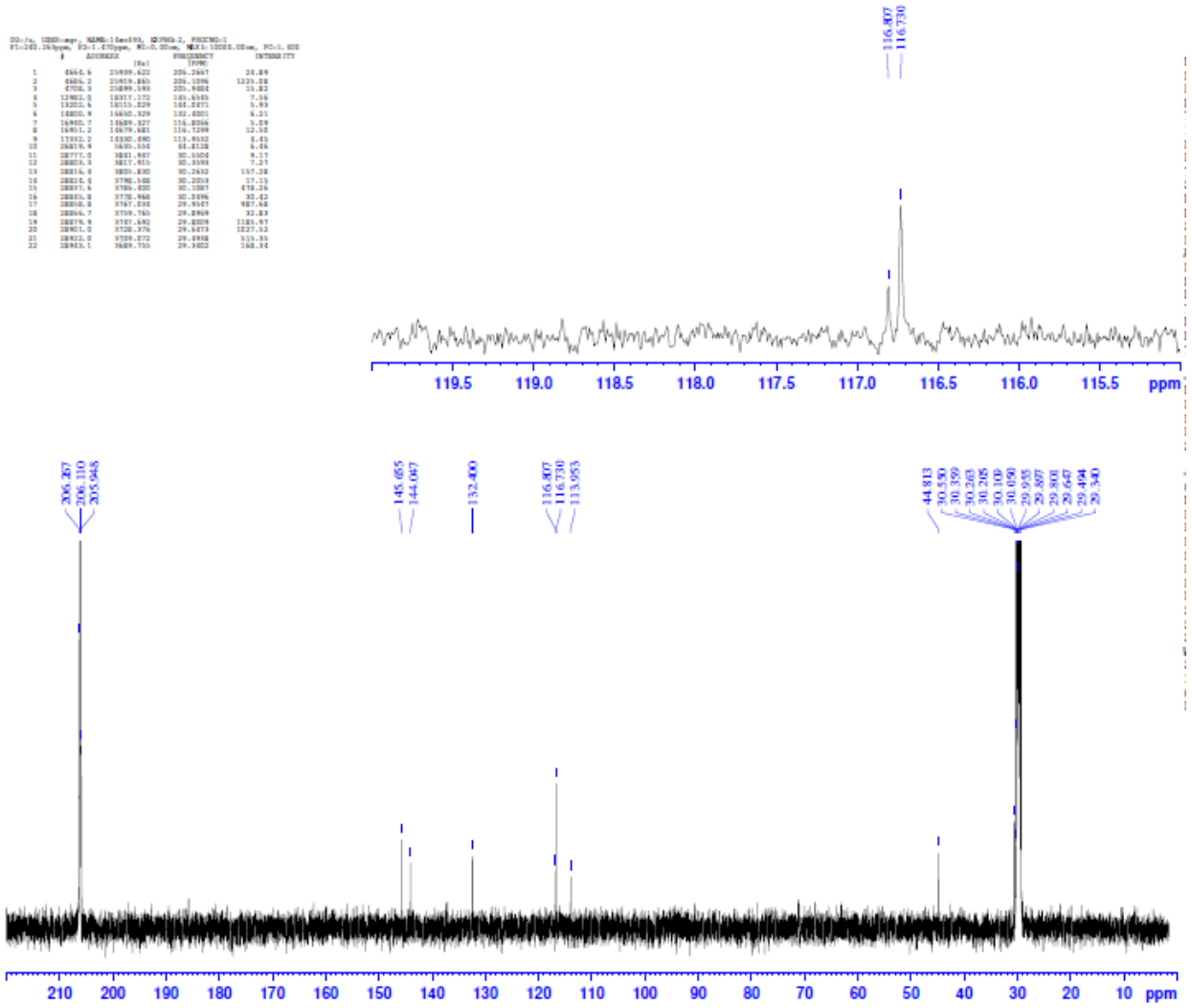

Figure 2-3-2-4. ^{13}C-NMR spectrum of compound **R5** (acetone-d_6, 125 MHz).

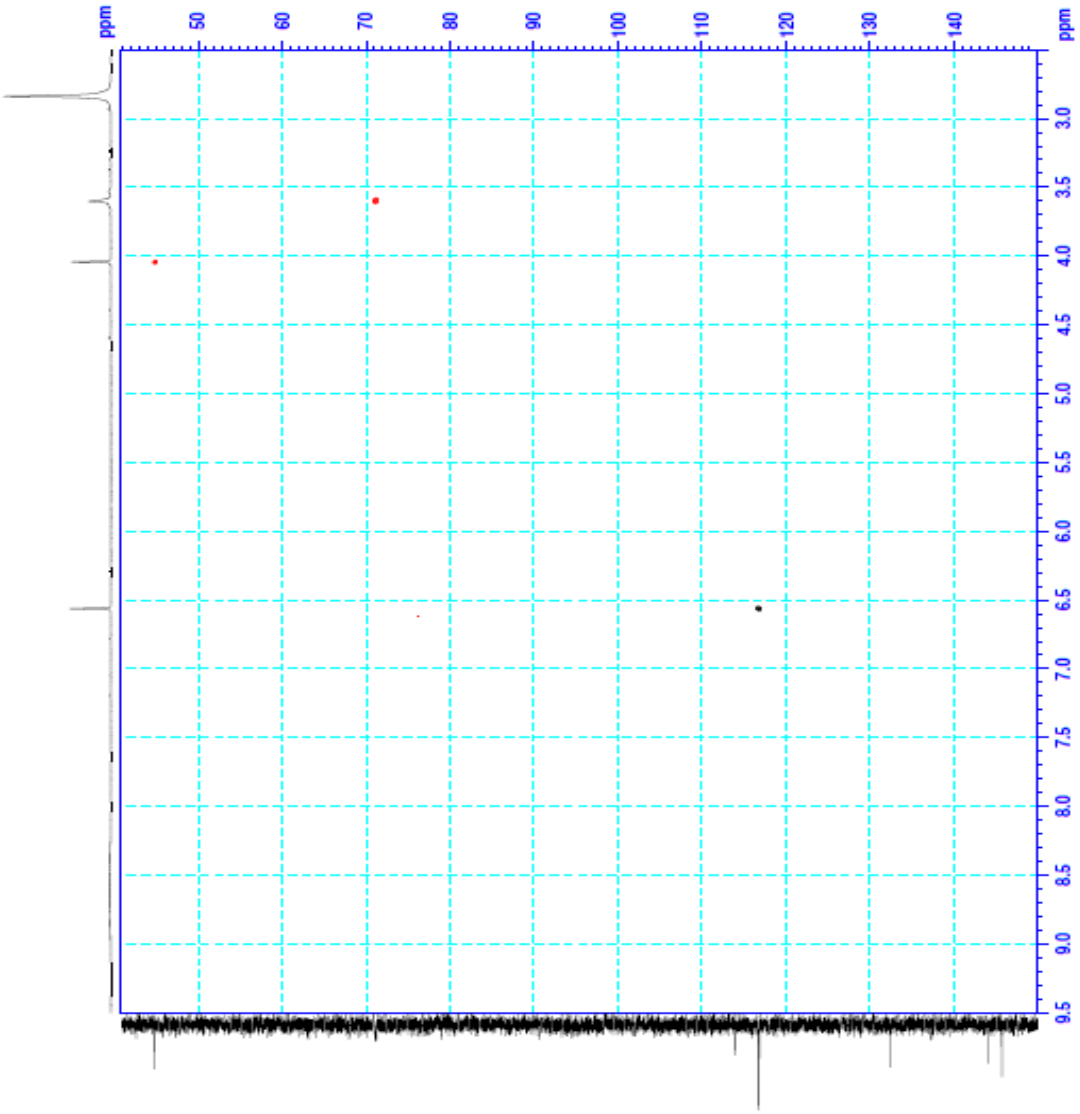

Figure 2-3-2-5. Editing HSQC spectrum of compound **R5**.

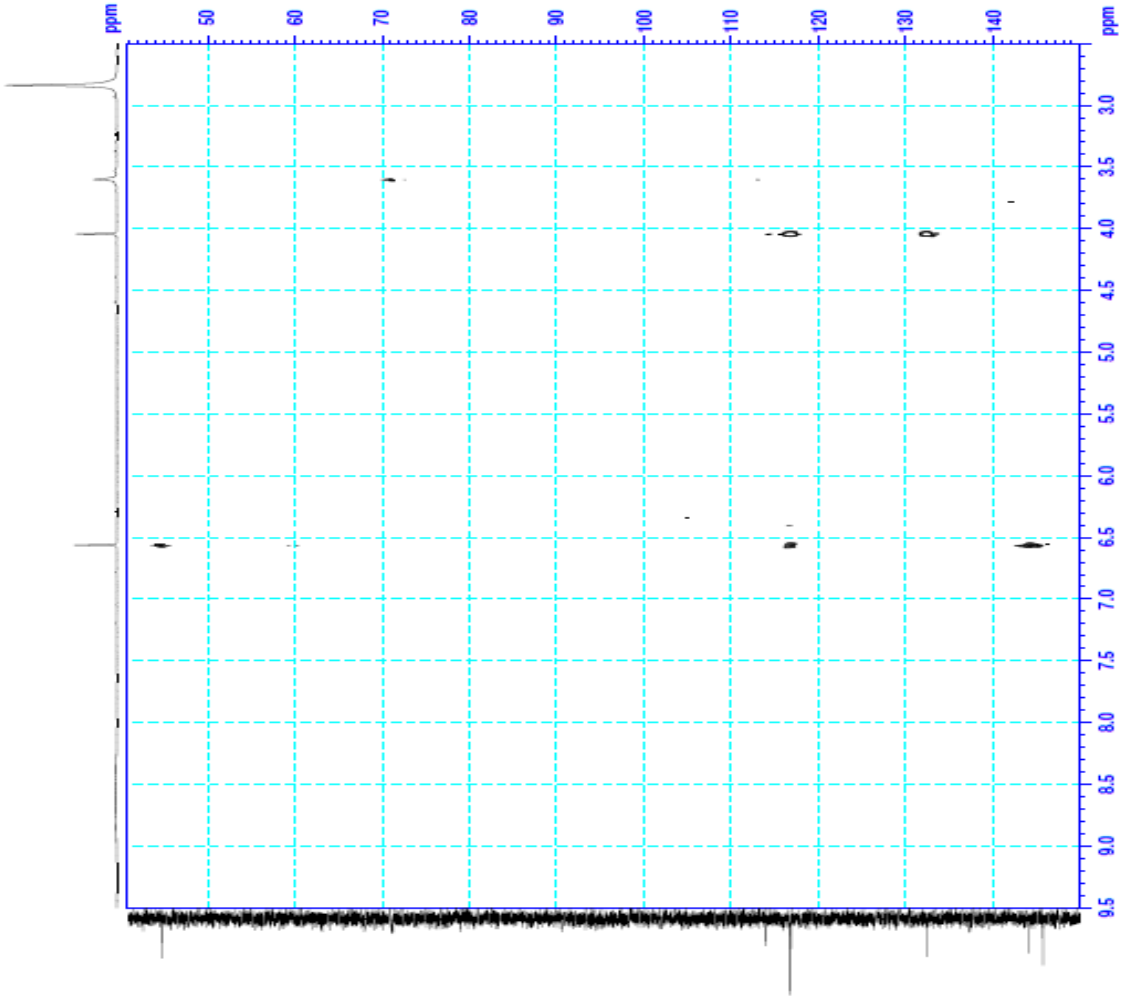

Figure 2-3-2-6. HMBC spectrum of compound **R5**.

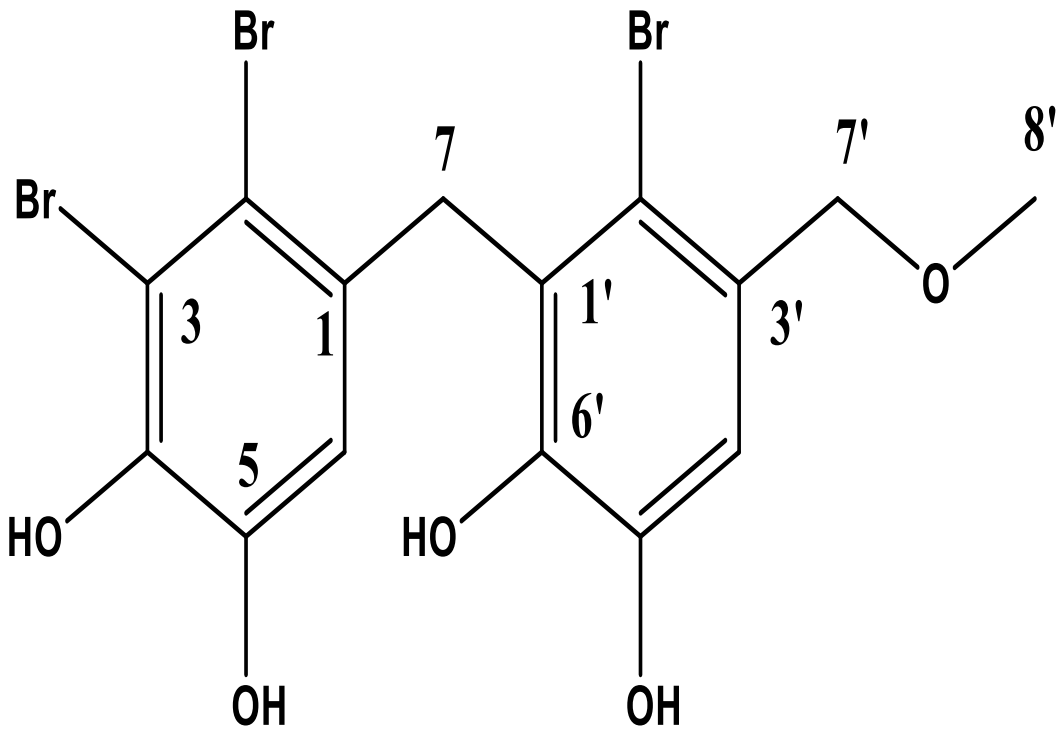

Figure 2-3-2-7. Structure of 2’-bromo-5’,6’-dihydroxy-1’-(2,3-dibromo-4,5-dihydroxybenzyl)benzyl methyl ether (compound **R6**).

Table 2-3-2-2. Comparison of compound **R6** observed and literature NMR data [55, 56, 69].

No.	^{1}H NMR (δ_H, ppm)		^{13}C NMR (δ_C, ppm)	
	Observed data	Literature data	Observed data	Literature data
1			132.4	130.4
2			116.5	114.3
3			115.7	113.0
4			143.5	142.5
5			146.1	144.5
6	6.14 (s, 1H)	6.15 (s, 1H)	114.0	115.3
7	4.14 (s, 2H)	4.12 (s, 2H)	38.2	37.8
1’			129.5	127.5
2’			117.0	114.4
3’			127.6	128.5
4’			143.5	144.8
5’			145.6	142.5
6’	6.92 (s, 1H)	6.92 (s, 1H)	115.0	113.7
7’	4.41 (s, 2H)	4.44 (s, 2H)	75.6	72.0
8’	3.29 (s, 3H)	3.35 (s, 3H)	58.5	57.3

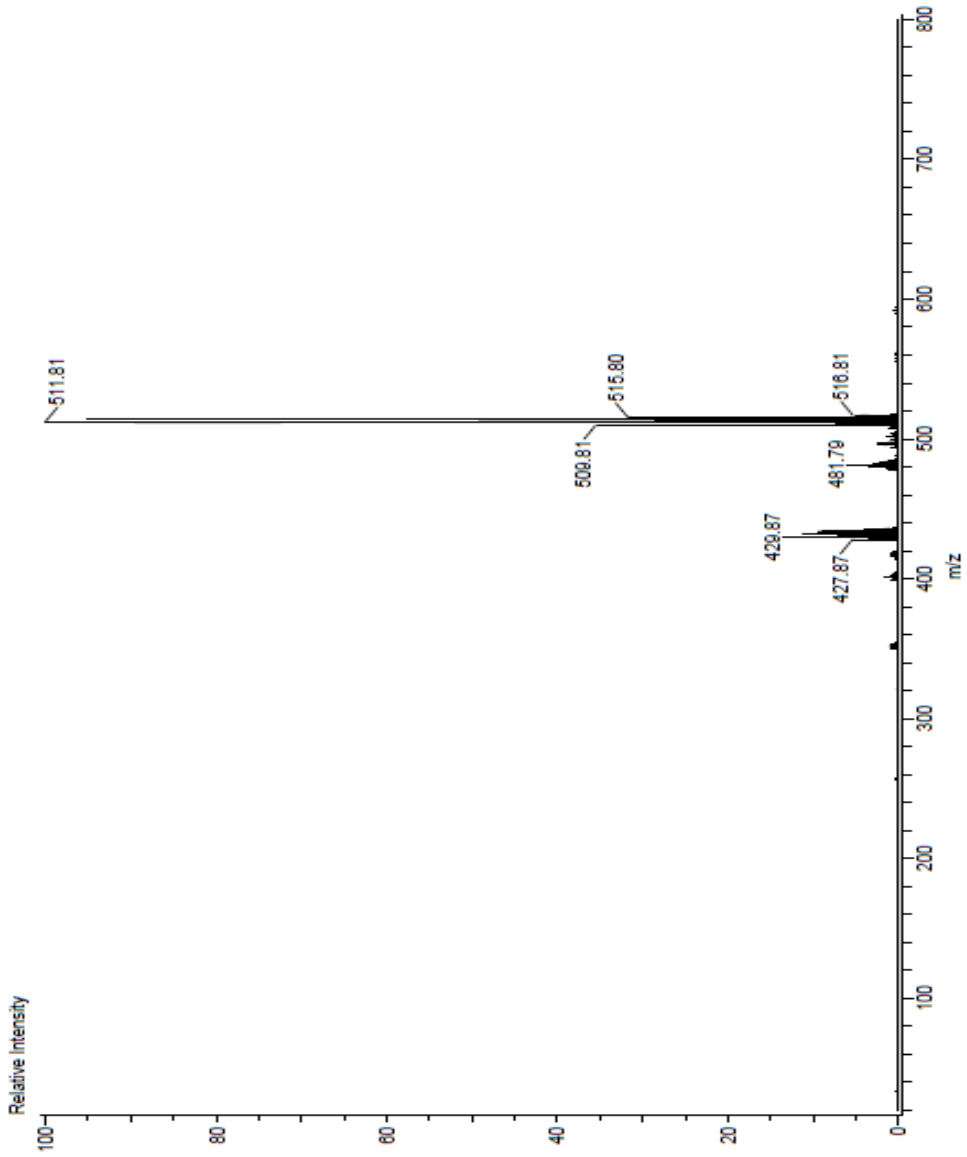

Figure 2-3-2-8. FD-MS spectrum of compound **R6**.

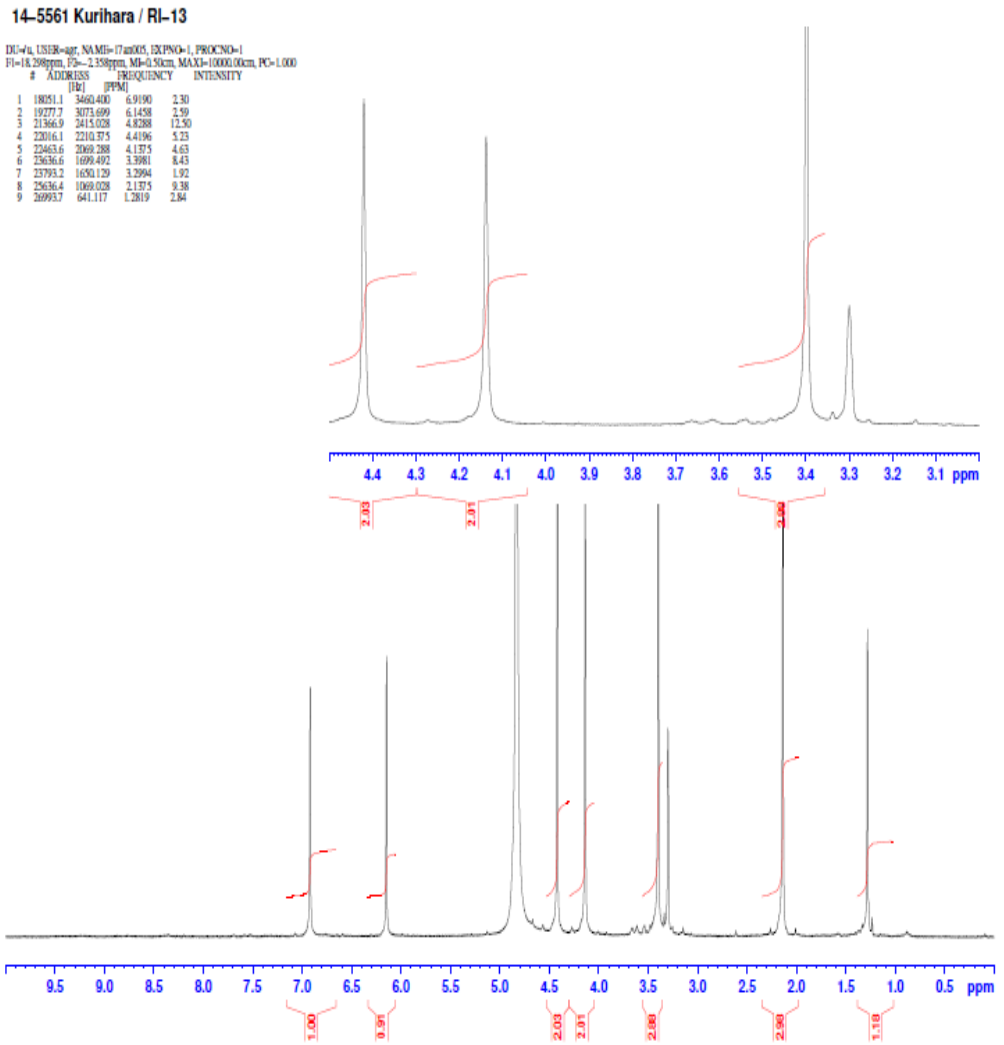

Figure 2-3-2-9. ^{1}H-NMR spectrum of compound **R6** (methanol-*d4*, 500 MHz).

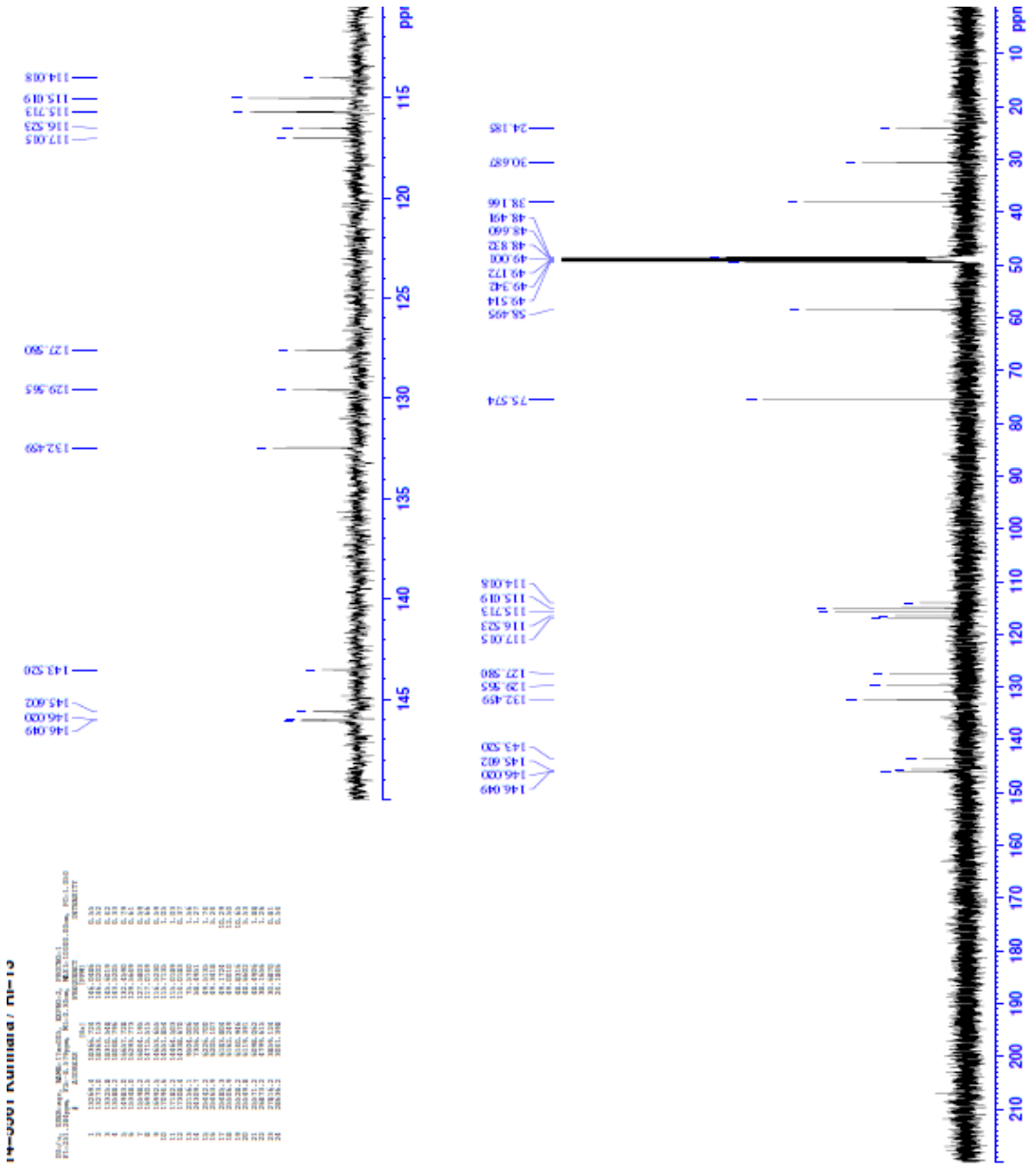

Figure 2-3-2-10. ^{13}C-NMR spectrum of compound **R6** (methanol-d_4, 125 MHz).

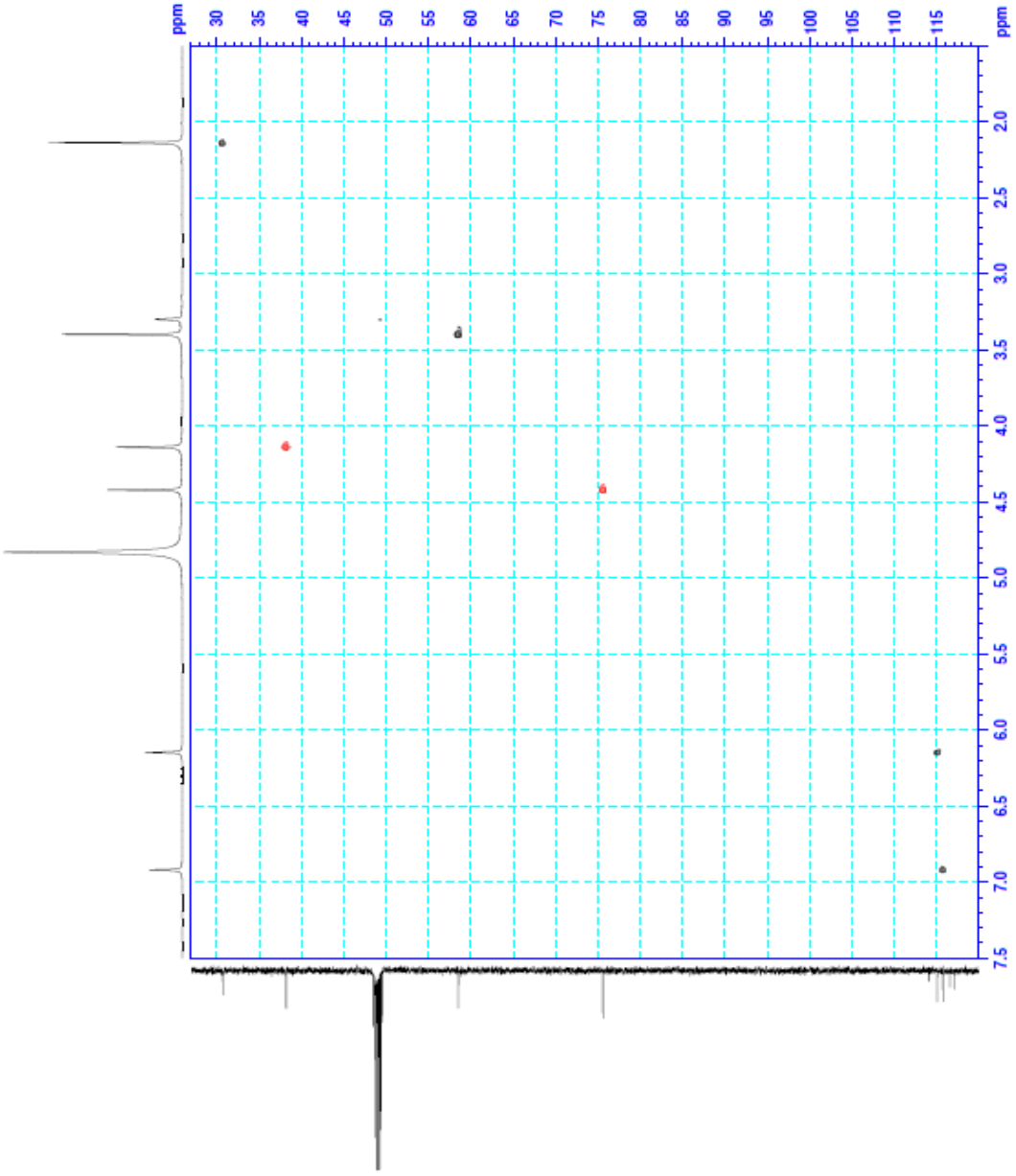

Figure 2-3-2-11. Editing HSQC spectrum of compound **R6**.

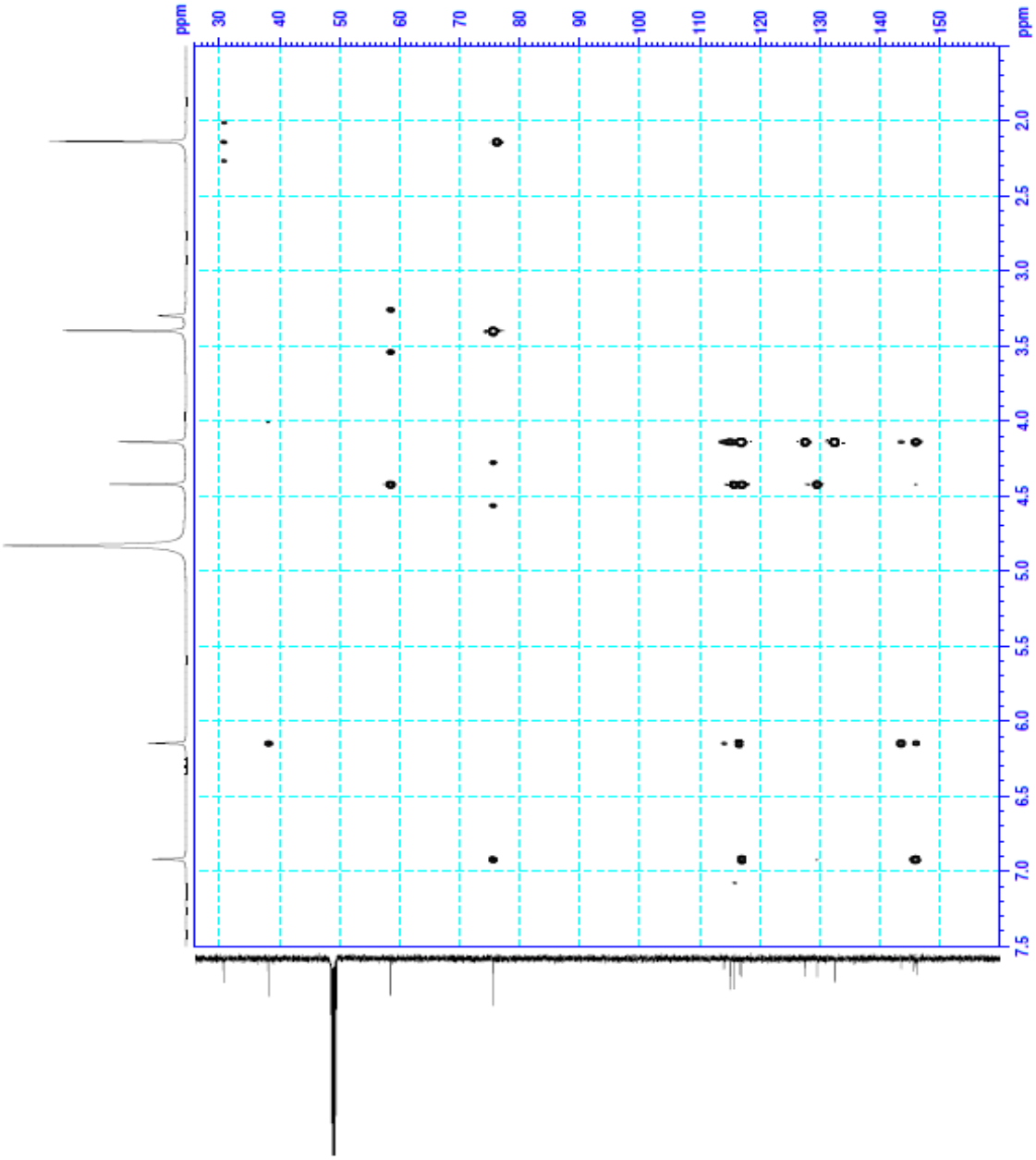

Figure 2-3-2-12. HMBC spectrum of compound **R6**.

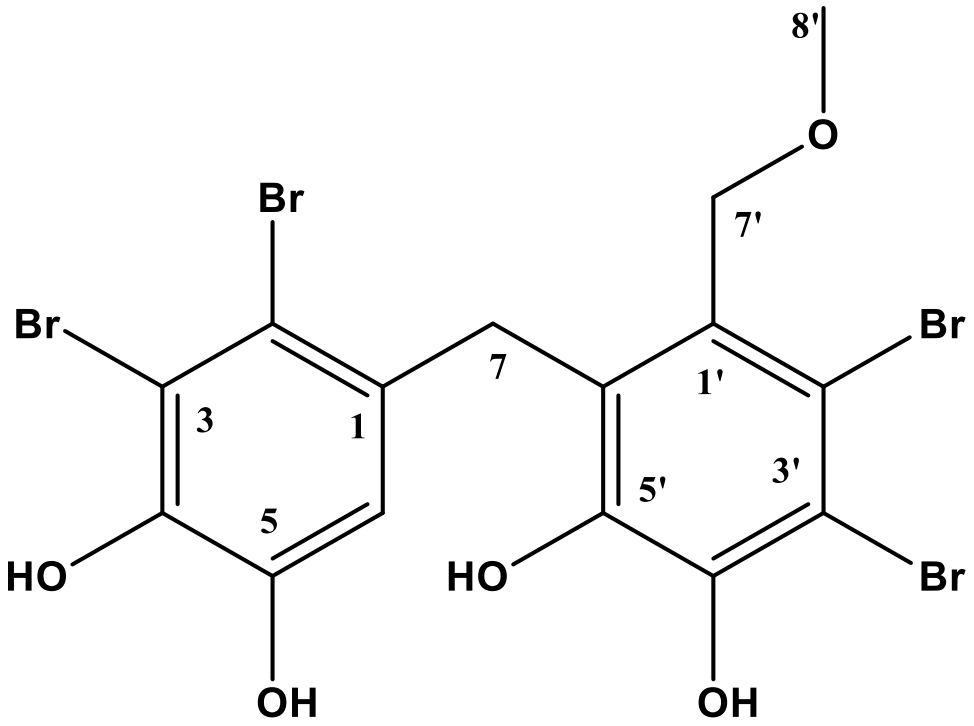

Figure 2-3-2-13. Structure of 2',3'-dibromo-4',5'-dihydroxy-6'-(2,3-dibromo-4,5-dihydroxybenzyl)benzyl methyl ether (compound **R7**).

Table 2-3-2-3. Comparison of compound **R7** observed and literature NMR data [36].

No.	^{1}H NMR (δ_H, ppm)		^{13}C NMR (δ_C, ppm)	
	Observed data	Literature data	Observed data	Literature data
1			132.8	132.4
2			117.3	116.3
3			115.1	113.6
4			143.9	143.5
5			146.2	145.3
6	6.12 (s, 1H)	6.18 (s, 1H)	116.2	114.9
7	4.11 (s, 2H)	4.15 (s, 2H)	34.6	34.4
1’			130.5	130.9
2’			119.2	118.9
3’			113.6	113.0
4’			145.7	144.8
5’			146.0	145.1
6’			128.8	128.2
7’	4.41 (s, 2H)	4.42 (s, 2H)	73.7	73.2
8’	3.30 (s, 3H)	3.28 (s, 3H)	58.5	58.3

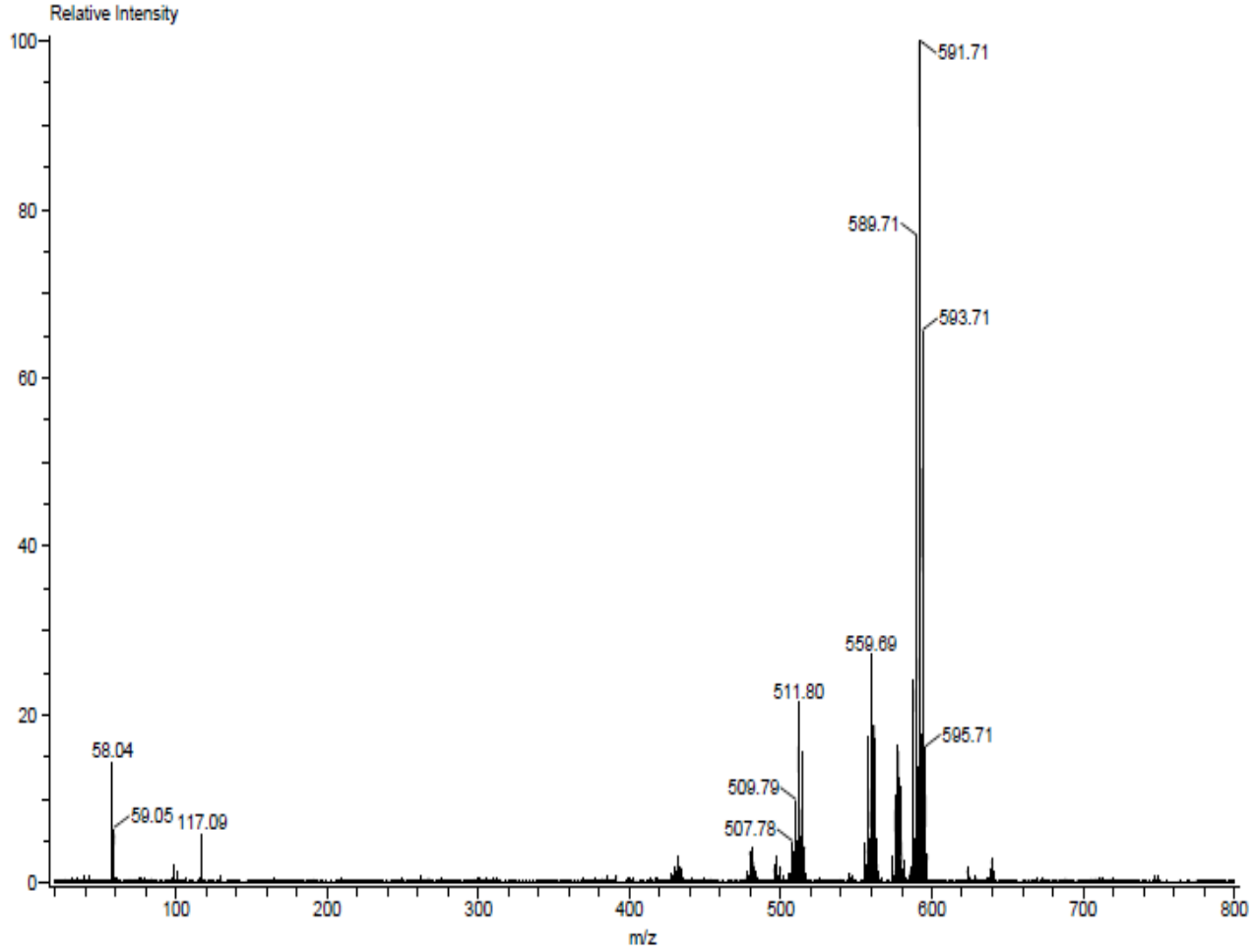

Figure 2-3-2-14. FD-MS spectrum of compound **R7**.

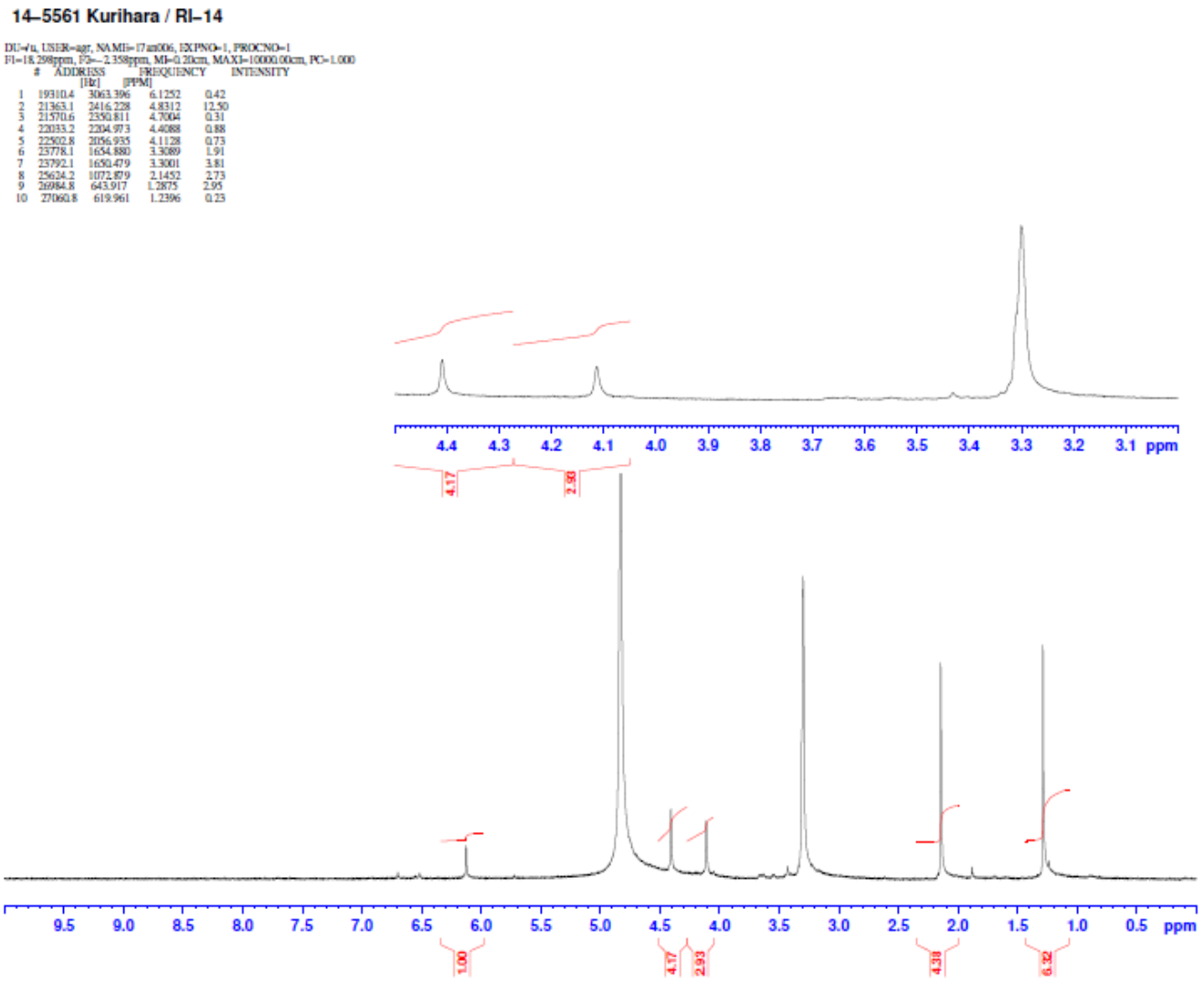

Figure 2-3-2-15. ^{1}H-NMR spectrum of compound **R7** (methanol-*d4*, 500 MHz).

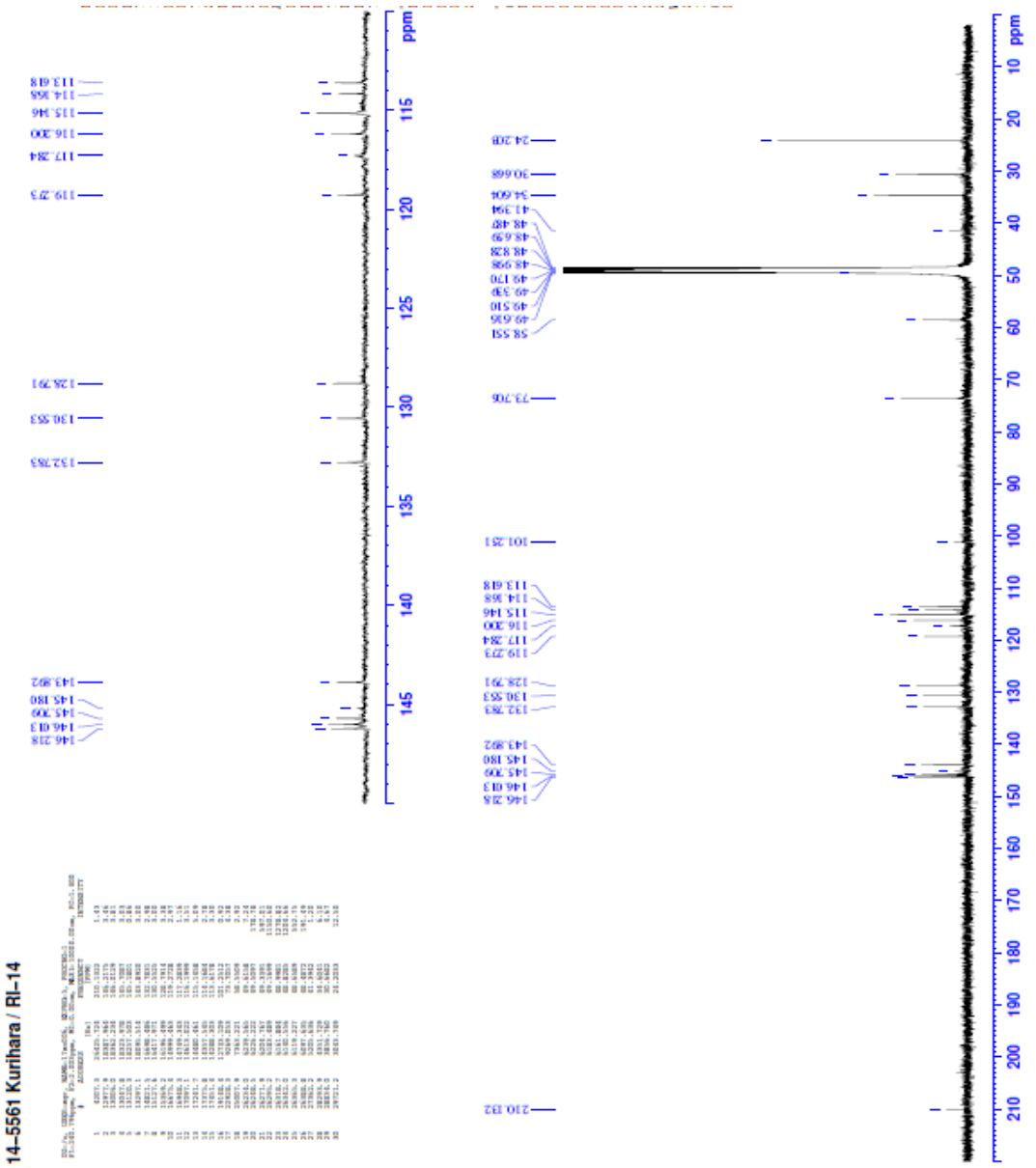

Figure 2-3-2-16. ^{13}C-NMR spectrum of compound **R7** (methanol-d_4, 125 MHz).

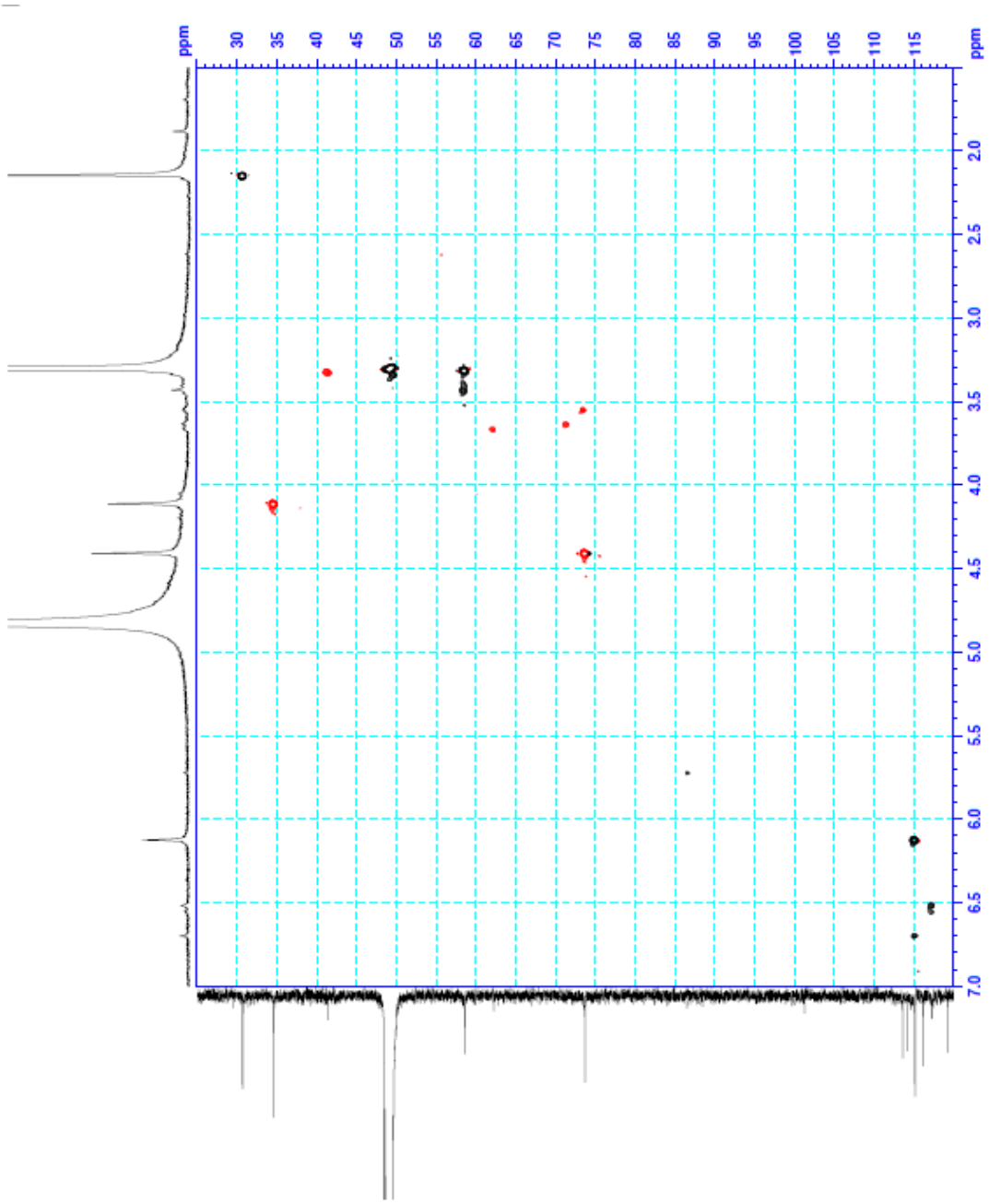

Figure 2-3-2-17. Editing HSQC spectrum of compound **R7**.

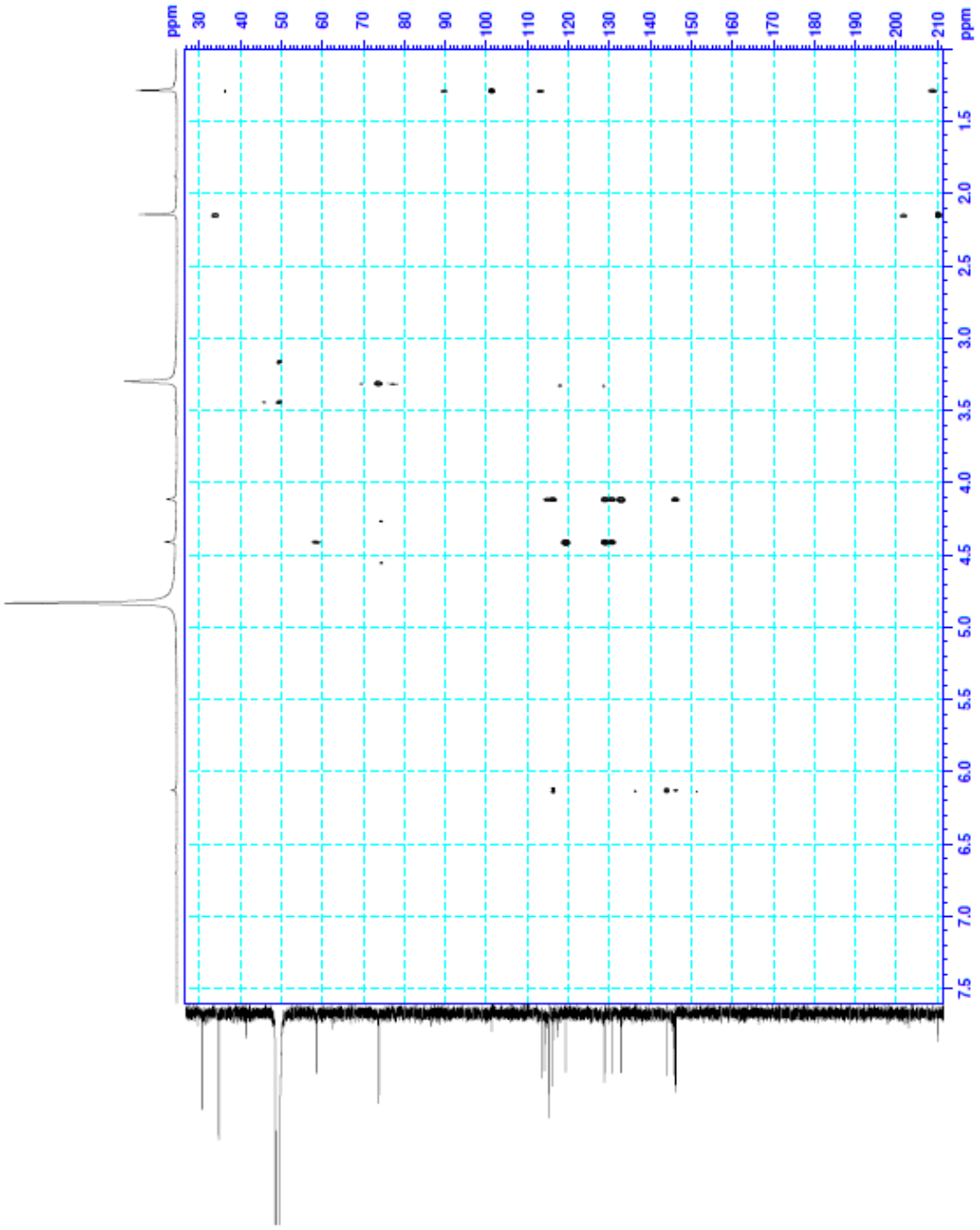

Figure 2-3-2-18. HMBC spectrum of compound **R7**.

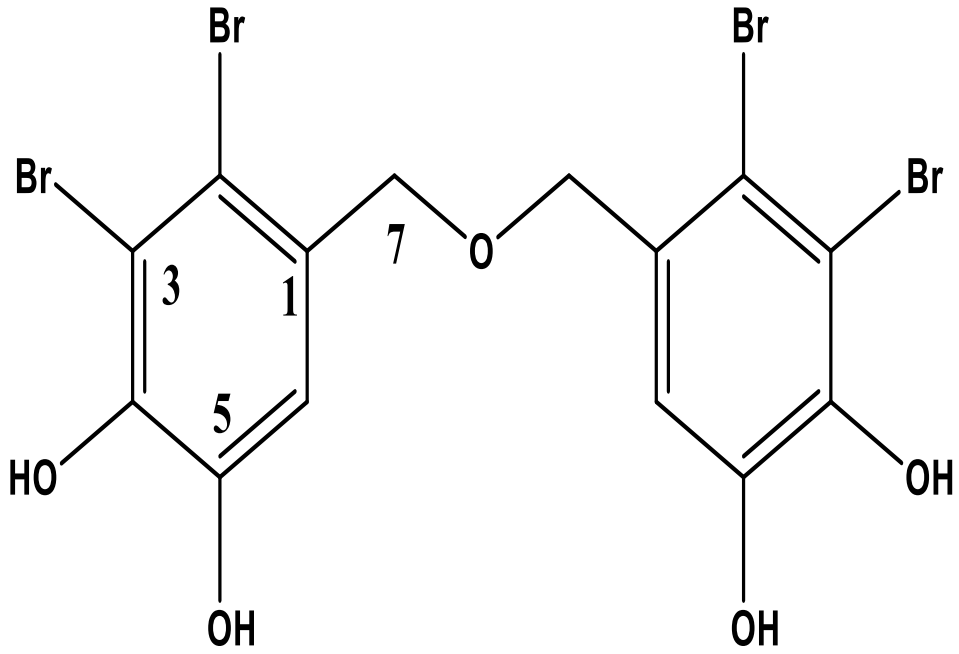

Figure 2-3-2-19. Structure of *bis*(2,3-dibromo-4,5-dihydroxybenzyl) ether (compound **R8**).

Table 2-3-2-4. Comparison of compound **R8** observed and literature NMR data [49].

No.	^{1}H NMR (δ_H, ppm)		^{13}C NMR (δ_C, ppm)	
	Observed data	Literature data	Observed data	Literature data
1			131.3	131.3
2			114.6	114.7
3			113.7	113.8
4			144.7	144.7
5			145.7	145.6
6	7.18 (s, 1H)	7.14 (s, 1H)	115.7	115.6
7	4.60 (s, 2H)	4.59 (s, 2H)	73.3	73.2

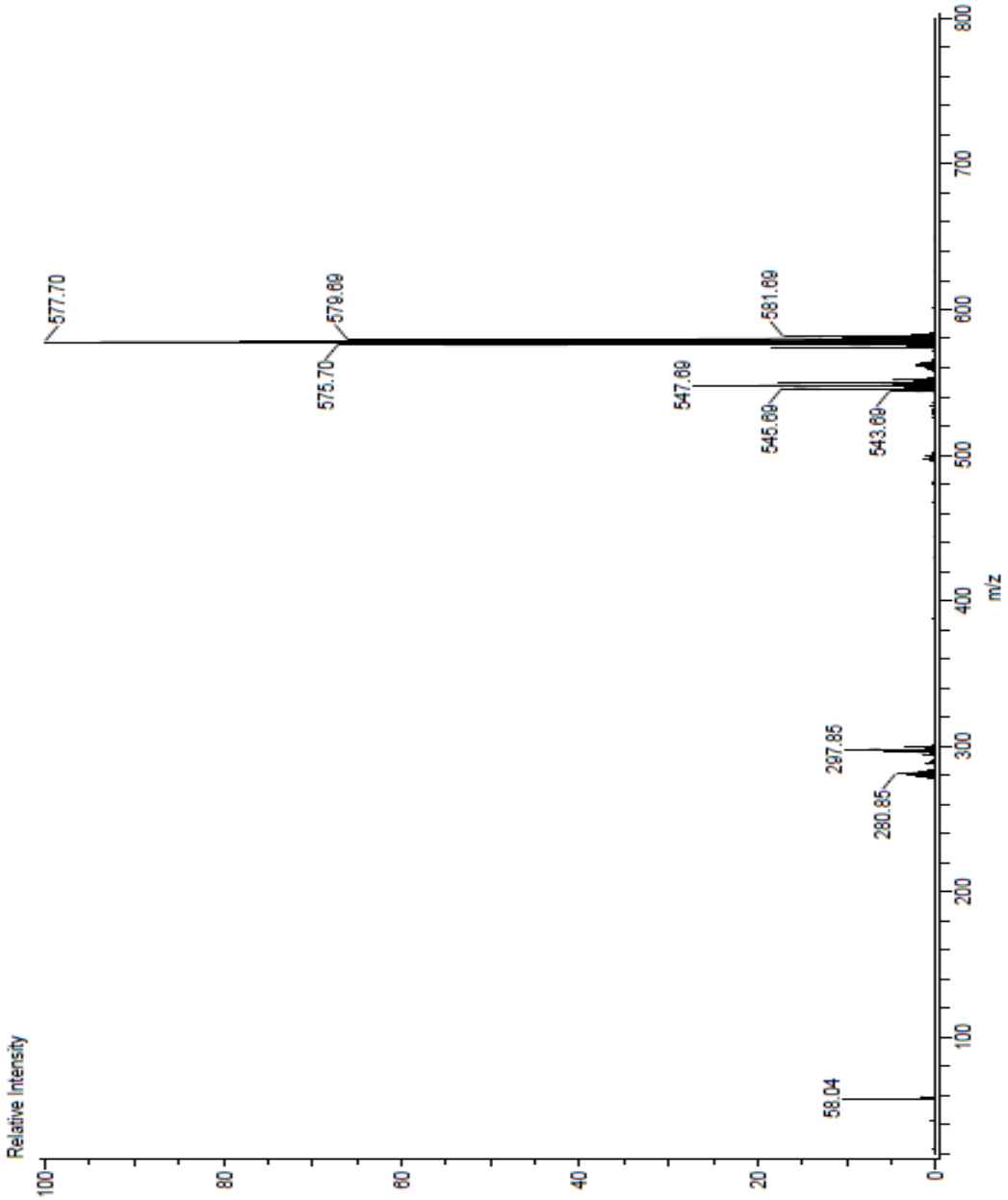

Figure 2-3-2-20. FD-MS spectrum of compound **R8**.

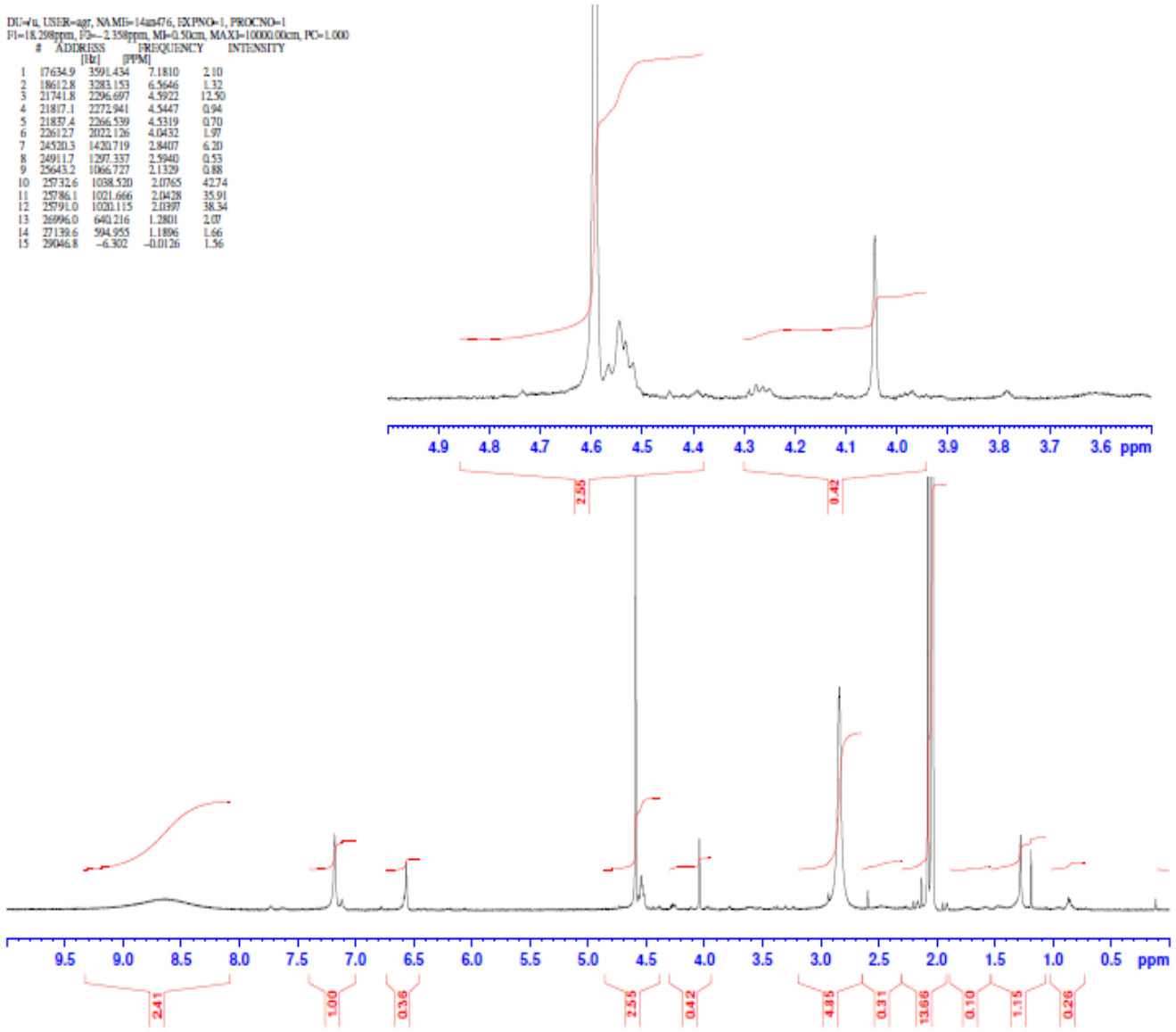

Figure 2-3-2-21. ^{1}H-NMR spectrum of compound **R8** (acetone-*d6*, 500 MHz).

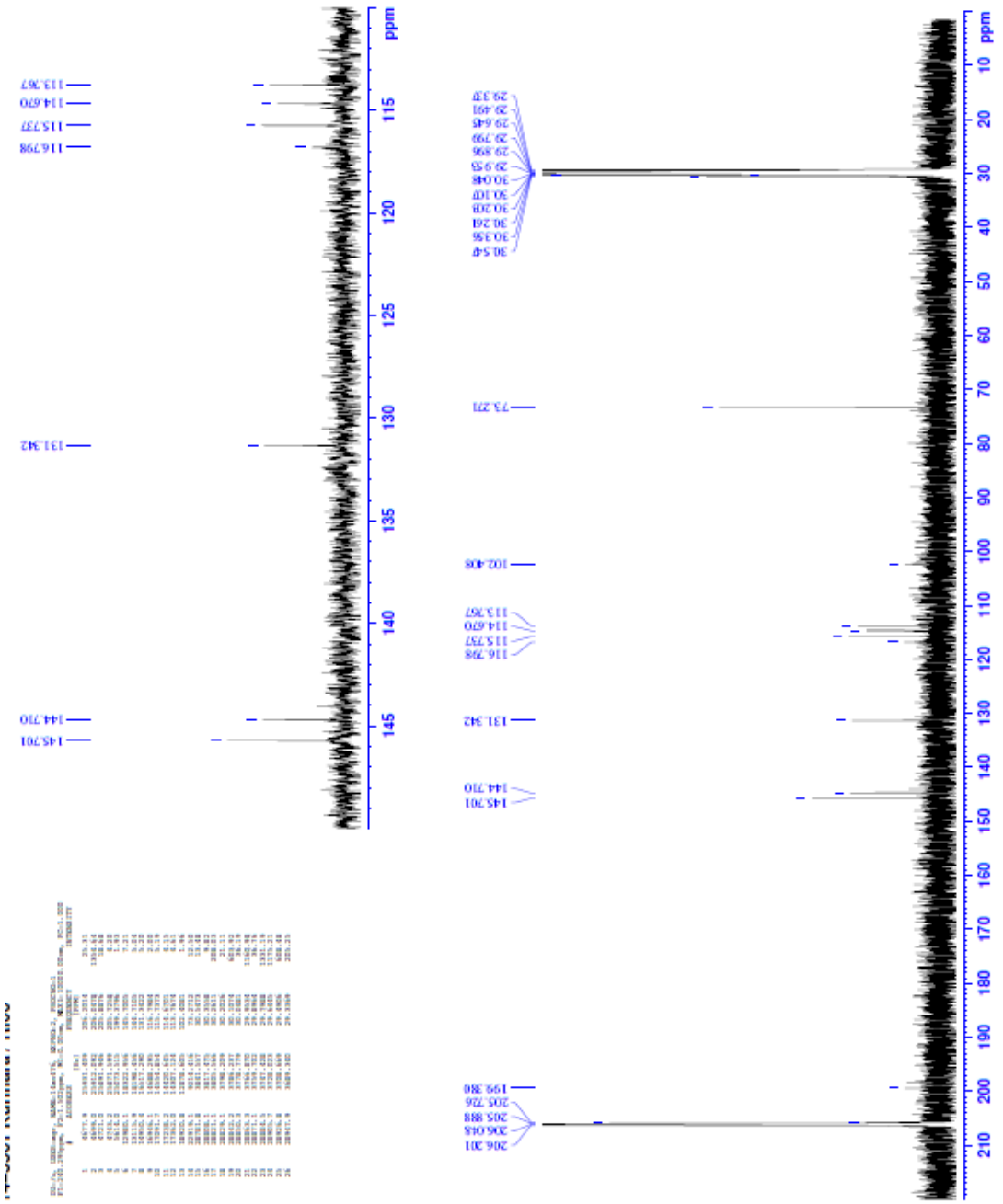

Figure 2-3-2-22. ^{13}C-NMR spectrum of compound **R8** (acetone-d_6, 125 MHz).

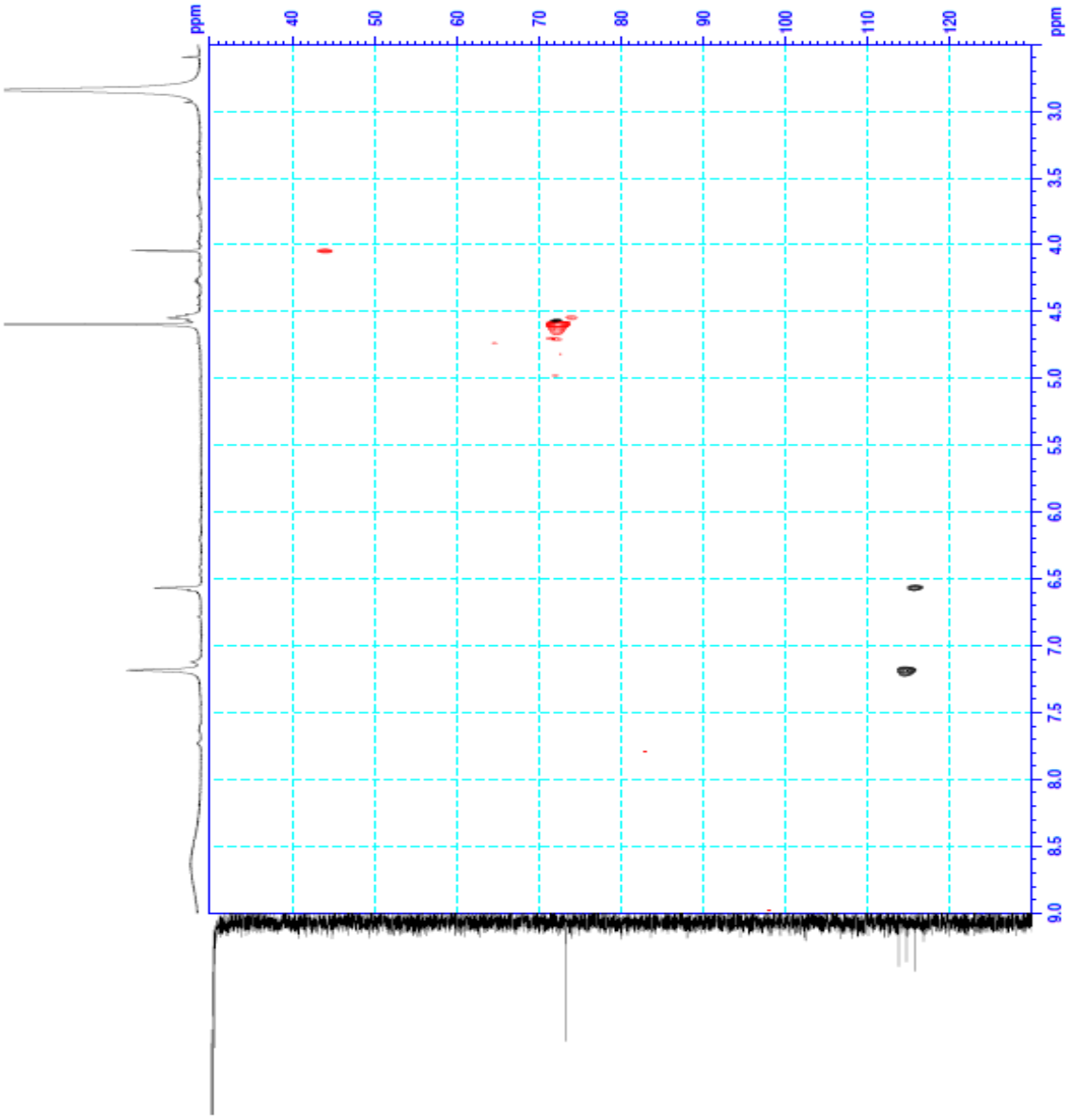

Figure 2-3-2-23. Editing HSQC spectrum of compound **R8**.

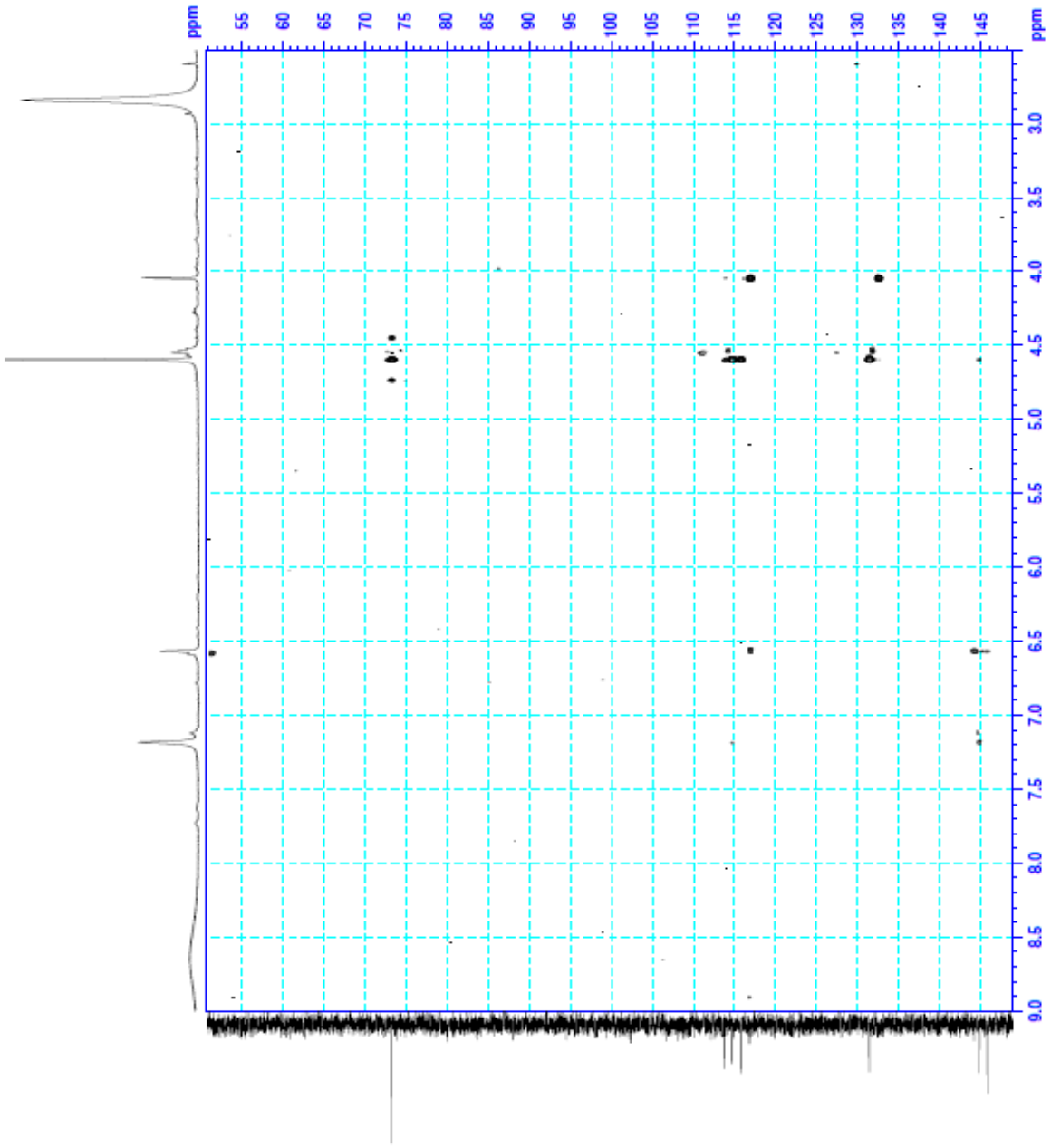

Figure 2-3-2-24. HMBC spectrum of compound **R8**.

2.3.3. Structural Elucidation of Compounds **R9** and **R10**

The FD-MS spectrum of compound **R9** gave the tribrominated molecular ion peak cluster at *m/z* 496/498/500/502 with a ratio of 1:3:3:1 (Figure 2-3-3-2). The molecular formula was determined as $C_{14}H_{11}Br_3O_5$ by HRFDMS at *m/z* 495.81586 (calcd for $C_{14}H_{11}Br_3O_5$ 495.81566). The ^{1}H NMR spectrum showed four singlets attributed to aromatic proton at δ 7.06, 6.16, and two methylenes at δ 4.52 and 4.12 ppm. The ^{13}C NMR and HSQC spectra of compound **R9** displayed 14 carbons assignable to two methylenes and two pentasubstituted benzene rings with four oxygenated carbons (δ > 142 ppm) (Figures 2-3-3-3 to 2-3-3-6, Table 2-3-3-1). The spectral data indicated that compound possessed a tribrominated diarylmethane structure with four hydroxy and one hydroxymethyl group. The structure of compound **R9** was determined as 3'-bromo-4',5'-dihydroxy-2'-(2,3-dibromo-4,5-dihydroxybenzyl)benzyl alcohol (Figure 2-3-3-1) [62].

Compound **R10** was obtained as colorless solid having the tribrominated molecular ion peak cluster at *m/z* 510/512/514/514 with a ratio of 1:3:3:1 (Figure 2-3-3-8). The molecular formula was determined as $C_{15}H_{13}Br_3O_5$ by HRFDMS at *m/z* 509.8306 (calcd for $C_{14}H_{11}Br_3O_5$ 509.8313). The ^{1}H NMR spectrum showed four singlets attributed to aromatic proton at δ 6.98 and 6.07, and two methylenes at δ 4.20 and 4.12, and one methoxy at 3.23 ppm. The ^{13}C NMR spectra of compound **R10** displayed 15 carbons assignable to two benzene rings; two methylenes; a methoxy with four oxygenated carbons (δ > 142 ppm) (Figures 2-3-3-9 to 2-3-3-12, Table 2-3-3-2). Connectivity of diphenyl moiety was determined from HMBC correlation of H-7 to C-1, C-2, C-6, C-1', C-2', C-3' and from H-7' to C-1', C-2', C-6'. Thus, the structure of compound **R10** was determined as 3'-bromo-4',5'-dihydroxy-2'-(2,3-dibromo-4,5-dihydroxybenzyl)benzyl methyl ether (Figure 2-3-3-7) [56].

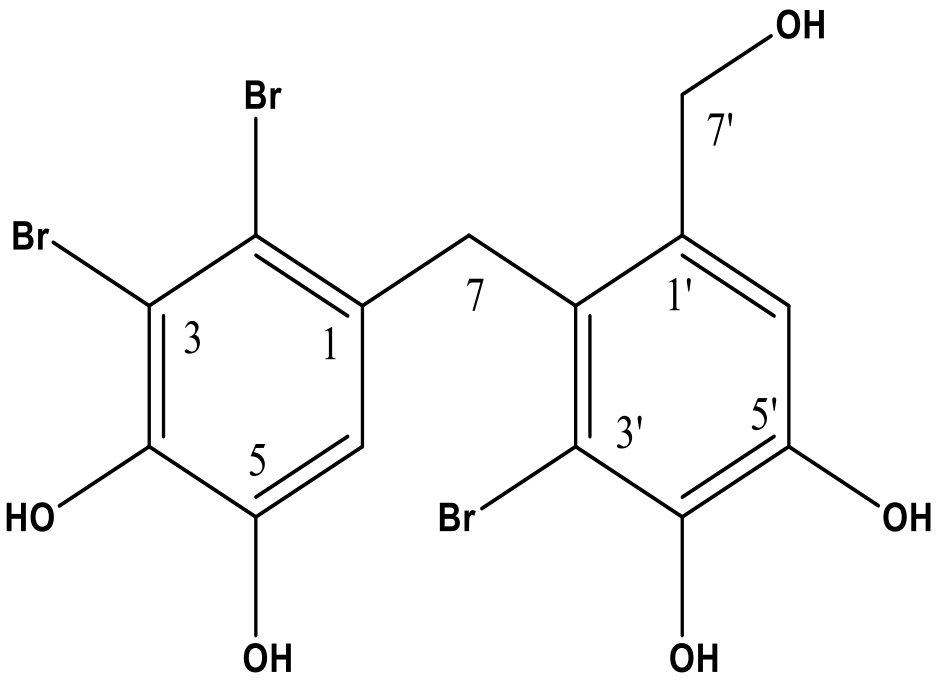

Figure 2-3-3-1. Structure of 3’-bromo-4’,5’-dihydroxy-2’-(2,3-dibromo-4,5-dihydroxybenzyl)benzyl alcohol (compound **R9**).

Table 2-3-3-1. Comparison of compound **R9** observed and literature NMR data [62].

No.	^{1}H NMR (δ_H, ppm)		^{13}C NMR (δ_C, ppm)	
	Observed data	Literature data	Observed data	Literature data
1			131.9	131.7
2			116.1	115.7
3			113.5	113.1
4			143.5	142.9
5			145.6	144.8
6	6.16 (s, 1H)	6.08 (s, 1H)	114.2	114.1
7	4.12 (s, 2H)	4.12 (s, 2H)	37.7	38.6
1’			132.9	133.5
2’			126.6	127.7
3’			114.9	114.2
4’			144.8	142.3
5’			145.2	144.4
6’	7.06 (s, 1H)	7.09 (s, 1H)	114.9	114.2
7’	4.52 (s, 2H)	4.42 (s, 2H)	64.5	62.1

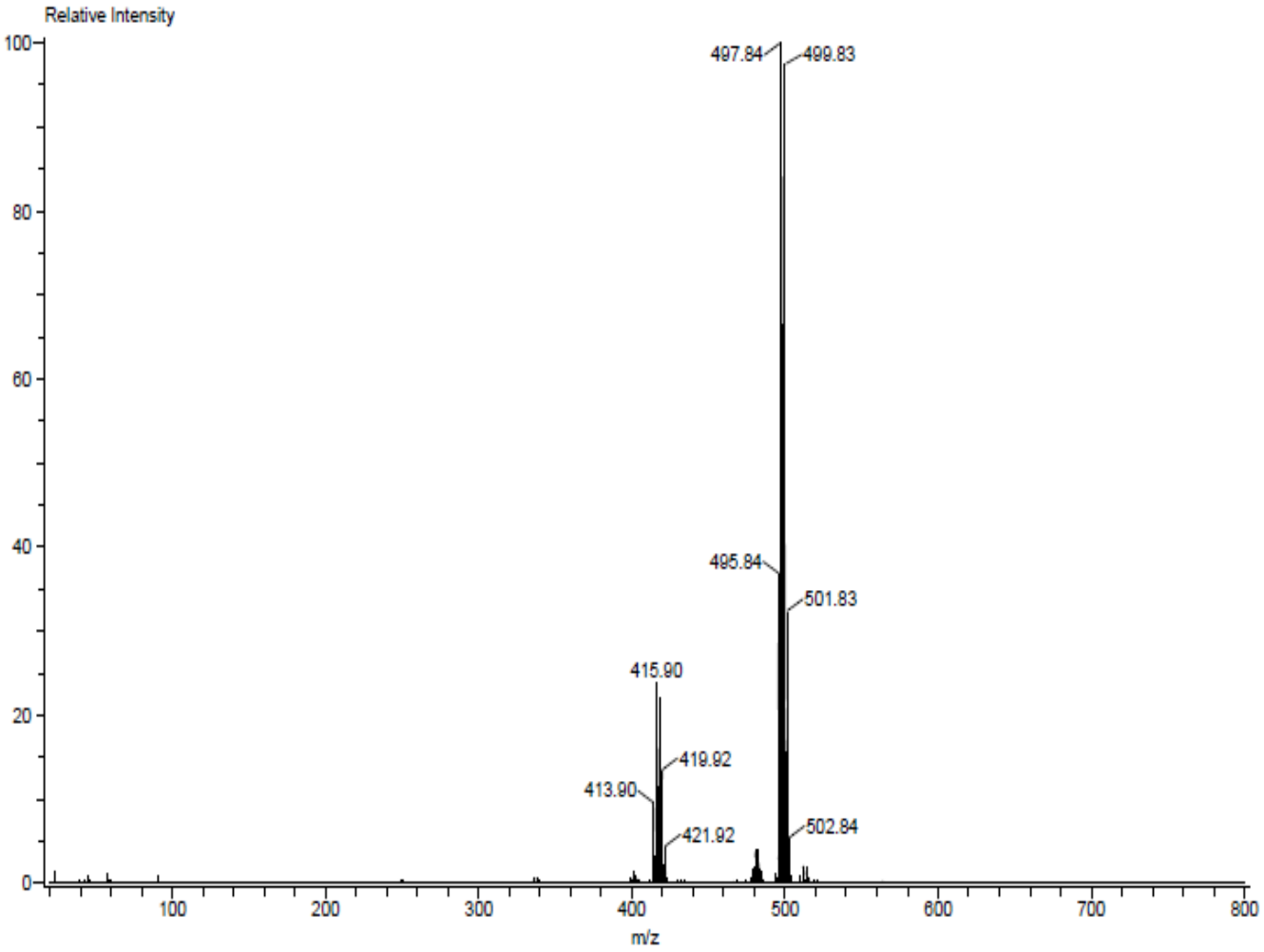

Figure 2-3-3-2. FD-MS spectrum of compound **R9**.

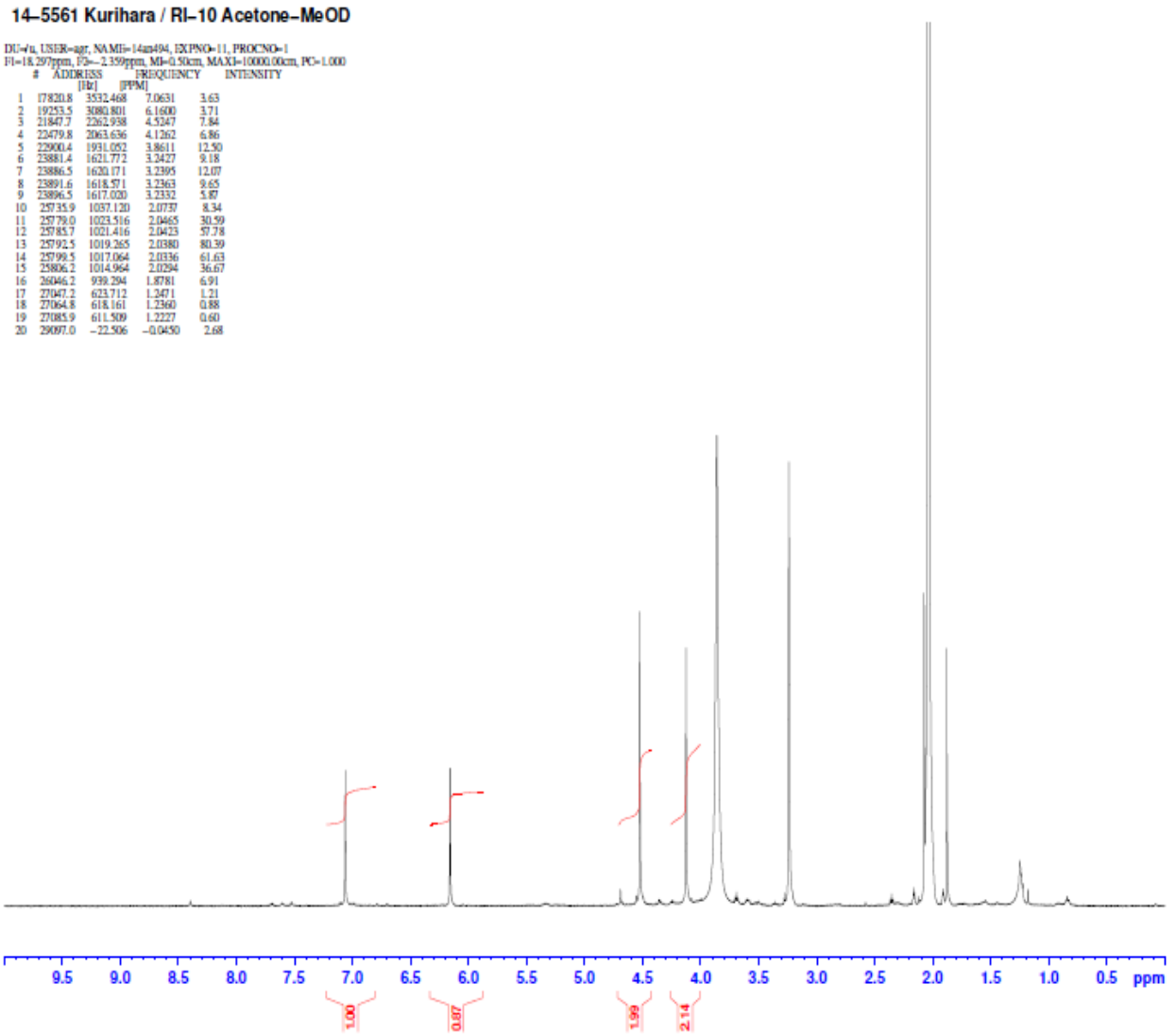

Figure 2-3-3-3. ^{1}H-NMR spectrum of compound **R9** (acetone-*d6*, 500 MHz).

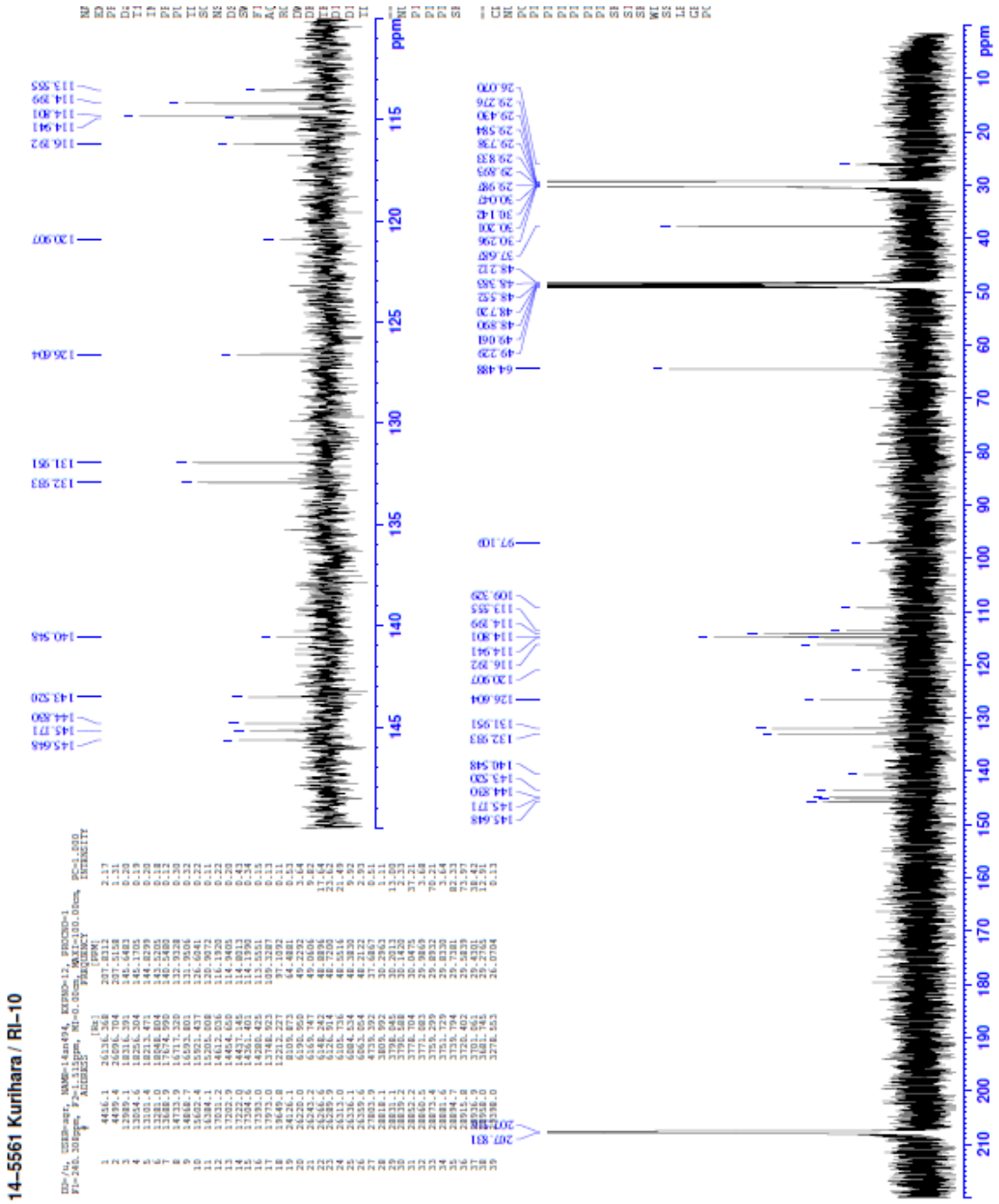

Figure 2-3-3-4. ^{13}C-NMR spectrum of compound **R9** (acetone-d_6, 125 MHz).

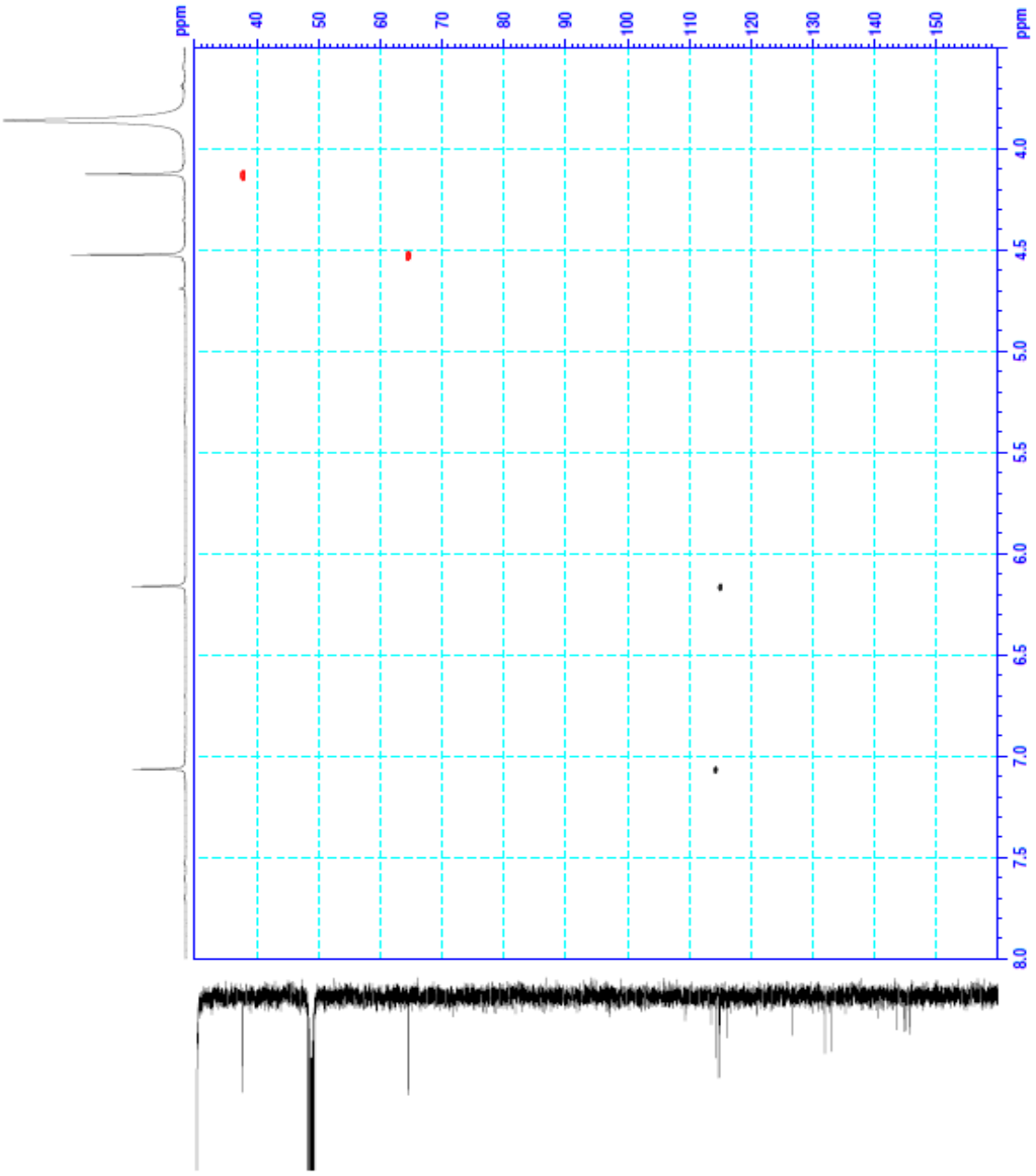

Figure 2-3-3-5. Editing HSQC spectrum of compound **R9**.

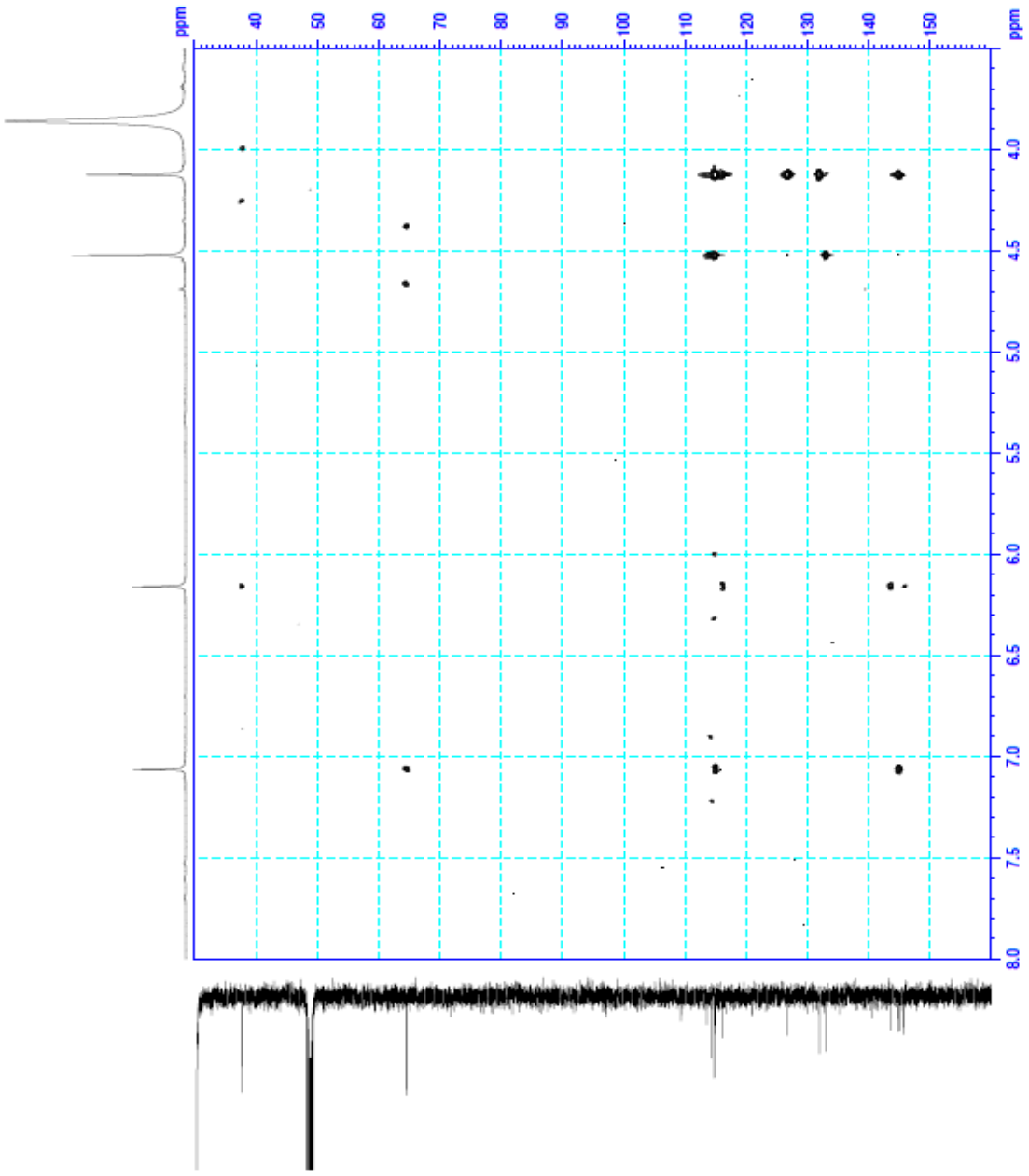

Figure 2-3-3-6. HMBC spectrum of compound **R9**.

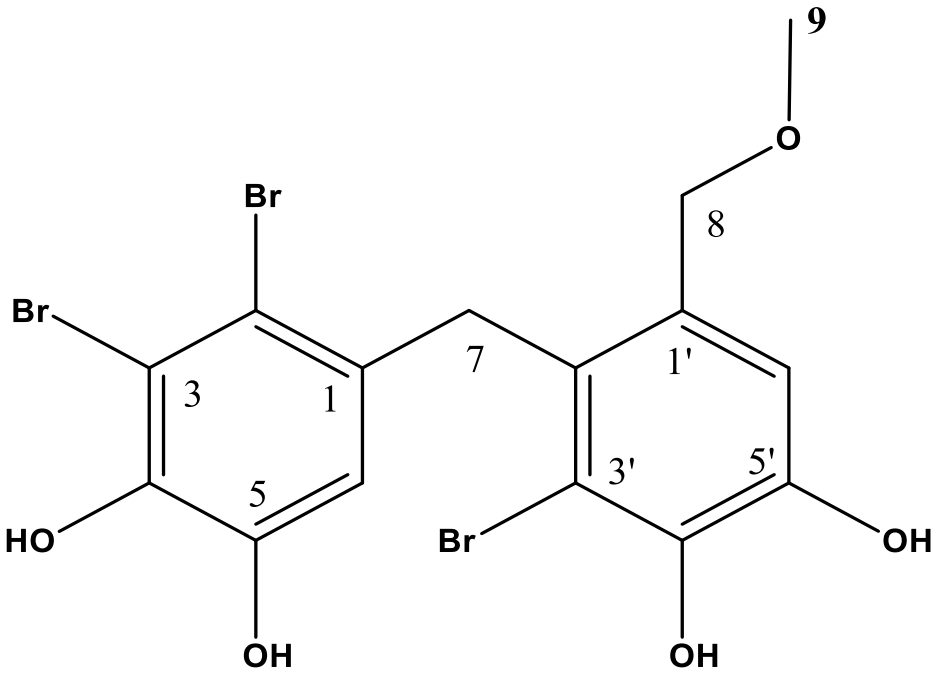

Figure 2-3-3-7. Structure of 3’-bromo-4’,5’-dihydroxy-2’-(2,3-dibromo-4,5-dihydroxybenzyl)benzyl methyl ether (compound **R10**).

Table 2-3-3-2. Comparison of compound **R10** observed and literature NMR data [56].

No.	^{1}H NMR (δ_H, ppm)		^{13}C NMR (δ_C, ppm)	
	Observed data	Literature data	Observed data	Literature data
1			132.4	131.5
2			114.8	115.4
3			113.6	112.8
4			143.3	142.6
5			144.7	144.0
6	6.07 (s, 1H)	6.08 (s, 1H)	114.9	114.0
7	4.11 (s, 2H)	4.12 (s, 2H)	39.4	38.4
8	4.19 (s, 2H)	4.21 (s, 2H)	73.3	72.3
9	3.23 (s, 3H)	3.24 (s, 3H)	58.1	57.9
1’			129.6	128.6
2’			130.8	129.8
3’			114.9	114.0
4’			143.4	142.6
5’			144.8	144.5
6’	6.98 (s, 1H)	7.00 (s, 1H)	116.3	115.4

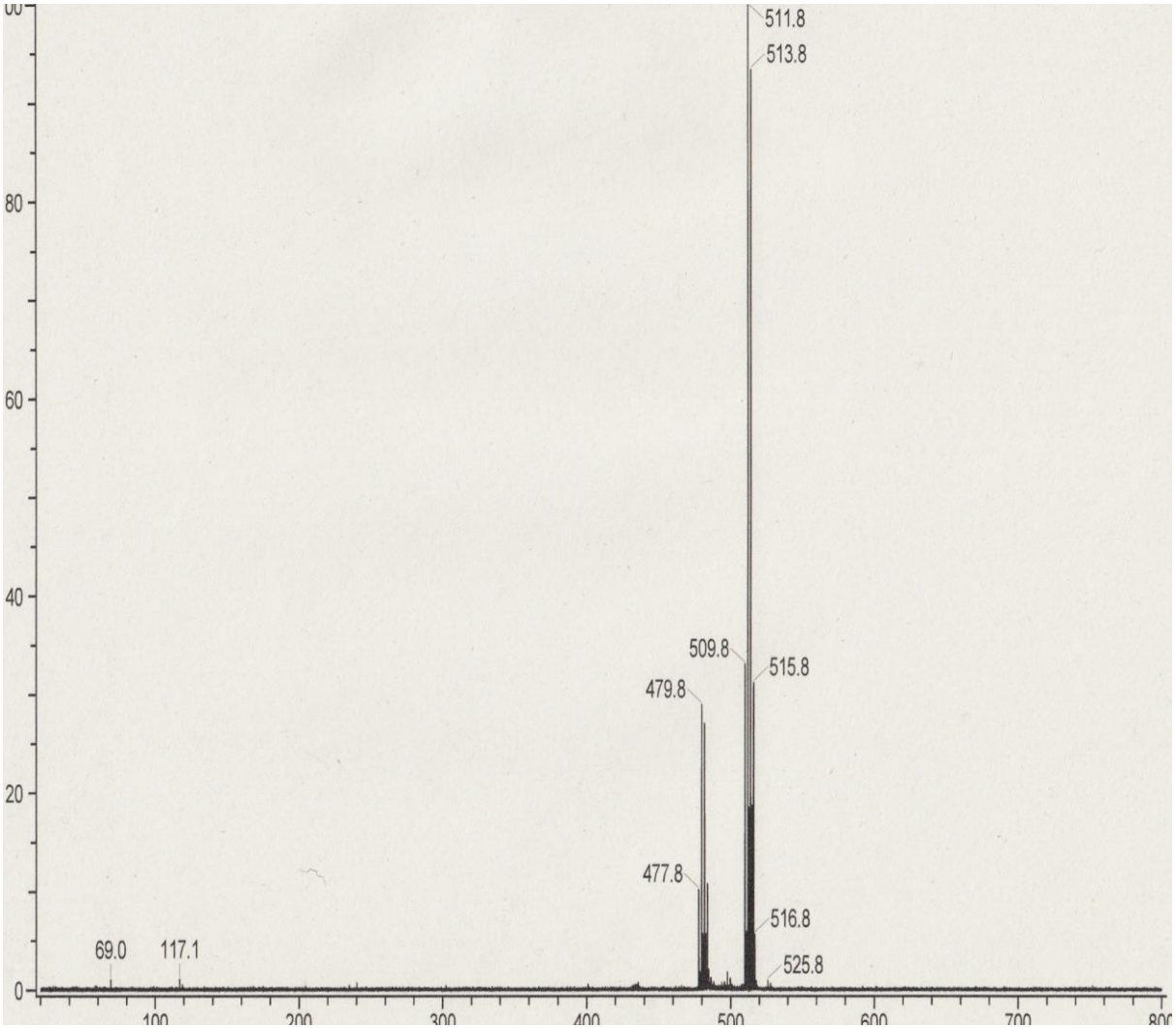

Figure 2-3-3-8. FD-MS spectrum of compound **R10**.

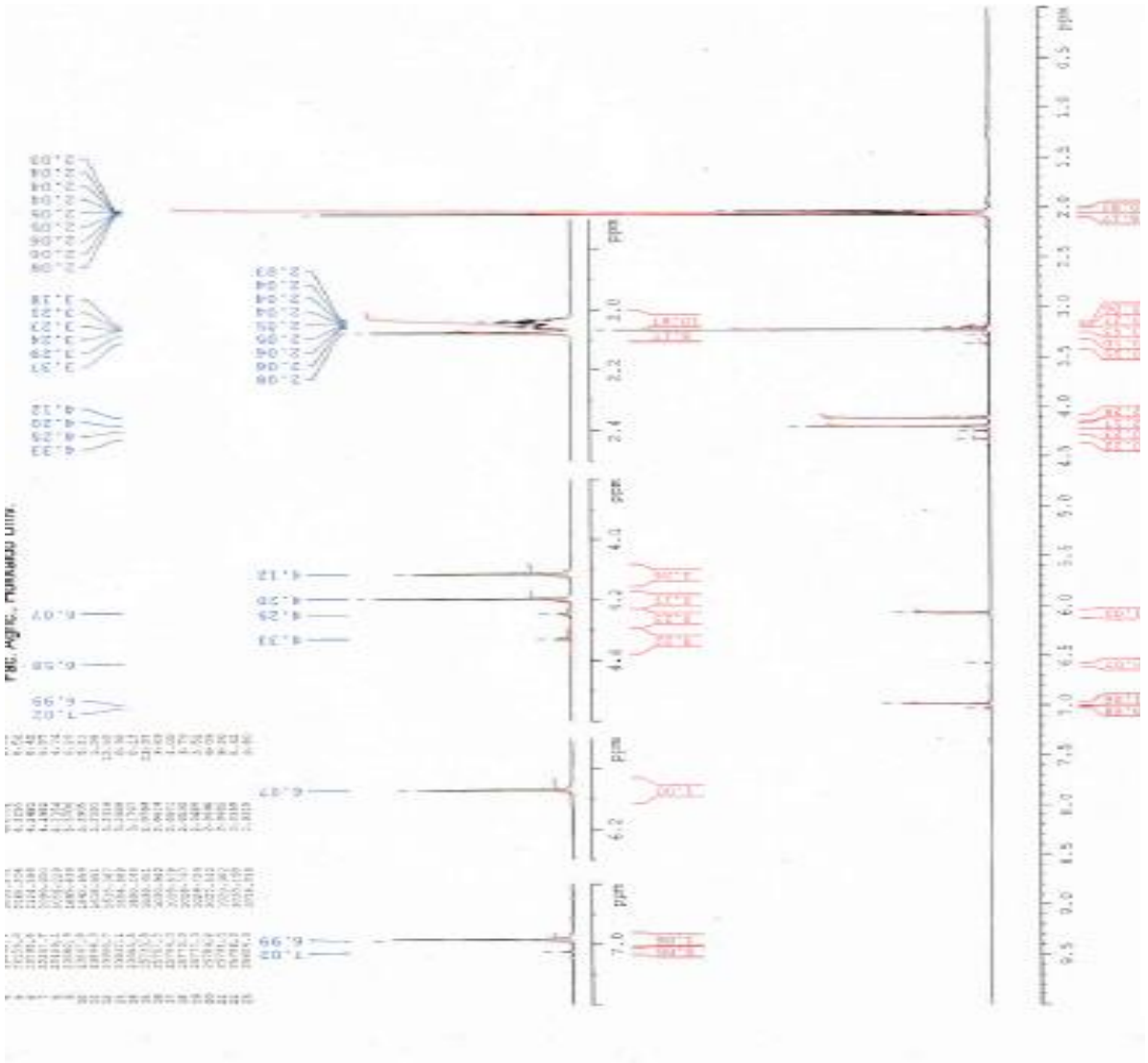

Figure 2-3-3-9. ^{1}H-NMR spectrum of compound **R10** (acetone-*d6*, 500 MHz).

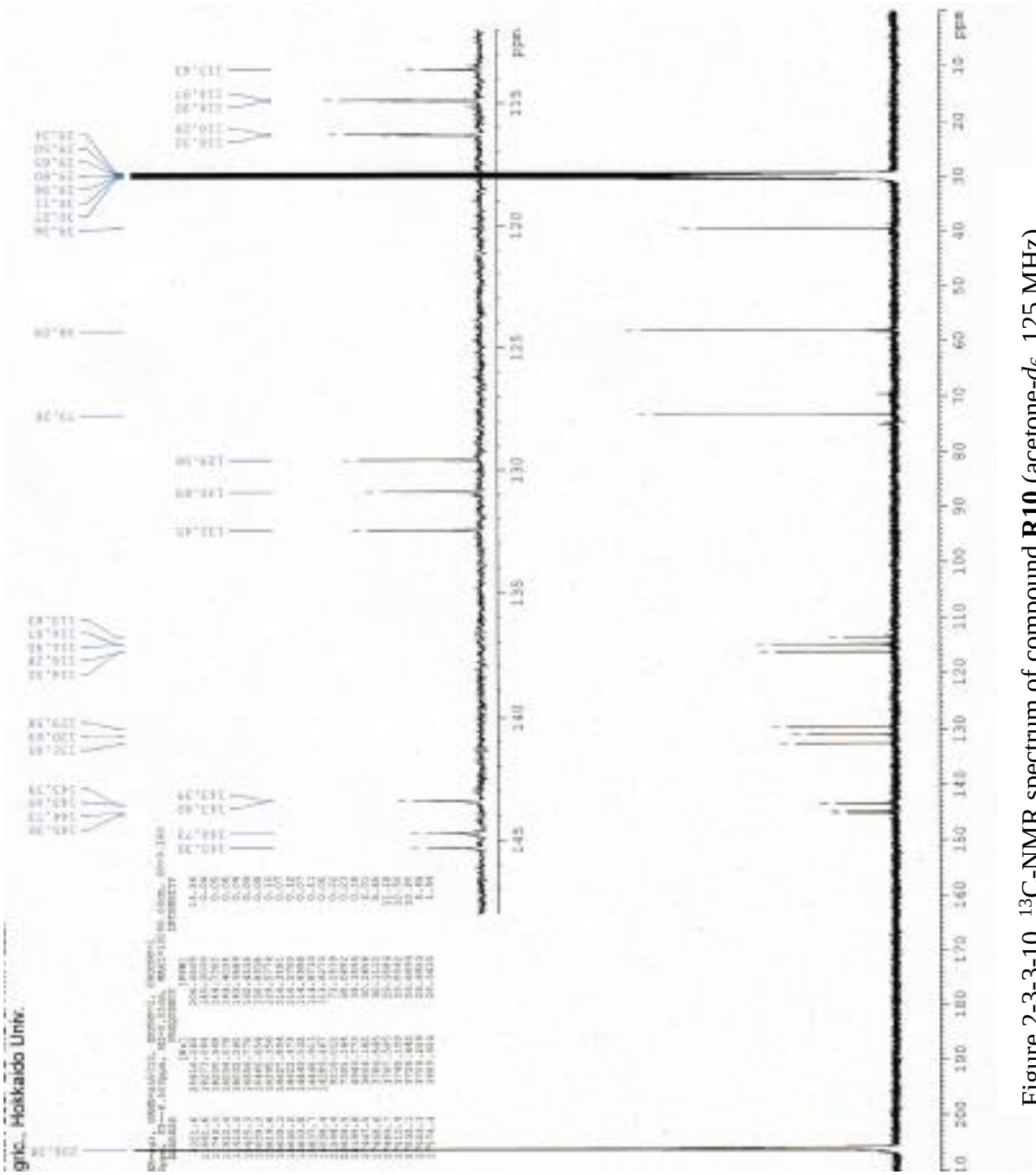

Figure 2-3-3-10. ^{13}C-NMR spectrum of compound **R10** (acetone-d_6, 125 MHz).

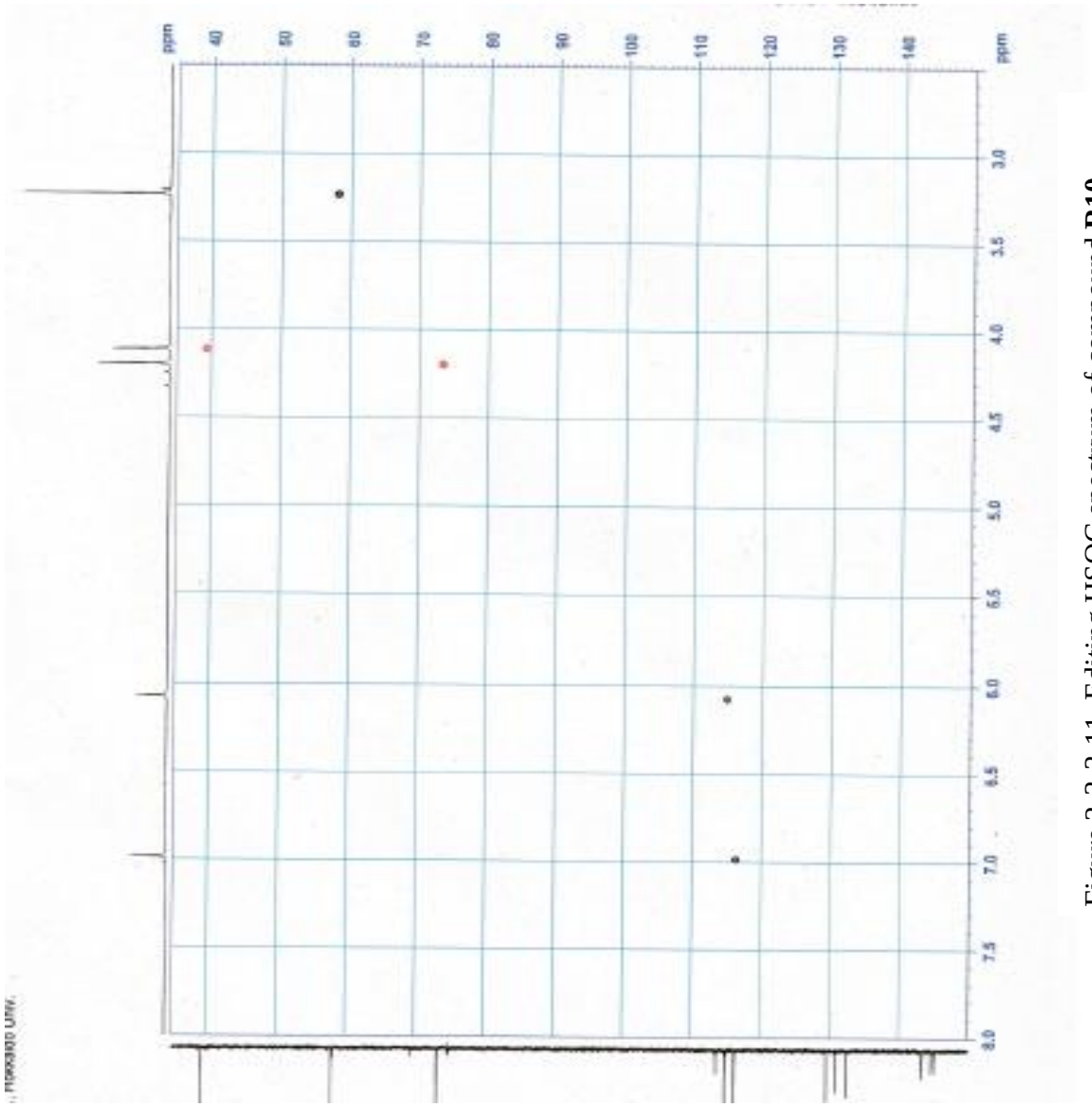

Figure 2-3-3-11. Editing HSQC spectrum of compound **R10**.

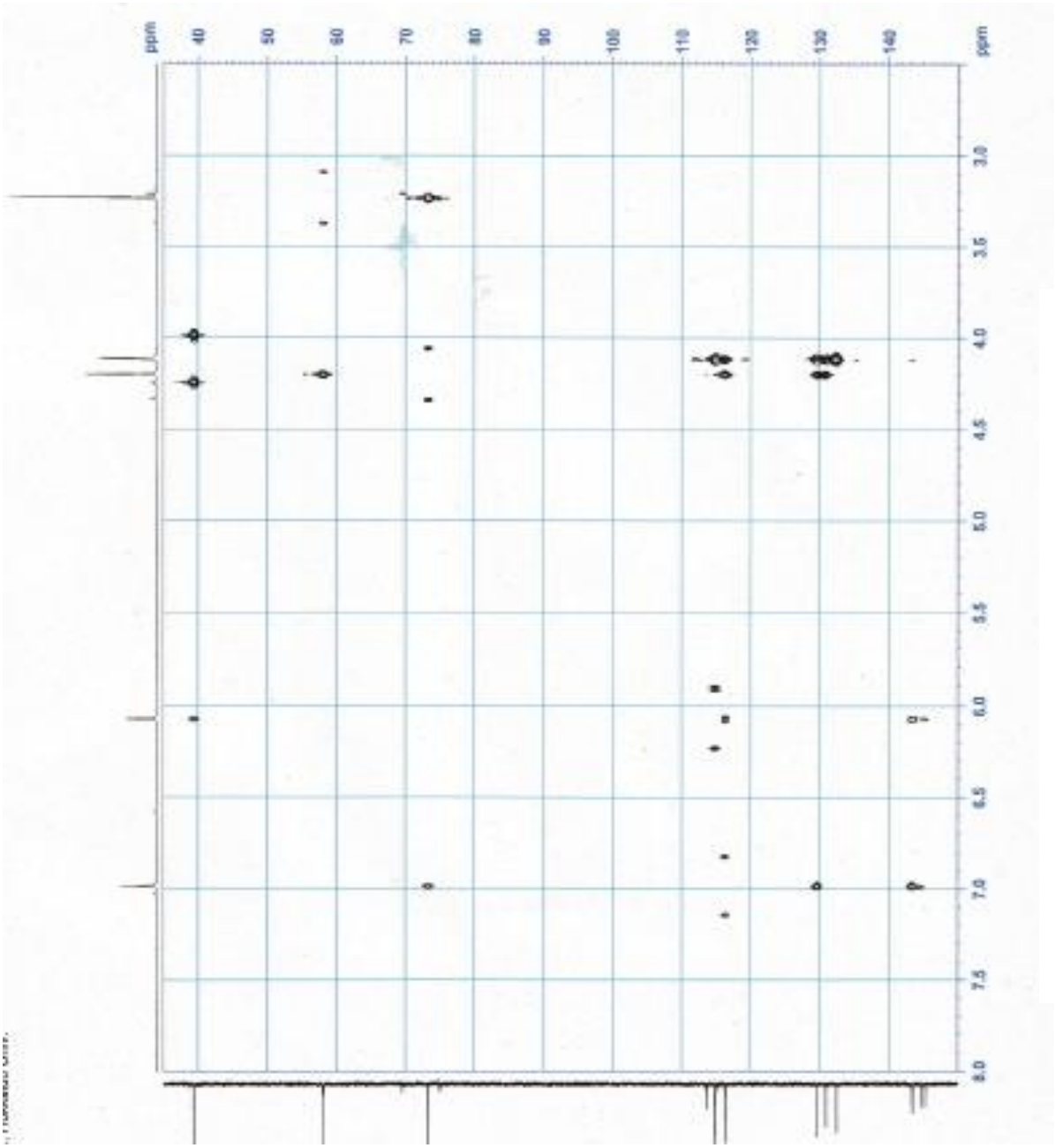

Figure 2-3-3-12. HMBC spectrum of compound **R10**.

2.4. Conclusion

The family of Rhodomelaceae is rich sources of bromophenols. This family contains many genera but *Rhodomela*, *Polysiphonia* and *Symphyocladia* have been reported for brominated phenolic compounds. On the basis of screening results, two red algae of Rhodomealaceae *N. aculeata* and *O. corymbifera* were selected for compound purification. Two known bromophenols **R3** & **R4** were purified from *N. aculeata* and six known bromophenols **R5**-**R10** from *O. corymbifera*. Structure confirmation was performed after comparison of reported spectroscopic data. On the basis of benzene ring, compounds **R3** & **R4** were monomers and **R5**-**R10** were dimers. BHB unit is a common feature in all compounds. Bromination is another typical characteristic of marine algae derived phenolic compounds. Tetrabromine substitutions were observed in compounds **R5**, **R7** & **R8**; tribromination in **R6**, **R9**, & **R10** while **R3** and **R4** were dibromosubstituted phenolic compounds. In the point of BHB units, compounds **R5** & **R8** were symmetric and remaining compounds were asymmetric.

Chapter 3
Tyrosinase Inhibitory and Antioxidant Activity of Bromophenols

3.1. Introduction

Many halogenated compounds were isolated from marine red algae of the family Rhodomelaceae. Usually halogenated phenols have a 2,3-dibromo-4,5-dihydroxybenzyl moiety and number of bromine substitution ranging from dibrominated to polybrominated ones. Halogenated phenols have been reported to showed wide range of functionalities such as antioxidant and enzyme inhibition [24, 31, 68, 70]. These functionalities are relying on number and position of either phenolic hydroxy group or bromine or both. Reactive oxygen species (ROS) are responsible of many human diseases. While human and agricultural commodity are suffering from hyperpigmentation caused by tyrosinase. Recently researcher found that free radical or reactive oxygen species (ROS) may induce α-melanocyte-stimulating hormone (α-MSH) resulting abnormal pigmentation such as age spot, freckles, skin aging, melasma [71]. Synthetic drugs are generally used as prevention method but these drugs have toxicity problem. Researchers have interest to find bioactive compounds from natural sources that can solve this problem. Ten bromophenols (**R1**-**R10**) were isolated from the marine red algae *Neorhodomela aculeata* and *Odonthalia corymbifera*. These bromophenols were investigated for tyrosinase inhibitory and antioxidant activity. To unveil the inhibitory mechanism, some phenolic compounds were purchased from chemical industries and inhibitory activities were compared with naturally occurring bromophenols (**R1**-**R10**). Kinetic study was performed to determine inhibition type and mode of inhibition of bromophenols against tyrosinase.

3.2. Materials and Methods

3.2.1. General Experimental Procedures

Synthetic phenolic compounds, 2,4-dichlorophenol (**62**), hexestrol (**63**), 2,4,6-trichlorophenol (**64**), 2,2'-biphenol (**65**), 2,2'-thiobis(4,6-dichlorophenol) (**66**), 2,4,6-tribromophenol (**67**), 2,2'-methylenebis-(4-chlorophenol) (**68**), tetrabromobisphenol A (**69**) and hexachlorophene (**70**) were purchased from Tokyo Chemical Industry Co. LTD. (Japan). Phenol crystal (**71**) was obtained from Kanto Chemical Co. LTD. (Japan). Catechol (**8**), pyrogallol (**72**) and phloroglucinol (**73**) were available from Wako Pure Chemical Industries LTD. (Japan). Mushroom tyrosinase (EC 1.14.18.1), 2,2´-azino-bis(3-ethylbenzothiazoline-6-sulfonic acid) diammonium salt (ABTS), 2,4,6-tris(2-pyridyl)-*s*-triazine (TPTZ), and 2,2-diphenyl-1-picrylhydrazyl (DPPH) were purchased from Sigma-Aldrich (St. Louis, MO, USA). Kojic acid was available from Tokyo Chemical Industry (Tokyo, Japan).

Ethylenediamine-*N,N,N',N'*-tetraacetic acid (EDTA) disodium salt was available from Dojindo Laboratories (Kumamoto, Japan). L-Tyrosine and 2(3)-*tert*-butyl-4-hydroxyanisole (BHA) were purchased from Wako Pure Chemical Industries (Kyoto, Japan).

3.2.2. Tyrosinase Inhibition Assay [72]

Sample solution (15 µl) was added into 50 mM sodium phosphate buffer (780 µl, pH 6.8) in test tube, followed by addition of 0.1 mg/ml L-tyrosine (0.5 ml) as substrate. Enzymatic reaction was started after adding 200 U/ml mushroom tyrosinase solution (205 µl). Reaction solution was incubated at 25 ^{0}C for 30 min and absorbance was measured at 490 nm. Kojic acid was used as a positive control. The IC_{50} value was expressed as sample concentration which can inhibit fitty percentage of tyrosinase reaction. The percent inhibition of tyrosinase activity was calculated as follows:

$$\% \text{ Inhibition} = [(A_2 - A_1) - (B_2 - B_1)]/ (A_2 - A_1) \times 100$$

Where A_1 is the absorbance at 490 nm without test compounds (control) at 0 min, A_2 is the absorbance at 490 nm without test compounds (control) at 30 min, B_1 is the absorbance at 490 nm with test compounds at 0 min, and B_2 is the absorbance at 490 nm with test compounds at 30 min.

3.2.3. DPPH Radical Scavenging Assay [67]

It was described in section 1.2.4.

3.2.4. ABTS Radical Scavenging Assay [73]

ABTS radical cation solution was prepared by adding 2.45 mM (final concentration) potassium persulfate to 7 mM ABTS in water and kept overnight in dark place. Before assay, the cation solution was diluted with ethanol to absorbance of 0.70 at 734 nm. Tested sample solution (10 µl) was added to the ABTS radical solution (1.0 ml). The mixture was left at room temperature for 10 min and absorbance was recorded at 734 nm. The EC_{50} value was expressed as sample concentration which can quench fitty percentage of ABTS radicals. The antioxidant activity of each sample was calculated from following equation:

$$\text{Antioxidant activity (\%)} = \{A_0 - A_S/A_0\} \times 100$$

Where A_0 is control absorbance, A_S is sample absorbance.

3.2.5. Cupric Reducing Antioxidant Capacity (CUPRAC) Assay [74]

Tested sample solution (0.1 ml) was added to the premixed reaction mixture containing 10 mM $CuCl_2$ solution (0.25 ml), 7.5 mM ethanolic neocuproine solution (0.25 ml), and 1 M ammonium acetate buffer solution (0.25 ml, pH 7.0) in each tube. The mixture was incubated for 30 min at room temperature, then absorbance was measured at 450 nm. $EC_{A0.50}$ means sample concentration with absorbance of 0.50 ($A_{0.50}$).

3.2.6. Ferric Reducing Antioxidant Power (FRAP) Assay [75]

Each tube contained freshly prepared FRAP reagent by mixing 300 mM sodium acetate buffer (750 µl, pH 3.6), 10 mM TPTZ in 40 mM HCl (75 µl) and of 20 mM $FeCl_3 \cdot 6H_2O$ (75 µl). Then sample solution (30 µl) was added along with water (100 µl) to the premixed FRAP reagent. The mixture was left for 4 min at room temperature and absorbance was measured at 593 nm. $EC_{A0.50}$ means sample concentration with absorbance of 0.50 ($A_{0.50}$).

3.2.7. Cupric Ion Chelation Assay [76]

Cupric ion chelation ability was assessed according to the method of Santos et al. with slight modification. Sample solution (120 µl) was mixed with 50 mM sodium acetate buffer (800 µl, pH 6.0). Then, 100 mg/l $CuSO_4 \cdot 5H_2O$ solution (120 µl), 2 mM pyrocatechol violet solution (34 µl) were added to reaction mixture and kept for 2 min. The mixture was shaken for 10 min and further incubated at 25 ^{0}C for another 10 min. Absorbance was measured at 632 nm and EDTA-Na_2 was used as positive control. The EC_{50} value was expressed as sample concentration which can chelate fitty percentage of Cu^{2+} ion. The percentage of chelation was calculated as follows:

$$Cu^{2+} \text{ chelating ability } (\%) = (Abs_{sample}/Abs_{control}) \times 100$$

3.3. Results and Discussion

3.3.1. Tyrosinase Inhibitory Activity of Compounds R1-R10

The isolated algal bromophenols **R1-R10** was investigated for tyrosinase inhibitory activity and structure-activity were speculated after comparison of other reported tyrosinase inhibitors. Antioxidant test employed as free radical scavenging (DPPH and ABTS), metal-reducing antioxidant (CUPRAC and FRAP), copper chelation assay.

3.3.1.1. Tyrosinase inhibitory activity

Compound **R1** displayed 2-fold stronger tyrosinase inhibitory activity while compound **R2** showed slightly higher activity with the positive control, kojic acid. Compound **R7** found as the most potent inhibitor (IC_{50} = 1.0 µM), 35-fold stronger than kojic acid (IC_{50} = 35.0 µM). Other two potent inhibitors were compounds **R5** and **R8** with IC_{50} values of 11.0 and 5.2 µM, respectively (Table 3-3-1).

Table 3-3-1. Tyrosinase inhibitory activity of compounds **R1-R10**.

Compound	Tyrosinase inhibition, IC_{50} (µM)[a]
R1	17.3±0.1
R2	31.0±0.1
R3	67.5±0.1
R4	96.8±0.1
R5	11.0±0.1
R6	39.2±0.0
R7	1.0±0.1
R8	5.2±0.0
R9	50.0±0.1
R10	39.0±0.0
Kojic acid	35.0±0.0

[a]Mean±standard error (n=3)

Compounds **R5**, **R7**, and **R8** possess two 2,3-dibromo-4,5-dihydroxylbenzyl moieties in their structures. Monomers compounds **R3** and **R4** displayed weaker inhibition than all dimers (compounds **R5**-**R10**). Thus number and position of phenolic hydroxy group is critical for tyrosinase inhibition. All the bromophenols (compounds **R1**-**R10)** possess the catechol moiety that behaves as a copper chelator of tyrosinase [71]. However, compound **R7** showed weak Cu-chelating potency than compounds **R5** and **R8**. Thus tyrosinase inhibition by bromophenol might be influenced by other mechanism different from copper chelation. This study has disclosed new functionality of naturally occurring bromophenol as a tyrosinase inhibitor. There are many plausible mechanisms for tyrosinase inhibition by phenolic compounds.

Polyphenols are the largest group of tyrosinase inhibitors [3]. Flavonoids are the well studied polyphenols that can inhibit tyrosinase due to their keto group which may be involved in complex formation with copper ions [4, 77]. Studies suggested that position and the number of hydroxy groups can affect the tyrosinase inhibitory activity such as norartocarpetin (**74**) showed higher inhibition than morusinol (**75**) and acacetin (**76**) (Figure 3-3-1-1) [78-80]. In flavonol, 3-hydroxy-4-keto moiety acts as key role in copper chelation [3] but showed weak inhibition than kojic acid. Inhibition strength ranks as quercetin (**77**) > kaempferol (**78**) > uralenol (**79**) > papyriflavonol A (**80**) (Figure 3-3-1-2) [4, 81]. The hydroxy groups near the carbonyl functional group on the C ring (C-3 position) compromised the tyrosinase quenching ability in flavonol [77]. Increasing isoprenyl substitutions also decrease inhibition potency.

Chalcone, a captured flavonoid-type tyrosinase inhibitor contains two aromatic rings linked by an unsaturated chain. Resorcinol subunit on both rings A and B might increase inhibition properties in morachalcone A (**81**) than isoliquiritigenin (**82**) and broussochalcone A (**83**) (Figure 3-3-1-3) [4, 81, 82]. Position of hydroxy groups and its substitution are very important in flavanones and flavanonols for tyrosinase inhibition. For example, steppogenin (**84**) showed more inhibition than artocarpanone (**85**), and kuwanon E (**86**) was powerful than kuwanon U (**87**) (Figure 3-3-1-4) [4, 80, 83].

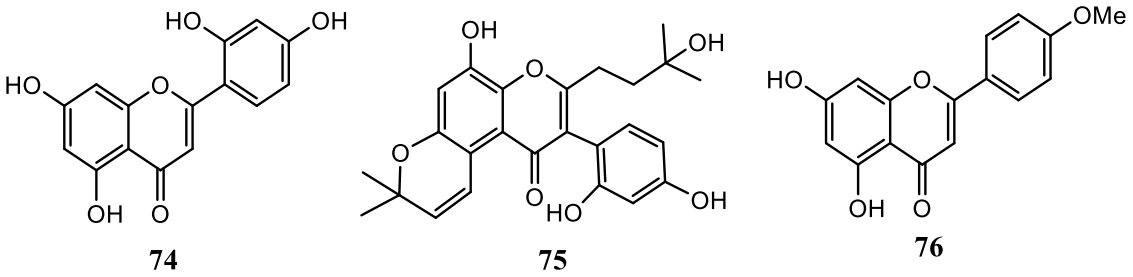

Figure 3-3-1-1. Flavones-type tyrosinase inhibitors.

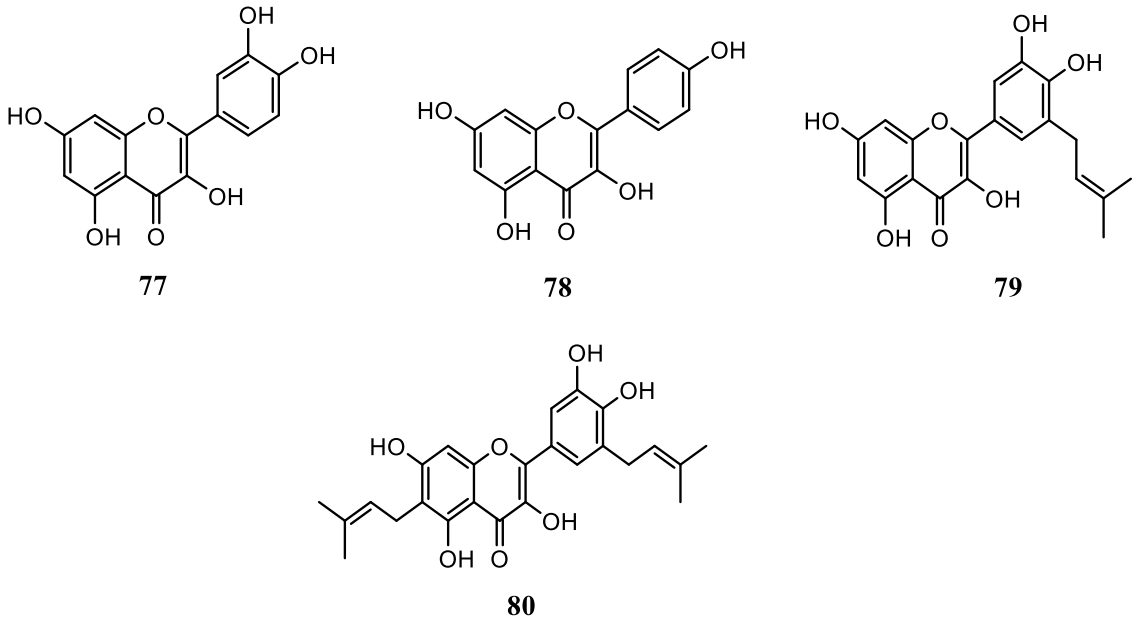

Figure 3-3-1-2. Flavonol-type tyrosinase inhibitors.

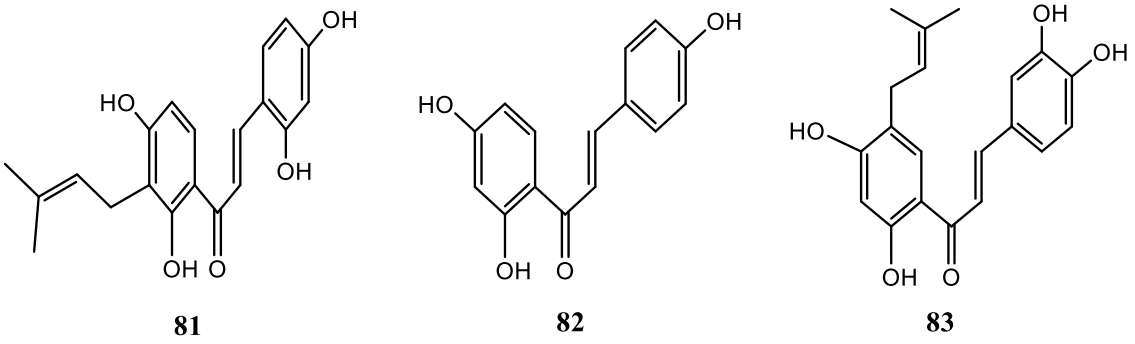

Figure 3-3-1-3. Chalcone-type tyrosinase inhibitors.

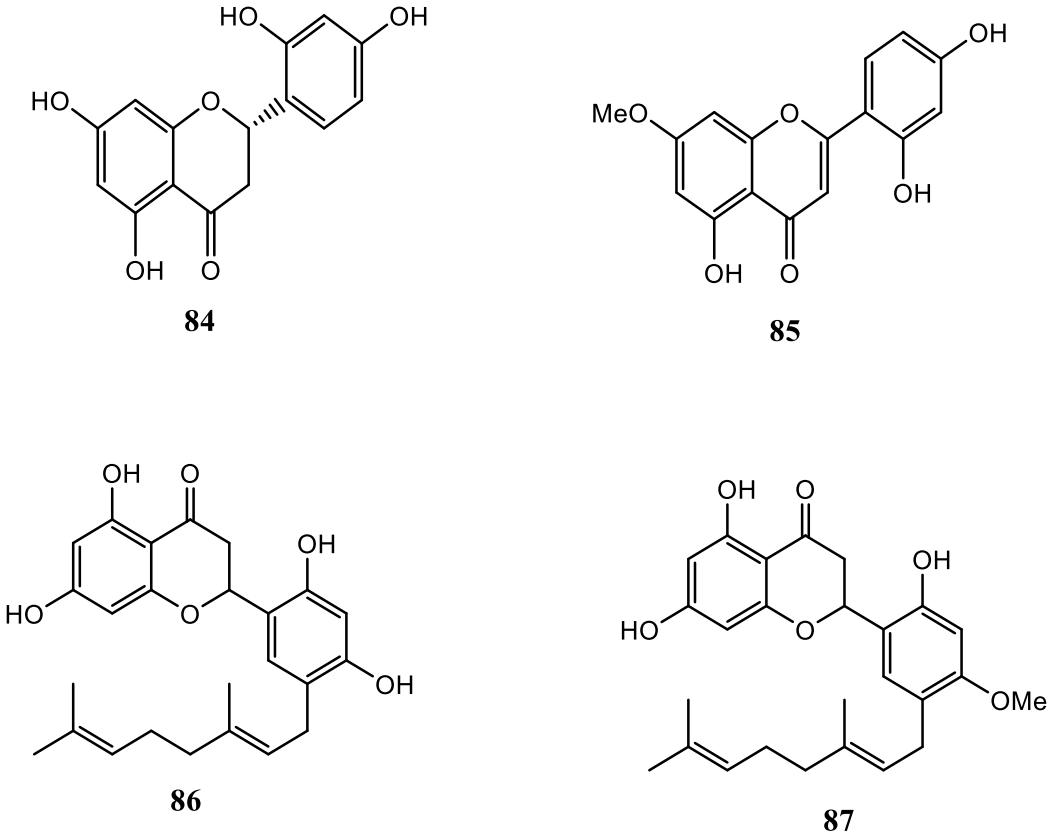

Figure 3-3-1-4. Flavanone-type tyrosinase inhibitors.

In the case of isoflavone-type tyrosinase inhibitor, position of hydroxy group in the A ring strongly affect inhibitory activity. Substitution of hydroxy group at C-6 and C-7 position increase inhibitory activity to a great extent than did substitution at C-7 position alone [4, 84]. Higher inhibitory activity found in 6,7,4'-trihydroxyisoflavone (**88**) compared to 5,7,8,4'-tetrahydroxyisoflavone (**89**) and 7,8,4'-trihydroxyisoflavone (**90**) (Figure 3-3-1-5). Phenolic hydroxy groups and *trans*-olefin structure of the parent stilbene skeleton are very significant for inhibitory potency of hydroxystilbene. This group also relies on number and position of hydroxy group substitution as tyrosinase inhibitors. Oxyresveratrol (**91**) has powerful inhibitory potency than artocarbene (**92**) and resveratrol (**93**) (Figure 3-3-1-6) [4, 85, 86].

The hydroxy groups at the C-6 and C-7 position of the coumarin skeleton were the determining factors for tyrosinase inhibitory activity. This speculation was proven as esculetin (**94**) showed higher inhibitory activity than umbelliferone (**95**) and scopoletin (**96**) (Figure 3-3-1-7) [4, 87]. Phenolic acid and phenolic acid ester showed weak inhibitory activity. Benzaldehyde-type inhibitors form Schiff base with a primary amino group in the enzyme while benzoate involves non-ionized interaction of the inhibitors with the copper of enzyme active site. Cinnamic acid (**97**), benzoic acid (**98**) and cinnamaldehyde (**99**) exhibited weak to moderate tyrosinase inhibitory activity and are weaker than kojic acid (Figure 3-3-1-8) [3, 4, 88]. In addition a steroid-type stigmast-5-ene-3β,26-diol (**100**) was 7-fold active, while trilinolein (**101**) a lipid compound proved to be as potent as kojic acid (Figure 3-3-1-9) [3, 4].

Bromination effect on tyrosinase activity was not investigated so far. Bromine substitution is a common characteristic of marine alga derived bromophenol. However, multibrominated compounds displayed higher protein tyrosine phosphatase inhibitory activity than monobrominated compounds [89, 90]. Compounds **R5**, **R7** and **R8** were also displayed inhibitory activity against protein tyrosine kinase and significant cytotoxicity against human cancer cell [36, 91]. Thus, the two 2, 3-dibromo-4, 5-dihydroxylbenzyl moieties are seemed to be important structures of tyrosinase inhibition, compared with tribrominated compounds. Although the reason why the asymmetric tetrabrominated compound **R7** showed strong inhibition is still unclear. These results suggest that both number of bromine substitution and orientation of bromine and phenolic hydroxy groups are important factors of tyrosinase inhibitory potency.

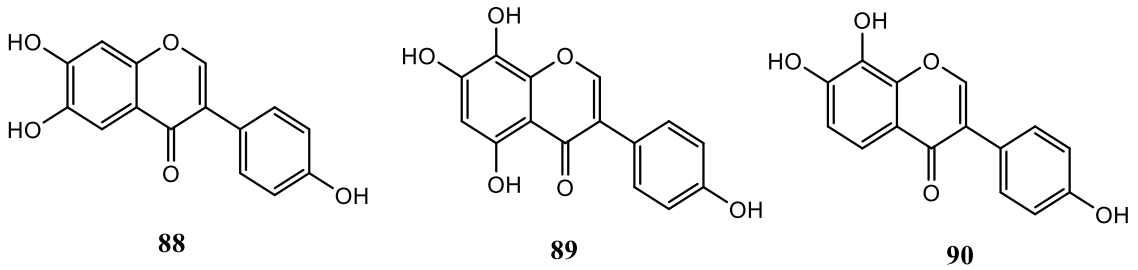

Figure 3-3-1-5. Isoflavone type-tyrosinase inhibitors.

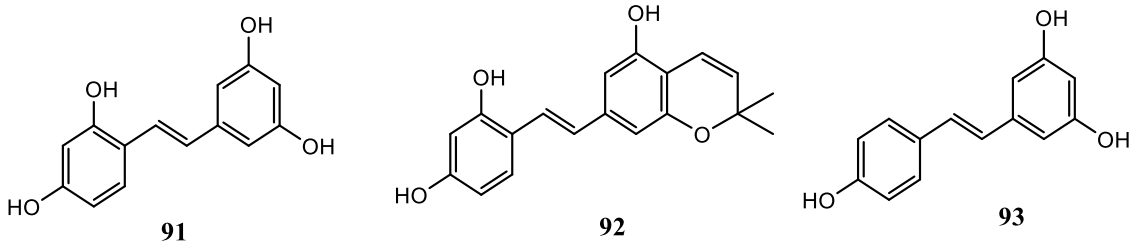

Figure 3-3-1-6. Stilbene-type-tyrosinase inhibitors.

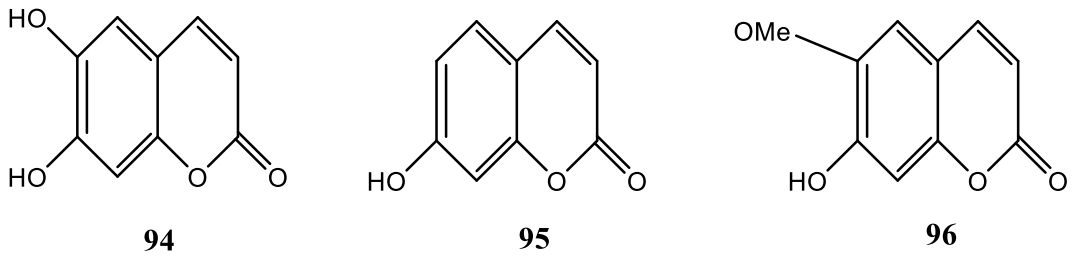

Figure 3-3-1-7. Coumarin type-tyrosinase inhibitors.

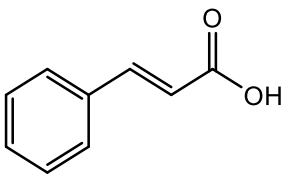

97

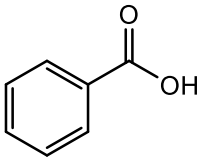

98

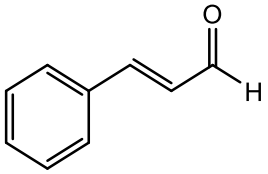

99

Figure 3-3-1-8. Phenolic acid-type tyrosinase inhibitors.

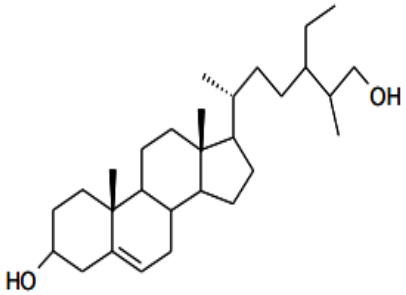

100

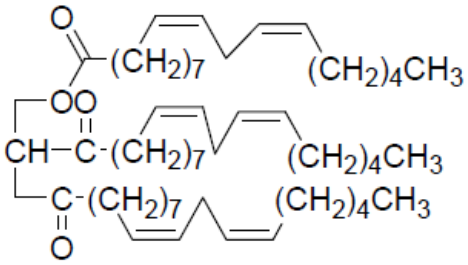

101

Figure 3-3-1-9. Steroid and long chain lipid type tyrosinase inhibitors.

3.3.2. Antioxidant Activity of Compounds R1-R10

Antioxidant test employed as free radical scavenging (DPPH and ABTS), metal-reducing antioxidant (CUPRAC and FRAP), copper chelation assay. Antioxidant properties of compounds **R1-R10** were investigated by using these assays. All the bromophenols examined showed radical scavenging properties. Compounds **R5**, **R8**, **R9** and **R10** exhibited potent DPPH radical scavenging activities with EC_{50} values of 5.0 to 10.0 μM while compounds **R2**, **R3**, **R4**, **R6** and **R7** exhibited relatively low activities with EC_{50} values around 20.0 μM (Table 3-3-2). Radical scavenging activity depends on hydrogen-donating ability. Many researchers [17, 92 93] have reported that increasing in the number of phenolic hydroxy groups led to higher radical scavenging activity. Thus, dimers (compounds **R5-R10**) showed strong radical scavenging than monomers (compounds **R3** and **R4**). This results support the relationship between molecular structure and antioxidant activity of bromophenols from marine red algae reported in Figures 3-3-2-1 to 3-3-2-5 [17, 24, 59, 94, 95]. However in the present study, bromophenols **R5-R10** possessed equal four phenolic hydroxy groups. This revealed antioxidant potency of bromophenols would be influenced not only by number of phenolic hydroxy groups but also by bromine and alkyl substitution. Compounds **R6** and **R10** were structural isomers, nevertheless, compound **R10** showed two-fold stronger scavenging activity than that of compound **R6**. This difference would rely on different positions of bromine atoms and methoxymethyl group [24]. Alternatively the different activity could depend on different orientation of *ortho*-dihydroxy groups to methylene or ether bridge, that is, positions of dihydroxy groups to bridge are *meta* and *para* position in compounds **R5**, **R8**-**R10**, and *ortho* and *meta* position in compounds **R6** and **R7**. In ABTS assay, scavenging trend showed similar patterns of DPPH assay results.

In CUPRAC and FRAP assays are indication of reducing power to donate electron to transition metals with a compound [96]. Compounds **R1-R10** exhibited relatively same reducing power compared with 2 or 3-*tert*-butyl-4-hydroxyanisole (BHA) and catechol as positive controls. Radical scavenging results were also supported compound reducing ability [97]. Compounds **R5, R8** and **R9** displayed the highest reducing potentiality in the bromophenols examined due to presence of catechol moieties and structural symmetry [98, 99]. In Cu^{2+}-chelation assay, compounds **R5**, **R8** and **R10** exhibited relatively high Cu^{2+}-chelating activity similar to the activity of ethylenediamine-*N,N,N',N'*-tetraacetic acid (EDTA) as a positive control. However compound **R6** showed the weakest chelating power.

Phenolic compound with catechol moieties can bind transition metal [76]. However, it is unclear the reason why compound **R6** showed weak chelating power.

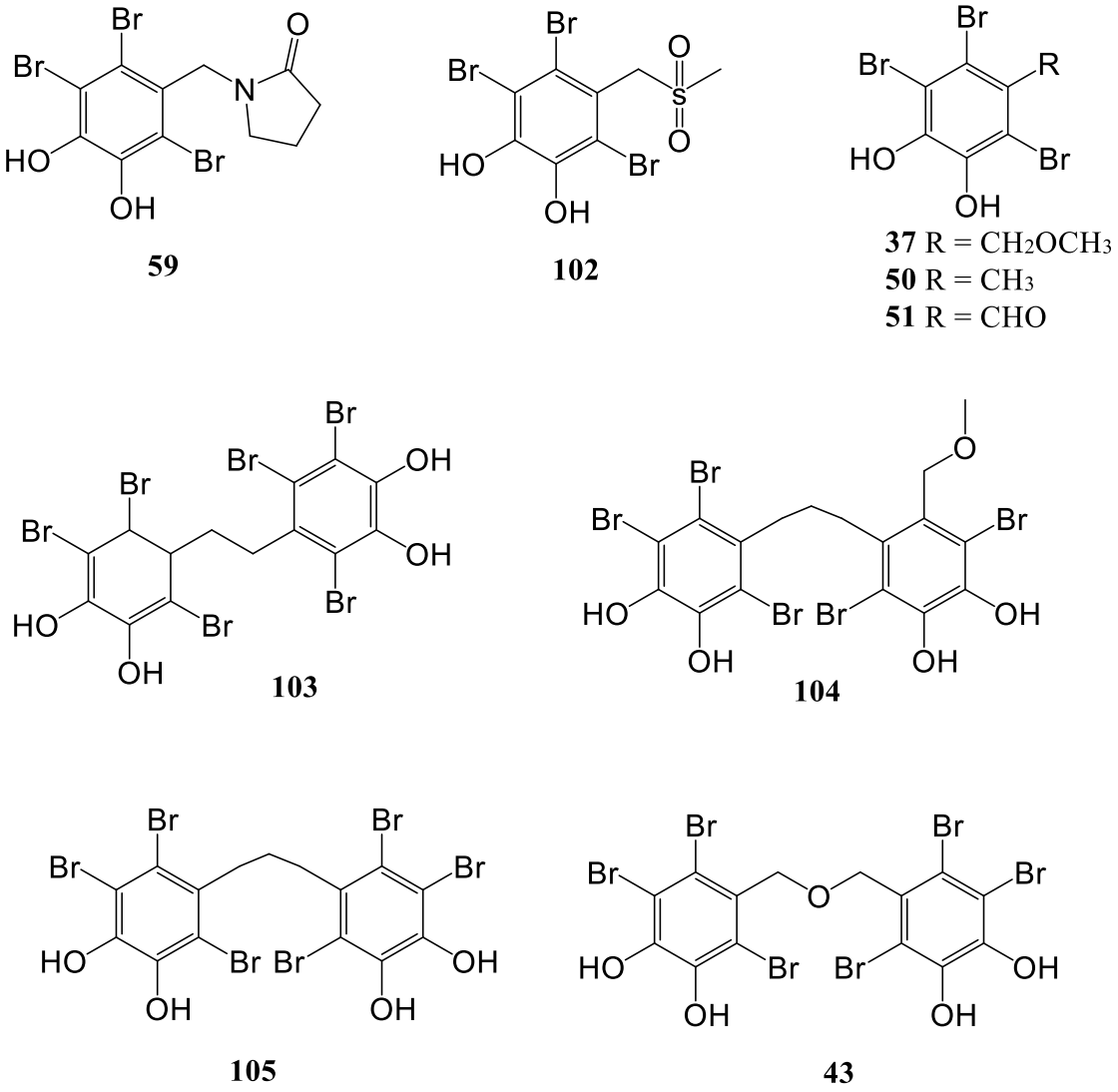

Figure 3-3-2-1. Bromophenols from the marine red alga *Symphyocladia latiuscula* [59].

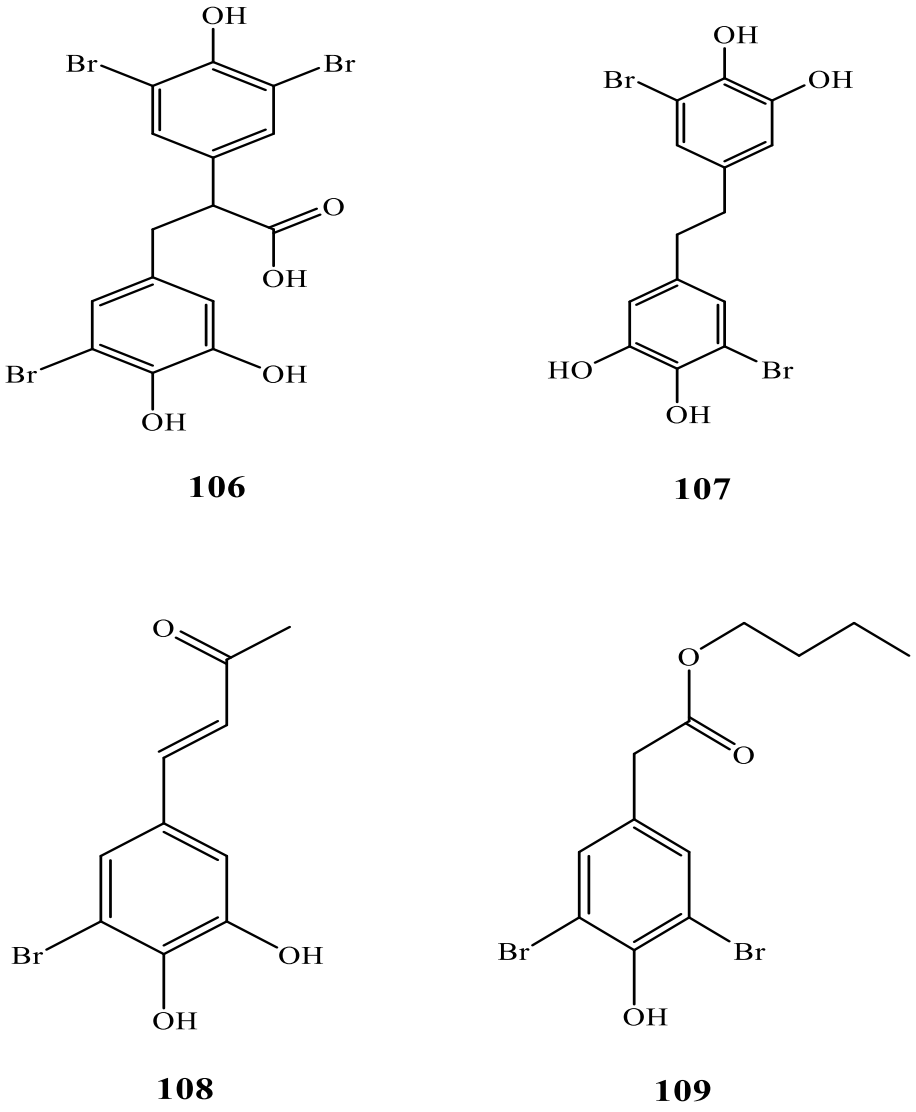

Figure 3-3-2-2. Bromophenols from the marine red alga *Polysiphonia urceolata* [94].

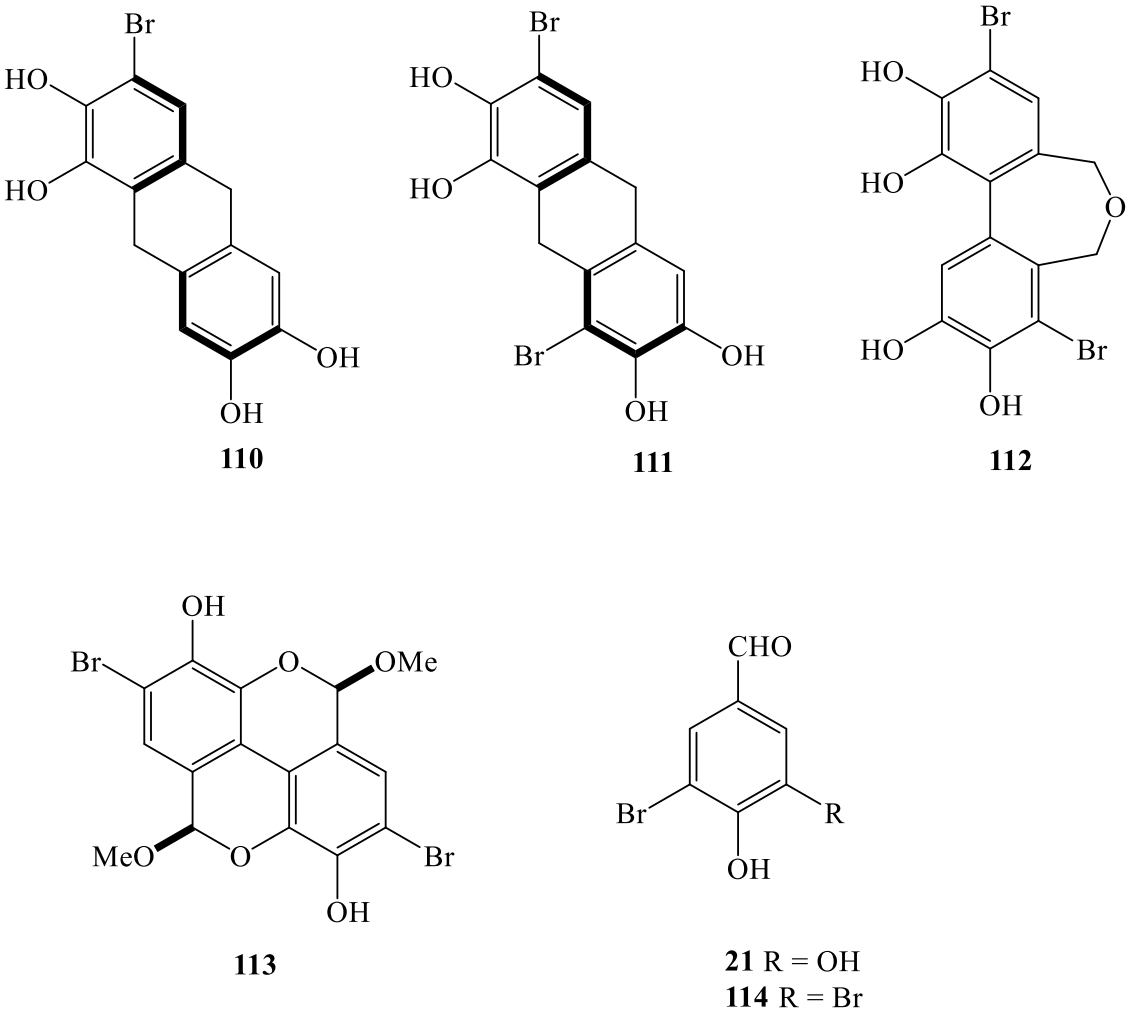

Figure 3-3-2-3. Bromophenols from the marine red alga *Polysiphonia urceolata* [95].

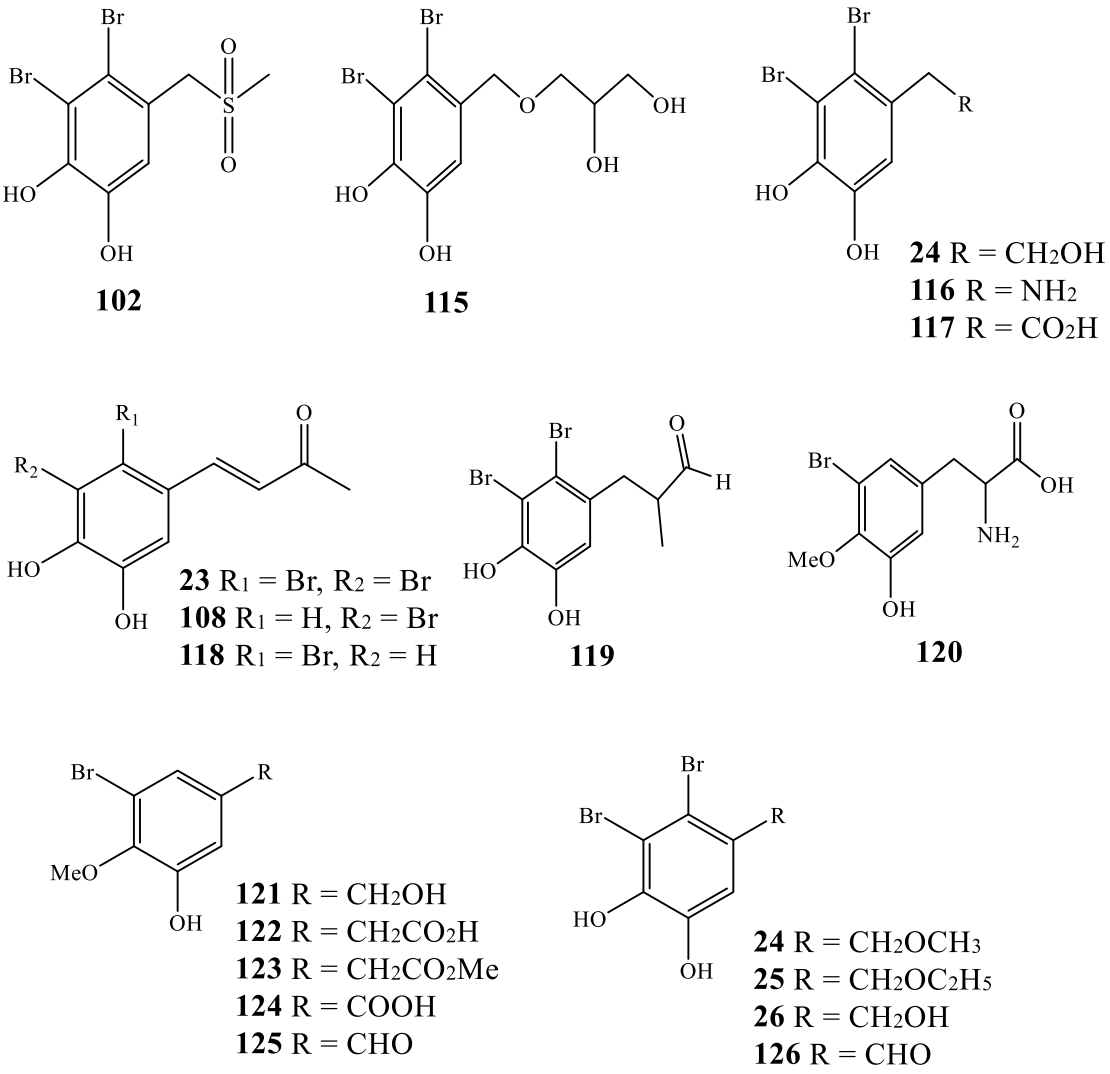

Figure 3-3-2-4. Bromophenols from the marine red alga *Rhodomela confervoides* [24].

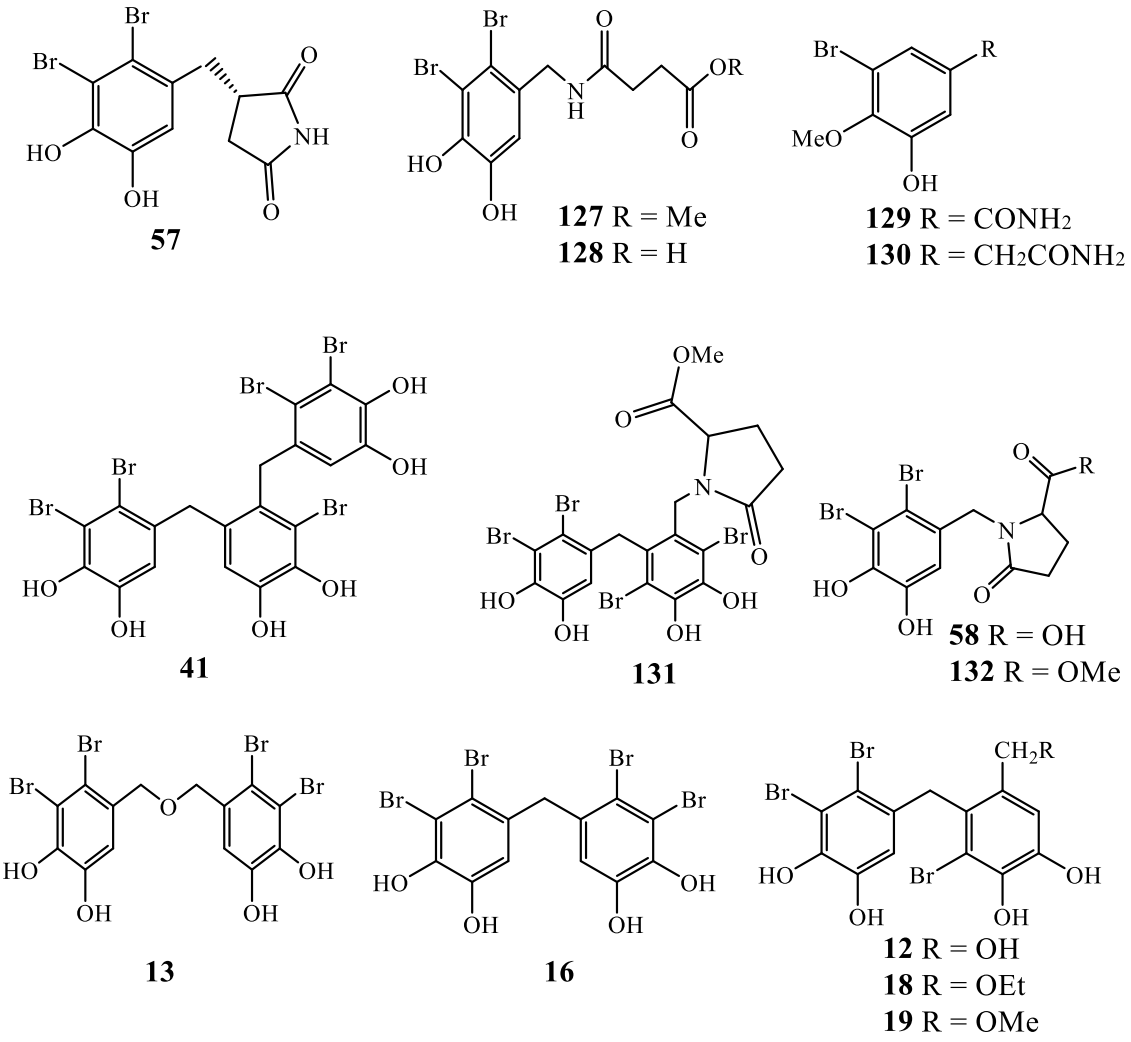

Figure 3-3-2-5. Bromophenols from the marine red alga *Rhodomela confervoides* [17].

Table 3-3-2. Antioxidant activity[a] of compounds **R1**-**R10**.

Compound	DPPH EC_{50}[b] (μM)	ABTS EC_{50}[b] (μM)	CUPRAC $EC_{A0.50}$[c] (μM)	FRAP $EC_{A0.50}$[c] (μM)	Cu^{2+}-chelation EC_{50}[b](μM)
R1	24.7±0.0	17.3±0.1	13.6±0.1	11.1±0.1	61.9±0.1
R2	13.5±0.0	6.7±0.1	7.8±0.1	10.8±0.1	74.3±0.1
R3	21.1±0.1	14.3±0.2	11.1±0.2	14.5±0.1	46.6±0.3
R4	25.5±0.5	10.1±0.4	9.3±0.1	12.9±0.1	41.9±0.3
R5	7.3±0.1	3.3±0.1	5.1±0.1	7.3±0.1	25.4±0.1
R6	19.6±0.1	9.8±0.0	10.9±0.1	7.8±0.1	107.8±0.1
R7	17.0±0.1	20.4±0.2	9.8±0.1	12.9±0.1	45.9±0.2
R8	8.7±0.1	3.4±0.2	5.5±0.2	7.1±0.1	24.0±0.1
R9	5.0±0.1	2.0±0.1	5.8±0.1	7.2±0.1	26.2±0.0
R10	9.8±0.2	7.7±0.0	6.4±0.1	8.0±0.1	29.6±0.1
BHA	34.0±0.1	10.4±0.2	16.0±0.1	8.3±0.1	
Catechol	16.9±0.1	7.3±0.0	25.4±0.1	9.1±0.1	
EDTA					31.6±0.1

[a] All values are represented as mean ± SE of triple mesurements.

[b] The half maximal effect concentration.

[c] The effective concentration of absorbance of 0.50.

3.3.3. Kinetic Study of Bromophenols against Tyrosinase

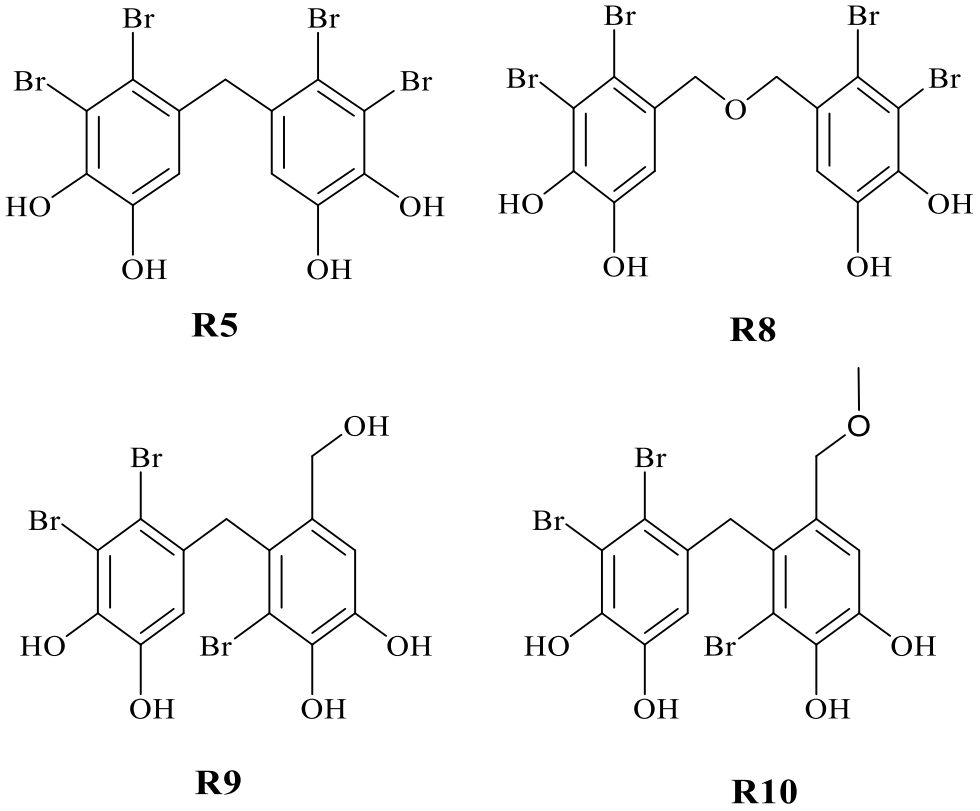

Figure 3-3-3-1. Examined bromophenols for kinetic study.

The inhibition types of bromophenols were determined from Lineweaver-Burk plot which shown in Figures 3-3-3-2(A) to 3-3-3-5(A). The results showed that inhibitors compounds **R5**, **R8**, **R9** and **R10** produced an intersection point of lines on 1/[S] axis. These results revealed that all the bromophenols examined were noncompetitive inhibitor. Dixon plot analysis was applied to determine inhibitor constant (K_i) in Figures 3-3-3-2(B) to 3-3-3-5(B) and values were enlisted in Table 3-3-3. 7-Phloroeckol, a phenolic compound derived from brown algae [100] and prenylated flavonoid derived from terrestrial plant also exhibited noncompetitive type inhibition against mushroom tyrosinase [71]. This suggests that bromophenols type tyrosinase inhibitors may bind other site of the active site and combine with either free enzyme or enzyme-substrate complex. In another hypothesis for mode of noncompetitive inhibition, the inhibitor caused a change in the structure and shape of enzyme, and the modified enzyme was no longer capable of binding correctly with the substrate [101]. Inhibitor constant, $K_{i,}$ is an indication of inhibitor binding affinity toward enzyme or enzyme-substrate complex [102]. Thus, bromophenol type tyrosinase inhibitors can be ranked as **R8** > **R5** > **R10** > **R9** on the basis of binding affinity.

Table 3-3-3. Inhibitor constant (K_i) value and inhibition type of bromophenols against tyrosinase activity.

Bromophenol	K_i value (μM)	Inhibition Type
R5	8.0	Non-competitive
R8	2.4	Non-competitive
R9	40.0	Non-competitive
R10	24.7	Non-competitive

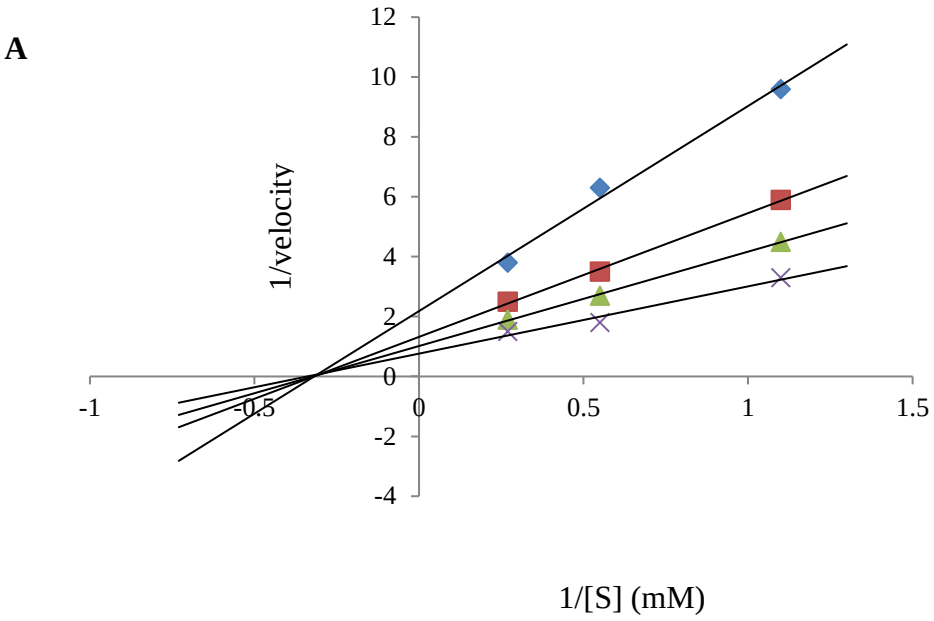

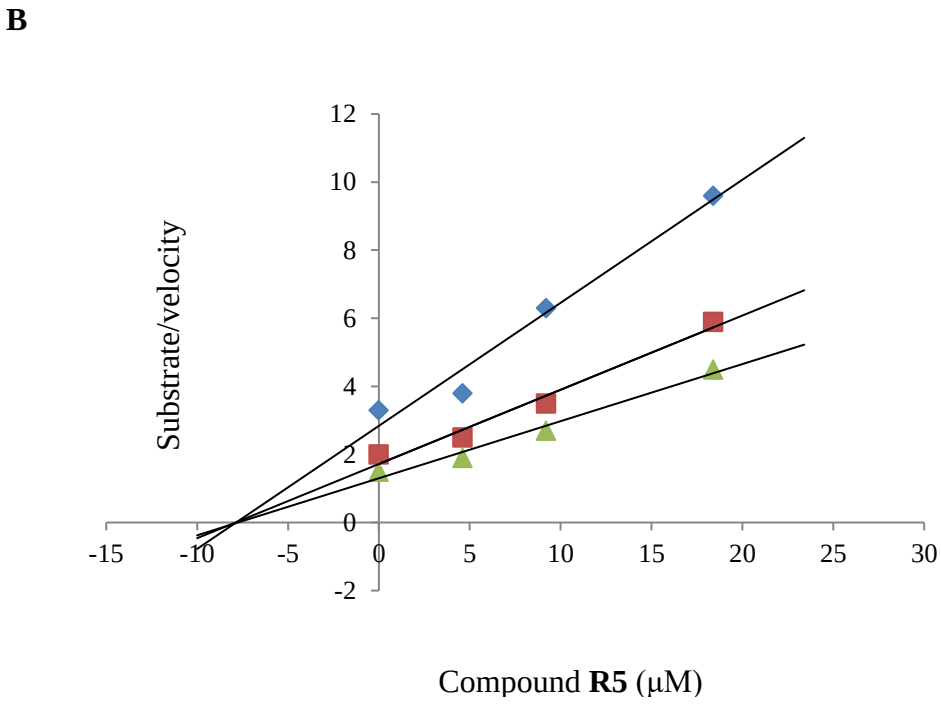

Figure 3-3-3-2. Kinetic analysis of compound **R5** against tyrosinase activity. **A**. Lineweaver-Burk plot, **B**. Dixon plot.

A

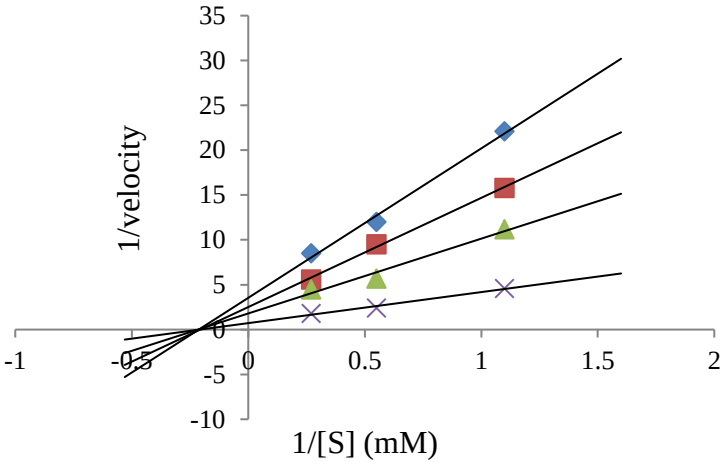

B

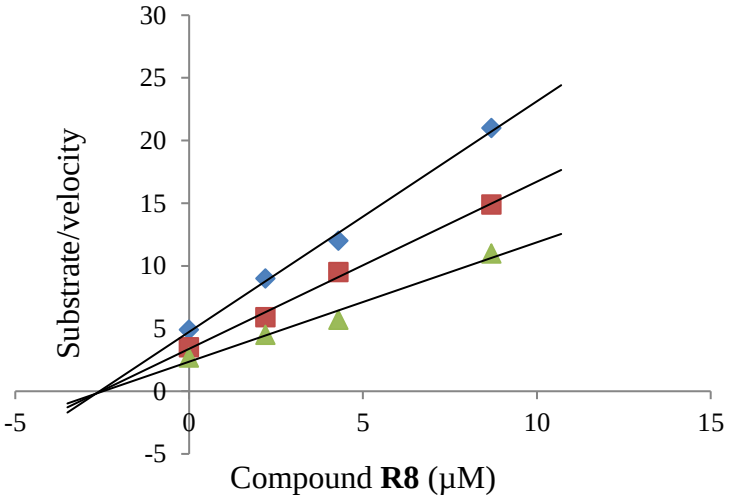

Figure 3-3-3-3. Kinetic analysis of compound **R8** against tyrosinase activity. **A**. Lineweaver-Burk plot, **B**. Dixon plot.

A

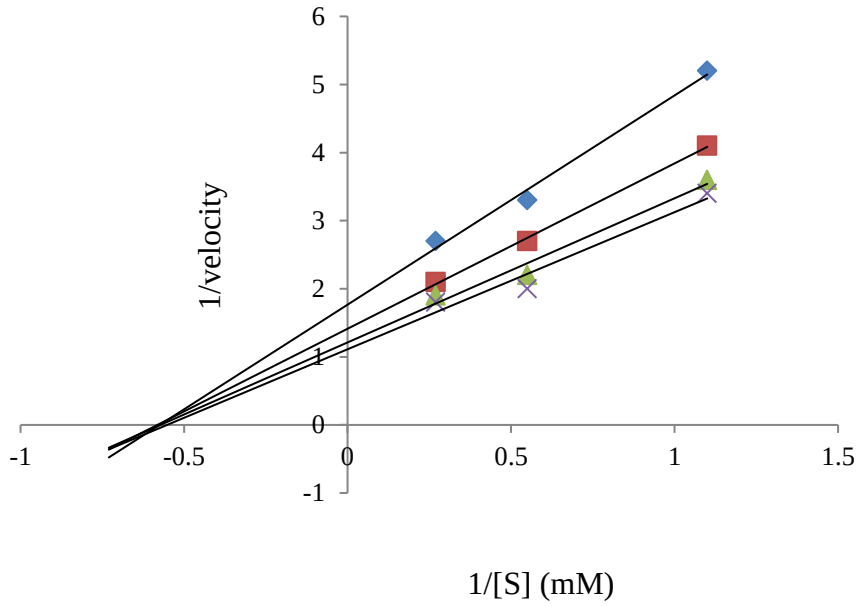

B

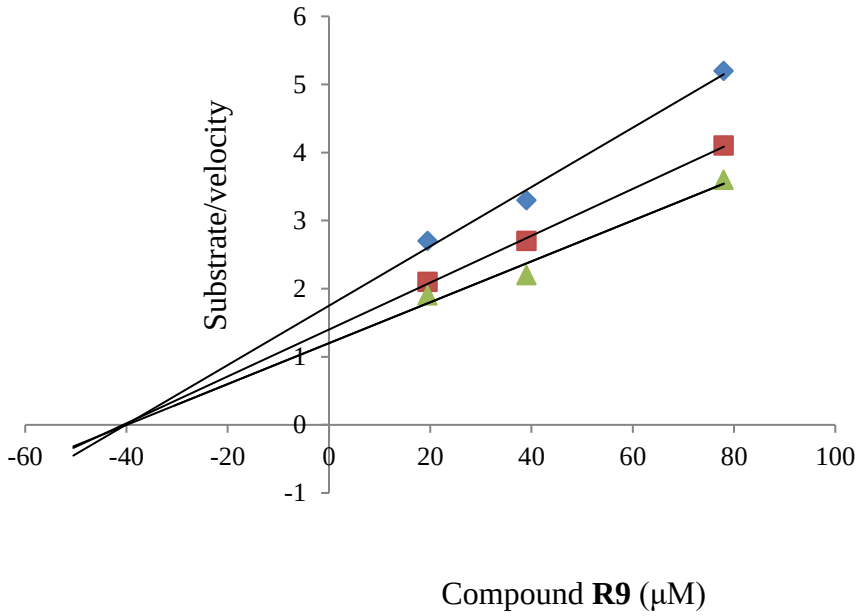

Figure 3-3-3-4. Kinetic analysis of compound **R9** against tyrosinase activity. **A**. Lineweaver-Burk plot, **B**. Dixon plot.

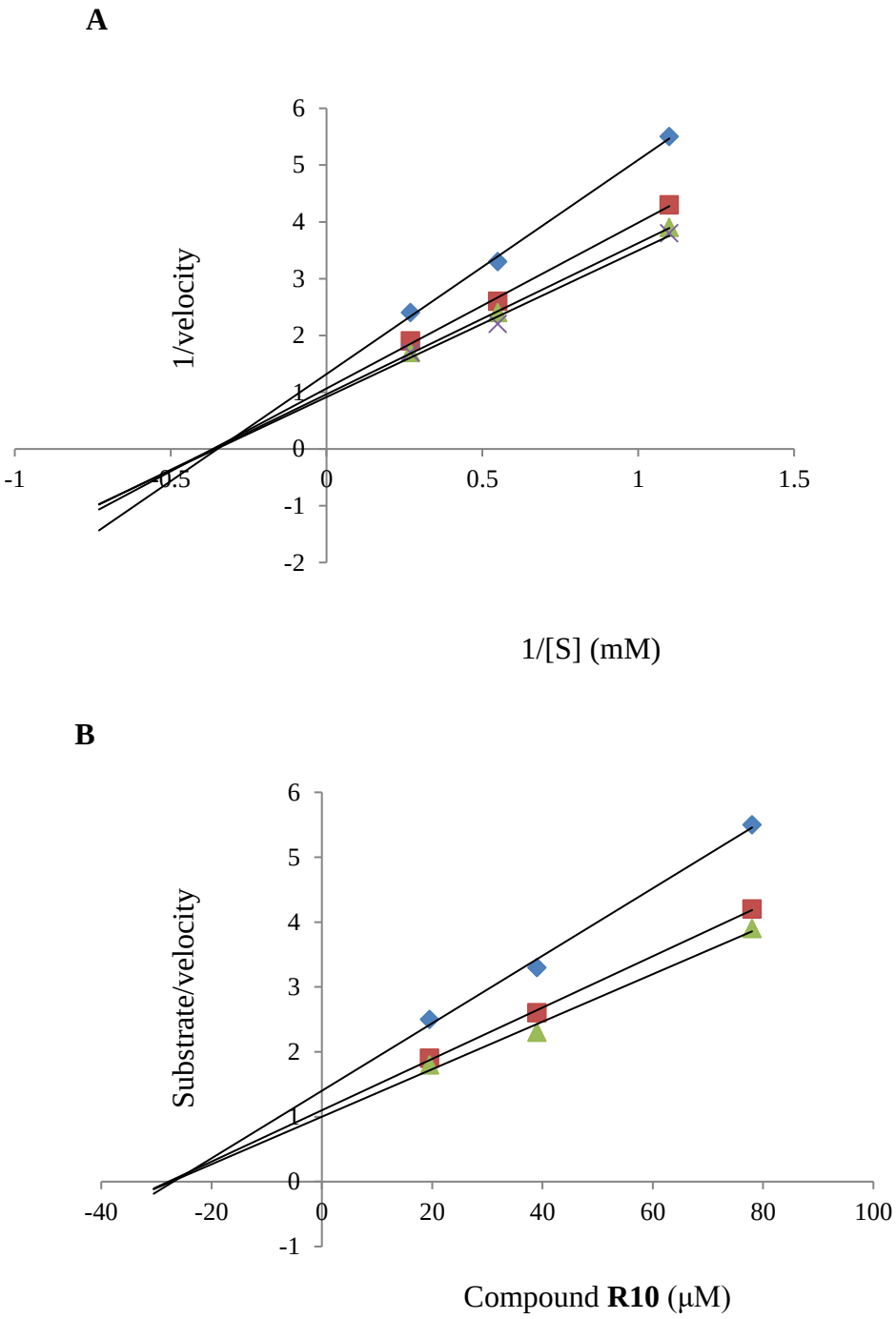

Figure 3-3-3-5. Kinetic analysis of compound **R10** against tyrosinase activity. **A**. Lineweaver-Burk plot, **B**. Dixon plot.

3.3.4. Tyrosinase Inhibitory Activity of Related Phenolic Compounds

In vitro results of tyrosinase inhibition of synthetic phenolic compounds (**8**, **62-73**) (Figure 3-3-4-1) and naturally occurring bromophenols (**R1**-**R10)** (Figure 3-3-4-2) were listed in Table 3-3-4-1.

Table 3-3-4-1. Tyrosinase inhibition of synthetic phenolic compounds and naturally occurring bromophenols.

Compound	Tyrosinase Inhibition IC_{50} (μM)[a]	Compound	Tyrosinase Inhibition, IC_{50} (μM)[a]
62	61.3±1.9	**R1**	17.3±0.1
63	>1000	**R2**	31.0±0.1
64	>1000	**R3**	67.5±0.2
65	>1000	**R4**	96.8±0.1
66	>1000	**R5**	11.0±0.1
67	>1000	**R6**	39.2±0.0
68	37.2±0.5	**R7**	1.0±0.1
69	>1000	**R8**	5.2±0.0
70	>1000	**R9**	50.0±0.1
71	>1000	**R10**	39.0±0.0
8	136.2±0.2	Kojic acid	35.0±0.0
72	>1000		
73	462.5±0.5		

[a]Mean±standard error (n=3).

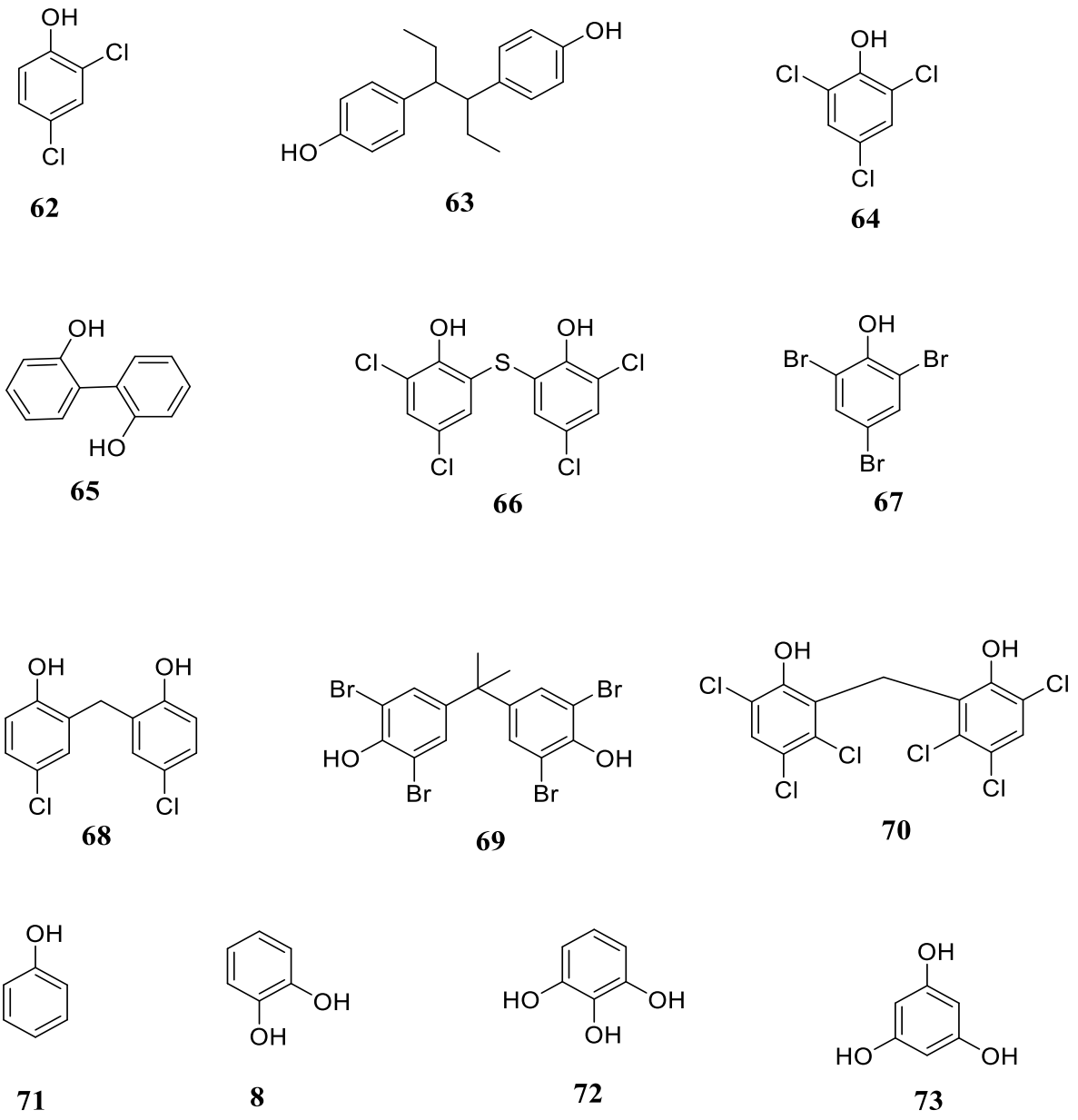

Figure 3-3-4-1. Synthetic phenolic compounds.

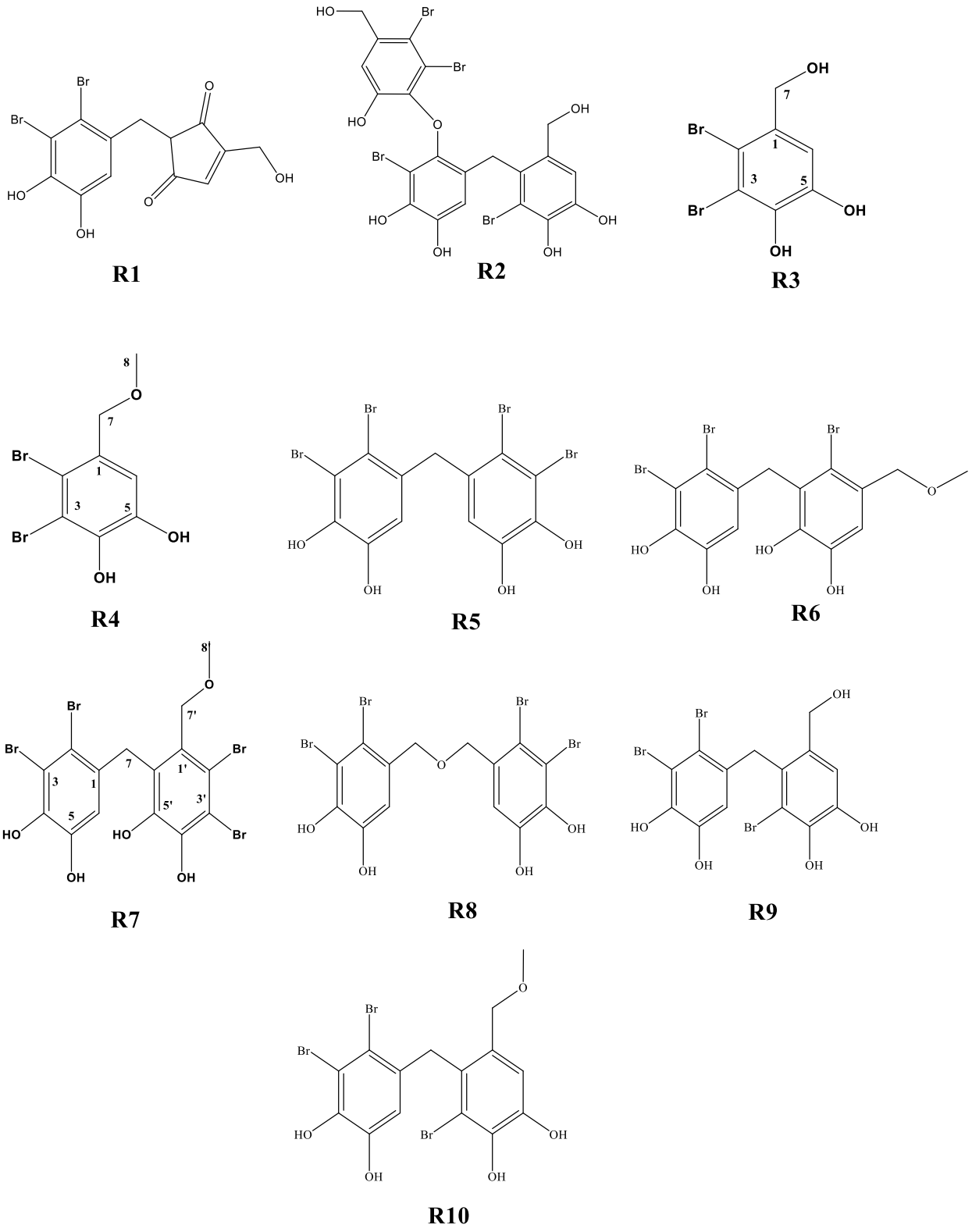

Figure 3-3-4-2. Naturally occurring bromophenols.

Number and position of hydroxy group and halogen, number of benzene ring, and asymmetric or symmetric structure of inhibitor are the key factors that can influence tyrosinase inhibition. In synthetic phenolic compounds **62** and **68** showed moderate inhibition, compounds **8** and **73** displayed weak inhibition while other synthetic compounds exhibited no inhibition. Compound **64** was a monomer and trichlorinated compound did not showed inhibitory potency while compound **62** was a diclorinataed phenol displayed moderated inhibition. Even tetra- and hexachlorinated phenolic compound (**66** and **70**) did not exhibit inhibition. Why only dichlorinated phenol displayed inhibition against tyrosinase did not clearly understood. Most of the tyrosinase inhibitor are phenolic-type compounds derived from terrestrial plant. Catechol moiety of inhibitors play a significant role as a copper chelator of tyrosinase enzyme [3]. This would be true because catechol (**8**) displayed moderate inhibition compared to other synthetic phenolic compounds. But this hypothesis does not always work as compounds **62** and **68** exhibited inhibitory activity despite without catechol moiety. Compound **62** and **68** might compete with L-tyrosine substrate. This result revealed that catechol moiety does not mandatory for chlorinated phenolic compound and tyrosinase can be inhibited other than copper chelation. Pyrogallol (**72**) moiety did not exhibit any effect on tyrosinase.

Naturally occurring dibrominated compound **R3** showed IC_{50} value of 67.5 μM but synthetic tribrominated (**67**) and tertrabrominated (**69**) phenolic compounds did not exhibit any inhibitory activity. There was a report on comparison between bromine and chlorine substitution and bromination lead to slightly more active compounds [31]. This speculation found true as naturally occurring bromophenols **R5**, **R7** and **R8** were the most powerful tyrosinase inhibitors. Then inhibitory potency followed by tribrominated and dibrominated naturally occurring bromophenols. Number and position of hydroxy group are important to antioxidant activity [103] but halogen substitution directly related with anticancer [31, 61], enzyme inhibition [70], antimicrobial [31], and anti-diabetic activity [31]. Specifically higher number of bromine substitution is gradually increased compound bioactive potency [103].

Synthetic symmetric chlorinated compounds **66** and **70** did not exhibit any inhibition but only compound **68** showed moderate tyrosinase inhibition. Compound **68** was reported to show glucose 6-phosphate dehydrogenase inhibitory activity [69]. Naturally occurring symmetric brominated compounds **R5** and **R7** displayed high tyrosinase inhibition as well.

3.4. Conclusion

Ten bromophenols **R1**-**R10** were isolated from the marine algae *Neorhodomela aculeata* and *Odonthalia corymbifera*. These bromophenols tyrosinase inhibitory and antioxidant activity were investigated. Novel compounds **R1** and **R2** showed stronger inhibition than positive control kojic acid. While dimers (**R5**-**R10**) displayed higher inhibition than monomers (**R3** & **R4**). Thus number and position of hydroxy group is very important for tyrosinase inhibition. All bromophenols possess catechol moiety that act as copper chelator of tyrosinase and play key role in enzyme inhibition. This property also supported by various reported phenolic tyrosinase inhibitors. Bromination also exhibited its role behind tyrosinase inhibition. Tetrabrominated compound (**R5**, **R7**, and **R8**) displayed the highest inhibition than dibrominated and tribrominated compounds. So, this study reveals possibility of different mechanism, other than Cu-chelation by catechol moiety of naturally occurring bromophenols for tyrosinase inhibition. Lineweaver-Burk and Dixon plot analysis were performed for the determination of inhibition type and inhibitor constant. The bromophenols examined (**R5**, **R8**-**R10**) showed non-competitive inhibition. This type of inhibitors may bind other site of the active site and combine with either free enzyme or enzyme-substrate complex. In another hypothesis the inhibitor caused a change in the structure and shape of enzyme, and the modified enzyme was no longer capable of binding correctly with the substrate. The antioxidant property strongly rely on number and position of hydroxy group and bromination relatively carry less significance which was opposite in tyrosinase inhibition. However, all the bromophenols showed antioxidant activities in varying degree which was comparable to positive controls. Synthetic phenolic compounds tyrosinase inhibitory activity was compared with naturally occurring bromophenols. Naturally occurring bromophenols were found as potent tyrosinase inhibitors than synthetic compounds.

General Summary

Hyperpigmentation and enzymatic browning is mainly caused by the activity of tyrosinase enzyme. Inhibition or delay of this enzymatic reaction is a very popular technique to overcome the problem. Synthetic inhibitors such as kojic acid, arbutin and hydroquinone are commonly used as skin whitening agents but these compounds are criticized for toxicity problem. Many tyrosinase inhibitors have already been isolated as phenolic compounds from plant, microorganism, and marine organism. Moreover, free radicals are continuously generated in a living systems but natural defense mechanism neutralize that radicals. When this balance does not work, there is possibility of arising many diseases from the attack of free radicals. Free radical or reactive oxygen species (ROS) may induce α-melanocyte-stimulating hormone (α-MSH) resulting abnormal pigmentation such as age spot, freckles, skin aging, melasma. The major objectives of this research were set as screening and identification of potential marine algae; isolation and purification of bioactive compounds, structural elucidation by MS and NMR analysis; activity and kinetic study for the inhibitors.

In Chapter 1, Marine algae were collected from Hakodate, Otaru and Nemuro, Japan and screened for DPPH antioxidant assay. Most of algae extract exhibited weak antioxidant activity except red algae of family Rhodomelaceae. Therefore, the marine alga *Odonthalia corymbifera* (Rhodomelaceae) was selected for purification. With the guidance of results of antioxidant assay, the extract was separated by several chromatographic techniques to obtain compounds **R1** and **R2**. Their structures were elucidated from instrumental analyses or chemical derivatization. Compound **R1** named odonthadione was determined as a new hybrid-type bromophenols consist of coupling between brominated hydroxylated benzyl (BHB) unit and a unique cyclopentene moiety with two ketone groups. Compound **R1** possessing a chiral center showed optically inactive. Thus compound **R1** could be a racemic mixture. Compound **R2** named odonthalol was determined as a new trimer of three BHB units. So far only four trimers have been purified and this compound will include as a new member of this group. Previously reported trimers BHB units were connected via methylene bridges but in compound **R2** BHB units were connected via methylene and ether bridges which were structurally unique.

In Chapter 2, eight known bromophenols were isolated from two kinds of Rhodomelaceae algae. Bromophenols were isolated from the two red algae *Neorhodomela aculeata* and *Odonthalia corymbifera*. The bromophenols were identified as two

bromophenol monomers **R3** and **R4**, two symmetric dimers **R5** and **R8**, and four asymmetric dimers **R6**, **R7**, **R9** and **R10**, from their MS and NMR data. Although compounds **R6**, **R7** and **R10** were isomers, they were determined from difference of HMBC correlations.

In Chapter 3, tyrosinase inhibitory and antioxidant activity were compared among the bromophenols isolated. All the bromophenols showed tyrosinase inhibitory activity which comparable to positive control kojic acid. Hybrid bromophenol **R1**, trimer **R2**, dimers **R5**-**R10** displayed higher inhibition than monomers **R3** and **R4**. Bromophenols **R1**-**R10** possess catechol moiety that act as copper chelator of tyrosinase and play key role in enzyme inhibition. Number of bromination affected tyrosinase inhibitory activity. These results suggested that tyrosinase activity influence not only from copper chelation but also bromination can enhance inhibitory activity. Bromophenols **R5**, **R8**, **R9** and **R10** showed non-competitive inhibition from Lineweaver-Burk plot analysis. This type of inhibitors may bind other site of the active site, combine with either free enzyme or enzyme-substrate complex, bring change in the structure and shape of enzyme, and the modified enzyme was no longer capable of binding correctly with the substrate. Although effect of bromination is still unclear, bromination may play an important role. The antioxidant activities of bromophenols **R1**-**R10** were examined by radical scavenging (DPPH & ABTS), metal reducing (CUPRAC & FRAP) and copper-chelation assay. Bromophenols **R1**-**R10** displayed antioxidant activity in varying degree which was comparable to respective positive controls. Result revealed that antioxidant properties strongly rely on number and position of hydroxy group. Bromination relatively carries less significance for antioxidant activity which found opposite in tyrosinase inhibition. Thirteen related phenolic compounds were purchased and compared inhibitory activity with bromophenols **R1**-**R10** to elucidate inhibition mechanism. Although two dichlorinated compounds showed moderate tyrosinase inhibition, the others displayed weak or no inhibition. These results suggest that tyrosinase inhibition requires catechol moiety and bromine substitution, not other halogen substitution.

Bromophenols are multifunctional compounds. Still researchers are interested to discover novel bromophenols and disclose new functionalities. Mostly reported tyrosinase inhibitior are phenolic ompounds but naturally ocurring bromophenol was not investigated for tyrosinase inhibition. These studies have revealed new functionality of bromophenol as tyrosinase inhibitor. Bromine substitutions inhibit tyrosinase activity to a great extent but further investigations are required for clear understanding of inhibitory mechanism. However, marine red algae can be source of bioactive compounds in pharmaceutical industries.

References

[1] Kim, Y. J.; Uyama, H. Tyrosinase inhibitors from natural and synthetic sources: structure, inhibition mechanism and perspective for the future. *Cell Mol. Life Sci.* 2005, 62, 1707-1723.

[2] Hamilton, A. J.; Gomez, B. L. Melanins in fungal pathogens. *J. Med. Microbiol*. 2002, 51, 189-191.

[3] Chang, T. S. An updated review of tyrosinase inhibitors. *Int. J. Mol. Sci*. 2009, 10, 2440-2475.

[4] Zongping, Z. Isolation and structural elucidation of tyrosinase inhibitors from five plant extracts. Ph.D. Thesis, The University of Hong Kong, January, 2011.

[5] Dev, S. K.; Mukherjee, A. Catechol oxidase and phenoxazinone synthase: Biomimetic functional models and mechanistic studies. *Coord. Chem. Rev*. 2016, 310, 80-115.

[6] Mayer, A. M.; Harel, E. Polyphenol oxidases in plants. *Phytochemistry*, 1979, 18, 193-215.

[7] Sánchez-Ferrer, A.; Rodríguez-López, J. N.; García-Cánovas, F.; García-Carmona, F. Tyrosinase: a comprehensive review of its mechanism. *Biochim. Biophys. Acta*, 1995, 1247, 1-11.

[8] Del, M. V.; Beermann, F. Tyrosinase and related protein in mammalian pigmentation. *FEBS Lett.* 1996, 381, 165-168.

[9] Prota, G. Progress in the chemistry of melanins and related metabolites. *Med. Res. Rev*. 1988, 8, 525-566.

[10] Solano, F.; Stefania, B.; Picardo, M.; Ghanem, G. Hyperpigmenting agents: an updated review on biological, chemical, and clinical aspects. *Pigment Cell Res*. 2006, 19, 550-571.

[11] Loizzo, M. R.; Tundis, R.; Menichini, F. Natural and synthetic tyrosinase inhibitors as antibrowning agents: an update. *Comp. Rev. Food Sci. Food Saf.* 2012, 11, 378-398.

[12] Hurrel, R. F.; Finot, P. A. Nutritional consequences of the reactions between proteins and oxidized polyphenolic acids. *Adv. Exp. Med. Biol*. 1984, 177, 423-435.

[13] Ando, H.; Kondoh, H.; Ichihashi, M.; Hearing, V. J. Approaches to indentify inhibitors of melanin biosynthesis via the quality control of tyrosinase. *J. Invest. Dermatol*. 2007, 127, 751-761.

[14] Chen, J. S.; Wei, C.; Marshall, M. R. Inhibition mechanism of kojic acid on polyphenol oxidase. *J. Agric. Food Chem*. 1991, 39, 1897-1901.

[15] Parvez, S.; Kang, M.; Chung, H. S.; Cho, C.; Hong, M. C.; Shin, M. K.; Bae, H. Survey and mechanism of skin depigmenting and lightening agents. *Phytother. Res*. 2006, 20, 921-934.

[16] Williams, G. M.; Iatropoulos, M. J.; Jeffrey, A. M; Duan, J. D. Inhibition by dietary hydroquinone of acetylaminofluorene induction of initiation of rat liver carcinogenesis. *Food Chem. Toxicol*. 2007, 45, 1620-1625.

[17] Li, K.; Li, X. M.; Gloer, J. B.; Wang, B. G. New nitrogen-containing bromophenols from the marine red alga *Rhodomela confervoides* and their radical scavenging activity. *Food Chem.* 2012, 135, 868-872.

[18] Balboa, E. M.; Conde, E.; Moure, A.; Falqué, E.; Domínguez, H. *In vitro* antioxidant properties of crude extracts and compounds from brown algae. *Food Chem.* 2013, 138, 1764-1785.

[19] Chung, Y. M.; Wang, H. C.; El-Shazly, M.; Leu, Y. L.; Cheng, M. C.; Lee, C. L.; Chang, F. R.; Wu, Y. C. Antioxidant and tyrosinase inhibitory constituents from a desugared sugar cane extract, a byproduct of sugar production. *J. Agric. Food Chem*. 2011, 59, 9219-9225.

[20] Firuzi, O.; Miri, R.; Tavakkoli, M.; Saso, L. Antioxidant therapy: current status and future prospects. *Cur. Med. Chem.* 2011, 18, 3871-3888.

[21] Brewer, M. S. Natural oxidants: sources, compounds, mechanisms of action, and potential applications. *Comp. Rev. Food Sci. Food Saf.* 2011, 10, 221-247.

[22] Andre, C.; Castanheira, I.; Cruz, J. M.; Paseiro, P.; Sanches-Silva, A. Analytical strategies to evaluate antioxidants in food: A review. *Trends Food Sci. Tecnhol.* 2010, 21, 229-246.

[23] Grillo, C. A.; Dulout, F. N. Cytogenetic evaluation of butylated hydroxytoluene. *Mutat. Res.* 1995, 345, 73-78.

[24] Li, K.; Li, X. M.; Gloer, J. B.; Wang, B. G. Isolation, characterization and antioxidant activity of bromophenols of the marine red alga *Rhodomela confervoides*. *J. Agric. Food Chem*. 2011, 59, 9916-9921.

[25] Bonilla, F.; Mayen, M.; Merida, J.; Medina, M. Extraction of phenolic compounds from red grape marc for use as food lipid antioxidants. *Food Chem.* 1999, 66, 209-215.

[26] Konczak, I.; Zabaras, D.; Dunstan, M.; Aguas, P. Antioxidant capacity and phenolic compounds in commercially grown native Australian herbs and spices. *Food Chem.* 2010, 122, 260-266.

[27] Öztaskin, N.; Taslimi, P.; Maras, A.; Gülcin, I.; Göksu, S. Novel antioxidant bromophenols with acetylcholinesterase, butyrylcholinesterase and carbonic anhydrase inhibitory actions. *Bioorg. Chem.* 2017, 74, 104-114.

[28] Huang, D.; Ou, B.; Prior, R. L. The chemistry behind antioxidant capacity assays. *J. Agric. Food Chem*. 2005, 53, 1841-1856.

[29] Nawar, W. F. Lipids. In: Fennema, O. editor. Food Chemistry, 3rd ed. New York: Marcel Dekker, Inc. 1996, 225-320.

[30] Shan, B.; Cai, Y. Z.; Sun, M.; Corke, H. Antioxidant capacity of 26 spice extracts and characterization of their phenolic constituents. *J. Agric. Food Chem*. 2005, 53, 7749-7759.

[31] Liu, M.; Hansen, P. E.; Lin, X. Bromophenols in marine algae and their bioactivities. *Mar. Drugs*, 2011, 9, 1273-1292.

[32] Flodin, C.; Whitfield, F. B. Biosynthesis of bromophenols in marine algae. *Water Sci. Technol*. 1999, 40, 53-58.

[33] Collén, J.; Ekdahl, A.; Abrahamsson, K.; Pedersén, M. The involvement of hydrogen peroxide in the production of volatile halogenated compounds by *Meristiella gelidium*. *Phytochemistry*, 1994, 36, 1197-1202.

[34] Kicklighter, C. E.; Kubanek, J.; Hay, M. E. Do brominated natural products defend marine worms from consumers? Some do, most don't. *Limnol. Oceanogr*. 2004, 49, 430-441.

[35] Whitfield, F. B.; Helidoniotis, F.; Shaw, K. J.; Svoronos, D. Distribution of bromophenols in species of marine algae from eastern Australia. *J. Agric. Food Chem*. 1999, 47, 2367-2373.

[36] Xu, X.; Song, F.; Wang, S.; Li, S.; Xiao, F.; Zhao, J.; Yang, Y.; Shang, S.; Yang, L.; Shi, J. Dibenzyl bromophenols with diverse dimerization patterns from the brown alga *Leathesia nana*. *J. Nat. Prod*. 2004, 67, 1661-1666.

[37] Xu, X. L.; Fan, X.; Song, F. H.; Zhao, J. L.; Han, L. J.; Yang, Y. C.; Shi, J. G. Bromophenols from the brown alga *Leathesia nana*. *J. Asian Nat. Prod. Res*. 2004, 6, 217-221.

[38] Sun, H. H.; Paul, V. J.; Fenical, W. Avrainvilleol, a brominated diphenylmethane derivative with feeding deterrent properties from the tropical green alga *Avrainvilla longicaulis*. *Phytochemistry*, 1983, 22, 743-745.

[39] Lindsay, B. S.; Battershill, C. N.; Copp, B. R. Isolation of 2-(3'-bromo-4'-hydroxyphenol)ethanamine from the New Zealand ascidian *Cnemidocarpa bicornuta*. *J. Nat. Prod*. 1998, 61, 857-858.

[40] Fu, X.; Schmitz, F. J.; Govindan, M.; Abbas, S. A.; Hanson, K. M.; Horton, P. A.; Crews, P.; Laney, M.; Schatzman, R. C. Enzyme inhibitors: new and known polybrominated phenols and diphenyl ethers from four Indo-Pacific *Dysidea* sponges. *J. Nat. Prod*. 1995, 58, 1384-1391.

[41] Olsen, E. K.; Hansen, E.; Isaksson, J.; Andersen, J. H. Cellular antioxidant effect of four bromophenols from the red algae, *Vertebrata lanosa*. *Mar. Drugs*, 2013, 11, 2769-2784.

[42] Xu, N.; Fan, X.; Yan, X.; Li, X.; Niu, R.; Tseng, C. K. Antibacterial bromophenols from the marine red alga *Rhodomela confervoides*. *Phytochemistry*, 2003, 62, 1221-1224.

[43] Popplewell, W. L.; Northcote, P. T. Colensolide A: a new nitrogenous bromophenol from the New Zealand marine red alga *Osmundaria colensoi*. *Tetrahedron Lett*. 2009, 50, 6814-6817.

[44] Kim, S. Y.; Kim, S.; Oh, M. J.; Jung, S. J. Kang, S. *In vitro* antiviral activity of red alga, *Polysiphonia morrowii* extract and its bromophenols against fish pathogenic infectious

hematopoietic necrosis virus and infectious pancreatic necrosis virus. *J. Microbiol*. 2011, 49, 102-106.

[45] Shi, D. Y.; Xu, F.; He, J.; Li, J.; Fan, X.; Han, L. J. Inhibition of bromophenols against PTP1B and anti-hyperglycemic effect of *Rhodomela confervoides* extract in diabetic rats. *Chin. Sci. Bull*. 2008, 53, 2476-2479.

[46] Kim, K. Y.; Nam, K. A.; Kurihara, H.; Kim, S. M. Potent alpha-glucosidase inhibitors from the red alga *Grateloupia elliptica*. *Phytochemistry*, 2008, 69, 2820-2825.

[47] Kurihara, H; Mitani, T.; Kawabata, J.; Takahashi, K. Inhibitory potencies of bromophenols from Rhodomelaceae algae against α-glucosidase activity. *Fish Sci*. 1999, 65, 300-303.

[48] Kim, K. Y.; Nguyen, T. H.; Kurihara, H.; Kim, S. M. Alpha-glucosidase inhibitory activity of bromophenol purified from the red alga *Polyopes lancifolia*. *J. Food Sci*. 2010, 75, H145-H150.

[49] Kurihara, H.; Mitani, T.; Kawabata, J.; Takahashi, K. Two new bromophenols from the red alga *Odonthalia corymbifera*. *J. Nat. Prod*. 1999, 62, 882-884.

[50] Wang, W.; Okada, Y.; Shi, H.; Wang, Y.; Okuyana, T. Structure and aldose reductase inhibitory effects of bromophenols from the red alga *Symphyocladia latiuscula*. *J. Nat. Prod.* 2005, 68, 620-622.

[51] Shi, D.; Li, X.; Li, J.; Guo, S.; Su, H.; Fan, X. Antithrombotic effects of bromophenol, an alga-derived thrombin inhibitor. *Chin. J. Oceanol. Limn*. 2010, 28, 96-98.

[52] Shi, D.; Li, J.; Guo, S.; Han, L. Antithrombotic effect of bromophenol, the alga-derived thrombin inhibitor. *J. Biotechnol*. 2008, 136, S579.

[53] Carte, B. K.; Troupe, N.; Chan, J. A.; Westley, J. W.; Faulkner, D. J. Rawsonol, an inhibitor of HMG-CoA reductase from the tropical green alga *Avrainvillea rawsoni*. *Phytochemistry*, 1989, 28, 2917-2919.

[54] Wiemer, D. F.; Idler, D. D.; Fenical, W. Vidalols A and B, new anti-inflammatory bromophenols from the Caribbean marine red alga *Vidalia obtusaloba*. *Experientia*, 1991, 47, 851-853.

[55] Kurata, K.; Taniguchii, K. Takashima, K.; Hayashi, I.; Suzuki, M. Feeding-deterrent bromophenols from *Odonthalia corymbifera*. *Phytochemistry*, 1997, 45, 485-487.

[56] Park, S. H.; Song, J. H.; Kim, T.; Shin, W. S.; Park, G. M.; Lee, S.; Kim, Y. J.; Choi, P.; Kim, H.; Kim, H. S.; Kwon, D. H.; Choi, H. J.; Ham, J. Anti-human rhinoviral activity of polybromocatechol compounds isolated from the rhodophyta, *Neorhodomela aculeata*. *Mar. Drugs*, 2012, 10, 2222-2233.

[57] Wang, B. G.; Gloer, J. B.; Ji, N. Y.; Zhao, J. C. Halogenated organic molecules of Rhodomelaceae origin: chemistry and biology. *Chem. Rev*. 2013, 113, 3632-3685.

[58] Zhao, J.; Fan, X.; Wang, S.; Li, S.; Shang, S.; Yang, Y.; Xu, N.; Lu, Y.; Shi, J. Bromophenol derivatives from the red alga *Rhodomela confervoides*. *J. Nat. Prod*. 2004, 67, 1032-1035.

[59] Duan, X. J.; Li, X. M.; Wang, B. G. Highly brominated mono and bis phenols from the marine red alga *Symphyocladia latiuscula* with radical scavenging activity. *J. Nat. Prod*. 2007, 70, 1210-1213.

[60] Zhao, J.; Ma, M.; Wang, S.; Li, S.; Cao, P.; Yang, Y.; Lu, Y.; Shi, J.; Xu, N.; Fan, X.; He, L. Bromophenols coupled with derivatives of amino acids and nucleosides from the red alga *Rhodomela confervoides*. *J. Nat. Prod*. 2005, 68, 691-694.

[61] Ma, M.; Zhao, J.; Wang, S.; Li, S.; Yang, Y.; Shi, J.; Fan, X.; He, L. Bromophenols coupled with methyl γ-ureidobutyrate and bromophenol sulfates from the red alga *Rhodomela confervoides*. *J. Nat. Prod*. 2006, 69, 206-210.

[62] Fan, X.; Xu, N. J.; Shi, J. G. Bromophenols from the red alga *Rhodomela confervoides*. *J. Nat. Prod*. 2003, 66, 455-458.

[63] Combaut, G.; Chantraine, J. M.; Teste, J.; Glombitza, K. W. Phenols bromes des algues rouges: Cyclotribromoveratrylene, nouvean derive obtenu an cours de l'extraction de *Halopytis pinastroides*. *Phytochemistry*, 1978, 17, 1791-1792.

[64] Li, K.; Li, X. M.; Ji, N. Y.; Gloer, J. B.; Wang, B. G. Urceolatin, a structurally unique bromophenol from *Polysiphonia urceolata*. *Org. Lett*. 2008, 10, 1429-1432.

[65] Xu, X. L.; Piggott, A. M.; Yin, L. Y.; Capon, R. J.; Song, F. H. Symphyocladins A-G: bromophenol adducts from a Chinese marine red alga *Symphyocladia latiuscula*. *Tetrahedron Lett*. 2012, 53, 2103-2106.

[66] Choi, J. S.; Park, H. J.; Jung, H. A.; Chung, H. Y.; Jung, J. H.; Choi, W. C. A cyclohexanonyl bromophenol from the red alga *Symphyocladia latiuscula*. *J. Nat. Prod*. 2000, 63, 1705-1706.

[67] Guo, Z.; Li, P.; Hung, W.; Wang, J.; Liu, Y.; Liu, B.; Wang, Y.; Wu, S. B.; Kennelly, E. J.; Long, C. Antioxidant and anti-inflammatory caffeoyl phenylpropanoid and secoiridoid glycosides from *Jasminum nervosum* stems, a Chinese folk medicine. *Phytochemistry*, 2014, 106, 124-133.

[68] Lee, H. S.; Lee, T. H.; Lee, J. H.; Chae, C. S.; Chung, S. C.; Shin, D. S.; Shin, J.; Oh, K. B. Inhibition of the pathogenicity of *Magnaporthe grisea* by bromophenols, isocitrate lyase inhibitors from the red alga, *Odonthalia corymbifera*. *J. Agric. Food Chem*. 2007, 55, 6923-6928.

[69] Kurata, K.; Amiya, T. Two new bromophenols from the red alga, *Rhodomela larix*. *Chem. Lett*. 1977, 6, 1435-1438.

[70] Mikami, D.; Kurihara, H.; Kim, S. M.; Takahashi, K. Red algal bromophenols as glucose 6-phosphate dehydrogenase inhibitors, *Mar. Drugs*, 2013, 11, 4050-4057.

[71] Lan, W. C.; Tzeng, C. W.; Lin, C. C.; Yen, F. L.; Ko, H. H. Prenylated flavonoids from *Artocarpus altilis*: Antioxidant activities and inhibitory effects on melanin production. *Phytochemistry*, 2013, 89, 78-88.

[72] Zheng Z. P.; Cheng, K. W.; Zhu, Q.; Wang, X. C.; Lin, Z. X.; Wang, M. Tyrosinase inhibition constituents in roots of *Morus nigra*: a structure-activity relationship study. *J. Agric. Food Chem.* 2010, 58, 5368–73.

[73] Re, R.; Pellegrini, N.; Proteggente, A.; Pannala, A.; Yang, M.; Evans, C. R. Antioxidant activity applying an improved ABTS radical cation decolorization assay. *Free Radical Biol. Med.* 1999, 26, 1231-1237.

[74] Sabudak, T.; Demirkiran, O.; Ozturk, M.; Topcu, G. Phenolic compounds from *Trifolium echinatum* Bieb and investigation of their tyrosinase inhibitory and antioxidant activities. *Phytochemistry*, 2013, 96, 305-311.

[75] Benzie, I. F. F.; Strain, J. J. The ferric reducing ability of plasma (FRAP) as a measure of antioxidant power: The FRAP assay. *Anal. Biochem.* 1996, 239, 70-76.

[76] Santos, J. S.; Brizola, V. R. A.; Granato, D. High-throughput assay comparison and standardization for metal chelating capacity screening: A proposal and application. *Food Chem.* 2017, 214, 515-522.

[77] Kim, D.; Park, J.; Kim, J.; Han, C.; Yoon, J.; Kim, J.; Kim, N.; Seo, J.; Lee, C. Flavonoids as mushroom tyrosinase inhibitors: a fluorescence quenching study. *J. Agric. Food Chem*. 2006, 54, 935-941.

[78] Likhitwitayawuid, K.; Sritularak, B.; De-Eknamkul, W.; Tyrosinase inhibitors from *Artocarpus gomezianus*. *Planta Med*. 2000, 66, 275-277.

[79] Roh, J. S.; Han, J. Y.; Kim, J. H.; Hwang, J. K. Inhibitory effects of active compounds isolated from safflower (*Carthamus tinctorius* L.) seeds for melanogenesis. *Biol. Pharm. Bull*. 2004, 27, 1976-1978.

[80] Jeong, S. H.; Ryu, Y. B.; Curtis-Long, M. J.; Ryu, W. H.; Baek, Y. S.; Kang, J. E.; Lee, W. S.; Park, K. H. Tyrosinase inhibitory polyphenols from roots of *Morus lhou*. *J. Agric. Food Chem*. 2009, 57, 1195-1203.

[81] Zheng, Z. P; Cheng, K. W.; Chao, J.; Wu, J.; Wang, M. Tyrosinase inhibitors from paper mulberry (*Broussonetia papyrifera*). *Food Chem.* 2008, 106, 529-535.

[82] Zhang, X. D.; Hu, X.; Hou, A. J.; Wang, H. Y. Inhibitory effect of 2, 4, 2', 4'-tetrahydroxy-3-(3-methyl-2-butenyl)-chalcone on tyrosinase activity and melanin biosynthesis. *Biol. Pharm. Bull*. 2009, 32, 86-90.

[83] Arung, E. T.; Shimizu, K.; Kondo, R. Inhibitory effect of artocarpanone from *Artocarpus heterophyllus* on melanin biosynthesis. *Biol. Pharm. Bull*. 2006, 29, 1966-1969.

[84] Chang, T. S.; Ding, H. Y.; Tai, S. S. K.; Wu, C. Y. Mushroom tyrosinase inhibitory effects of isoflavones isolated from soygerm koji fermented with *Aspergillus oryzae* BCRC 32288. *Food Chem.* 2007, 105, 1430-1438.

[85] Shimizu, K.; Kondo, R.; Sakai, K. Inhibition of tyrosinase by flavonoids, stilbenes and related 4-substituted resorcinols: structure acitivity investigations. *Planta Med*. 2000, 66, 11-15.

[86] Shimizu, K.; Kondo, R.; Sakai, K.; Lee, S. H. The inhibitory components from *Artocarpus incius* on melanin biosynthesis. *Planta Med*. 1998, 64, 408-412.

[87] Masamoto, Y.; Ando, H.; Murata, Y.; Shimoishi, Y.; Tada, M.; Takahata, K. Mushroom tyrosinase inhibitory activity of esculetin isolated from seeds of *Euphorbia lathyris*. *Biosci. Biotechnol. Biochem*. 2003, 67, 631-634.

[88] Lee, H. S. Tyrosinase inhibitors of *Pulsatilla cernua* root-derived materials. *J. Agric. Food Chemistry,* 2002, 50, 1400-1403.

[89] Shi, D.; Li, J.; Jiang, B.; Guo, S.; Su, H.; Wang, T. Bromophenols as inhibitors of protein tyrosine phosphatase 1B with antidiabetic properties. *Bioorg. Med. Chem. Lett*. 2012, 22, 2827-2832.

[90] Jiang, B.; Guo, S.; Shi, D.; Guo, C.; Wang, T. Discovery of novel bromophenol 3, 4-dibromo-5-(2-bromo-3,4-dihydroxy-6-(isobutoxymethyl)benzyl)benzene-1,2-diol as protein tyrosine phosphatase 1B inhibitor and its anti-diabetic properties in C57BL/KsJ-*db/db* mice. *Eur. J. Med. Chem*. 2013, 64, 129-136.

[91] Dayong, S.; Jing, L.; Shuju, G.; Hua, S.; Xiao, F. The antitumor effect of bromophenol derivatives *in vitro* and *Leathesia nana* extract *in vivo*. *Chin. J. Oceanol. Limnol*. 2009, 27, 277-282.

[92] Al-Qudah, M. A.; Al-Jaber, H. L.; Zarga, M. H. A.; Qrabi, S. T. A. Flavonoid and phenolic compounds from *Salvia palaestina* L. growing wild in Jordan and their antioxidant activities. *Phytochemistry*, 2014, 99, 115-120.

[93] Son, S.; Lewis, B. A. Free radical scavenging and antioxidative activity of caffeic acid amide and ester analogues: structure-activity relationship. *J. Agric. Food Chem.* 2002, 50, 468-472.

[94] Li, K.; Li, X. M.; Ji, N. Y.; Wang, B. G. Natural bromophenols from the marine red alga *Polysiphonia urceolata* (Rhodomelaceae): Structural elucidation and DPPH radical scavenging activity. *Bioorg. Med. Chem*. 2007, 15, 6627-6631.

[95] Li, K.; Li, X. M.; Ji, N. Y.; Wang, B. G. Bromophenols from the marine red alga *Polysiphonia urceolata* with DPPH radical scavenging activity. *J. Nat. Prod*. 2008, 71, 28-30.

[96] Öztaskin, N.; Ćetinkaya, Y.; Taslimi, P.; Goksu, S.; Gulcin, I. Antioxidant and acetylcholinesterase inhibition properties of novel bromophenol derivatives. *Bioorg. Chem.* 2015, 60, 49-57.

[97] Demirkiran, O.; Sabudak, T.; Ozturk, M.; Topcu, G. Antioxidant and tyrosinase inhibitory activities of flavonoids from *Trifolium nigrescens* subsp. *petrisavi*. *J. Agric. Food Chem*. 2013, 61, 12598-12603.

[98] Mikami, D.; Kurihara, H.; Ono, M.; Kim, S. M.; Takahashi, K. Inhibition of algal bromophenols and their related phenols against glucose 6-phosphate dehydrogenase. *Fitoterapia*, 2016, 108, 20-25.

[99] Hung, A. C.; Wilde, A.; Ebmeyer, J.; Skouroumounis, G. K.; Taylor, D. K. Examination of the phenolic profile and antioxidant activity of the leaves of the Australian native plant *Smilax glyciphylla*. *J. Nat. Prod*. 2013, 76, 1930-1936.

[100] Yoon, N. Y.; Eom, T. K.; Kim, M. M.; Kim, S. K. Inhibitory effect of phlorotannins isolated from *Ecklonia cava* on mushroom tyrosinase activity and melanin formation in mouse B16F10 melanoma cells. *J. Agric. Food Chem*. 2009, 57, 4124-4129.

[101] Higa, T. Phenolic substances. In *Marine Natural Products, Chemical and Biological Perspectives*; Scheuer, P. J., Ed.; Academic Press: New York, 1981, 4, 119-123.

[102] Yang, M. H.; Chen, C. M.; Hu, Y. H.; Zheng, C. Y.; Li, Z. C.; Ni, L. L.; Sun, L.; Chen, Q. X. Inhibitory kinetics of DABT and DABPT as novel tyrosinase inhibitors. *J. Biosci. Bioeng*. 2013, 115, 514-517.

[103] Zhao, W.; Feng, X.; Ban, S.; Lin, W.; Li, Q. Synthesis and biological activity of halophenols as potent antioxidant and cytoprotective agents. *Bioorg. Med. Chem. Lett*. 2010, 20, 4132-4134.